Glucocerebrosidase and glycolipids:
in and beyond the lysosome

PROEFSCHIFT

ter verkrijging van
de graad van Doctor aan de Universiteit Leiden,
op het gezag van Rector Magnificus prof.mr. C.J.J.M. Stolker,
volgens besluit van het College voor Promoties
te verdedigen op 7 januari 2021.
klokke 11:15 uur

door

Daphne Elisabeth Cornelia Boer
geboren te Voorschoten 1988

Promotiecommissie

Promotor: Prof. dr. J.M.F.G Aerts

Copromotor: Prof. dr. J.A. Bouwstra

Overige leden: Prof. Dr. Marcellus Ubbink
Prof Dr Derralynn Hughes
Prof. Dr. Thierry Levade
Prof. Dr. Thomas Hankemeier

ISBN/EAN: 978-94-6332-714-5
Printed by: GVO drukkers & vormgevers B.V. | proefschriften.nl
Quote page 3: Quoted, without source in Wennergren G, Lagercrantz H. "One sometimes finds what one is not looking for" (Sir Alexander Fleming): the most important medical discovery of the 20th century. *Acta Paediatr*. 2007;96(1):141-144.

One sometimes finds what one is not looking for
— Sir Alexander Fleming

Table of contents

Chapter 1

General introduction and scope of the thesis

General introduction and scope of the thesis

Introduction

The human body contains numerous macromolecular constituents of which many contain sugar moieties. Among these glycoconjugates, glycosphingolipids (GSLs) form a distinct class of molecules. They uniquely consist of a lipid moiety (ceramide) to which a single sugar or a chain of sugar carbohydrates can be linked (Figure 1A). The biosynthesis and versatile functions of GSL have been recently reviewed [1-3], (see also **Chapter 2**).

The simplest GSL is glucosylceramide (GlcCer), ubiquitously present in cells of multi-cellular organisms. It is synthesized by the transfer of glucose from UDP-glucose to ceramide by the enzyme glucosylceramide synthase and acts as precursor of many complex GSLs [4]. GSLs are stepwise degraded in lysosomes of cells. The penultimate step in GSL degradation is deglucosylation of GlcCer to ceramide and glucose. This reaction is catalyzed by the lysosomal acid β-glucosidase, commonly named glucocerebrosidase (GCase; GBA) encoded by the *GBA* gene [5, 6]. Inherited deficiencies in GCase result in lysosomal accumulation of GlcCer, which forms the basis for Gaucher disease (GD) [7], (Figure 1B).

GD is heterogeneous in clinical manifestation, involving symptoms such as hepatosplenomegaly, thrombocytopenia, anemia, skeletal deterioration, osteoporosis, neurological symptoms and aberrant skin barrier properties [7]. Besides the most extreme variant, the collodion baby with lethal skin abnormality, three GD phenotypes are generally discerned: type 1, the non-neuronopathic variant; type 2, the acute (infantile) neuronopathic variant, and type 3, the sub-acute (juvenile) neuronopathic variant (see **Chapter 2** for a review). The complete absence of GCase activity leads to a lethally disrupted skin barrier due the crucial role of GCase in the skin for proper conversion of

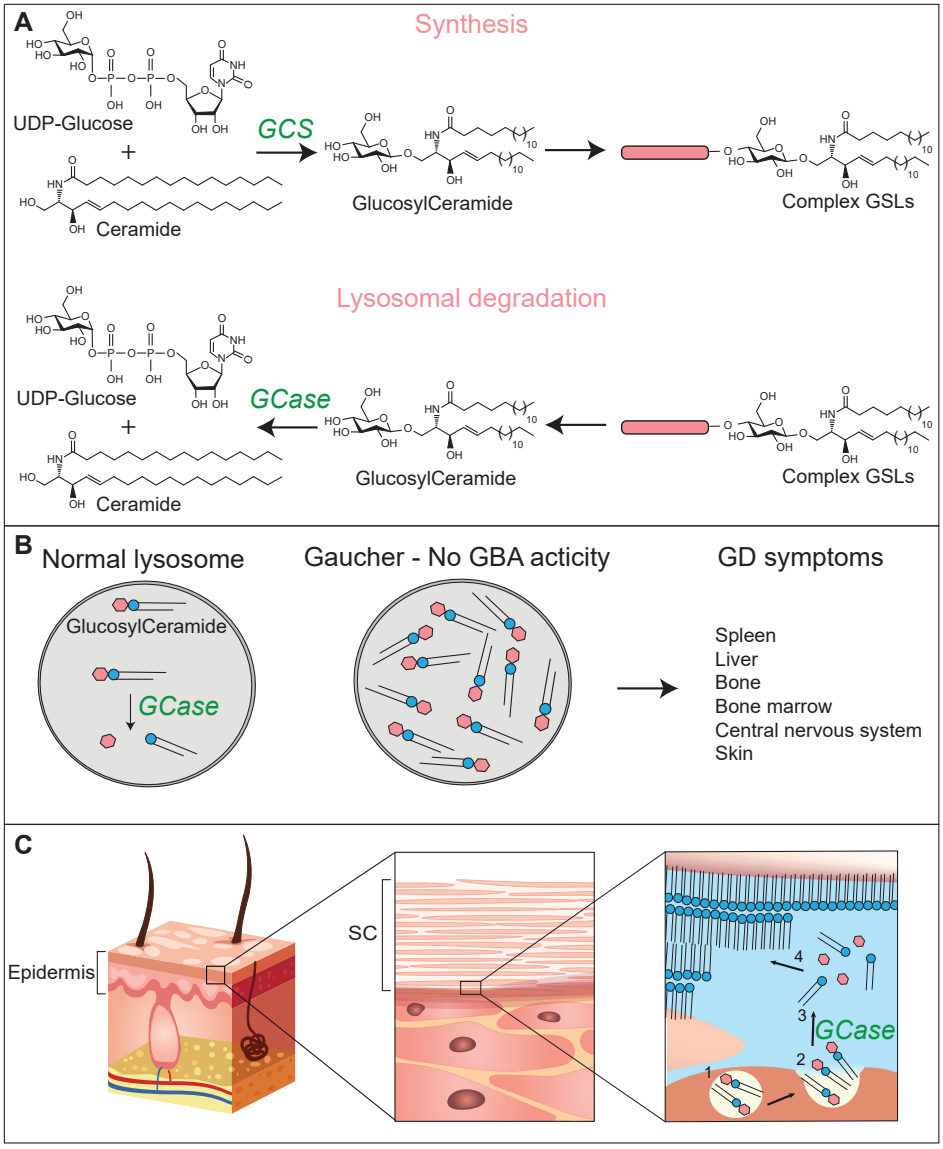

Figure 1: Formation and degradation of glucosylceramide in lysosomes and skin. A. Formation and lysosomal degradation of glucosylceramide (GlcCer). B. Conversion of GlcCer to ceramide by GCase in the lysosome, a lack of GCase activity leads to an accumulation of GlcCer in the lysosome with associated symptoms in GD patients. C. Schematic overview of SC lipid layer formation in the epidermis. 1. Lamellar Bodies (LBs) in the keratinocytes are filled with ceramide precursor GlcCer together with GCase. 2. Extrusion process. 3. Conversion of GlcCer by GCase to ceramides. 4. Formation of the extracellular stacked lipid layers: the lipid barrier in the SC.

skin generating local ceramides [8, 9]. The barrier function of the skin, offering protection against external hazardous factors and preventing water loss, resides in the outer part, the epidermis (Figure 1C).

The outermost part of the epidermis, the stratum corneum (SC), contains a high level GCase [10-12]. The SC consist of corneocytes (cornified keratinocytes) embedded in layers of lipid lamellae in a 'brick-and-mortar" like structure [13]. The lipid lamellae are the 'mortar' and contain approximately 50% ceramides, 25% cholesterol, and 15% free fatty acids with little phospholipid. The GlcCer and sphingomyelin precursors of the SC ceramides are first packed in lamellar bodies (LBs) of keratinocytes along with their hydrolyzing enzymes including GCase. The internal content of LBs (lipids and enzymes) is released by keratinocytes into the SC where ceramides are enzymatically generated (Figure 1C). A proper lipid composition is essential for a correct structure and barrier property of the SC. In various skin diseases, like atopic dermatitis, psoriasis and forms of ichthyosis the SC composition is abnormal [14-16].

Glucocerebrosidase

Following the discovery of the molecular basis of GD in the sixties, GCase has been intensively studied. The features of the enzyme are reviewed in **Chapter 2**. It has become apparent that GCase is a protein of 497 amino acids that contains 4 N-linked glycans (Figure 2A). Contrary to the situation for other lysosomal hydrolases, the glycans of GCase acquire no mannose-6-phosphate recognition signal and consequently the enzyme's transport is normal in Mucolipidoses II and III where mannos-6-phosphate formation is impaired [17]. The delivery of newly formed GCase to lysosomes is mediated by the membrane protein LIMP-2 (Lysosomal integral membrane protein 2) to which folded GCase binds in the endoplasmic reticulum (Figure 2A) [18]. In the acid lysosome, the enzyme is released from its binding partner [19]. Inside the lysosome, GCase is assisted by saposin C in degradation of GlcCer, as illustrated by the Gaucher-like phenotype of individuals with a defective saposin C (Figure 2A) [20].

GCase is a retaining β-glucosidase of which the crystal structure has been resolved (Figure 2B) [21]. In its catalytic TIM-barrel domain, a nucleophile (E340) and acid-base residue (E235) mediate catalysis with a glucosyl-E340 intermediate (Figure 2C) [22]. This reaction-mechanism has allowed the design of activity-based probes (ABPs), existing of cyclophellitol-based compounds that covalently bind to the catalytic nucleophile E340 (Figure 2D) [23]. The mechanism-based labeling of GCase with ABP allows ultrasensitive visualization of active enzyme molecules *in situ* and cross species (see also **Chapter 2**) [24-26].

GCase is encoded by the *GBA* gene (locus 1q21) and numerous mutations have meanwhile been identified in association with GD [7]. Most mutations concern amino acid substitutions of which N370S GCase and L444P GCase are most commonly encountered. The former mutation results in an enzyme with catalytic abnormalities, whereas the latter impairs folding of newly formed GCase in the endoplasmic reticulum which results in markedly reduced lysosomal levels [27].

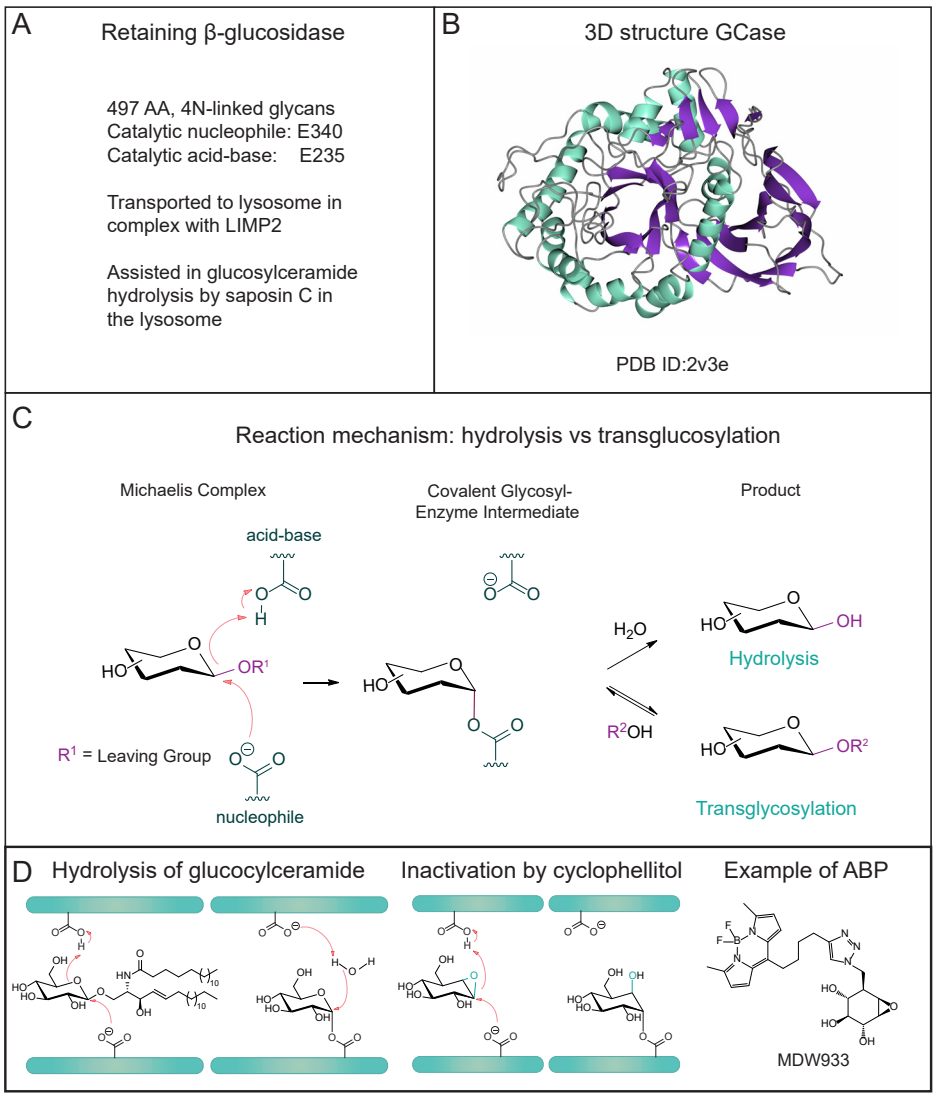

Figure 2: Features of Glucocerebrosidase. A. 3D-structure of GCase. B. Composition, transport and lysosomal activation. C. Reaction mechanisms: hydrolysis versus transglycosylation. D. Mechanism-based suicide inhibition: activity-based probes.

Pathophysiology during GCase deficiency.

Despite the detailed knowledge on GCase, many aspects of the pathophysiology of GD are still poorly understood. For example, while some GCase mutations are associated with more severe disease (L444P GCase) and other with milder and exclusively visceral pathology (N370S GCase), the *GBA* genotype of individual GD patients poorly predicts the precise course of disease and organs involved in this [28]. The nature of the apparent modifiers of disease manifestation is still largely elusive, (see **Chapter 2**).

It has been recognized that adaptive metabolism occurs during GCase deficiency with clinical implications. The characteristic excessive presence of gangliosides in GD patients seems to underly their insulin resistance [29]. Conversion in lysosomes of accumulating GlcCer by acid ceramidase generates glucosylsphingosine (GlcSph) that may leave lysosomes spread through the body of GD patients [30, 31]. Recently, GlcSph is considered as pathogenic, for example in relation to osteoporosis, complement activation and gammopathy that may develop into multiple myeloma [32-34]. The markedly increased risk for Parkinson's disease among carriers of a mutant *GBA* is still unexplained [35]. It has been hypothesized that excessive GlcSph promotes α-synuclein aggregation, a hallmark of Parkinson's disease [36]. However, a clear relation between GlcSph levels and Parkinson's disease does not exist.

Catalytic features of GCase.

In view of the unresolved questions regarding pathophysiology during GCase deficiency, careful investigation of the catalytic features of GCase seems warranted. It has quite recently been recognized that GCase, as reported earlier for other retaining glycosidases, is able to perform tranglucosylation [37, 38]. This reaction implies the transfer of the glucose moiety from the sugar donor (GlcCer) to an acceptor (Figure 2C). It has been demonstrated that cholesterol is a suitable acceptor for GCase. The enzyme may generate glucosylated cholesterol (GlcChol) when cholesterol accumulates in lysosomes, as is the case in Niemann Pick disease type C [38]. At normal conditions, GlcChol is primarily hydrolyzed to cholesterol and glucose by GCase in lysosomes. The physiological relevance of GlcChol is presently unknown.

Another aspect is the potential activity of GCase towards β-xylosides. Many β-glucosidases are known to also acts as β-xylsoidases and this is also the case for GCase. Recent studies (see **Chapter 6**) demonstrate that GCase not only hydrolyzes β-xylosides but also performs transxylosylation and generates xylosylated cholesterol (XylChol). The physiological relevance of recently identified endogenous XylChol and xylosylated ceramide warrants follow-up investigations on the physiological impact of these newly discovered lipids.

Role of GCase beyond the lysosome.

Studies with cultured cells have indicated that normally secretion of GCase molecules is prevented. While other lysosomal hydrolases are partly secreted due to aberrant sorting, this is not apparent for GCase. Only during overexpression some enzyme is secreted, likely due to levels exceeding the capacity of the binding partner LIMP-2. One important exception in this respect form keratinocytes. As discussed above, in these cells GCase is partly sorted to LBs to be actively delivered into the acid extracellular space of the SC where it generates essential ceramide molecules from secreted GlcCer precursor lipids (see **Chapter 3**). Other roles for the high amounts of extracellular GCase in the SC deserve attention (**Chapter 5**).

Visualization of active GCase.

A multitude of techniques has become available over the years to visualize active GCase molecules. Activity assays employing GlcCer that is radioactively labeled in the glucose or ceramide moiety to monitor enzyme levels in biological materials are available for some decades [5]. Great use has also been made of artificial GlcCer with a fluorescent acyl-NBD moiety allowing visualization of active enzyme when combined with chromatography methods (high performance liquid chromatography (HPLC) and high-performance thin layer chromatography (HPTLC)) [39]. Likewise, isotope-encoded GlcCer and ultra-performance liquid chromatography – tandem mass spectrometry (ULC-MS/MS) may be employed. Feeding of cells with radioactive serine and with isotope encoded or radioactive sphinganine or sphingosine when used in combination with available specific inhibitors of the GCase allow the analysis of GCase activity *in vivo*. Given their convenient use, popular artificial substrates for GCase activity assays are chromogenic para-nitrophenyl-β-glucoside and fluorogenic 4-methylumbelliferyl-β-glucoside [40].

Of particular interest is the visualization of active GCase *in situ*. Antibodies directed against GCase have been widely employed to visualize GCase molecules with histochemistry, immunofluorescence, and immune-electron microscopy [23, 41]. However, these methods do not discern inactive and active enzyme molecules. The recently availability of highly specific ABP directed towards GCase has opened up new possibilities to study the presence of active GCase molecules *in situ*. Examples is the recent application of ABPs to visualize endogenous GCase, and endocytosed exogenous therapeutic enzyme in lysosomes with correlative light and electron microscopy [42]. Along the same line is the visualization with ABP of active GCase in the SC of skin [43], (**Chapter 3**).

For the detection of activity of GCase towards β-xylosides specific assays have been developed, see **Chapter 6**. The commercial fluorogenic substrate 4-mehylumbelliferyl-β-xyloside can be used to monitor β-xylosidase activity exerted by GCase, in particular in combination with specific inhibitors of the enzymes to account for contaminating activity of other enzymes in samples.

Specific assays have been developed to monitor transglycosylation activity of GCase (Figure 3), see **Chapter 6**. One method is HPTLC based separation of glycosylated product of NBD-cholesterol that is quantified with a Typhoon (Fluorescence mode, Emission 520 BP, laser 488 nm). Alternatively, LC-MS/MS can be employed to detect sensitively and specifically formed trans-products. With this method liquid chromatography is used to separate metabolites of interest. The effluent from the column is ionized in charged particles that migrate under vacuum through the quadrupoles (mass analyzers). A preset mass/charge (m/z) is targeted to pass through the first quadrupole: the parent (precursor) ion. All other particles with a different m/z ratio are then excluded. The selected ions are then fragmented in the collision cell: the daughter ions

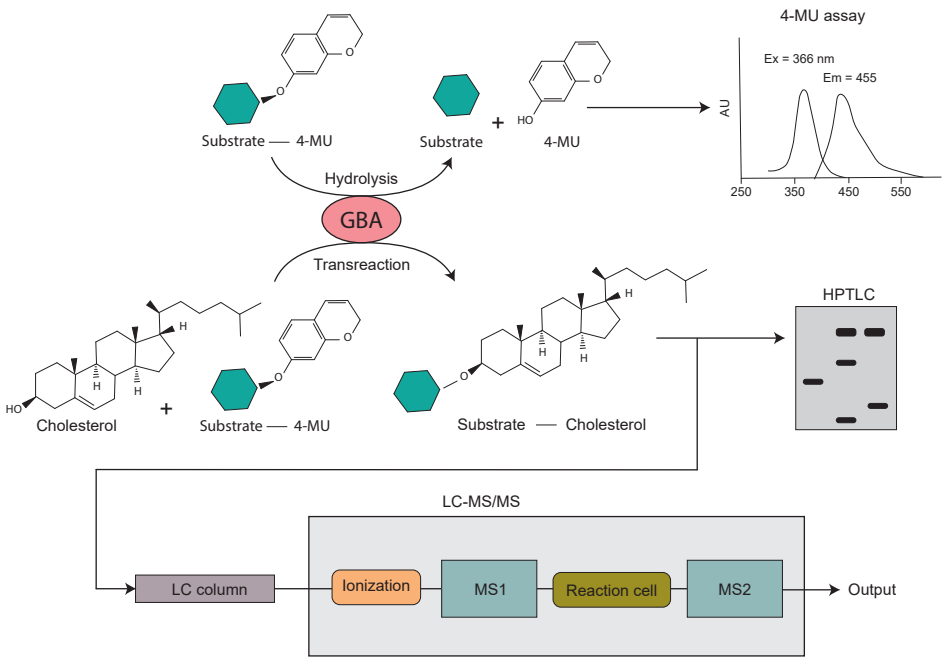

Figure 3: Method to determine in parallel hydrolysis and transglucosylation by GCase. Hydrolysis can be determined by measuring the released fluorescent 4-methylumbelliferone (4-MU) from the non-fluorescent substrate. Transglucosylation by GCase can be in parallel visualized by separation of transproduct using high-performance thin-layer chromatography (HPTLC) or mass spectrometry (MS).

(product ions). The final quadrupole isolates specific daughters followed by quantification via an electron multiplier (Figure 3). This selection of a parent ion with a particular m/z at the first stage and (multiple) daughter ions in the final stage is also referred to as Multiple Reaction Monitoring (MRM, or Selective Reaction Monitoring; SRM).

Analysis of glycolipids.

LC-MS/MS is a powerful method to identify and quantify complex lipids in biological materials. The availability of isotope-encoded standards of lipids of interest is of great value in this respect [44, 45]. Analysis of the lipid composition of the SC of the skin is particularly challenging. The SC can be isolated by tape stripping of the skin or by dermatoming skin and subsequent isolation of the SC by tryptic digestion. Alternatively, skin biopsies from subjects followed by tryptic digestion can be used to isolate the SC. Lipids can be subsequently extracted from SC, as from other tissues.

Challenges.

At present costly therapeutic interventions are available to treat visceral symptoms of GD such as hepatosplenomegaly and hematological symptoms. These therapies are based on supplementation of macrophages with intravenously infused recombinant GCase (enzyme replacement therapy; ERT) or the oral administration of small compound inhibitor of GlcCer synthesis (substrate reduction therapy; SRT) [46-48]. In clinical trials are compounds aiming to stabilize and promote folding of mutant GCase in amenable GD patients (enzyme enhancement therapy, pharmacological chaperone therapy) [49, 50], see **Chapter 2**. Present therapies fail to prevent bone disease and central nervous system manifestations during GCase deficiency. A better understanding of the function of GCase at various body locations and detailed knowledge on its substrates and products is required to improve treatment of GCase deficiency in the future.

Scope of the thesis investigations

The central aim of the undertaken studies was to increase insight in the catalytic versatility and potential functions of glucocerebrosidase (GCase), inside and beyond the lysosome.

Chapter 2 provides a review of the present knowledge on GCase, covering its composition, life cycle and roles in the lysosome and beyond the organelle in the skin. Attention is also paid to the metabolism of glycosphingolipids and Gaucher disease.

Chapter 3 describes the application of ABPs to visualize active GCase *in situ* in skin. The sensitivity of the newly developed method is compared to zymography. The investigation confirmed the presence of high amounts of active GCase at the interface of the vital epidermis and SC. In addition, the effect of inhibition of GCase on GlcCer and ceramide in a 3D-cultured skin model was investigated.

Chapter 4 reports the visualization of active GCase in SC samples of skin from normal individuals and those suffering from atopic dermatitis. In parallel to ABP-labelled GCase, acid sphingomyelinase was visualized by zymography. The data on localization of the ceramide-generating enzymes were compared with measured lipid composition of SC samples. The study illustrated the relation between correct localization of (active) enzymes and desired SC lipid composition for proper skin barrier function.

Chapter 5 deals with the occurrence of GlcChol in the skin, the glucosylated sterol that can be formed by GCase via transglucosylation using GlcCer as glucose donor and cholesterol as acceptor. The investigation revealed the presence of GlcChol in SC. This finding is not surprising given the local abundance of GCase, GlcCer and cholesterol.

Chapter 6 presents an investigation on the ability of GCase to metabolize β-xylosides. It is demonstrated that GCase can hydrolyze various β-xylosides. Moreover, it can use β-xylosides as sugar donor in the transglycosylation of cholesterol, rendering XylChol. The natural presence of XylChol in cells and tissues was subsequently demonstrated. In search for a natural β-xyloside metabolite that acts as sugar donor in the formation of XylChol, a completely novel glycosphingolpid was identified: xylosylated ceramide (XylCer). XylCer was found to be generated by glucosylceramide synthase using UDP-xyloside as sugar donor.

Chapter 7 discusses the findings of the conducted investigations in view of the literature. Moreover, it proposes future investigations on GCase and other β-glucosidases, in and beyond the lysosome.

References

1. A.H. Merrill, Jr., Sphingolipid and glycosphingolipid metabolic pathways in the era of sphingolipidomics, Chem Rev, 111 (2011) 6387-6422.
2. J. Aerts, C.L. Kuo, L.T. Lelieveld, D.E.C. Boer, M.J.C. van der Lienden, H.S. Overkleeft, M. Artola, Glycosphingolipids and lysosomal storage disorders as illustrated by gaucher disease, Curr Opin Chem Biol, 53 (2019) 204-215.
3. G. van Meer, J. Wolthoorn, S. Degroote, The fate and function of glycosphingolipid glucosylceramide, Philos Trans R Soc Lond B Biol Sci, 358 (2003) 869-873.
4. S. Ichikawa, H. Sakiyama, G. Suzuki, K.I. Hidari, Y. Hirabayashi, Expression cloning of a cDNA for human ceramide glucosyltransferase that catalyzes the first glycosylation step of glycosphingolipid synthesis, Proc Natl Acad Sci U S A, 93 (1996) 4638-4643.
5. R.O. Brady, J.N. Kanfer, R.M. Bradley, D. Shapiro, Demonstration of a deficiency of glucocerebroside-cleaving enzyme in Gaucher's disease, J Clin Invest, 45 (1966) 1112-1115.
6. M. Horowitz, S. Wilder, Z. Horowitz, O. Reiner, T. Gelbart, E. Beutler, The human glucocerebrosidase gene and pseudogene: structure and evolution, Genomics, 4 (1989) 87-96.
7. E. Beutler, G.A. Grabowski, Glucosylceramide Lipidosis-Gaucher Disease, The metabolic and molecular bases of inherited disease eighth edition: Edited by C R Sriver, A L Beaudet, W S Sly and D Valle. McGraw-Hill, New York, (2001).
8. E. Sidransky, D.M. Sherer, E.I. Ginns, Gaucher disease in the neonate: a distinct Gaucher phenotype is analogous to a mouse model created by targeted disruption of the glucocerebrosidase gene, Pediatr Res, 32 (1992) 494-498.
9. V.L. Tybulewicz, M.L. Tremblay, M.E. LaMarca, R. Willemsen, B.K. Stubblefield, S. Winfield, B. Zablocka, E. Sidransky, B.M. Martin, S.P. Huang, et al., Animal model of Gaucher's disease from targeted disruption of the mouse glucocerebrosidase gene, Nature, 357 (1992) 407-410.
10. Y. Takagi, E. Kriehuber, G. Imokawa, P.M. Elias, W.M. Holleran, Beta-glucocerebrosidase activity in mammalian stratum corneum, J Lipid Res, 40 (1999) 861-869.
11. M. Schmuth, K. Schoonjans, Q.C. Yu, J.W. Fluhr, D. Crumrine, J.P. Hachem, P. Lau, J. Auwerx, P.M. Elias, K.R. Feingold, Role of peroxisome proliferator-activated receptor alpha in epidermal development in utero, J Invest Dermatol, 119 (2002) 1298-1303.
12. J.P. Hachem, D. Crumrine, J. Fluhr, B.E. Brown, K.R. Feingold, P.M. Elias, pH directly regulates epidermal permeability barrier homeostasis, and stratum corneum integrity/cohesion, J Invest Dermatol, 121 (2003) 345-353.
13. P.M. Elias, E.R. Cooper, A. Korc, B.E. Brown, Percutaneous transport in relation to stratum corneum structure and lipid composition, J Invest Dermatol, 76 (1981) 297-301.
14. M. Janssens, J. van Smeden, G.J. Puppels, A.P. Lavrijsen, P.J. Caspers, J.A. Bouwstra, Lipid to protein ratio plays an important role in the skin barrier function in patients with atopic eczema, Br J Dermatol, 170 (2014) 1248-1255.
15. S. Motta, M. Monti, S. Sesana, R. Caputo, S. Carelli, R. Ghidoni, Ceramide composition of the psoriatic scale, Biochim Biophys Acta, 1182 (1993) 147-151.
16. P.M. Elias, M.L. Williams, D. Crumrine, M. Schmuth, Inherited clinical disorders of lipid metabolism, Curr Probl Dermatol, 39 (2010) 30-88.
17. J.M. Aerts, A.W. Schram, A. Strijland, S. van Weely, L.M. Jonsson, J.M. Tager, S.H. Sorrell, E.I. Ginns, J.A. Barranger, G.J. Murray, Glucocerebrosidase, a lysosomal enzyme that does not undergo oligosaccharide phosphorylation, Biochim Biophys Acta, 964 (1988) 303-308.
18. D. Reczek, M. Schwake, J. Schroder, H. Hughes, J. Blanz, X. Jin, W. Brondyk, S. Van Patten, T. Edmunds, P. Saftig, LIMP-2 is a receptor for lysosomal mannose-6-phosphate-independent targeting of beta-glucocerebrosidase, Cell, 131 (2007) 770-783.
19. F. Zunke, L. Andresen, S. Wesseler, J. Groth, P. Arnold, M. Rothaug, J.R. Mazzulli, D. Krainc, J. Blanz, P. Saftig, M. Schwake, Characterization of the complex formed by beta-glucocerebrosidase and the lysosomal integral membrane protein type-2, Proc Natl Acad Sci U S A, 113 (2016) 3791-3796.
20. A. Tylki-Szymanska, J.E. Groener, M.L. Kaminski, A. Lugowska, E. Jurkiewicz, B. Czartoryska, Gaucher disease due to saposin C deficiency, previously described as non-neuronopathic form--no positive effects after 2-years of miglustat therapy, Mol Genet Metab, 104 (2011) 627-630.
21. B. Brumshtein, H.M. Greenblatt, T.D. Butters, Y. Shaaltiel, D. Aviezer, I. Silman, A.H. Futerman, J.L. Sussman, Crystal structures of complexes of N-butyl- and N-nonyl-deoxynojirimycin bound to acid beta-glucosidase: insights into the mechanism of chemical chaperone action in Gaucher disease, J Biol Chem, 282 (2007) 29052-29058.

22. W.W. Kallemeijn, M.D. Witte, T. Wennekes, J.M. Aerts, Mechanism-based inhibitors of glycosidases: design and applications, Adv Carbohydr Chem Biochem, 71 (2014) 297-338.
23. M.D. Witte, W.W. Kallemeijn, J. Aten, K.Y. Li, A. Strijland, W.E. Donker-Koopman, A.M. van den Nieuwendijk, B. Bleijlevens, G. Kramer, B.I. Florea, B. Hooibrink, C.E. Hollak, R. Ottenhoff, R.G. Boot, G.A. van der Marel, H.S. Overkleeft, J.M. Aerts, Ultrasensitive in situ visualization of active glucocerebrosidase molecules, Nat Chem Biol, 6 (2010) 907-913.
24. W.W. Kallemeijn, K.Y. Li, M.D. Witte, A.R. Marques, J. Aten, S. Scheij, J. Jiang, L.I. Willems, T.M. Voorn-Brouwer, C.P. van Roomen, R. Ottenhoff, R.G. Boot, H. van den Elst, M.T. Walvoort, B.I. Florea, J.D. Codee, G.A. van der Marel, J.M. Aerts, H.S. Overkleeft, Novel activity-based probes for broad-spectrum profiling of retaining beta-exoglucosidases in situ and in vivo, Angew Chem Int Ed Engl, 51 (2012) 12529-12533.
25. C.L. Kuo, E. van Meel, K. Kytidou, W.W. Kallemeijn, M. Witte, H.S. Overkleeft, M.E. Artola, J.M. Aerts, Activity-Based Probes for Glycosidases: Profiling and Other Applications, Methods Enzymol, 598 (2018) 217-235.
26. L.T. Lelieveld, M. Mirzaian, C.L. Kuo, M. Artola, M.J. Ferraz, R.E.A. Peter, H. Akiyama, P. Greimel, R. van den Berg, H.S. Overkleeft, R.G. Boot, A.H. Meijer, J. Aerts, Role of beta-glucosidase 2 in aberrant glycosphingolipid metabolism: model of glucocerebrosidase deficiency in zebrafish, J Lipid Res, 60 (2019) 1851-1867.
27. T. Ohashi, C.M. Hong, S. Weiler, J.M. Tomich, J.M. Aerts, J.M. Tager, J.A. Barranger, Characterization of human glucocerebrosidase from different mutant alleles, J Biol Chem, 266 (1991) 3661-3667.
28. M.J. Ferraz, W.W. Kallemeijn, M. Mirzaian, D. Herrera Moro, A. Marques, P. Wisse, R.G. Boot, L.I. Willems, H.S. Overkleeft, J.M. Aerts, Gaucher disease and Fabry disease: new markers and insights in pathophysiology for two distinct glycosphingolipidoses, Biochim Biophys Acta, 1841 (2014) 811-825.
29. M. Langeveld, J.M. Aerts, Glycosphingolipids and insulin resistance, Prog Lipid Res, 48 (2009) 196-205.
30. N. Dekker, L. van Dussen, C.E. Hollak, H. Overkleeft, S. Scheij, K. Ghauharali, M.J. van Breemen, M.J. Ferraz, J.E. Groener, M. Maas, F.A. Wijburg, D. Speijer, A. Tylki-Szymanska, P.K. Mistry, R.G. Boot, J.M. Aerts, Elevated plasma glucosylsphingosine in Gaucher disease: relation to phenotype, storage cell markers, and therapeutic response, Blood, 118 (2011) e118-127.
31. M.J. Ferraz, A.R. Marques, M.D. Appelman, M. Verhoek, A. Strijland, M. Mirzaian, S. Scheij, C.M. Ouairy, D. Lahav, P. Wisse, H.S. Overkleeft, R.G. Boot, J.M. Aerts, Lysosomal glycosphingolipid catabolism by acid ceramidase: formation of glycosphingoid bases during deficiency of glycosidases, FEBS Lett, 590 (2016) 716-725.
32. P.K. Mistry, J. Liu, L. Sun, W.L. Chuang, T. Yuen, R. Yang, P. Lu, K. Zhang, J. Li, J. Keutzer, A. Stachnik, A. Mennone, J.L. Boyer, D. Jain, R.O. Brady, M.I. New, M. Zaidi, Glucocerebrosidase 2 gene deletion rescues type 1 Gaucher disease, Proc Natl Acad Sci U S A, 111 (2014) 4934-4939.
33. M.K. Pandey, G.A. Grabowski, J. Kohl, An unexpected player in Gaucher disease: The multiple roles of complement in disease development, Semin Immunol, 37 (2018) 30-42.
34. S. Nair, A.R. Branagan, J. Liu, C.S. Boddupalli, P.K. Mistry, M.V. Dhodapkar, Clonal Immunoglobulin against Lysolipids in the Origin of Myeloma, N Engl J Med, 374 (2016) 555-561.
35. E. Sidransky, M.A. Nalls, J.O. Aasly, J. Aharon-Peretz, G. Annesi, E.R. Barbosa, A. Bar-Shira, D. Berg, J. Bras, A. Brice, C.M. Chen, L.N. Clark, C. Condroyer, E.V. De Marco, A. Durr, M.J. Eblan, S. Fahn, M.J. Farrer, H.C. Fung, Z. Gan-Or, T. Gasser, R. Gershoni-Baruch, N. Giladi, A. Griffith, T. Gurevich, C. Januario, P. Kropp, A.E. Lang, G.J. Lee-Chen, S. Lesage, K. Marder, I.F. Mata, A. Mirelman, J. Mitsui, I. Mizuta, G. Nicoletti, C. Oliveira, R. Ottman, A. Orr-Urtreger, L.V. Pereira, A. Quattrone, E. Rogaeva, A. Rolfs, H. Rosenbaum, R. Rozenberg, A. Samii, T. Samaddar, C. Schulte, M. Sharma, A. Singleton, M. Spitz, E.K. Tan, N. Tayebi, T. Toda, A.R. Troiano, S. Tsuji, M. Wittstock, T.G. Wolfsberg, Y.R. Wu, C.P. Zabetian, Y. Zhao, S.G. Ziegler, Multicenter analysis of glucocerebrosidase mutations in Parkinson's disease, N Engl J Med, 361 (2009) 1651-1661.
36. Y.V. Taguchi, J. Liu, J. Ruan, J. Pacheco, X. Zhang, J. Abbasi, J. Keutzer, P.K. Mistry, S.S. Chandra, Glucosylsphingosine Promotes alpha-Synuclein Pathology in Mutant GBA-Associated Parkinson's Disease, J Neurosci, 37 (2017) 9617-9631.
37. H. Akiyama, S. Kobayashi, Y. Hirabayashi, K. Murakami-Murofushi, Cholesterol glucosylation is catalyzed by transglucosylation reaction of beta-glucosidase 1, Biochem Biophys Res Commun, 441 (2013) 838-843.
38. A.R. Marques, M. Mirzaian, H. Akiyama, P. Wisse, M.J. Ferraz, P. Gaspar, K. Ghauharali-van der Vlugt, R. Meijer, P. Giraldo, P. Alfonso, P. Irun, M. Dahl, S. Karlsson, E.V. Pavlova, T.M. Cox, S. Scheij, M. Verhoek, R. Ottenhoff, C.P. van Roomen, N.S. Pannu, M. van Eijk, N. Dekker, R.G. Boot, H.S. Overkleeft, E. Blommaart, Y. Hirabayashi, J.M. Aerts, Glucosylated cholesterol in mammalian cells and tissues: formation and degradation by multiple cellular beta-glucosidases, J Lipid Res, 57 (2016) 451-463.
39. S. Van Weely, M.B. Van Leeuwen, I.D. Jansen, M.A. De Bruijn, E.M. Brouwer-Kelder, A.W. Schram, M.C. Sa

Miranda, J.A. Barranger, E.M. Petersen, J. Goldblatt, et al., Clinical phenotype of Gaucher disease in relation to properties of mutant glucocerebrosidase in cultured fibroblasts, Biochim Biophys Acta, 1096 (1991) 301-311.
40. J.M. Aerts, W.E. Donker-Koopman, M.K. van der Vliet, L.M. Jonsson, E.I. Ginns, G.J. Murray, J.A. Barranger, J.M. Tager, A.W. Schram, The occurrence of two immunologically distinguishable beta-glucocerebrosidases in human spleen, Eur J Biochem, 150 (1985) 565-574.
41. R. Willemsen, J.M. van Dongen, J.M. Aerts, A.W. Schram, J.M. Tager, R. Goudsmit, A.J. Reuser, An immunoelectron microscopic study of glucocerebrosidase in type 1 Gaucher's disease spleen, Ultrastruct Pathol, 12 (1988) 471-478.
42. E. van Meel, E. Bos, M.J.C. van der Lienden, H.S. Overkleeft, S.I. van Kasteren, A.J. Koster, J. Aerts, Localization of active endogenous and exogenous beta-glucocerebrosidase by correlative light-electron microscopy in human fibroblasts, Traffic, 20 (2019) 346-356.
43. J. van Smeden, I.M. Dijkhoff, R.W.J. Helder, H. Al-Khakany, D.E.C. Boer, A. Schreuder, W.W. Kallemeijn, S. Absalah, H.S. Overkleeft, J. Aerts, J.A. Bouwstra, In situ visualization of glucocerebrosidase in human skin tissue: zymography versus activity-based probe labeling, J Lipid Res, 58 (2017) 2299-2309.
44. H. Gold, M. Mirzaian, N. Dekker, M. Joao Ferraz, J. Lugtenburg, J.D. Codee, G.A. van der Marel, H.S. Overkleeft, G.E. Linthorst, J.E. Groener, J.M. Aerts, B.J. Poorthuis, Quantification of globotriaosylsphingosine in plasma and urine of fabry patients by stable isotope ultraperformance liquid chromatography-tandem mass spectrometry, Clin Chem, 59 (2013) 547-556.
45. M. Mirzaian, P. Wisse, M.J. Ferraz, A.R.A. Marques, P. Gaspar, S.V. Oussoren, K. Kytidou, J.D.C. Codee, G. van der Marel, H.S. Overkleeft, J.M. Aerts, Simultaneous quantitation of sphingoid bases by UPLC-ESI-MS/MS with identical (13)C-encoded internal standards, Clin Chim Acta, 466 (2017) 178-184.
46. R.O. Brady, Enzyme replacement therapy: conception, chaos and culmination, Philos Trans R Soc Lond B Biol Sci, 358 (2003) 915-919.
47. F.M. Platt, M. Jeyakumar, U. Andersson, D.A. Priestman, R.A. Dwek, T.D. Butters, T.M. Cox, R.H. Lachmann, C. Hollak, J.M. Aerts, S. Van Weely, M. Hrebicek, C. Moyses, I. Gow, D. Elstein, A. Zimran, Inhibition of substrate synthesis as a strategy for glycolipid lysosomal storage disease therapy, J Inherit Metab Dis, 24 (2001) 275-290.
48. P.K. Mistry, M. Balwani, H.N. Baris, H.B. Turkia, T.A. Burrow, J. Charrow, G.F. Cox, S. Danda, M. Dragosky, G. Drelichman, A. El-Beshlawy, C. Fraga, S. Freisens, S. Gaemers, E. Hadjiev, P.S. Kishnani, E. Lukina, P. Maison-Blanche, A.M. Martins, G. Pastores, M. Petakov, M.J. Peterschmitt, H. Rosenbaum, B. Rosenbloom, L.H. Underhill, T.M. Cox, Safety, efficacy, and authorization of eliglustat as a first-line therapy in Gaucher disease type 1, Blood Cells Mol Dis, 71 (2018) 71-74.
49. A. Narita, K. Shirai, S. Itamura, A. Matsuda, A. Ishihara, K. Matsushita, C. Fukuda, N. Kubota, R. Takayama, H. Shigematsu, A. Hayashi, T. Kumada, K. Yuge, Y. Watanabe, S. Kosugi, H. Nishida, Y. Kimura, Y. Endo, K. Higaki, E. Nanba, Y. Nishimura, A. Tamasaki, M. Togawa, Y. Saito, Y. Maegaki, K. Ohno, Y. Suzuki, Ambroxol chaperone therapy for neuronopathic Gaucher disease: A pilot study, Ann Clin Transl Neurol, 3 (2016) 200-215.
50. C.K. Fog, P. Zago, E. Malini, L.M. Solanko, P. Peruzzo, C. Bornaes, R. Magnoni, A. Mehmedbasic, N.H.T. Petersen, B. Bembi, J. Aerts, A. Dardis, T. Kirkegaard, The heat shock protein amplifier arimoclomol improves refolding, maturation and lysosomal activity of glucocerebrosidase, EBioMedicine, 38 (2018) 142-153.

Chapter 2

Glucocerebrosidase: Functions in and beyond the lysosome

Glucocerebrosidase: Functions in and beyond the lysosome

D.E.C. Boer, J. van Smeden, J.A. Bouwstra, J.M.F.G Aerts.

Abstract

Glucocerebrosidase (GCase) is a retaining β-glucosidase with acid pH optimum metabolizing the glycosphingolipid glucosylceramide (GlcCer) to ceramide and glucose. Inherited deficiency of GCase causes the lysosomal storage disorder named Gaucher disease (GD). In GCase-deficient GD patients the accumulation of GlcCer in lysosomes of tissue macrophages is prominent. Based on the above, the key function of GCase as lysosomal hydrolase is well recognized, however it has become apparent that GCase fulfills in the human body at least one other key function beyond lysosomes. Crucially, GCase generates ceramides from GlcCer molecules in the outer part of the skin, an essential process for optimal skin barrier properties compatible with terrestrial life. This review covers the functions of GCase in and beyond lysosomes and also pays attention to the increasing insight in hitherto unexpected catalytic versatility of the enzyme.

Introduction

The cellular acid β-glucosidase (E.C.3.2.1.45) was firstly reported to be located in lysosomes already more than fifty years ago [1]. There it degrades the glycosphingolipid glucosylceramide (GlcCer), a.k.a. glucocerebroside (Figure 1A) [2]. The enzyme, commonly named glucocerebrosidase (GCase), is active towards GlcCer molecules with different fatty acyl moieties. Deficiency of GCase causes the recessively inherited disorder Gaucher disease (GD, OMIM #230800, ORPHA355), named after the French dermatologist Ernest Gaucher who published the first case report [3]. A hallmark of GD are lipid-laden macrophages with lysosomal GlcCer deposits, referred to as Gaucher cells [4]. Numerous mutations in the *GBA* gene encoding GCase have been associated with GD [5]. The genetic heterogeneity contributes to the highly

variable clinical manifestation of the disorder that may involve various organs and tissues [4]. A complete absence of GCase activity is incompatible with terrestrial life due to a disturbed skin barrier [6, 7]. The lethal impairment stems from the crucial extracellular role of GCase in the stratum corneum (SC). This review covers the functions of GCase in metabolism of GlcCer inside lysosomes and beyond.

Part I: GCase and lysosomal glucosylceramide degradation

Glucosylceramide as intermediate of glycosphingolipids.

The primary physiological substrate of GCase is GlcCer, the simplest glycosphingolipid (GSL) in which a single glucose β-glucosidic is linked to the 1-hydroxy of ceramide (Cer) [8]. Figure 2 present an overview of the GSL metabolism. *De novo* formation of Cer starts on the endoplasmic reticulum (ER) with formation of 3-keto-dihydrosphingosine by the enzyme serine palmitoyl transferase (SPT) that conjugates the amino acid serine with a palmitoyl chain [9-12]. Next, the enzyme 3-ketosphinganine reductase (KSR) converts 3-keto-hydrosphingosine to dihydrosphingosine (sphinganine). Ceramide synthases (CERS) are responsible for acylation of dihydrosphingosine, thus generating diverse dihydroceramides [13-15]. In mammals six distinct CERS enzymes with different fatty acyl-CoA affinities have been identified. Subsequently, dihydroceramide desaturase (DES) catalyzes the conversion of dihydroceramides into ceramides [15]. Ceramide is alternatively formed in the salvage pathway by acylation of sphingosine molecules released from lysosomes [16, 17]. Cer can be further metabolized by conjugation of its 1-hydroxy, resulting in very diverse structures like ceramide 1-phosphate (C1P), sphingomyelin (SM), 1-O-acylceramide, galactosylceramide (GalCer) and GlcCer (reviewed in ref [18]). Formation of GlcCer, the key GSL of this review, involves transfer of Cer to the cytosolic surface of the Golgi apparatus where the membrane bound glucosylceramide synthase (GCS) generates GlcCer using UDP-glucose as sugar donor and Cer as acceptor [19, 20]. Next, some of the newly formed GlcCer molecules are converted back to Cer by the cytosol facing β-glucosidase GBA2 [21], but most reach via an unknown mechanism the luminal membrane of the Golgi apparatus. There, conversion to more complex GSLs like gangliosides and globosides occurs through stepwise addition of additional sugar and sulfate moieties (the biosynthesis and vast structural heterogeneity of GSL is excellently reviewed in refs [13] and [22]).

The major destination of newly formed GSLs is the outer leaflet of the plasma membrane. At the cell surface, GSLs fulfill a variety of important functions. GSLs interact with cholesterol molecules via hydrogen bonds and hydrophobic van der Waal's forces and spontaneously form semi-ordered lipid microdomains, commonly referred to as lipid rafts [23, 24]. Hydrophilic cis-interactions

among GSL headgroups promote lateral associations with surrounding lipid and proteins. Residing in the GSL-enriched domains are proteins involved in interactions of cells with the exterior (extracellular space and other cells) and mediating the associated intracellular signaling processes [24-26]. The GSL composition of lipid rafts may exert modulating effects in the cell's response to triggers. One example in this respect is the insulin receptor whose signaling is negatively influenced by neighboring gangliosides such as GM3 in lipid rafts [27-29]. Pharmacological reduction of GSLs results in improved glucose homeostasis in obese insulin-resistant rodents [30]. Similarly, the epidermal growth factor (EGF) receptor is influenced by the GSL composition of microdomains in which it resides [31]. GSLs at the cell surface also play direct roles in adhesion/recognition processes. For example, specific GSLs are involved in binding of pathogenic viruses, microorganisms and bacterial toxins [32-34]. The topic has been recently reviewed 34. Glycosphingolipid-enriched lipid rafts essentially contribute to immunological functions as for example activation of T cells [35-38].

Lysosomal turnover of glycosphingolipid.

GSLs leave cells from the plasma membrane through incorporation in high density-lipoproteins [39, 40]. However, most of the GSLs are internalized from the plasma membrane via endocytosis, involving multi-vesicular bodies within late endosomes. Upon the delivery of internalized membranes to lysosomes, fragmentation of GSL components takes place by step-wise removal of terminal sugars by specialized glycosidases assisted by corresponding accessory proteins such as saposins A-D and GM2 activator protein (reviewed in ref [41]). Exogenous GSLs, such as constituents of lipoproteins or components of phagocytosed apoptotic cells, also reach lysosomes by endocytic processes. The final lipid product of lysosomal fragmentation of GSLs, GalCer and SM is in all cases Cer [41]. The lysosomal acid ceramidase (EC 3.5.1.23) subsequently splits Cer into free fatty acid and sphingosine to be exported to the cytosol [42]. Next, cytosolic sphingosine can be used to form again Cer or alternatively it is converted by sphingosine kinases (SK1 and SK2) to sphingosine-1-phosphate (S1P) [43].

Glucocerebrosidase

GCase protein and life cycle.

The penultimate step in GSL degradation is the deglucosylation of GlcCer yielding glucose and Cer. This reaction is catalyzed by GCase, a 495 amino acid glycoprotein with four N-linked glycans [2, 44]. GCase, based on its structural features, is classified in the glycoside hydrolase family GH30 (formerly in the related family GH5 [45]. The 3D-structure of GCase has been resolved by

crystallography [46, 47]. GCase, like other GH5 and GH30 glycosidases, has an (α/β)8 TIM barrel catalytic domain. In the case of GCase this is fused with a β-structure consisting of an immunoglobulin-like fold [45]. GCase is a retaining β-glucosidase hydrolyzing a glucosidic substrate with net retention of glucose stereochemistry (Figure 1 B). Retaining beta-glucosidases generally use a two-step catalytic mechanism. The Koshland double displacement mechanism involves a catalytic nucleophile and acid/base residue [48]. A nucleophilic attack to the anomeric carbon of the glycosidic substrate is the first step. The aglycon is released assisted by a proton transfer from the acid/base residue and a covalent enzyme-glycoside complex is formed. Next, an activated water molecule deglycosylates the nucleophile, allowing a new round catalysis. The reaction involves two transient oxocarbenium ion-like states and the sugar substrate adopts different itineraries depending on its pyranose ring configuration [49]. In the case of retaining β-glucosidases like GCase, the substrate itinerary is $^{1}S_{3}$ -> $^{4}H_{3}$ -> $^{4}C_{1}$ -> $^{4}H_{3}$ -> $^{4}C_{1}$ for the Michaelis complex -> transition state -> covalent intermediate -> transition state -> product [[50, 51]. In the $(\alpha/\beta)_{8}$ TIM barrel catalytic domain of GCase, E340 acts as nucleophile and E235 as acid/base residue [52, 53].

Cyclophellitol, present in the mushroom *Phellinus sp.*, is a potent irreversible inhibitor that binds covalently, in mechanism-based manner, to the nucleophile E340 of GCase [52-54]. The structurally related compounds cyclophellitol aziridine and conduritol B-epoxide inactivate GCase via the same mechanism [52, 55]. Recently, superior suicide inhibitors for GCase have been designed [56]. Cyclophellitol derivatives carrying a large hydrophobic substituent at C8 inactivate GCase with even higher affinity and with great specificity (not reacting with another retaining β-glucosidase like GBA2 and GBA3) [56, 57]. Using cyclophellitol as scaffold, selective activity-based probes (ABPs) toward GCase were designed [52]. A reporter group (biotin or BODIPY) was attached to the C8 of cyclophellitol via a pentyl linker rendering ABPs allowing ultrasensitive and specific visualization of GCase *in vitro* and *in vivo* [58]. Subsequently, cyclophellitol aziridine ABPs with attached reporter groups via alkyl or acyl linkers were designed reacting with multiple retaining glycosidases in the same class [55, 59]. Cyclophellitol aziridine ABPs labeling α-galactosidases, α-glucosidases, α-fucosidase, α-iduronidase, β-galactosidases, and β-glucuronidase as well as cyclophellitol ABPs labelling galactocerebrosidase have been designed [60-65]. Applications of ABPs are the quantitative detection and localization of glycosidases in cells and tissues, as well as identification and characterization of glycosidase inhibitors by competitive ABP profiling [66, 67].

GCase shows an acid pH optimum of hydrolytic activity, coinciding with the lysosomal pH [44]. The activity of the enzyme towards GlcCer is promoted by negatively charged lipids and saposin C, an activator protein generated in the

lysosome by proteolytic processing of prosaposin [41, 68]. The half-life of GCase in lysosomes is relatively short due to proteolytic degradation by cathepsins as suggested by the protective effect of leupeptin [69, 70]. It has been noted that unfolding and degradation of GCase is protected by occupation of the catalytic pocket [69].

GCase fundamentally differs from other lysosomal hydrolases in the mechanism underlying sorting and transport to lysosomes [44]. Whilst most soluble lysosomal hydrolases are transported to lysosomes by mannose-6-phosphate receptors, this is not the case for GCase. In the inherited disorders mucolipidoses II and III where formation of mannose-6-phosphate recognition signal in N-glycans of lysosomal hydrolases is impaired and consequently these enzymes are largely secreted, the transport of GCase to lysosomes is normal. In fact, in cultured skin fibroblasts the four N-glycans of GCase do not acquire mannose-6-phosphate [71]. Following correct folding of newly formed GCase molecules in the ER, these bind to the membrane protein LIMP2 (lysosomal membrane protein 2) [72-74]. This binding involves is mediated by hydrophobic helical interfaces on both proteins [75]. Action myoclonus renal failure syndrome (AMRF) is a recessively inherited disease caused by mutations in LIMP2 [76]. In most cell types of AMRF patients except for phagocytic cells, GCase is markedly reduced due to faulty transport to lysosomes [76, 77]. More recently, progranulin (PGRN) has been identified as another factor influencing GCase [78, 79]. PGRN is thought to function as a chaperone facilitating the transport of GCase to lysosomes. It recruits heat shock protein 70 (HSP70) to the GCase/LIMP2 complex in the ER and thus promotes delivery of GCase to lysosomes [80]. Another protein found to interact with newly formed GCase in the ER is ERdj3 [81].

Catalytic activity of GCase.

The primary substrate of GCase is GlcCer, as is reflected by the prominent accumulation of this lipid during GCase deficiency [82-84]. However, it recently has become apparent that catalytic versatility of the enzymes needs consideration. Firstly, GCase has been found able to hydrolyze artificial β-xylosides [20]. Secondly, several retaining β-glycosidases are reported to be able to transglycosylate when provided with a suitable aglycon acceptor (Figure 1B) [85]. Such catalytic activity has also been observed for GCase, the enzyme being able to generate glucosylated cholesterol (GlcChol) by transglucosylation [86-88]. This reaction occurs during cholesterol accumulation in lysosomes as occurs in Niemann Pick disease type C (NPC) [86]. Massive accumulation of GlcChol in liver of NPC mice has been demonstrated. Inducing lysosomal cholesterol accumulation in cultured cells by their exposure to U1986663A is accompanied by formation of GlcChol [86]. Of note, under normal conditions GlcChol is primarily degraded by GCase into glucose and cholesterol. It may be

envisioned that further research will reveal that there exist more β-glucosidic metabolites being substrates (and products) of GCase.

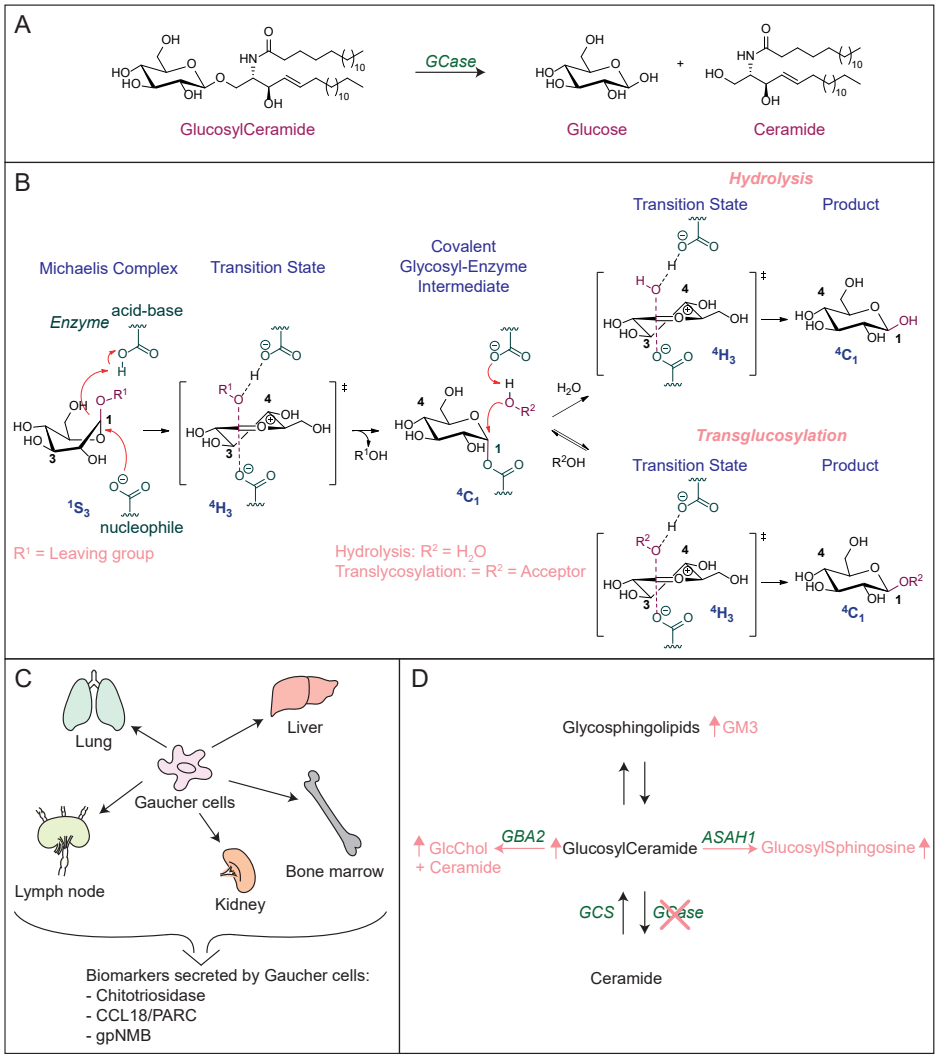

Figure 1: A. Structure of GlucosylCeramide (GlcCer) and degradation by GCase to glucose and ceramide. B. Catalytic activity GCase: Hydrolyzation of β-glucosides and transglucosylation activity. C. Occurrence of Gaucher cells and the biomarkers they secrete in plasma. D. Metabolic adaptations to GCase deficiency: increase of GlcCer as a result of lack of degradation by GCase. Accumulated GlcCer is converted by ASAH1 to glucosylsphingosine, Glucosylated cholesterol (GlcChol) formed by GBA2 increases and GM3 levels rise because increased anabolism by glycosyltransferases to complex GSLs. Enzymes are depicted in green. ASAH1: acid ceramidase, GBA2: cytosolic β-glucosidase, GCase: β-glucocerebrosidase, GCS: glucosylceramide synthase.

Gaucher disease, inherited deficiency in GCase

Gaucher disease, a lysosomal storage disorder.

Since degradation of GSLs is catalyzed by lysosomal glycosidases, inherited deficiencies in these enzymes cause lysosomal accumulation of their GSL substrates, so-called glycosphingolipidoses [9, 41, 89-91]. Examples of such disorders are Gaucher disease, Krabbe disease, GM2-gangliosidosis, Sandhoff disease, and GM1-gangliosidosis. The glycosphingolipidoses are clinically diverse and generally show marked heterogeneity in severity of disease that usually involves neuropathy in more severely affected patients.

Gaucher disease is a prototype glycosphingolipidosis. The first case report was published in 1882 by Ernest Gaucher concerning a female patient with unexplained massive splenomegaly without leukemia [3]. Soon it was recognized that this patient represented a distinct disease entity that was subsequently referred to as Gaucher's disease or Gaucher disease (GD). Following the demonstration of abnormal accumulation of GlcCer in GD patients as the result of deficient GCase activity, the *GBA* gene encoding the acid β-glucosidase was cloned and characterized [4]. The *GBA* gene is located at locus 1q21 and neighbored by a pseudogene [92]. Numerous mutations in *GBA* have now been associated with GD. The consequences of mutations at the level of the GCase protein may markedly differ. For example, the common N370S GCase mutation among Caucasians results in near normal production of a mutant enzyme with aberrant catalytic properties [93]. The heteroallelic presence of this mutation protects against a neuronopathic disease course [4, 44, 94]. This *GBA* mutation occurs relatively frequent among Ashkenazim and has been proposed to have offered some advantage against an infectious disease, for example bubonic plaque or tuberculosis [95-99]. In contrast, another common pan-ethnic mutation encoding L444P GCase, results in a mutant enzyme that largely misfolds in the ER and consequently only a small fraction (<10% of normal) reaches lysosomes. Homozygosity for the L444P mutation is always associated with a severe neuronopathic disease manifestation [4]. The L444P mutation is thought to have arisen repeatedly by homologous recombination of the *GBA* gene with its pseudogene.

The genetic heterogeneity of GD is accompanied by clinical heterogeneity of the disorder. Common symptoms manifesting in GD patients are hepatosplenomegaly, hematological abnormalities like anemia and thrombocytopenia, skeletal disease and neuropathology. A very severe manifestation (referred to as collodion baby) involves lethal skin barrier dysfunction [4]. Discrete phenotypic variants of GD are historically discerned: type 1, the non-neuronopathic variant; type 2, the acute neuronopathic variant; type 3, the subacute neuronopathic variant and the collodion baby or neonatal variant. It has been proposed to no longer adhere to this classification, but rather view GD as a continuum of phenotypes [99]. Marked

intraindividual variation occurs in type 1 GD patients in the nature and degree of organ involvement and particular symptoms such as skeletal disease [4].

The correlation of *GBA* genotype with GD phenotype is limited in some aspects. While the presence of N370S GCase protects GD patients against neuropathology, there are several reports of monozygotic GD twins with discordant severity of visceral disease [100, 101]. A very specific clinical course is associated with the presence of D409H GCase involving yet unexplained cardiac symptoms, including aortic valve, mitral valve, and ascending aorta calcifications [102-104].

Modifier genes, and possibly epigenetics and external factors, are considered to impact on the clinical manifestation of GCase deficiency. The transmembrane protein CLN8 (ceroid-lipofuscinosis, neuronal 8), recycling between the ER and Golgi apparatus, is a putative modifier [105] CLN8, identified as putative modifier of GD in a genome-wide association study, has recently been reported to be involved in the transport of newly formed lysosomal enzymes between ER and Golgi [106]. Other proteins are known to directly influence the life cycle and activity of GCase. Saposin C is the lysosomal activator protein of GCase and patients with a defective saposin C develop symptoms similar to GD patients [68]. LIMP2, encoded by the SCARB2 (scavenger receptor class B, 2) gene, transporting GCase to lysosomes has been reported to be a GD modifier [107]. Polymorphisms in the UGCG gene coding for GCS catalyzing synthesis of GlcCer have also been proposed as GD modifiers [108]. Recently, microRNAs up- or down-regulating GCase and down-regulating LIMP2 have been reported [109].

It has recently been appreciated that carrying a mutant *GBA* gene is not without health risk. Carriers of GD have a yet unexplained significantly increased (20-fold) risk for developing Parkinson disease (PD) and Lewy body dementia (LBD) [110-112]. A recent study in the United Kingdom revealed that 5% to 25% of patients with PD carry glucocerebrosidase gene mutations, and 10% to 30% of glucocerebrosidase carriers will develop PD by age 80 [113]. Of note, active GCase activity is also decreased, and corresponding glycosphingolipid substrate levels elevated, in the brain in PD without *GBA* mutations [114, 115]. Abnormalities in multiple enzymes and other proteins involved in sphingolipid metabolism have been observed in association with PD [114, 116, 117]. With increasing age, the brain of mice shows reduced GCase levels and increased amounts of lipid substrate [115]. PD is historically viewed as a "proteinopathy" with cellular protein aggregates like that of α-synuclein (αSyn). It has more recently been hypothesized that sphingolipid abnormalities may be primary disturbances which can produce protein aggregation [114]. Indeed, inactivation of GCase promotes accumulation of αSyn aggregates [118]. It has been observed that insoluble alpha-synuclein positive aggregates in sporadic PD midbrain linearly correlate with loss of GCase activity [119].

Likewise, protein aggregates develop in mice with primary *GBA* mutations [120]. Supplementation of GCase or reduction of accumulating glycolipids prevents and reverses α-synucleinopathy [121, 122]. It has been furthermore observed that over-expression of aggregating αSyn causes a reduction of GCase, suggesting a potential harmful interaction between the two proteins in a self-amplifying manner [123-125]. *In vitro* experiments showed that GCase and aSyn may directly interact at lysosomal pH [126]. Different explanations have been proposed for ways by which mutant GCase may induce α-synucleinopathy (reviewed in refs [125, 127, 128]). For example, it has been hypothesized that the accumulation of substrates of GCase is pathogenic; that GCase deficiency causes inhibition of autophagy and lysosomal degradative capacity and subsequently reduces turnover of αSyn; that increased αSyn levels impair the activity of GCase and vice versa; and, that GCase deficiency impairs mitochondria. Contrarily, it has been proposed that mutant GCase protein may be toxic by inducing an excessive unfolded protein response in the ER or saturating the ubiquitin–proteasome pathway [129, 130]. It is conceivable that multiple mechanisms may be involved in the GCase-PD pathology.

Lysosomal GlcCer deposits in macrophages: Gaucher cells.

The storage of GlcCer in GD patients occurs almost exclusively in macrophages residing in the spleen, liver, bone marrow, lymph nodes and lung (Figure 1C) [131]. The lipid-laden Gaucher cells are viable, alternatively activated macrophages [132]. These cells overproduce and secrete specific proteins resulting in massively elevated plasma levels in symptomatic GD patients. These proteins are now used as biomarkers of body burden of Gaucher cells. The first identified plasma biomarker is the chitinase named chitotriosidase encoded by the CHIT1 gene [133, 134]. It can be conveniently detected by the measurement of its activity towards 4-methylumbelliferyl-chitotrioside [133] and the superior substrate 4-metylumbelliferyl-4'-deoxy-chitobioside [135, 136]. Plasma chitotriosidase is on average about 1000-fold elevated in type 1 GD patients. Immunohistochemistry and *in situ* hybridization revealed that the enzyme is produced by Gaucher cells. Common is a 24 base pair duplication in the CHIT1 gene that excludes synthesis of active chitinase [137]. The chemokine CCL18/PARC (Chemokine (C-C motif) ligand 18; Pulmonary and activation-regulated chemokine) serves as an alternative plasma marker of Gaucher cells, being 20 to 50-fold elevated plasma of type 1 GD patients [138, 139]. The chemokine is over-produced and secreted by Gaucher cells [139]. More recently the glycoprotein nonmetastatic melanoma protein B (gpNMB) has been found to be overproduced by Gaucher cells [140]. A soluble fragment of gpNMB is released into plasma and is over 50-fold elevated in type 1 GD patients [140, 141]. In cerebral spine fluid and brain of type 3 GD patients elevated gpNMB levels have also been observed [142]. Likewise,

recently an increased level of gpNMB in the substantia nigra of PD patients has been reported [143]. In mice with conditional deficiency in GCase in the white blood cell lineage Gaucher-like cells are formed. These do not produce chitotriosidase or CCL18, but gpNMB does [140, 144]. Inactivation of GCase with an irreversible inhibitor was found to increase gpNMB in the brain [143]. Interestingly, zebrafish and fruit flies overproduce a chitinase during GCase deficiency [130, 145].

There is compelling evidence for a direct role of Gaucher cells in GD pathology. Their presence in spleen, liver and bone marrow is associated with splenomegaly, hepatomegaly and hematological abnormalities, respectively [4]. The same holds for these symptoms in GD mice with induced GCase deficiency in white blood cells [144]. In GD spleens the storage lesions contain a core of mature Gaucher cells surrounded by pro-inflammatory macrophages [132]. These lesions likely contribute to the complex cytokine, chemokine and protease abnormalities in GD patients [91, 146, 147]. Type 1 GD patients, show low-grade inflammation and activation of both coagulation and the complement cascade [148, 149]. Of note, many of the visceral symptoms of type 1 Gaucher disease patients resemble those of Niemann Pick type A and B patients suffering from lysosomal acid sphingomyelinase (ASMase) deficiency causing lysosomal sphingomyelin storage [42]. In both disorders, lipid storage in visceral macrophages is a hallmark. In sharp contrast, whilst GCase is markedly reduced in most cell types of LIMP2-deficient AMRF patients, their symptoms differ from those of type 1 Gaucher patients. Likely this is due to the fact that macrophages of AMRF patients contain a high residual GCase and consequently no lipid-laden macrophages are formed [77].

Therapies of Gaucher disease: ERT, SRT, PCT/EET.

The prominence of lipid-laden macrophages in GD and their relationship to pathology has prompted the design of rational therapies aiming to prevent and/or correct the lipid-laden macrophages. The first effective treatment designed for type 1 GD is enzyme replacement therapy (ERT) aiming to supplement patient's macrophages with lacking enzyme by repeated intravenous enzyme infusion [150]. Therapeutic GCase, nowadays recombinant but initially isolated from placenta, has enzymatically modified N-linked glycans with terminal mannose groups to favor uptake via the mannose receptor (or another mannose-binding lectin) at the surface of tissue macrophages. Two-weekly ERT reverses hepatosplenomegaly and hematological abnormalities in type 1 GD patients [67]. In addition, it reduces storage cells in the bone marrow [151]. Present ERT does however not prevent neurological symptoms due to the inability of enzyme to pass the blood brain barrier.

An alternative GD treatment is substrate reduction therapy (SRT) [152-154]. SRT aims to balance synthesis of GlcCer with reduced GCase activity of GD

patients. Oral inhibitors of GCS (Miglustat and Eliglustat) are approved drugs. Eliglustat therapy resembles ERT in efficacy [155]. Brain-permeable inhibitors of GCS are presently designed and tested [156]. The response to treatment of GD patients is primarily monitored by clinical assessments. A retrospective evaluation revealed that reductions in plasma chitotriosidase during ERT correlate with corrections in liver and spleen volumes, improvements in hemoglobin, platelet count and bone marrow composition [157]. Given the observed positive outcome of bone marrow transplantation in type 1 GD patients, genetic modification of hematopoietic stem cells has been, and still is, seriously considered as therapeutic avenue [144].

At present there is still an unmet need for neuronopathic GD. Small compounds are actively studied as potential therapeutic agent in this respect. One envisioned approach is pharmacological chaperone therapy (PCT). Chemical chaperones are small compounds improving folding of mutant GCase in the ER, thus increasing lysosomal enzyme levels. Current studies with ambroxol, a weak inhibitor of GCase indicate impressive reductions in spleen and liver volumes in ambroxol-treated type 1 GD patients as well as clinical improvements in type 3 GD patients [158-160]. Another approach is enzyme enhancement therapy with small compounds (EET). An example of this is arimoclomol, a heat shock protein amplifier, found to improve refolding, maturation and lysosomal activity of GCase in GD fibroblasts and neuronal cells [161].

Metabolic adaptations to lysosomal GCase deficiency

Formation of glucosylsphingosine from accumulating GlcCer.

Important metabolic adaptations occur during GCase deficiency in lysosomes (Figure 1D) [162]. We demonstrated that part of the accumulating GlcCer is actively converted by lysosomal acid ceramidase to glucosylsphingosine (GlcSph) [163]. GlcSph is sometimes also referred to as lyso-GL1 or lyso-GB1. It was earlier observed that GlcSph is increased in the brain and spleen of GD patients [164, 165]. We firstly reported an average 200-fold increased GlcSph level in plasma of symptomatic type 1 GD patients [166]. Urine of GD patients also contains increases GlcSph isoforms [167]. Pharmacological inhibition of GCase in cultured cells and zebrafish embryos causes a rapid increase in GlcSph [168]. The quantitative detection of GlcSph in biological samples was improved by o-phthaldialdehyde (OPA) derivatization and high-performance liquid chromatography [169]. Further improvement was reached by the introduction of LC-MS/MS (liquid chromatography-mass spectrometry) employing an identical (13)C-encoded glucosylsphingosine standard [168]. Measurement of elevated plasma GlcSph is now regularly used in the confirmation of GD

diagnosis.

Excessive GlcSph in GD patients is believed to contribute to various symptoms. GlcSph has been linked to the common reduced bone mineral density (osteopenia) in GD patients by impairing osteoblasts [170]. It is reported to promote α-synuclein aggregation, a hallmark of Parkinson disease [171]. Antigenicity of GlcCer, and possibly GlcSph, is thought to cause the common gammopathies in GD patients gammopathies that can lead to multiple myeloma [172]. The same lipids have been proposed to activate the complement cascade activation and associated local tissue inflammation [173]. GlcSph is hypothesized to diminished cerebral microvascular density in mice based on the observed interference of the lipid with endothelial cytokinesis [174]. Earlier studies have provided evidence that GlcSph promotes lysis of red blood cells, impairs cell fission during cytokinesis, damages specific neurons, interferes with growth, and activates pro-inflammatory phospholipase A2 (see for a review ref [91]). In line with these observations is the occurrence of hemolysis, multinucleated macrophages, neuropathology, growth retardation, and chronic low-grade inflammation in GD patients [4]. Of note, in brain of ageing mice reduction of active GCase in combination with increased glucosylceramide and glucosylsphingosine levels have been observed 116.

The conversion of accumulating GSL in lysosomes to glycosphingoid bases (lyso-lipids) is not unique to Gaucher disease. Comparable acid ceramidase-dependent formation of sphingoid bases occurs in Krabbe disease (galactosylsphingosine), Fabry disease (globotriaosylsphingosine; lysoGb3), GM2-gangliosidosis (lysoGM1) and GM2-gangliosidoses (lysoGM2) [91, 175]. In Niemann Pick disease types A and B, the water soluble lysoSM is formed from accumulating SM [176]. As for GlcSph in GD, toxicity of excessive galactosylsphingosine in Krabbe disease and excessive lysoGb3 in Fabry disease has been proposed [91, 177-182].

Excessive gangliosides.

In GD patients increases of the ganglioside GM3 (monosialodihexosylganglioside) in plasma and spleen have been observed [183]. It is unknown whether this abnormality is caused by increased metabolic shuttling of newly formed GlcCer to gangliosides and/or impaired recycling of gangliosides. Not surprisingly (see section 2.1), the elevated concentrations of GM3 in GD patients are accompanied by insulin insensitivity, without overt hyperglycemia [184].

Increased activity of cytosol-faced GBA2 and GlcChol.

Cells contain besides GCase another retaining β-glucosidase that metabolizes GlcCer. The enzyme GBA2 was discovered during studies with GCase-deficient cells [21]. GBA2 is synthesized as soluble cytosolic protein that

rapidly associates to the cytosolic leaflet membranes with its catalytic pocket inserted in the lipid layer. GBA2 shows prominent transglucosylase capacity and is largely responsible for the (reversible) formation of GlcChol from GlcCer and cholesterol [86]. The *GBA2* gene (locus 1p13) was identified and GBA2-deficient mice have meanwhile been generated [185, 186]. The animals develop normally without overt abnormality, except for incidences of male infertility [185]. GBA2-deficient zebrafish also develop normally [168]. Inhibition of GBA2 in GD and NPC patients treated with N-butyldeoxynojirimycin causes no major complications, whereas on the other hand individuals with spastic paraplegia and cerebellar ataxia have been found to be GBA2 deficient [187-190] The physiological role of the highly conserved GBA2 is still an enigma [191].

Reducing GBA2 activity, genetically or using small compound inhibitors such AMP-DNM, has remarkable beneficial effects in NPC mice, ameliorating neuropathology and prolonging lifespan significantly [52, 53]. A comparable neuro-protective effect of the iminosugar AMP-DNM was also observed in mice with Sandhoff disease, another neuropathic glycosphingolipidosis [54]. Presently zebrafish models are used to study the poorly understood interplay between GCase and GBA2 mediated metabolism of GlcCer [168]. The possible toxic effect of excessive glucosylated metabolites generated by GBA2 during GCase deficiency warrants further investigation.

Part II: GCase and glucosylceramide metabolism beyond the lysosome

GCase: other locations than lysosomes.

As discussed in section 3.1, GCase does not rely on mannose-6-phosphate receptor mediated intracellular sorting and re-uptake after secretion. The intracellular transport of GCase is tightly governed by the membrane protein LIMP2 and secretion of GCase into the extracellular space is normally prevented [77]. Immuno-electron microscopy has revealed that specific organelles are involved in trafficking of GCase-LIMP2 complexes from the Golgi apparatus to lysosomes [192]. The delivery of GCase to other locations than lysosomes warrants consideration and discussion.

Lysosome Related Organelles.

TTo fulfil specific physiological functions several cell types have adapted their endolysosomal apparatus and evolved specialized secretory compartments, the lysosome related organelles (LROs) (for reviews see refs [193, 194]). The LROs are diverse and comprise endothelial cell Weibel-Palade bodies, cytotoxic T cell lytic granules pigment cell melanosomes and platelet dense and alpha granules. Common components of LROs are tetraspanin CD63, and GTPases

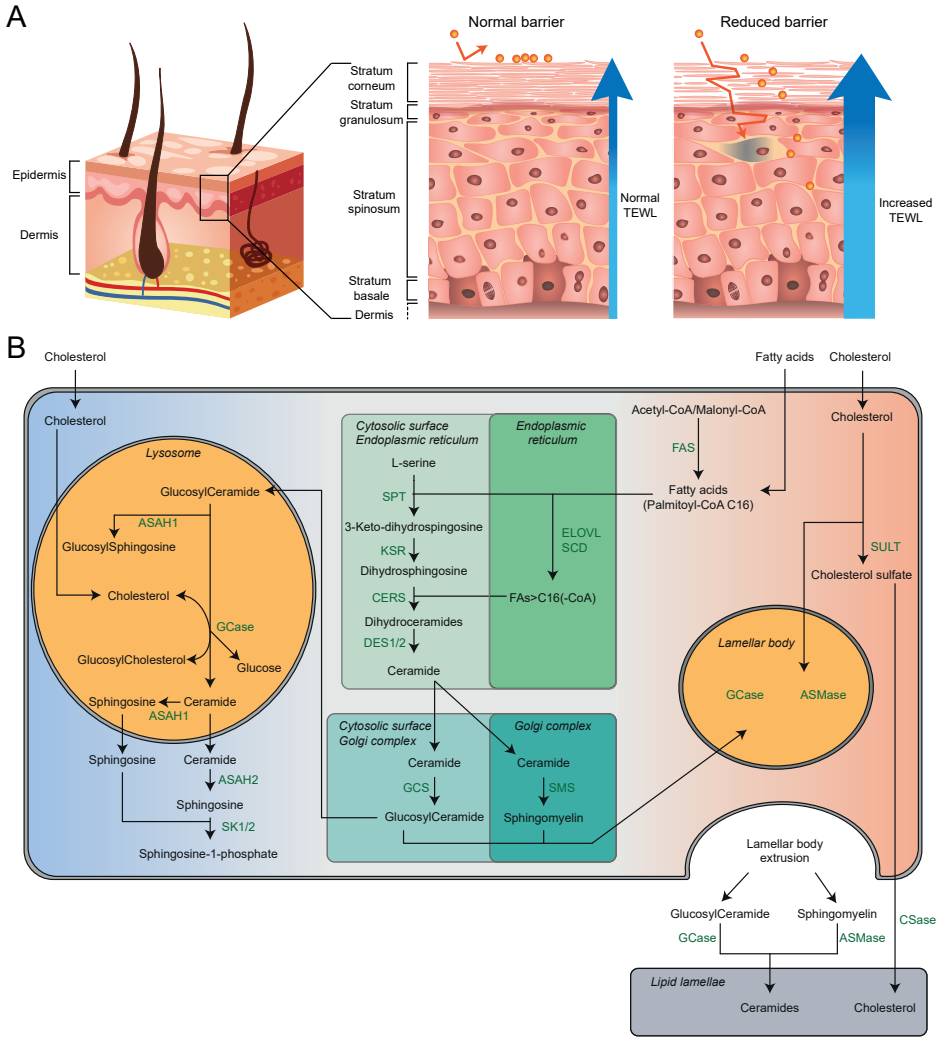

Figure 2: Schematic overview of the human skin and the main processes involved around GCase and its related lipids. A. Schematic overview of a cross section of the skin showing the epidermis, dermis and subcutaneous tissue. The middle illustration shows a more detailed view of the epidermis under healthy conditions. The right illustration depicts a more detailed view of the epidermis with a reduced barrier. Exogenous compounds can get into deeper layers of the epidermis when the barrier is reduced, resulting in an immune response. It also leads to an increased transepidermal water loss (TEWL). B. Schematic overview of the main processes involved around GCase within the cell. Arrows indicate the transport or conversion of lipids, associated enzymes are listed adjacent by their abbreviations. ASAH1: acid ceramidase, ASAH2: neutral ceramidase, ASMase: acid sphingomyelinase, CERS: ceramide synthase family, CSase: cholesterol sulfatase, DES1/2: dihydroceramide desaturase 1 and 2, ELOVL: elongation of very long chain fatty acids family, FAS: fatty acid synthase, GCase: β-glucocerebrosidase, GCS: glucosylceramide synthase, KSR: 3-ketosphinganine reductase, PLA-2: phospholipase, SCD: stearoyl-CoA desaturase, SMS: sphingomyelin synthase, SPT: serine palmitoyltransferase, SULT: cholesterol sulfotransferase type 2 isoform 1b.

RAB27A or RAB27B. The same proteins also occur in multivesicular endosomes (MVEs) that excrete intraluminal vesicles (ILVs) as exosomes upon fusion with the plasma membrane [195]. The notochord vacuole in the zebrafish is also considered to be a LRO [196, 197]. Interestingly, LIMP2, the GCase transporter protein, has been implicated in the formation of this LRO [198].

An established link between GSLs and LROs concerns the pigmented melanosomes in melanocytes. The formation of melanosomes requires GSLs: melanoma cells when deficient in GCS loose pigmentation due to aberrant transport of the enzyme tyrosinase synthesizing melanin [199]. Similarly, cultured melanocytes loose pigmentation when treated with a GCS inhibitor (Smit & Aerts, unpublished observations).

Keratinocytes contain a special kind of LRO, the lamellar body (LB), that justifies more detailed discussion regarding GSLs and their metabolism (see sections 8 and 9). Prior to this, the composition of the mammalian skin is introduced in the section below.

Composition of the Skin

Skin differentiation and barrier formation.

The mammalian skin acts as a key barrier offering protection against xenobiotics and harmful pathogens and preventing excessive water loss from the body (Figure 2A) [200]. The barrier function resides in the epidermis, the outermost part of the skin that consists of four distinct layers: the stratum basale (SB), stratum spinosum (SS), stratum granulosum (SG) and stratum corneum (SC) [201]. The innermost SB, SS and SG are the vital part of the epidermis (thickness: 50–100 μm) whilst the SC is the non-vital differentiation product (thickness: 10–20 μm). The SB contains proliferating keratinocytes that after escape from this single cell layer start to differentiate and migrate towards the SC, where the keratinocytes differentiate to terminal corneocytes. During this differentiation process the keratinocytes flatten, and diminish their water content. During the flattening process cells become filled with keratin. At the interface between the SG and SC, subcellular structures like organelles and nuclei are degraded and corneocytes are formed (as reviewed in ref [202]).

Stratum corneum: hydration and skin-pH.

Proper function and features of the SC are dependent on optimal water content and acidity. The SC hydration level depends on multiple factors such as amino acids, specific sugars and salts, referred to as the natural moisturizing factor (NMF) [203]. Amino acids of NMF are breakdown products of the major SC protein filaggrin. Mutations in the filaggrin gene FLG cause a reduced NMF level associated with dry skin [204, 205]. NMF also plays a key role in

maintenance of pH in the SC. At the outside of the SC the pH is 4.5–5.3 and it gradually increases to pH 6.8 in the inner SC [206]. The local pH likely modulates the activity of various enzymes in the SC, includifng GCase and ASMase with optimal catalytic activity at a more acid pH, and thus also impacts on lipid structures [207].

Stratum corneum: composition.

The SC has a 'brick-and-mortar' like structure, where the corneocytes are the 'bricks' embedded in a lipid matrix that is the 'mortar' of the SC [206, 208]. During the terminal differentiation of corneocytes, plasma membranes develop into the cornified lipid envelope, a lipid-linked crosslinked protein structure [209]. The cornified lipid envelope acts as template for the formation and organization of extracellular lipid lamellae [210, 211]. The lipid matrix contains approximately on a total lipid mass basis 50% ceramides, 25% cholesterol, and 15% free fatty acids with very little phospholipid. The adequate balance of lipid components is essential for proper lipid organization and SC barrier competence [212]. Alterations in the lipid composition have been associated to various skin diseases, particularly to psoriasis, atopic dermatitis and several forms of ichthyosis [213-218].

Sphingolipids of the stratum corneum

Role of lamellar bodies.

Keratinocytes have a specific ovoid shaped LROs with a diameter of about 200 nm are called lamellar body (LB), or alternatively lamellar granule, membrane-coating granule, cementsome, or Odland body [219]. LBs have a bounding membrane surrounding lipid disks. The main lipids packed in LBs are precursors of ceramides and fatty acids constituting the lamellar matrix in the SC. In the uppermost granular cells, the bounding membrane of the LB fuses into the cell plasma membrane, and the lipid disks are extruded into the intercellular space between the SC and SG. The initially extruded content of the LB is largely metabolized to ceramides and fatty acids and rearranged to form together with cholesterol the intercellular lamellae of the SC.

Keratinocytes serve as initial factory of the permeability barrier of the skin [219]. Briefly, the generation of SC barrier lipids initiates in keratinocytes where ceramides are *de novo* formed by ceramide synthase 3 (CerS3). The sphingolipid content of keratinocytes increases along with differentiation. Newly formed ceramides are rapidly modified into glucosylceramides (GlcCers) and sphingomyelins (SMs), thereby likely protecting keratinocytes from cytotoxic ceramide effects. Next these sphingolipids are packaged into LBs [212]. The membrane protein ABCA12 (ATP-binding cassette sub-family A member 12) is essential for the presence of GlcCer in LBs [220-222]. Several

mutations in the ABCA12 gene cause Harlequin-type ichthyosis, characterized thickened skin over nearly the entire body at birth and causing early death. Incorporated in LBs besides lipids are also acid hydrolases including GCase, ASMase and phospholipase A as well as proteases and antimicrobial peptides. Following exocytotic secretion of LBs, the SM and GlcCer molecules are largely enzymatically re-converted to ceramides [223, 224].

Chemical composition of skin sphingolipids.

The sphingolipids in the skin differ in their complexity of chemical composition from those encountered in most tissues. Firstly, their sphingosine backbones are modified to yield from dihydroceramide [DS] precursors not only the regular ceramide [S] but as well 6-hydroxyceramide [H], phytoceramide [P] and 4,X-dihydroxysphinganine containing ceramide [T] [225-228]. In addition, skin ceramides have unique fatty acyl moieties. Besides regular non-hydroxylated fatty acyls of variable chain length, there are α-hydroxylated and ω-esterified structures (acylceramides) [229].

In keratinocytes, fatty acids can be elongated by elongases (mainly ELVOL1, ELVOL4 and ELVOL6) [230, 231]. Very long chain fatty acids are incorporated in phospholipids and sphingolipids are packaged in LBs. Cholesterol does not require a conversion to be transported into LBs. Cholesterol can furthermore be metabolized to oxysterol or cholesterol sulfate. Oxysterol and cholesterol sulfate can both stimulate keratinocyte differentiation, additionally cholesterol sulfate has a key role in [232-235]. Since cholesterol sulfate is highly amphiphilic it can cross the cell membrane and directly enter the SC where it is metabolized by LB-derived steroid sulfatase to cholesterol [236, 237]. Because cholesterol sulfate inhibits proteases that are involved in desquamation [238], its decrease in the upper layers of the SC results in the initiation of desquamation [239, 240].

Besides the presence of regular ceramides, the scaffold of the lipid matrix in the SC is built of acylceramides, containing ω-hydroxylated very long chain fatty acids acylated at the ω-position with linoleic acid [212, 228]. Also, the acylceramides are synthetized in the keratinocytes where after they and regular ceramides are glucosylated at Golgi membranes and secreted via LB secretion. Extracellularly the linoleic acid residues are replaced by glutamate residues at proteins exposed on the surface of corneocytes, thus completing the corneocyte lipid envelope [212, 228, 241].

GCase: crucial Extracellular Role in the Skin

Inhibition of either cholesterol, phospholipid, ceramide or glucosylceramide synthesis prevents the delivery of lipids into LBs disrupting LB formation, thereby impairing barrier homeostasis [242]. LB secretion and lipid structure is abnormal in the outer-epidermis of multiple skin diseases, like Atopic Dermatitis and Netherton syndrome [215, 243, 244]. A complete lack of GCase results in a disease phenotype (collodion baby) with fatal skin abnormalities and inhibition of GCase activity reduces the permeability barrier formation [245-248]. Gaucher mice homozygous for a null allele develop skin abnormalities that are lethal within the first day of life [6, 7]. Holleran and colleagues showed increased trans epidermal water loss (TEWL) and altered barrier function in GCase deficient mice [247]. Suggesting deficient conversion of GlcCer to ceramides by GCase alters the skin barrier function. Identical changes were observed in hairless mice treated with GCase inhibitor bromoconduritol B epoxide, however ceramide levels remained normal [246, 247]. Similarly, mice deficient for prosaposin, and therefore also lacking the GCase activator protein saposin C, accumulate GlcCer in the SC and show abnormal SC lamellar membrane structures [249]. Interestingly, deficiency of LIMP2 in AMRF patients is not associated with skin abnormalities. No prominent abnormalities have also been noted in LIMP2-deficient mice. Apparently, GCase is reaching the SC also sufficiently without its regular transporting protein.

GlcCer and GCase appear to be co-localized in the LB [250-252]. GCase activity has been observed throughout the outer parts of the epidermis [253-255] and recently a novel *in situ* method with the use of activity-based probes (ABPs) confirmed predominant localization of active GCase in the extracellular space of the SC lipid matrix [256], (**Chapter 3**).

GD is not the only lysosomal storage disease associated with skin barrier abnormalities. In Niemann-Pick disease a deficiency in ASMase causes an impaired conversion of SM into ceramides in the SC and therefore into a disturbed skin barrier [247, 257]. Reduction of epidermal ASMase activity by the inhibitor imipramine causes delayed permeability barrier repair after SC injury [258].

Atopic Dermatitis

A common skin disease is atopic dermatitis (AD, OMIM #603165). Clinical manifestation of AD involves eczematous lesions as well as erythema, xerosis and pruritis [259-261]. In AD there is a complex interplay between inflammation, genetic background and the skin barrier. Inflammation can affect the skin barrier and subsequent entry of compounds promotes an immune response. Additionally, it has been observed that AD is associated with loss of function

mutations in the filaggrin gene FLG [262, 263]. As discussed in section 7.2, filaggrin is essential for SC hydration and may affect the sensitivity of the skin [264]. Even though FLG mutations have been suggested as a predisposing factor for AD, it does not influence SC ceramide synthesis [264-266].

SC lipids in AD.

SC lipid metabolism and composition have been substantially studied in AD, however there is some disagreement in literature about the lipid composition in skin of AD patients. Farwanah and co-workers reported no change in non-lesional AD skin compared to control [267]. Though other studies report a decrease in total ceramide level as well as an increase in ceramide [AS] and a decrease ceramide [EOS] and [EOH] mainly in lesional AD skin compared to control [215, 265, 268-271]. Additionally, Di Nardo et al. have reported a decrease in ceramide/cholesterol ratio in AD skin [271].

Besides subclass composition also ceramide chain length has been studied in AD. Some report an increase of short chain ceramides (total chain length of 34 carbon atoms) in lesional AD skin that also correlated with an increased TEWL [268, 272]. Moreover, levels of ω-O-acyl-ceramides correlated negatively with TEWL [268]. A reduction in ω-O-acyl-ceramide in AD compared to control was also reported by Jungersted et al. they additionally observed no statistically difference between their FLG mutant and wild type group in relation to the

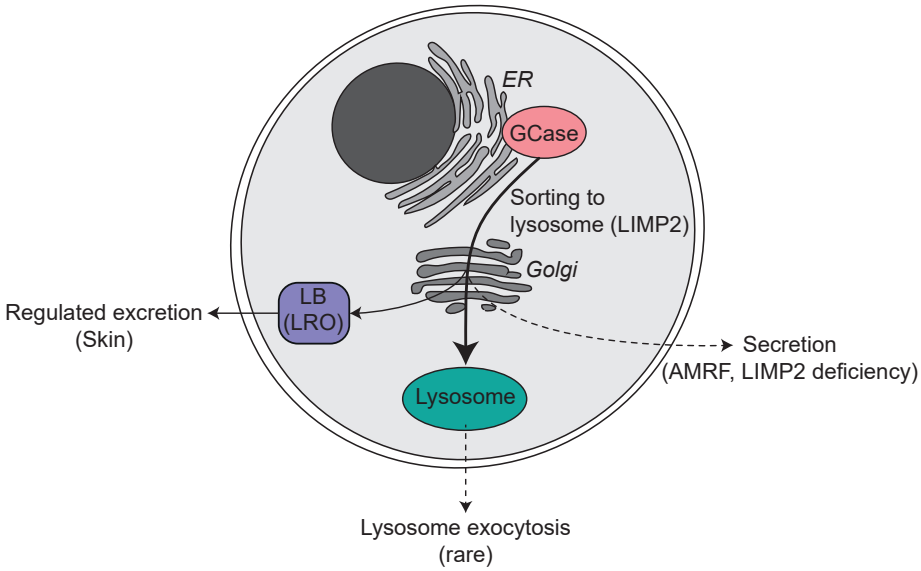

Figure 3 : The life cycle of GCase in and beyond the lysosome. AMRF: Action myoclonus renal failure syndrome, ER: endoplasmic reticulum, LB: lamellar body, LIMP2: lysosomal membrane protein 2LRO: lysosome related organelle.

ω-O-acyl-ceramide decrease [266].

Data on fatty acids in relation to AD skin are limited, but there are a few reports reporting a reduced fatty acid chain length [273, 274]. A study by van Smeden et al. described an increase of shorter fatty acids, mainly saturated fatty acids with 16 and 18 carbon atoms, as well as a reduction in fatty acids with 24 carbons or more in non-lesional AD patients [273]. However, another study observed an increased level of very long fatty acid chains in non-lesional as well as lesional AD [274]. It has been hypothesized that SC ceramides and fatty acids share a common synthetic pathway and this is consistent with the observation that ceramide composition is paralleled by the chain length of fatty acids [275].

The expression of enzymes involved in the biosynthesis of fatty acids and ceramides has been related to the SC lipid composition in lesional AD skin [276]. Danso et al. observed an altered expression of GCase, ASMase and CerS3 in lesional AD skin with a corresponding increase in ceramide [AS] and [NS] and decrease in esterified ω-hydroxy CERs. Additionally, they noted increased levels of unsaturated fatty acids and reduced levels of C22-C28 fatty acids in combination with an altered expression of stearoyl CoA desaturase (SCD) and elongase 1 (ELOVL1) [276].

Potential role for glucosylsphingosine in AD pathology.

Deficiency of ceramides in the SC is thought to contribute to the dry and barrier-disrupted skin of patients with AD. It has been proposed that this deficiency involves a tentative novel enzyme, named sphingomyelin-glucosylceramide deacylase, forming sphingosylphosphorylcholine (SPC; lysoSM) and GlcSph from SM and GlcCer. Increased deacylase activity is thought to contribute to reduced formation and subsequent deficiency of ceramide in the AD skin [277]. The deacylase enzyme is considered to be distinct from acid ceramidase as based by apparent isoelectric point [278]. Increased deacylase activity was observed for involved SC and epidermis from patients with AD [279]. Unfortunately, the deacylase has so far not been isolated and characterized. At present it can't be excluded that the intriguing observations are explained by some neutral ceramidase, a bacterial amidase, or even acid ceramidase that in lipid-laden macrophages of GD patients shows GlcCer deacylase activity.

A common symptom in AD is pruritis. It has been observed that GlcSph induces scratching in mice and more recently it was demonstrated that GlcSph activates the Serotonin Receptor 2 a and b, considered to be part of a novel itch signaling pathway [280, 281].

Direct role of GCase in AD?

As discussed above, GCase expression has been found to be altered in (particularly lesional) AD skin [276]. However, no abnormality in GCase activity level in AD skin was previously noted [282]. Earlier research in mice has pointed to changes in location of GCase activity in mice with a skin barrier disruption [246]. Using the specific and sensitive ABP technology, the localization of active GCase molecules in AD skin has been studied. An abnormal GCase localization in (mainly lesional) AD skin has been observed together with abnormal SC lipids (**Chapter 4**). It will be of interest to comparably study other skin diseases. It should be stressed that abnormalities in GCase are not a sole cause for AD, however an acquired local abnormal enzyme activity might contribute to the pathology.

Summary and Conclusion

This review addresses the multiple functions of the enzyme GCase that degrades the ubiquitous glycosphingolipid GlcCer. In the first part of the review, the metabolism and various functions of glycosphingolipids in health and disease are discussed. The structural features and catalytic mechanism of GCase are described as well as its remarkable life cycle involving LIMP2-mediated transport to lysosomes. Highlighted is the essential cellular role of GCase in turnover of GlcCer in lysosomes, as illustrated by the lysosomal storage disorder Gaucher disease (GD) resulting from inherited GCase deficiency. Reviewed are the variable symptoms of GD patients, the presumed underlying pathophysiological mechanisms and the present effective treatments of visceral manifestations. In the second part of the review, attention is focused to another, extracellular, role of GCase in the skin. In the stratum corneum, GCase converts secreted GlcCer to ceramide, an essential component of lipid lamellae contributing to the barrier properties of the skin. Lack of GCase activity causes a lethal skin pathology, the collodion baby.

To conclude, the catalytic ability of the enzyme GCase has been exploited in evolution for two different functions: in lysosomes, it essentially contributes to cellular glycosphingolipid metabolism and in the extracellular space of the stratum corneum, it generates an essential building block for lipid lamellae.

References

1. Weinreb, N. J.; Brady, R. O.; Tappel, A. L., The lysosomal localization of sphingolipid hydrolases. Biochim Biophys Acta 1968, 159 (1), 141-6.
2. Brady, R. O.; Kanfer, J. N.; Bradley, R. M.; Shapiro, D., Demonstration of a deficiency of glucocerebroside-cleaving enzyme in Gaucher's disease. J Clin Invest 1966, 45 (7), 1112-5.
3. Gaucher, P. C. E., De l'epithelioma primitif de la rate, hypertrophie idiopathique de la rate sans leucemie, Faculté de Médecine, Thèse de Paris. 1882.
4. Beutler, E.; Grabowski, G. A., Glucosylceramide Lipidosis-Gaucher Disease. The metabolic and molecular bases of inherited disease eighth edition: Edited by C R Sriver, A L Beaudet, W S Sly and D Valle. McGraw-Hill, New York 2001.
5. Smith, L.; Mullin, S.; Schapira, A. H. V., Insights into the structural biology of Gaucher disease. Exp Neurol 2017, 298 (Pt B), 180-190.
6. Sidransky, E.; Sherer, D. M.; Ginns, E. I., Gaucher disease in the neonate: a distinct Gaucher phenotype is analogous to a mouse model created by targeted disruption of the glucocerebrosidase gene. Pediatr Res 1992, 32 (4), 494-8.
7. Tybulewicz, V. L.; Tremblay, M. L.; LaMarca, M. E.; Willemsen, R.; Stubblefield, B. K.; Winfield, S.; Zablocka, B.; Sidransky, E.; Martin, B. M.; Huang, S. P.; et al., Animal model of Gaucher's disease from targeted disruption of the mouse glucocerebrosidase gene. Nature 1992, 357 (6377), 407-10.
8. van Meer, G.; Wolthoorn, J.; Degroote, S., The fate and function of glycosphingolipid glucosylceramide. Philos Trans R Soc Lond B Biol Sci 2003, 358 (1433), 869-73.
9. Merrill, A. H., Jr., Sphingolipid and glycosphingolipid metabolic pathways in the era of sphingolipidomics. Chem Rev 2011, 111 (10), 6387-422.
10. Wennekes, T.; van den Berg, R. J.; Boot, R. G.; van der Marel, G. A.; Overkleeft, H. S.; Aerts, J. M., Glycosphingolipids--nature, function, and pharmacological modulation. Angew Chem Int Ed Engl 2009, 48 (47), 8848-69.
11. Tidhar, R.; Futerman, A. H., The complexity of sphingolipid biosynthesis in the endoplasmic reticulum. Biochim Biophys Acta 2013, 1833 (11), 2511-8.
12. Mandon, E. C.; Ehses, I.; Rother, J.; van Echten, G.; Sandhoff, K., Subcellular localization and membrane topology of serine palmitoyltransferase, 3-dehydrosphinganine reductase, and sphinganine N-acyltransferase in mouse liver. J Biol Chem 1992, 267 (16), 11144-8.
13. Levy, M.; Futerman, A. H., Mammalian ceramide synthases. IUBMB Life 2010, 62 (5), 347-56.
14. Lahiri, S.; Lee, H.; Mesicek, J.; Fuks, Z.; Haimovitz-Friedman, A.; Kolesnick, R. N.; Futerman, A. H., Kinetic characterization of mammalian ceramide synthases: determination of K(m) values towards sphinganine. FEBS Lett 2007, 581 (27), 5289-94.
15. Fabrias, G.; Munoz-Olaya, J.; Cingolani, F.; Signorelli, P.; Casas, J.; Gagliostro, V.; Ghidoni, R., Dihydroceramide desaturase and dihydrosphingolipids: debutant players in the sphingolipid arena. Prog Lipid Res 2012, 51 (2), 82-94.
16. Chigorno, V.; Riva, C.; Valsecchi, M.; Nicolini, M.; Brocca, P.; Sonnino, S., Metabolic processing of gangliosides by human fibroblasts in culture--formation and recycling of separate pools of sphingosine. Eur J Biochem 1997, 250 (3), 661-9.
17. Kitatani, K.; Idkowiak-Baldys, J.; Hannun, Y. A., The sphingolipid salvage pathway in ceramide metabolism and signaling. Cell Signal 2008, 20 (6), 1010-8.
18. D'Angelo, G.; Capasso, S.; Sticco, L.; Russo, D., Glycosphingolipids: synthesis and functions. FEBS J 2013, 280 (24), 6338-53.
19. Hanada, K.; Kumagai, K.; Yasuda, S.; Miura, Y.; Kawano, M.; Fukasawa, M.; Nishijima, M., Molecular machinery for non-vesicular trafficking of ceramide. Nature 2003, 426 (6968), 803-9.
20. Ichikawa, S.; Sakiyama, H.; Suzuki, G.; Hidari, K. I.; Hirabayashi, Y., Expression cloning of a cDNA for human ceramide glucosyltransferase that catalyzes the first glycosylation step of glycosphingolipid synthesis. Proc Natl Acad Sci U S A 1996, 93 (10), 4638-43.
21. van Weely, S.; Brandsma, M.; Strijland, A.; Tager, J. M.; Aerts, J. M., Demonstration of the existence of a second, non-lysosomal glucocerebrosidase that is not deficient in Gaucher disease. Biochim Biophys Acta 1993, 1181 (1), 55-62.
22. Sandhoff, R.; Sandhoff, K., Emerging concepts of ganglioside metabolism. FEBS Lett 2018, 592 (23), 3835-3864.
23. Mukherjee, S.; Maxfield, F. R., Membrane domains. Annu Rev Cell Dev Biol 2004, 20, 839-66.
24. Sonnino, S.; Prinetti, A., Membrane domains and the "lipid raft" concept. Curr Med Chem 2013, 20 (1), 4-21.

25. Lingwood, D.; Simons, K., Lipid rafts as a membrane-organizing principle. Science 2010, 327 (5961), 46-50.
26. Tagami, S.; Inokuchi Ji, J.; Kabayama, K.; Yoshimura, H.; Kitamura, F.; Uemura, S.; Ogawa, C.; Ishii, A.; Saito, M.; Ohtsuka, Y.; Sakaue, S.; Igarashi, Y., Ganglioside GM3 participates in the pathological conditions of insulin resistance. J Biol Chem 2002, 277 (5), 3085-92.
27. Langeveld, M.; Aerts, J. M., Glycosphingolipids and insulin resistance. Prog Lipid Res 2009, 48 (3-4), 196-205.
28. Kabayama, K.; Sato, T.; Saito, K.; Loberto, N.; Prinetti, A.; Sonnino, S.; Kinjo, M.; Igarashi, Y.; Inokuchi, J., Dissociation of the insulin receptor and caveolin-1 complex by ganglioside GM3 in the state of insulin resistance. Proc Natl Acad Sci U S A 2007, 104 (34), 13678-83.
29. Yamashita, T.; Hashiramoto, A.; Haluzik, M.; Mizukami, H.; Beck, S.; Norton, A.; Kono, M.; Tsuji, S.; Daniotti, J. L.; Werth, N.; Sandhoff, R.; Sandhoff, K.; Proia, R. L., Enhanced insulin sensitivity in mice lacking ganglioside GM3. Proc Natl Acad Sci U S A 2003, 100 (6), 3445-9.
30. Aerts, J. M.; Ottenhoff, R.; Powlson, A. S.; Grefhorst, A.; van Eijk, M.; Dubbelhuis, P. F.; Aten, J.; Kuipers, F.; Serlie, M. J.; Wennekes, T.; Sethi, J. K.; O'Rahilly, S.; Overkleeft, H. S., Pharmacological inhibition of glucosylceramide synthase enhances insulin sensitivity. Diabetes 2007, 56 (5), 1341-9.
31. Coskun, U.; Grzybek, M.; Drechsel, D.; Simons, K., Regulation of human EGF receptor by lipids. Proc Natl Acad Sci U S A 2011, 108 (22), 9044-8.
32. Nakayama, H.; Nagafuku, M.; Suzuki, A.; Iwabuchi, K.; Inokuchi, J. I., The regulatory roles of glycosphingolipid-enriched lipid rafts in immune systems. FEBS Lett 2018, 592 (23), 3921-3942.
33. Hanada, K., Sphingolipids in infectious diseases. Jpn J Infect Dis 2005, 58 (3), 131-48.
34. Aerts, J.; Artola, M.; van Eijk, M.; Ferraz, M. J.; Boot, R. G., Glycosphingolipids and Infection. Potential New Therapeutic Avenues. Front Cell Dev Biol 2019, 7, 324.
35. Inokuchi, J. I.; Inamori, K. I.; Kabayama, K.; Nagafuku, M.; Uemura, S.; Go, S.; Suzuki, A.; Ohno, I.; Kanoh, H.; Shishido, F., Biology of GM3 Ganglioside. Prog Mol Biol Transl Sci 2018, 156, 151-195.
36. Iwabuchi, K., Gangliosides in the Immune System: Role of Glycosphingolipids and Glycosphingolipid-Enriched Lipid Rafts in Immunological Functions. Methods Mol Biol 2018, 1804, 83-95.
37. Aerts, J.; Kuo, C. L.; Lelieveld, L. T.; Boer, D. E. C.; van der Lienden, M. J. C.; Overkleeft, H. S.; Artola, M., Glycosphingolipids and lysosomal storage disorders as illustrated by gaucher disease. Curr Opin Chem Biol 2019, 53, 204-215.
38. Nagata, M.; Izumi, Y.; Ishikawa, E.; Kiyotake, R.; Doi, R.; Iwai, S.; Omahdi, Z.; Yamaji, T.; Miyamoto, T.; Bamba, T.; Yamasaki, S., Intracellular metabolite beta-glucosylceramide is an endogenous Mincle ligand possessing immunostimulatory activity. Proc Natl Acad Sci U S A 2017, 114 (16), E3285-E3294.
39. van den Bergh, F. A.; Tager, J. M., Localization of neutral glycosphingolipids in human plasma. Biochim Biophys Acta 1976, 441 (3), 391-402.
40. Ghauharali, K.; Kallemeijn, W.; Vergeer, M.; Motazacker, M.; van Eijk, M.; Aerts, H.; Groener, A., The role of ABCA1 in glycosphingolipid trafficking and efflux. Chem Phys Lipids 2009, 160, S15-S15.
41. Kolter, T.; Sandhoff, K., Lysosomal degradation of membrane lipids. FEBS Lett 2010, 584 (9), 1700-12.
42. Park, J. H.; Schuchman, E. H., Acid ceramidase and human disease. Biochim Biophys Acta 2006, 1758 (12), 2133-8.
43. Pyne, S.; Adams, D. R.; Pyne, N. J., Sphingosine 1-phosphate and sphingosine kinases in health and disease: Recent advances. Prog Lipid Res 2016, 62, 93-106.
44. Aerts, J. M.; Hollak, C.; Boot, R.; Groener, A., Biochemistry of glycosphingolipid storage disorders: implications for therapeutic intervention. Philos Trans R Soc Lond B Biol Sci 2003, 358 (1433), 905-14.
45. Ben Bdira, F.; Artola, M.; Overkleeft, H. S.; Ubbink, M.; Aerts, J., Distinguishing the differences in beta-glycosylceramidase folds, dynamics, and actions informs therapeutic uses. J Lipid Res 2018, 59 (12), 2262-2276.
46. Brumshtein, B.; Greenblatt, H. M.; Butters, T. D.; Shaaltiel, Y.; Aviezer, D.; Silman, I.; Futerman, A. H.; Sussman, J. L., Crystal structures of complexes of N-butyl- and N-nonyl-deoxynojirimycin bound to acid beta-glucosidase: insights into the mechanism of chemical chaperone action in Gaucher disease. J Biol Chem 2007, 282 (39), 29052-8.
47. Dvir, H.; Harel, M.; McCarthy, A. A.; Toker, L.; Silman, I.; Futerman, A. H.; Sussman, J. L., X-ray structure of human acid-beta-glucosidase, the defective enzyme in Gaucher disease. EMBO Rep 2003, 4 (7), 704-9.
48. Koshland, D. E., Stereochemistry and the Mechanism of Enzymatic Reactions. Biol Rev 1953, 28 (4), 416-436.
49. Rye, C. S.; Withers, S. G., Glycosidase mechanisms. Curr Opin Chem Biol 2000, 4 (5), 573-80.
50. Speciale, G.; Thompson, A. J.; Davies, G. J.; Williams, S. J., Dissecting conformational contributions to

glycosidase catalysis and inhibition. Curr Opin Struct Biol 2014, 28, 1-13.
51. Ardevol, A.; Rovira, C., Reaction Mechanisms in Carbohydrate-Active Enzymes: Glycoside Hydrolases and Glycosyltransferases. Insights from ab Initio Quantum Mechanics/Molecular Mechanics Dynamic Simulations. J Am Chem Soc 2015, 137 (24), 7528-47.
52. Legler, G., Glycoside hydrolases: mechanistic information from studies with reversible and irreversible inhibitors. Adv Carbohydr Chem Biochem 1990, 48, 319-84.
53. Withers, S. G.; Aebersold, R., Approaches to labeling and identification of active site residues in glycosidases. Protein Sci 1995, 4 (3), 361-72.
54. Atsumi, S.; Umezawa, K.; Iinuma, H.; Naganawa, H.; Nakamura, H.; Iitaka, Y.; Takeuchi, T., Production, isolation and structure determination of a novel beta-glucosidase inhibitor, cyclophellitol, from Phellinus sp. J Antibiot (Tokyo) 1990, 43 (1), 49-53.
55. Kallemeijn, W. W.; Li, K. Y.; Witte, M. D.; Marques, A. R.; Aten, J.; Scheij, S.; Jiang, J.; Willems, L. I.; Voorn-Brouwer, T. M.; van Roomen, C. P.; Ottenhoff, R.; Boot, R. G.; van den Elst, H.; Walvoort, M. T.; Florea, B. I.; Codee, J. D.; van der Marel, G. A.; Aerts, J. M.; Overkleeft, H. S., Novel activity-based probes for broad-spectrum profiling of retaining beta-exoglucosidases in situ and in vivo. Angew Chem Int Ed Engl 2012, 51 (50), 12529-33.
56. Artola, M.; Kuo, C. L.; Lelieveld, L. T.; Rowland, R. J.; van der Marel, G. A.; Codee, J. D. C.; Boot, R. G.; Davies, G. J.; Aerts, J.; Overkleeft, H. S., Functionalized Cyclophellitols Are Selective Glucocerebrosidase Inhibitors and Induce a Bona Fide Neuropathic Gaucher Model in Zebrafish. J Am Chem Soc 2019, 141 (10), 4214-4218.
57. Kuo, C. L.; Kallemeijn, W. W.; Lelieveld, L. T.; Mirzaian, M.; Zoutendijk, I.; Vardi, A.; Futerman, A. H.; Meijer, A. H.; Spaink, H. P.; Overkleeft, H. S.; Aerts, J.; Artola, M., In vivo inactivation of glycosidases by conduritol B epoxide and cyclophellitol as revealed by activity-based protein profiling. FEBS J 2019, 286 (3), 584-600.
58. Witte, M. D.; Kallemeijn, W. W.; Aten, J.; Li, K. Y.; Strijland, A.; Donker-Koopman, W. E.; van den Nieuwendijk, A. M.; Bleijlevens, B.; Kramer, G.; Florea, B. I.; Hooibrink, B.; Hollak, C. E.; Ottenhoff, R.; Boot, R. G.; van der Marel, G. A.; Overkleeft, H. S.; Aerts, J. M., Ultrasensitive in situ visualization of active glucocerebrosidase molecules. Nat Chem Biol 2010, 6 (12), 907-13.
59. Jiang, J.; Beenakker, T. J.; Kallemeijn, W. W.; van der Marel, G. A.; van den Elst, H.; Codee, J. D.; Aerts, J. M.; Overkleeft, H. S., Comparing Cyclophellitol N-Alkyl and N-Acyl Cyclophellitol Aziridines as Activity-Based Glycosidase Probes. Chemistry 2015, 21 (30), 10861-9.
60. Willems, L. I.; Beenakker, T. J.; Murray, B.; Scheij, S.; Kallemeijn, W. W.; Boot, R. G.; Verhoek, M.; Donker-Koopman, W. E.; Ferraz, M. J.; van Rijssel, E. R.; Florea, B. I.; Codee, J. D.; van der Marel, G. A.; Aerts, J. M.; Overkleeft, H. S., Potent and selective activity-based probes for GH27 human retaining alpha-galactosidases. J Am Chem Soc 2014, 136 (33), 11622-5.
61. Jiang, J.; Kuo, C. L.; Wu, L.; Franke, C.; Kallemeijn, W. W.; Florea, B. I.; van Meel, E.; van der Marel, G. A.; Codee, J. D.; Boot, R. G.; Davies, G. J.; Overkleeft, H. S.; Aerts, J. M., Detection of Active Mammalian GH31 alpha-Glucosidases in Health and Disease Using In-Class, Broad-Spectrum Activity-Based Probes. ACS Cent Sci 2016, 2 (5), 351-8.
62. Jiang, J.; Kallemeijn, W. W.; Wright, D. W.; van den Nieuwendijk, A.; Rohde, V. C.; Folch, E. C.; van den Elst, H.; Florea, B. I.; Scheij, S.; Donker-Koopman, W. E.; Verhoek, M.; Li, N.; Schurmann, M.; Mink, D.; Boot, R. G.; Codee, J. D. C.; van der Marel, G. A.; Davies, G. J.; Aerts, J.; Overkleeft, H. S., In vitro and in vivo comparative and competitive activity-based protein profiling of GH29 alpha-l-fucosidases. Chem Sci 2015, 6 (5), 2782-false.
63. Artola, M.; Kuo, C. L.; McMahon, S. A.; Oehler, V.; Hansen, T.; van der Lienden, M.; He, X.; van den Elst, H.; Florea, B. I.; Kermode, A. R.; van der Marel, G. A.; Gloster, T. M.; Codee, J. D. C.; Overkleeft, H. S.; Aerts, J., New Irreversible alpha-l-Iduronidase Inhibitors and Activity-Based Probes. Chemistry 2018, 24 (71), 19081-19088.
64. Wu, L.; Jiang, J.; Jin, Y.; Kallemeijn, W. W.; Kuo, C. L.; Artola, M.; Dai, W.; van Elk, C.; van Eijk, M.; van der Marel, G. A.; Codee, J. D. C.; Florea, B. I.; Aerts, J.; Overkleeft, H. S.; Davies, G. J., Activity-based probes for functional interrogation of retaining beta-glucuronidases. Nat Chem Biol 2017, 13 (8), 867-873.
65. Marques, A. R.; Willems, L. I.; Herrera Moro, D.; Florea, B. I.; Scheij, S.; Ottenhoff, R.; van Roomen, C. P.; Verhoek, M.; Nelson, J. K.; Kallemeijn, W. W.; Biela-Banas, A.; Martin, O. R.; Cachon-Gonzalez, M. B.; Kim, N. N.; Cox, T. M.; Boot, R. G.; Overkleeft, H. S.; Aerts, J. M., A Specific Activity-Based Probe to Monitor Family GH59 Galactosylceramidase, the Enzyme Deficient in Krabbe Disease. Chembiochem 2017, 18 (4), 402-412.
66. Kuo, C. L.; van Meel, E.; Kytidou, K.; Kallemeijn, W. W.; Witte, M.; Overkleeft, H. S.; Artola, M. E.; Aerts, J. M., Activity-Based Probes for Glycosidases: Profiling and Other Applications. Methods Enzymol 2018, 598,

217-235.
67. Lahav, D.; Liu, B.; van den Berg, R.; van den Nieuwendijk, A.; Wennekes, T.; Ghisaidoobe, A. T.; Breen, I.; Ferraz, M. J.; Kuo, C. L.; Wu, L.; Geurink, P. P.; Ovaa, H.; van der Marel, G. A.; van der Stelt, M.; Boot, R. G.; Davies, G. J.; Aerts, J.; Overkleeft, H. S., A Fluorescence Polarization Activity-Based Protein Profiling Assay in the Discovery of Potent, Selective Inhibitors for Human Nonlysosomal Glucosylceramidase. J Am Chem Soc 2017, 139 (40), 14192-14197.
68. Tylki-Szymanska, A.; Groener, J. E.; Kaminski, M. L.; Lugowska, A.; Jurkiewicz, E.; Czartoryska, B., Gaucher disease due to saposin C deficiency, previously described as non-neuronopathic form--no positive effects after 2-years of miglustat therapy. Mol Genet Metab 2011, 104 (4), 627-30.
69. Ben Bdira, F.; Kallemeijn, W. W.; Oussoren, S. V.; Scheij, S.; Bleijlevens, B.; Florea, B. I.; van Roomen, C.; Ottenhoff, R.; van Kooten, M.; Walvoort, M. T. C.; Witte, M. D.; Boot, R. G.; Ubbink, M.; Overkleeft, H. S.; Aerts, J., Stabilization of Glucocerebrosidase by Active Site Occupancy. ACS Chem Biol 2017, 12 (7), 1830-1841.
70. Jonsson, L. M.; Murray, G. J.; Sorrell, S. H.; Strijland, A.; Aerts, J. F.; Ginns, E. I.; Barranger, J. A.; Tager, J. M.; Schram, A. W., Biosynthesis and maturation of glucocerebrosidase in Gaucher fibroblasts. Eur J Biochem 1987, 164 (1), 171-9.
71. Aerts, J. M.; Schram, A. W.; Strijland, A.; van Weely, S.; Jonsson, L. M.; Tager, J. M.; Sorrell, S. H.; Ginns, E. I.; Barranger, J. A.; Murray, G. J., Glucocerebrosidase, a lysosomal enzyme that does not undergo oligosaccharide phosphorylation. Biochim Biophys Acta 1988, 964 (3), 303-8.
72. Reczek, D.; Schwake, M.; Schroder, J.; Hughes, H.; Blanz, J.; Jin, X.; Brondyk, W.; Van Patten, S.; Edmunds, T.; Saftig, P., LIMP-2 is a receptor for lysosomal mannose-6-phosphate-independent targeting of beta-glucocerebrosidase. Cell 2007, 131 (4), 770-83.
73. Rijnboutt, S.; Aerts, H. M.; Geuze, H. J.; Tager, J. M.; Strous, G. J., Mannose 6-phosphate-independent membrane association of cathepsin D, glucocerebrosidase, and sphingolipid-activating protein in HepG2 cells. J Biol Chem 1991, 266 (8), 4862-8.
74. Rijnboutt, S.; Kal, A. J.; Geuze, H. J.; Aerts, H.; Strous, G. J., Mannose 6-phosphate-independent targeting of cathepsin D to lysosomes in HepG2 cells. J Biol Chem 1991, 266 (35), 23586-92.
75. Zunke, F.; Andresen, L.; Wesseler, S.; Groth, J.; Arnold, P.; Rothaug, M.; Mazzulli, J. R.; Krainc, D.; Blanz, J.; Saftig, P.; Schwake, M., Characterization of the complex formed by beta-glucocerebrosidase and the lysosomal integral membrane protein type-2. Proc Natl Acad Sci U S A 2016, 113 (14), 3791-6.
76. Balreira, A.; Gaspar, P.; Caiola, D.; Chaves, J.; Beirao, I.; Lima, J. L.; Azevedo, J. E.; Miranda, M. C., A nonsense mutation in the LIMP-2 gene associated with progressive myoclonic epilepsy and nephrotic syndrome. Hum Mol Genet 2008, 17 (14), 2238-43.
77. Gaspar, P.; Kallemeijn, W. W.; Strijland, A.; Scheij, S.; Van Eijk, M.; Aten, J.; Overkleeft, H. S.; Balreira, A.; Zunke, F.; Schwake, M.; Sa Miranda, C.; Aerts, J. M., Action myoclonus-renal failure syndrome: diagnostic applications of activity-based probes and lipid analysis. J Lipid Res 2014, 55 (1), 138-45.
78. Chen, Y.; Sud, N.; Hettinghouse, A.; Liu, C. J., Molecular regulations and therapeutic targets of Gaucher disease. Cytokine Growth Factor Rev 2018, 41, 65-74.
79. Jian, J.; Zhao, S.; Tian, Q. Y.; Liu, H.; Zhao, Y.; Chen, W. C.; Grunig, G.; Torres, P. A.; Wang, B. C.; Zeng, B.; Pastores, G.; Tang, W.; Sun, Y.; Grabowski, G. A.; Kong, M. X.; Wang, G.; Chen, Y.; Liang, F.; Overkleeft, H. S.; Saunders-Pullman, R.; Chan, G. L.; Liu, C. J., Association Between Progranulin and Gaucher Disease. EBioMedicine 2016, 11, 127-137.
80. Jian, J.; Tian, Q. Y.; Hettinghouse, A.; Zhao, S.; Liu, H.; Wei, J.; Grunig, G.; Zhang, W.; Setchell, K. D. R.; Sun, Y.; Overkleeft, H. S.; Chan, G. L.; Liu, C. J., Progranulin Recruits HSP70 to beta-Glucocerebrosidase and Is Therapeutic Against Gaucher Disease. EBioMedicine 2016, 13, 212-224.
81. Tan, Y. L.; Genereux, J. C.; Pankow, S.; Aerts, J. M.; Yates, J. R., 3rd; Kelly, J. W., ERdj3 is an endoplasmic reticulum degradation factor for mutant glucocerebrosidase variants linked to Gaucher's disease. Chem Biol 2014, 21 (8), 967-76.
82. Aghion, H. La Maladie de Gaucher dans l'enfance, Faculte de Medecine. Paris, 1934.
83. Rosenberg, A.; Chargaff, E., A reinvestigation of the cerebroside deposited in Gaucher's disease. J Biol Chem 1958, 233 (6), 1323-6.
84. Aerts, J. M.; Cox, T. M., Roscoe O. Brady: Physician whose pioneering discoveries in lipid biochemistry revolutionized treatment and understanding of lysosomal diseases. Blood Cells Mol Dis 2018, 68, 4-8.
85. Danby, P. M.; Withers, S. G., Advances in Enzymatic Glycoside Synthesis. ACS Chem Biol 2016, 11 (7), 1784-94.
86. Marques, A. R.; Mirzaian, M.; Akiyama, H.; Wisse, P.; Ferraz, M. J.; Gaspar, P.; Ghauharali-van der Vlugt, K.; Meijer, R.; Giraldo, P.; Alfonso, P.; Irun, P.; Dahl, M.; Karlsson, S.; Pavlova, E. V.; Cox, T. M.; Scheij, S.;

Verhoek, M.; Ottenhoff, R.; van Roomen, C. P.; Pannu, N. S.; van Eijk, M.; Dekker, N.; Boot, R. G.; Overkleeft, H. S.; Blommaart, E.; Hirabayashi, Y.; Aerts, J. M., Glucosylated cholesterol in mammalian cells and tissues: formation and degradation by multiple cellular beta-glucosidases. J Lipid Res 2016, 57 (3), 451-63.
87. Akiyama, H.; Kobayashi, S.; Hirabayashi, Y.; Murakami-Murofushi, K., Cholesterol glucosylation is catalyzed by transglucosylation reaction of beta-glucosidase 1. Biochem Biophys Res Commun 2013, 441 (4), 838-43.
88. Akiyama, H.; Hirabayashi, Y., A novel function for glucocerebrosidase as a regulator of sterylglucoside metabolism. Biochim Biophys Acta Gen Subj 2017, 1861 (10), 2507-2514.
89. Ballabio, A.; Gieselmann, V., Lysosomal disorders: from storage to cellular damage. Biochim Biophys Acta 2009, 1793 (4), 684-96.
90. Platt, F. M.; d'Azzo, A.; Davidson, B. L.; Neufeld, E. F.; Tifft, C. J., Lysosomal storage diseases. Nat Rev Dis Primers 2018, 4 (1), 27.
91. Ferraz, M. J.; Kallemeijn, W. W.; Mirzaian, M.; Herrera Moro, D.; Marques, A.; Wisse, P.; Boot, R. G.; Willems, L. I.; Overkleeft, H. S.; Aerts, J. M., Gaucher disease and Fabry disease: new markers and insights in pathophysiology for two distinct glycosphingolipidoses. Biochim Biophys Acta 2014, 1841 (5), 811-25.
92. Horowitz, M.; Wilder, S.; Horowitz, Z.; Reiner, O.; Gelbart, T.; Beutler, E., The human glucocerebrosidase gene and pseudogene: structure and evolution. Genomics 1989, 4 (1), 87-96.
93. Ohashi, T.; Hong, C. M.; Weiler, S.; Tomich, J. M.; Aerts, J. M.; Tager, J. M.; Barranger, J. A., Characterization of human glucocerebrosidase from different mutant alleles. J Biol Chem 1991, 266 (6), 3661-7.
94. Boot, R. G.; Hollak, C. E.; Verhoek, M.; Sloof, P.; Poorthuis, B. J.; Kleijer, W. J.; Wevers, R. A.; van Oers, M. H.; Mannens, M. M.; Aerts, J. M.; van Weely, S., Glucocerebrosidase genotype of Gaucher patients in The Netherlands: limitations in prognostic value. Hum Mutat 1997, 10 (5), 348-58.
95. Diamond, J. M., Human genetics. Jewish lysosomes. Nature 1994, 368 (6469), 291-2.
96. Boas, F. E., Linkage to Gaucher mutations in the Ashkenazi population: effect of drift on decay of linkage disequilibrium and evidence for heterozygote selection. Blood Cells Mol Dis 2000, 26 (4), 348-59.
97. Colombo, R., Age estimate of the N370S mutation causing Gaucher disease in Ashkenazi Jews and European populations: A reappraisal of haplotype data. Am J Hum Genet 2000, 66 (2), 692-7.
98. Meijer, A. H.; Aerts, J. M., Linking Smokers' Susceptibility to Tuberculosis with Lysosomal Storage Disorders. Dev Cell 2016, 37 (2), 112-3.
99. Sidransky, E., Gaucher disease: complexity in a "simple" disorder. Mol Genet Metab 2004, 83 (1-2), 6-15.
100. Biegstraaten, M.; van Schaik, I. N.; Aerts, J. M.; Langeveld, M.; Mannens, M. M.; Bour, L. J.; Sidransky, E.; Tayebi, N.; Fitzgibbon, E.; Hollak, C. E., A monozygotic twin pair with highly discordant Gaucher phenotypes. Blood Cells Mol Dis 2011, 46 (1), 39-41.
101. Lachmann, R. H.; Grant, I. R.; Halsall, D.; Cox, T. M., Twin pairs showing discordance of phenotype in adult Gaucher's disease. QJM 2004, 97 (4), 199-204.
102. Uyama, E.; Takahashi, K.; Owada, M.; Okamura, R.; Naito, M.; Tsuji, S.; Kawasaki, S.; Araki, S., Hydrocephalus, corneal opacities, deafness, valvular heart disease, deformed toes and leptomeningeal fibrous thickening in adult siblings: a new syndrome associated with beta-glucocerebrosidase deficiency and a mosaic population of storage cells. Acta Neurol Scand 1992, 86 (4), 407-20.
103. Chabas, A.; Cormand, B.; Grinberg, D.; Burguera, J. M.; Balcells, S.; Merino, J. L.; Mate, I.; Sobrino, J. A.; Gonzalez-Duarte, R.; Vilageliu, L., Unusual expression of Gaucher's disease: cardiovascular calcifications in three sibs homozygous for the D409H mutation. J Med Genet 1995, 32 (9), 740-2.
104. Abrahamov, A.; Elstein, D.; Gross-Tsur, V.; Farber, B.; Glaser, Y.; Hadas-Halpern, I.; Ronen, S.; Tafakjdi, M.; Horowitz, M.; Zimran, A., Gaucher's disease variant characterised by progressive calcification of heart valves and unique genotype. Lancet 1995, 346 (8981), 1000-3.
105. Zhang, C. K.; Stein, P. B.; Liu, J.; Wang, Z.; Yang, R.; Cho, J. H.; Gregersen, P. K.; Aerts, J. M.; Zhao, H.; Pastores, G. M.; Mistry, P. K., Genome-wide association study of N370S homozygous Gaucher disease reveals the candidacy of CLN8 gene as a genetic modifier contributing to extreme phenotypic variation. Am J Hematol 2012, 87 (4), 377-83.
106. di Ronza, A.; Bajaj, L.; Sharma, J.; Sanagasetti, D.; Lotfi, P.; Adamski, C. J.; Collette, J.; Palmieri, M.; Amawi, A.; Popp, L.; Chang, K. T.; Meschini, M. C.; Leung, H. E.; Segatori, L.; Simonati, A.; Sifers, R. N.; Santorelli, F. M.; Sardiello, M., CLN8 is an endoplasmic reticulum cargo receptor that regulates lysosome biogenesis. Nat Cell Biol 2018, 20 (12), 1370-1377.
107. Velayati, A.; DePaolo, J.; Gupta, N.; Choi, J. H.; Moaven, N.; Westbroek, W.; Goker-Alpan, O.; Goldin, E.; Stubblefield, B. K.; Kolodny, E.; Tayebi, N.; Sidransky, E., A mutation in SCARB2 is a modifier in Gaucher disease. Hum Mutat 2011, 32 (11), 1232-8.

108. Alfonso, P.; Navascues, J.; Navarro, S.; Medina, P.; Bolado-Carrancio, A.; Andreu, V.; Irun, P.; Rodriguez-Rey, J. C.; Pocovi, M.; Espana, F.; Giraldo, P., Characterization of variants in the glucosylceramide synthase gene and their association with type 1 Gaucher disease severity. Hum Mutat 2013, 34 (10), 1396-403.
109. Siebert, M.; Westbroek, W.; Chen, Y. C.; Moaven, N.; Li, Y.; Velayati, A.; Saraiva-Pereira, M. L.; Martin, S. E.; Sidransky, E., Identification of miRNAs that modulate glucocerebrosidase activity in Gaucher disease cells. RNA Biol 2014, 11 (10), 1291-300.
110. Sidransky, E.; Nalls, M. A.; Aasly, J. O.; Aharon-Peretz, J.; Annesi, G.; Barbosa, E. R.; Bar-Shira, A.; Berg, D.; Bras, J.; Brice, A.; Chen, C. M.; Clark, L. N.; Condroyer, C.; De Marco, E. V.; Durr, A.; Eblan, M. J.; Fahn, S.; Farrer, M. J.; Fung, H. C.; Gan-Or, Z.; Gasser, T.; Gershoni-Baruch, R.; Giladi, N.; Griffith, A.; Gurevich, T.; Januario, C.; Kropp, P.; Lang, A. E.; Lee-Chen, G. J.; Lesage, S.; Marder, K.; Mata, I. F.; Mirelman, A.; Mitsui, J.; Mizuta, I.; Nicoletti, G.; Oliveira, C.; Ottman, R.; Orr-Urtreger, A.; Pereira, L. V.; Quattrone, A.; Rogaeva, E.; Rolfs, A.; Rosenbaum, H.; Rozenberg, R.; Samii, A.; Samaddar, T.; Schulte, C.; Sharma, M.; Singleton, A.; Spitz, M.; Tan, E. K.; Tayebi, N.; Toda, T.; Troiano, A. R.; Tsuji, S.; Wittstock, M.; Wolfsberg, T. G.; Wu, Y. R.; Zabetian, C. P.; Zhao, Y.; Ziegler, S. G., Multicenter analysis of glucocerebrosidase mutations in Parkinson's disease. N Engl J Med 2009, 361 (17), 1651-61.
111. Nalls, M. A.; Duran, R.; Lopez, G.; Kurzawa-Akanbi, M.; McKeith, I. G.; Chinnery, P. F.; Morris, C. M.; Theuns, J.; Crosiers, D.; Cras, P.; Engelborghs, S.; De Deyn, P. P.; Van Broeckhoven, C.; Mann, D. M.; Snowden, J.; Pickering-Brown, S.; Halliwell, N.; Davidson, Y.; Gibbons, L.; Harris, J.; Sheerin, U. M.; Bras, J.; Hardy, J.; Clark, L.; Marder, K.; Honig, L. S.; Berg, D.; Maetzler, W.; Brockmann, K.; Gasser, T.; Novellino, F.; Quattrone, A.; Annesi, G.; De Marco, E. V.; Rogaeva, E.; Masellis, M.; Black, S. E.; Bilbao, J. M.; Foroud, T.; Ghetti, B.; Nichols, W. C.; Pankratz, N.; Halliday, G.; Lesage, S.; Klebe, S.; Durr, A.; Duyckaerts, C.; Brice, A.; Giasson, B. I.; Trojanowski, J. Q.; Hurtig, H. I.; Tayebi, N.; Landazabal, C.; Knight, M. A.; Keller, M.; Singleton, A. B.; Wolfsberg, T. G.; Sidransky, E., A multicenter study of glucocerebrosidase mutations in dementia with Lewy bodies. JAMA Neurol 2013, 70 (6), 727-35.
112. Siebert, M.; Sidransky, E.; Westbroek, W., Glucocerebrosidase is shaking up the synucleinopathies. Brain 2014, 137 (Pt 5), 1304-22.
113. Mullin, S.; Beavan, M.; Bestwick, J.; McNeill, A.; Proukakis, C.; Cox, T.; Hughes, D.; Mehta, A.; Zetterberg, H.; Schapira, A. H. V., Evolution and clustering of prodromal parkinsonian features in GBA1 carriers. Mov Disord 2019, 34 (9), 1365-1373.
114. Isacson, O.; Brekk, O. R.; Hallett, P. J., Novel Results and Concepts Emerging From Lipid Cell Biology Relevant to Degenerative Brain Aging and Disease. Front Neurol 2019, 10, 1053.
115. Rocha, E. M.; Smith, G. A.; Park, E.; Cao, H.; Brown, E.; Hallett, P.; Isacson, O., Progressive decline of glucocerebrosidase in aging and Parkinson's disease. Ann Clin Transl Neurol 2015, 2 (4), 433-8.
116. Hallett, P. J.; Huebecker, M.; Brekk, O. R.; Moloney, E. B.; Rocha, E. M.; Priestman, D. A.; Platt, F. M.; Isacson, O., Glycosphingolipid levels and glucocerebrosidase activity are altered in normal aging of the mouse brain. Neurobiol Aging 2018, 67, 189-200.
117. Huebecker, M.; Moloney, E. B.; van der Spoel, A. C.; Priestman, D. A.; Isacson, O.; Hallett, P. J.; Platt, F. M., Reduced sphingolipid hydrolase activities, substrate accumulation and ganglioside decline in Parkinson's disease. Mol Neurodegener 2019, 14 (1), 40.
118. Rocha, E. M.; Smith, G. A.; Park, E.; Cao, H.; Graham, A. R.; Brown, E.; McLean, J. R.; Hayes, M. A.; Beagan, J.; Izen, S. C.; Perez-Torres, E.; Hallett, P. J.; Isacson, O., Sustained Systemic Glucocerebrosidase Inhibition Induces Brain alpha-Synuclein Aggregation, Microglia and Complement C1q Activation in Mice. Antioxid Redox Signal 2015, 23 (6), 550-64.
119. Brekk, O. R.; Moskites, A.; Isacson, O.; Hallett, P. J., Lipid-dependent deposition of alpha-synuclein and Tau on neuronal Secretogranin II-positive vesicular membranes with age. Sci Rep 2018, 8 (1), 15207.
120. Xu, Y. H.; Sun, Y.; Ran, H.; Quinn, B.; Witte, D.; Grabowski, G. A., Accumulation and distribution of alpha-synuclein and ubiquitin in the CNS of Gaucher disease mouse models. Mol Genet Metab 2011, 102 (4), 436-47.
121. Sardi, S. P.; Clarke, J.; Kinnecom, C.; Tamsett, T. J.; Li, L.; Stanek, L. M.; Passini, M. A.; Grabowski, G. A.; Schlossmacher, M. G.; Sidman, R. L.; Cheng, S. H.; Shihabuddin, L. S., CNS expression of glucocerebrosidase corrects alpha-synuclein pathology and memory in a mouse model of Gaucher-related synucleinopathy. Proc Natl Acad Sci U S A 2011, 108 (29), 12101-6.
122. Sardi, S. P.; Viel, C.; Clarke, J.; Treleaven, C. M.; Richards, A. M.; Park, H.; Olszewski, M. A.; Dodge, J. C.; Marshall, J.; Makino, E.; Wang, B.; Sidman, R. L.; Cheng, S. H.; Shihabuddin, L. S., Glucosylceramide synthase inhibition alleviates aberrations in synucleinopathy models. Proc Natl Acad Sci U S A 2017, 114 (10), 2699-2704.
123. Mazzulli, J. R.; Xu, Y. H.; Sun, Y.; Knight, A. L.; McLean, P. J.; Caldwell, G. A.; Sidransky, E.; Grabowski,

G. A.; Krainc, D., Gaucher disease glucocerebrosidase and alpha-synuclein form a bidirectional pathogenic loop in synucleinopathies. Cell 2011, 146 (1), 37-52.
124. Mazzulli, J. R.; Zunke, F.; Tsunemi, T.; Toker, N. J.; Jeon, S.; Burbulla, L. F.; Patnaik, S.; Sidransky, E.; Marugan, J. J.; Sue, C. M.; Krainc, D., Activation of beta-Glucocerebrosidase Reduces Pathological alpha-Synuclein and Restores Lysosomal Function in Parkinson's Patient Midbrain Neurons. J Neurosci 2016, 36 (29), 7693-706.
125. Stojkovska, I.; Krainc, D.; Mazzulli, J. R., Molecular mechanisms of alpha-synuclein and GBA1 in Parkinson's disease. Cell Tissue Res 2018, 373 (1), 51-60.
126. Yap, T. L.; Gruschus, J. M.; Velayati, A.; Westbroek, W.; Goldin, E.; Moaven, N.; Sidransky, E.; Lee, J. C., Alpha-synuclein interacts with Glucocerebrosidase providing a molecular link between Parkinson and Gaucher diseases. J Biol Chem 2011, 286 (32), 28080-8.
127. Toffoli, M.; Smith, L.; Schapira, A. H. V., The biochemical basis of interactions between Glucocerebrosidase and alpha-synuclein in GBA1 mutation carriers. J Neurochem 2020.
128. Balestrino, R.; Schapira, A. H. V., Parkinson disease. Eur J Neurol 2020, 27 (1), 27-42.
129. Maor, G.; Cabasso, O.; Krivoruk, O.; Rodriguez, J.; Steller, H.; Segal, D.; Horowitz, M., The contribution of mutant GBA to the development of Parkinson disease in Drosophila. Hum Mol Genet 2016, 25 (13), 2712-2727.
130. Cabasso, O.; Paul, S.; Dorot, O.; Maor, G.; Krivoruk, O.; Pasmanik-Chor, M.; Mirzaian, M.; Ferraz, M.; Aerts, J.; Horowitz, M., Drosophila melanogaster Mutated in its GBA1b Ortholog Recapitulates Neuronopathic Gaucher Disease. J Clin Med 2019, 8 (9).
131. Bussink, A. P.; van Eijk, M.; Renkema, G. H.; Aerts, J. M.; Boot, R. G., The biology of the Gaucher cell: the cradle of human chitinases. Int Rev Cytol 2006, 252, 71-128.
132. Boven, L. A.; van Meurs, M.; Boot, R. G.; Mehta, A.; Boon, L.; Aerts, J. M.; Laman, J. D., Gaucher cells demonstrate a distinct macrophage phenotype and resemble alternatively activated macrophages. Am J Clin Pathol 2004, 122 (3), 359-69.
133. Hollak, C. E.; van Weely, S.; van Oers, M. H.; Aerts, J. M., Marked elevation of plasma chitotriosidase activity. A novel hallmark of Gaucher disease. J Clin Invest 1994, 93 (3), 1288-92.
134. Boot, R. G.; Renkema, G. H.; Strijland, A.; van Zonneveld, A. J.; Aerts, J. M., Cloning of a cDNA encoding chitotriosidase, a human chitinase produced by macrophages. J Biol Chem 1995, 270 (44), 26252-6.
135. Aguilera, B.; Ghauharali-van der Vlugt, K.; Helmond, M. T.; Out, J. M.; Donker-Koopman, W. E.; Groener, J. E.; Boot, R. G.; Renkema, G. H.; van der Marel, G. A.; van Boom, J. H.; Overkleeft, H. S.; Aerts, J. M., Transglycosidase activity of chitotriosidase: improved enzymatic assay for the human macrophage chitinase. J Biol Chem 2003, 278 (42), 40911-6.
136. Schoonhoven, A.; Rudensky, B.; Elstein, D.; Zimran, A.; Hollak, C. E.; Groener, J. E.; Aerts, J. M., Monitoring of Gaucher patients with a novel chitotriosidase assay. Clin Chim Acta 2007, 381 (2), 136-9.
137. Boot, R. G.; Renkema, G. H.; Verhoek, M.; Strijland, A.; Bliek, J.; de Meulemeester, T. M.; Mannens, M. M.; Aerts, J. M., The human chitotriosidase gene. Nature of inherited enzyme deficiency. J Biol Chem 1998, 273 (40), 25680-5.
138. Deegan, P. B.; Moran, M. T.; McFarlane, I.; Schofield, J. P.; Boot, R. G.; Aerts, J. M.; Cox, T. M., Clinical evaluation of chemokine and enzymatic biomarkers of Gaucher disease. Blood Cells Mol Dis 2005, 35 (2), 259-67.
139. Boot, R. G.; Verhoek, M.; de Fost, M.; Hollak, C. E.; Maas, M.; Bleijlevens, B.; van Breemen, M. J.; van Meurs, M.; Boven, L. A.; Laman, J. D.; Moran, M. T.; Cox, T. M.; Aerts, J. M., Marked elevation of the chemokine CCL18/PARC in Gaucher disease: a novel surrogate marker for assessing therapeutic intervention. Blood 2004, 103 (1), 33-9.
140. Kramer, G.; Wegdam, W.; Donker-Koopman, W.; Ottenhoff, R.; Gaspar, P.; Verhoek, M.; Nelson, J.; Gabriel, T.; Kallemeijn, W.; Boot, R. G.; Laman, J. D.; Vissers, J. P.; Cox, T.; Pavlova, E.; Moran, M. T.; Aerts, J. M.; van Eijk, M., Elevation of glycoprotein nonmetastatic melanoma protein B in type 1 Gaucher disease patients and mouse models. FEBS Open Bio 2016, 6 (9), 902-13.
141. Murugesan, V.; Liu, J.; Yang, R.; Lin, H.; Lischuk, A.; Pastores, G.; Zhang, X.; Chuang, W. L.; Mistry, P. K., Validating glycoprotein non-metastatic melanoma B (gpNMB, osteoactivin), a new biomarker of Gaucher disease. Blood Cells Mol Dis 2018, 68, 47-53.
142. Zigdon, H.; Savidor, A.; Levin, Y.; Meshcheriakova, A.; Schiffmann, R.; Futerman, A. H., Identification of a biomarker in cerebrospinal fluid for neuronopathic forms of Gaucher disease. PLoS One 2015, 10 (3), e0120194.
143. Moloney, E. B.; Moskites, A.; Ferrari, E. J.; Isacson, O.; Hallett, P. J., The glycoprotein GPNMB is selectively elevated in the substantia nigra of Parkinson's disease patients and increases after lysosomal

stress. Neurobiol Dis 2018, 120, 1-11.
144. Dahl, M.; Doyle, A.; Olsson, K.; Mansson, J. E.; Marques, A. R. A.; Mirzaian, M.; Aerts, J. M.; Ehinger, M.; Rothe, M.; Modlich, U.; Schambach, A.; Karlsson, S., Lentiviral gene therapy using cellular promoters cures type 1 Gaucher disease in mice. Mol Ther 2015, 23 (5), 835-844.
145. Keatinge, M.; Bui, H.; Menke, A.; Chen, Y. C.; Sokol, A. M.; Bai, Q.; Ellett, F.; Da Costa, M.; Burke, D.; Gegg, M.; Trollope, L.; Payne, T.; McTighe, A.; Mortiboys, H.; de Jager, S.; Nuthall, H.; Kuo, M. S.; Fleming, A.; Schapira, A. H.; Renshaw, S. A.; Highley, J. R.; Chacinska, A.; Panula, P.; Burton, E. A.; O'Neill, M. J.; Bandmann, O., Glucocerebrosidase 1 deficient Danio rerio mirror key pathological aspects of human Gaucher disease and provide evidence of early microglial activation preceding alpha-synuclein-independent neuronal cell death. Hum Mol Genet 2015, 24 (23), 6640-52.
146. Aerts, J. M.; Hollak, C. E., Plasma and metabolic abnormalities in Gaucher's disease. Baillieres Clin Haematol 1997, 10 (4), 691-709.
147. Aerts, J. M.; Kallemeijn, W. W.; Wegdam, W.; Joao Ferraz, M.; van Breemen, M. J.; Dekker, N.; Kramer, G.; Poorthuis, B. J.; Groener, J. E.; Cox-Brinkman, J.; Rombach, S. M.; Hollak, C. E.; Linthorst, G. E.; Witte, M. D.; Gold, H.; van der Marel, G. A.; Overkleeft, H. S.; Boot, R. G., Biomarkers in the diagnosis of lysosomal storage disorders: proteins, lipids, and inhibodies. J Inherit Metab Dis 2011, 34 (3), 605-19.
148. Vissers, J. P.; Langridge, J. I.; Aerts, J. M., Analysis and quantification of diagnostic serum markers and protein signatures for Gaucher disease. Mol Cell Proteomics 2007, 6 (5), 755-66.
149. Hollak, C. E.; Levi, M.; Berends, F.; Aerts, J. M.; van Oers, M. H., Coagulation abnormalities in type 1 Gaucher disease are due to low-grade activation and can be partly restored by enzyme supplementation therapy. Br J Haematol 1997, 96 (3), 470-6.
150. Brady, R. O., Enzyme replacement therapy: conception, chaos and culmination. Philos Trans R Soc Lond B Biol Sci 2003, 358 (1433), 915-9.
151. Maas, M.; van Kuijk, C.; Stoker, J.; Hollak, C. E.; Akkerman, E. M.; Aerts, J. F.; den Heeten, G. J., Quantification of bone involvement in Gaucher disease: MR imaging bone marrow burden score as an alternative to Dixon quantitative chemical shift MR imaging--initial experience. Radiology 2003, 229 (2), 554-61.
152. Aerts, J. M.; Hollak, C. E.; Boot, R. G.; Groener, J. E.; Maas, M., Substrate reduction therapy of glycosphingolipid storage disorders. J Inherit Metab Dis 2006, 29 (2-3), 449-56.
153. Platt, F. M.; Jeyakumar, M.; Andersson, U.; Priestman, D. A.; Dwek, R. A.; Butters, T. D.; Cox, T. M.; Lachmann, R. H.; Hollak, C.; Aerts, J. M.; Van Weely, S.; Hrebicek, M.; Moyses, C.; Gow, I.; Elstein, D.; Zimran, A., Inhibition of substrate synthesis as a strategy for glycolipid lysosomal storage disease therapy. J Inherit Metab Dis 2001, 24 (2), 275-90.
154. Heitner, R.; Elstein, D.; Aerts, J.; Weely, S.; Zimran, A., Low-dose N-butyldeoxynojirimycin (OGT 918) for type I Gaucher disease. Blood Cells Mol Dis 2002, 28 (2), 127-33.
155. Mistry, P. K.; Balwani, M.; Baris, H. N.; Turkia, H. B.; Burrow, T. A.; Charrow, J.; Cox, G. F.; Danda, S.; Dragosky, M.; Drelichman, G.; El-Beshlawy, A.; Fraga, C.; Freisens, S.; Gaemers, S.; Hadjiev, E.; Kishnani, P. S.; Lukina, E.; Maison-Blanche, P.; Martins, A. M.; Pastores, G.; Petakov, M.; Peterschmitt, M. J.; Rosenbaum, H.; Rosenbloom, B.; Underhill, L. H.; Cox, T. M., Safety, efficacy, and authorization of eliglustat as a first-line therapy in Gaucher disease type 1. Blood Cells Mol Dis 2018, 71, 71-74.
156. Shayman, J. A.; Larsen, S. D., The development and use of small molecule inhibitors of glycosphingolipid metabolism for lysosomal storage diseases. J Lipid Res 2014, 55 (7), 1215-25.
157. van Dussen, L.; Hendriks, E. J.; Groener, J. E.; Boot, R. G.; Hollak, C. E.; Aerts, J. M., Value of plasma chitotriosidase to assess non-neuronopathic Gaucher disease severity and progression in the era of enzyme replacement therapy. J Inherit Metab Dis 2014, 37 (6), 991-1001.
158. Maegawa, G. H.; Tropak, M. B.; Buttner, J. D.; Rigat, B. A.; Fuller, M.; Pandit, D.; Tang, L.; Kornhaber, G. J.; Hamuro, Y.; Clarke, J. T.; Mahuran, D. J., Identification and characterization of ambroxol as an enzyme enhancement agent for Gaucher disease. J Biol Chem 2009, 284 (35), 23502-16.
159. Zimran, A.; Altarescu, G.; Elstein, D., Pilot study using ambroxol as a pharmacological chaperone in type 1 Gaucher disease. Blood Cells Mol Dis 2013, 50 (2), 134-7.
160. Narita, A.; Shirai, K.; Itamura, S.; Matsuda, A.; Ishihara, A.; Matsushita, K.; Fukuda, C.; Kubota, N.; Takayama, R.; Shigematsu, H.; Hayashi, A.; Kumada, T.; Yuge, K.; Watanabe, Y.; Kosugi, S.; Nishida, H.; Kimura, Y.; Endo, Y.; Higaki, K.; Nanba, E.; Nishimura, Y.; Tamasaki, A.; Togawa, M.; Saito, Y.; Maegaki, Y.; Ohno, K.; Suzuki, Y., Ambroxol chaperone therapy for neuronopathic Gaucher disease: A pilot study. Ann Clin Transl Neurol 2016, 3 (3), 200-15.
161. Fog, C. K.; Zago, P.; Malini, E.; Solanko, L. M.; Peruzzo, P.; Bornaes, C.; Magnoni, R.; Mehmedbasic, A.; Petersen, N. H. T.; Bembi, B.; Aerts, J.; Dardis, A.; Kirkegaard, T., The heat shock protein amplifier

arimoclomol improves refolding, maturation and lysosomal activity of glucocerebrosidase. EBioMedicine 2018, 38, 142-153.
162. Aerts, J. M.; Ferraz, M. J.; Mirzaian, M.; Gaspar, P.; Oussoren, S. V.; Wisse, P.; Kuo, C. L.; Lelieveld, L. T.; Kytidou, K.; Hazeu, M. D.; Boer, D. E. C.; Meijer, R.; van der Lienden, M. J. C.; Herrera, D.; Gabriel, T. L.; Aten, J.; Overkleeft, H. S.; van Eijk, M. C.; Boot, R. G.; Marques, A. R. A., Lysosomal Storage Diseases. For Better or Worse: Adapting to Defective Lysosomal Glycosphingolipid. In eLs, John Wiley & Sons, Ltd.: Chichester, UK, 2017; pp 1-13.
163. Ferraz, M. J.; Marques, A. R.; Appelman, M. D.; Verhoek, M.; Strijland, A.; Mirzaian, M.; Scheij, S.; Ouairy, C. M.; Lahav, D.; Wisse, P.; Overkleeft, H. S.; Boot, R. G.; Aerts, J. M., Lysosomal glycosphingolipid catabolism by acid ceramidase: formation of glycosphingoid bases during deficiency of glycosidases. FEBS Lett 2016, 590 (6), 716-25.
164. Raghavan, S. S.; Mumford, R. A.; Kanfer, J. N., Isolation and characterization of glucosylsphingosine from Gaucher's spleen. J Lipid Res 1974, 15 (5), 484-90.
165. Nilsson, O.; Svennerholm, L., Accumulation of glucosylceramide and glucosylsphingosine (psychosine) in cerebrum and cerebellum in infantile and juvenile Gaucher disease. J Neurochem 1982, 39 (3), 709-18.
166. Dekker, N.; van Dussen, L.; Hollak, C. E.; Overkleeft, H.; Scheij, S.; Ghauharali, K.; van Breemen, M. J.; Ferraz, M. J.; Groener, J. E.; Maas, M.; Wijburg, F. A.; Speijer, D.; Tylki-Szymanska, A.; Mistry, P. K.; Boot, R. G.; Aerts, J. M., Elevated plasma glucosylsphingosine in Gaucher disease: relation to phenotype, storage cell markers, and therapeutic response. Blood 2011, 118 (16), e118-27.
167. Mirzaian, M.; Wisse, P.; Ferraz, M. J.; Gold, H.; Donker-Koopman, W. E.; Verhoek, M.; Overkleeft, H. S.; Boot, R. G.; Kramer, G.; Dekker, N.; Aerts, J. M., Mass spectrometric quantification of glucosylsphingosine in plasma and urine of type 1 Gaucher patients using an isotope standard. Blood Cells Mol Dis 2015, 54 (4), 307-14.
168. Lelieveld, L. T.; Mirzaian, M.; Kuo, C. L.; Artola, M.; Ferraz, M. J.; Peter, R. E. A.; Akiyama, H.; Greimel, P.; van den Berg, R.; Overkleeft, H. S.; Boot, R. G.; Meijer, A. H.; Aerts, J., Role of beta-glucosidase 2 in aberrant glycosphingolipid metabolism: model of glucocerebrosidase deficiency in zebrafish. J Lipid Res 2019, 60 (11), 1851-1867.
169. Groener, J. E.; Poorthuis, B. J.; Kuiper, S.; Helmond, M. T.; Hollak, C. E.; Aerts, J. M., HPLC for simultaneous quantification of total ceramide, glucosylceramide, and ceramide trihexoside concentrations in plasma. Clin Chem 2007, 53 (4), 742-7.
170. Mistry, P. K.; Liu, J.; Sun, L.; Chuang, W. L.; Yuen, T.; Yang, R.; Lu, P.; Zhang, K.; Li, J.; Keutzer, J.; Stachnik, A.; Mennone, A.; Boyer, J. L.; Jain, D.; Brady, R. O.; New, M. I.; Zaidi, M., Glucocerebrosidase 2 gene deletion rescues type 1 Gaucher disease. Proc Natl Acad Sci U S A 2014, 111 (13), 4934-9.
171. Taguchi, Y. V.; Liu, J.; Ruan, J.; Pacheco, J.; Zhang, X.; Abbasi, J.; Keutzer, J.; Mistry, P. K.; Chandra, S. S., Glucosylsphingosine Promotes alpha-Synuclein Pathology in Mutant GBA-Associated Parkinson's Disease. J Neurosci 2017, 37 (40), 9617-9631.
172. Nair, S.; Branagan, A. R.; Liu, J.; Boddupalli, C. S.; Mistry, P. K.; Dhodapkar, M. V., Clonal Immunoglobulin against Lysolipids in the Origin of Myeloma. N Engl J Med 2016, 374 (6), 555-61.
173. Pandey, M. K.; Grabowski, G. A.; Kohl, J., An unexpected player in Gaucher disease: The multiple roles of complement in disease development. Semin Immunol 2018, 37, 30-42.
174. Smith, N. J.; Fuller, M.; Saville, J. T.; Cox, T. M., Reduced cerebral vascularization in experimental neuronopathic Gaucher disease. J Pathol 2018, 244 (1), 120-128.
175. Ferraz, M. J.; Marques, A. R.; Gaspar, P.; Mirzaian, M.; van Roomen, C.; Ottenhoff, R.; Alfonso, P.; Irun, P.; Giraldo, P.; Wisse, P.; Sa Miranda, C.; Overkleeft, H. S.; Aerts, J. M., Lyso-glycosphingolipid abnormalities in different murine models of lysosomal storage disorders. Mol Genet Metab 2016, 117 (2), 186-93.
176. Kuchar, L.; Sikora, J.; Gulinello, M. E.; Poupetova, H.; Lugowska, A.; Malinova, V.; Jahnova, H.; Asfaw, B.; Ledvinova, J., Quantitation of plasmatic lysosphingomyelin and lysosphingomyelin-509 for differential screening of Niemann-Pick A/B and C diseases. Anal Biochem 2017, 525, 73-77.
177. Suzuki, K., Twenty five years of the "psychosine hypothesis": a personal perspective of its history and present status. Neurochem Res 1998, 23 (3), 251-9.
178. Aerts, J. M.; Groener, J. E.; Kuiper, S.; Donker-Koopman, W. E.; Strijland, A.; Ottenhoff, R.; van Roomen, C.; Mirzaian, M.; Wijburg, F. A.; Linthorst, G. E.; Vedder, A. C.; Rombach, S. M.; Cox-Brinkman, J.; Somerharju, P.; Boot, R. G.; Hollak, C. E.; Brady, R. O.; Poorthuis, B. J., Elevated globotriaosylsphingosine is a hallmark of Fabry disease. Proc Natl Acad Sci U S A 2008, 105 (8), 2812-7.
179. Choi, L.; Vernon, J.; Kopach, O.; Minett, M. S.; Mills, K.; Clayton, P. T.; Meert, T.; Wood, J. N., The Fabry disease-associated lipid Lyso-Gb3 enhances voltage-gated calcium currents in sensory neurons and causes pain. Neurosci Lett 2015, 594, 163-8.

180. Sanchez-Nino, M. D.; Carpio, D.; Sanz, A. B.; Ruiz-Ortega, M.; Mezzano, S.; Ortiz, A., Lyso-Gb3 activates Notch1 in human podocytes. Hum Mol Genet 2015, 24 (20), 5720-32.
181. Kaissarian, N.; Kang, J.; Shu, L.; Ferraz, M. J.; Aerts, J. M.; Shayman, J. A., Dissociation of globotriaosylceramide and impaired endothelial function in alpha-galactosidase-A deficient EA.hy926 cells. Mol Genet Metab 2018, 125 (4), 338-344.
182. Rombach, S. M.; Twickler, T. B.; Aerts, J. M.; Linthorst, G. E.; Wijburg, F. A.; Hollak, C. E., Vasculopathy in patients with Fabry disease: current controversies and research directions. Mol Genet Metab 2010, 99 (2), 99-108.
183. Ghauharali-van der Vlugt, K.; Langeveld, M.; Poppema, A.; Kuiper, S.; Hollak, C. E.; Aerts, J. M.; Groener, J. E., Prominent increase in plasma ganglioside GM3 is associated with clinical manifestations of type I Gaucher disease. Clin Chim Acta 2008, 389 (1-2), 109-13.
184. Langeveld, M.; Ghauharali, K. J.; Sauerwein, H. P.; Ackermans, M. T.; Groener, J. E.; Hollak, C. E.; Aerts, J. M.; Serlie, M. J., Type I Gaucher disease, a glycosphingolipid storage disorder, is associated with insulin resistance. J Clin Endocrinol Metab 2008, 93 (3), 845-51.
185. Yildiz, Y.; Matern, H.; Thompson, B.; Allegood, J. C.; Warren, R. L.; Ramirez, D. M.; Hammer, R. E.; Hamra, F. K.; Matern, S.; Russell, D. W., Mutation of beta-glucosidase 2 causes glycolipid storage disease and impaired male fertility. J Clin Invest 2006, 116 (11), 2985-94.
186. Boot, R. G.; Verhoek, M.; Donker-Koopman, W.; Strijland, A.; van Marle, J.; Overkleeft, H. S.; Wennekes, T.; Aerts, J. M., Identification of the non-lysosomal glucosylceramidase as beta-glucosidase 2. J Biol Chem 2007, 282 (2), 1305-12.
187. Hammer, M. B.; Eleuch-Fayache, G.; Schottlaender, L. V.; Nehdi, H.; Gibbs, J. R.; Arepalli, S. K.; Chong, S. B.; Hernandez, D. G.; Sailer, A.; Liu, G.; Mistry, P. K.; Cai, H.; Shrader, G.; Sassi, C.; Bouhlal, Y.; Houlden, H.; Hentati, F.; Amouri, R.; Singleton, A. B., Mutations in GBA2 cause autosomal-recessive cerebellar ataxia with spasticity. Am J Hum Genet 2013, 92 (2), 245-51.
188. Martin, E.; Schule, R.; Smets, K.; Rastetter, A.; Boukhris, A.; Loureiro, J. L.; Gonzalez, M. A.; Mundwiller, E.; Deconinck, T.; Wessner, M.; Jornea, L.; Oteyza, A. C.; Durr, A.; Martin, J. J.; Schols, L.; Mhiri, C.; Lamari, F.; Zuchner, S.; De Jonghe, P.; Kabashi, E.; Brice, A.; Stevanin, G., Loss of function of glucocerebrosidase GBA2 is responsible for motor neuron defects in hereditary spastic paraplegia. Am J Hum Genet 2013, 92 (2), 238-44.
189. Kancheva, D.; Atkinson, D.; De Rijk, P.; Zimon, M.; Chamova, T.; Mitev, V.; Yaramis, A.; Maria Fabrizi, G.; Topaloglu, H.; Tournev, I.; Parman, Y.; Parma, Y.; Battaloglu, E.; Estrada-Cuzcano, A.; Jordanova, A., Novel mutations in genes causing hereditary spastic paraplegia and Charcot-Marie-Tooth neuropathy identified by an optimized protocol for homozygosity mapping based on whole-exome sequencing. Genet Med 2016, 18 (6), 600-7.
190. Sultana, S.; Reichbauer, J.; Schule, R.; Mochel, F.; Synofzik, M.; van der Spoel, A. C., Lack of enzyme activity in GBA2 mutants associated with hereditary spastic paraplegia/cerebellar ataxia (SPG46). Biochem Biophys Res Commun 2015, 465 (1), 35-40.
191. Woeste, M. A.; Stern, S.; Raju, D. N.; Grahn, E.; Dittmann, D.; Gutbrod, K.; Dormann, P.; Hansen, J. N.; Schonauer, S.; Marx, C. E.; Hamzeh, H.; Korschen, H. G.; Aerts, J.; Bonigk, W.; Endepols, H.; Sandhoff, R.; Geyer, M.; Berger, T. K.; Bradke, F.; Wachten, D., Species-specific differences in nonlysosomal glucosylceramidase GBA2 function underlie locomotor dysfunction arising from loss-of-function mutations. J Biol Chem 2019, 294 (11), 3853-3871.
192. Saftig, P.; Klumperman, J., Lysosome biogenesis and lysosomal membrane proteins: trafficking meets function. Nat Rev Mol Cell Biol 2009, 10 (9), 623-35.
193. Luzio, J. P.; Hackmann, Y.; Dieckmann, N. M.; Griffiths, G. M., The biogenesis of lysosomes and lysosome-related organelles. Cold Spring Harb Perspect Biol 2014, 6 (9), a016840.
194. Bowman, S. L.; Bi-Karchin, J.; Le, L.; Marks, M. S., The road to lysosome-related organelles: Insights from Hermansky-Pudlak syndrome and other rare diseases. Traffic 2019, 20 (6), 404-435.
195. Delevoye, C.; Marks, M. S.; Raposo, G., Lysosome-related organelles as functional adaptations of the endolysosomal system. Curr Opin Cell Biol 2019, 59, 147-158.
196. Bahadori, R.; Rinner, O.; Schonthaler, H. B.; Biehlmaier, O.; Makhankov, Y. V.; Rao, P.; Jagadeeswaran, P.; Neuhauss, S. C., The Zebrafish fade out mutant: a novel genetic model for Hermansky-Pudlak syndrome. Invest Ophthalmol Vis Sci 2006, 47 (10), 4523-31.
197. Ellis, K.; Bagwell, J.; Bagnat, M., Notochord vacuoles are lysosome-related organelles that function in axis and spine morphogenesis. J Cell Biol 2013, 200 (5), 667-79.
198. Diaz-Tellez, A.; Zampedri, C.; Ramos-Balderas, J. L.; Garcia-Hernandez, F.; Maldonado, E., Zebrafish scarb2a insertional mutant reveals a novel function for the Scarb2/Limp2 receptor in notochord

development. Dev Dyn 2016, 245 (4), 508-19.
199. Groux-Degroote, S.; van Dijk, S. M.; Wolthoorn, J.; Neumann, S.; Theos, A. C.; De Maziere, A. M.; Klumperman, J.; van Meer, G.; Sprong, H., Glycolipid-dependent sorting of melanosomal from lysosomal membrane proteins by lumenal determinants. Traffic 2008, 9 (6), 951-63.
200. McLean, W. H.; Hull, P. R., Breach delivery: increased solute uptake points to a defective skin barrier in atopic dermatitis. J Invest Dermatol 2007, 127 (1), 8-10.
201. Yousef, H.; Alhajj, M.; Sharma, S., Anatomy, Skin (Integument), Epidermis. . In StatPearls, Treasure Island (FL), 2019.
202. Eckhart, L.; Lippens, S.; Tschachler, E.; Declercq, W., Cell death by cornification. Biochim Biophys Acta 2013, 1833 (12), 3471-3480.
203. Rawlings, A. V.; Harding, C. R., Moisturization and skin barrier function. Dermatol Ther 2004, 17 Suppl 1, 43-8.
204. Takahashi, M.; Tezuka, T., The content of free amino acids in the stratum corneum is increased in senile xerosis. Arch Dermatol Res 2004, 295 (10), 448-52.
205. Voegeli, D., The role of emollients in the care of patients with dry skin. Nurs Stand 2007, 22 (7), 62, 64-8.
206. Fluhr, J. W.; Elias, P. M., Stratum corneum pH: formation and function of the "acid mantle". Exog Dermatol 2002, 163-75.
207. Proksch, E., pH in nature, humans and skin. J Dermatol 2018, 45 (9), 1044-1052.
208. Elias, P. M., Epidermal lipids, membranes, and keratinization. Int J Dermatol 1981, 20 (1), 1-19.
209. Rinnerthaler, M.; Duschl, J.; Steinbacher, P.; Salzmann, M.; Bischof, J.; Schuller, M.; Wimmer, H.; Peer, T.; Bauer, J. W.; Richter, K., Age-related changes in the composition of the cornified envelope in human skin. Exp Dermatol 2013, 22 (5), 329-35.
210. Meguro, S.; Arai, Y.; Masukawa, Y.; Uie, K.; Tokimitsu, I., Relationship between covalently bound ceramides and transepidermal water loss (TEWL). Arch Dermatol Res 2000, 292 (9), 463-8.
211. Elias, P. M.; Gruber, R.; Crumrine, D.; Menon, G.; Williams, M. L.; Wakefield, J. S.; Holleran, W. M.; Uchida, Y., Formation and functions of the corneocyte lipid envelope (CLE). Biochim Biophys Acta 2014, 1841 (3), 314-8.
212. Rabionet, M.; Gorgas, K.; Sandhoff, R., Ceramide synthesis in the epidermis. Biochim Biophys Acta 2014, 1841 (3), 422-34.
213. Lampe, M. A.; Burlingame, A. L.; Whitney, J.; Williams, M. L.; Brown, B. E.; Roitman, E.; Elias, P. M., Human stratum corneum lipids: characterization and regional variations. J Lipid Res 1983, 24 (2), 120-30.
214. Janssens, M.; van Smeden, J.; Gooris, G. S.; Bras, W.; Portale, G.; Caspers, P. J.; Vreeken, R. J.; Kezic, S.; Lavrijsen, A. P.; Bouwstra, J. A., Lamellar lipid organization and ceramide composition in the stratum corneum of patients with atopic eczema. J Invest Dermatol 2011, 131 (10), 2136-8.
215. Imokawa, G.; Abe, A.; Jin, K.; Higaki, Y.; Kawashima, M.; Hidano, A., Decreased level of ceramides in stratum corneum of atopic dermatitis: an etiologic factor in atopic dry skin? J Invest Dermatol 1991, 96 (4), 523-6.
216. Motta, S.; Monti, M.; Sesana, S.; Caputo, R.; Carelli, S.; Ghidoni, R., Ceramide composition of the psoriatic scale. Biochim Biophys Acta 1993, 1182 (2), 147-51.
217. Coderch, L.; Lopez, O.; de la Maza, A.; Parra, J. L., Ceramides and skin function. Am J Clin Dermatol 2003, 4 (2), 107-29.
218. Elias, P. M.; Williams, M. L.; Crumrine, D.; Schmuth, M., Inherited clinical disorders of lipid metabolism. Curr Probl Dermatol 2010, 39, 30-88.
219. Wertz, P., Epidermal Lamellar Granules. Skin Pharmacol Physiol 2018, 31 (5), 262-268.
220. Mitsutake, S.; Suzuki, C.; Akiyama, M.; Tsuji, K.; Yanagi, T.; Shimizu, H.; Igarashi, Y., ABCA12 dysfunction causes a disorder in glucosylceramide accumulation during keratinocyte differentiation. J Dermatol Sci 2010, 60 (2), 128-9.
221. Akiyama, M., The roles of ABCA12 in epidermal lipid barrier formation and keratinocyte differentiation. Biochim Biophys Acta 2014, 1841 (3), 435-40.
222. Akiyama, M.; Sugiyama-Nakagiri, Y.; Sakai, K.; McMillan, J. R.; Goto, M.; Arita, K.; Tsuji-Abe, Y.; Tabata, N.; Matsuoka, K.; Sasaki, R.; Sawamura, D.; Shimizu, H., Mutations in lipid transporter ABCA12 in harlequin ichthyosis and functional recovery by corrective gene transfer. J Clin Invest 2005, 115 (7), 1777-84.
223. Schurer, N. Y.; Elias, P. M., The biochemistry and function of stratum corneum lipids. Adv Lipid Res 1991, 24, 27-56.
224. Feingold, K. R., Lamellar bodies: the key to cutaneous barrier function. J Invest Dermatol 2012, 132 (8), 1951-3.
225. Geeraert, L.; Mannaerts, G. P.; van Veldhoven, P. P., Conversion of dihydroceramide into ceramide:

involvement of a desaturase. Biochem J 1997, 327 (Pt 1), 125-32.
226. Michel, C.; van Echten-Deckert, G.; Rother, J.; Sandhoff, K.; Wang, E.; Merrill, A. H., Jr., Characterization of ceramide synthesis. A dihydroceramide desaturase introduces the 4,5-trans-double bond of sphingosine at the level of dihydroceramide. J Biol Chem 1997, 272 (36), 22432-7.
227. Savile, C. K.; Fabrias, G.; Buist, P. H., Dihydroceramide delta(4) desaturase initiates substrate oxidation at C-4. J Am Chem Soc 2001, 123 (19), 4382-5.
228. Mizutani, Y.; Kihara, A.; Igarashi, Y., Identification of the human sphingolipid C4-hydroxylase, hDES2, and its up-regulation during keratinocyte differentiation. FEBS Lett 2004, 563 (1-3), 93-7.
229. Breiden, B.; Sandhoff, K., The role of sphingolipid metabolism in cutaneous permeability barrier formation. Biochim Biophys Acta 2014, 1841 (3), 441-52.
230. Park, Y. H.; Jang, W. H.; Seo, J. A.; Park, M.; Lee, T. R.; Park, Y. H.; Kim, D. K.; Lim, K. M., Decrease of ceramides with very long-chain fatty acids and downregulation of elongases in a murine atopic dermatitis model. J Invest Dermatol 2012, 132 (2), 476-9.
231. Uchida, Y., The role of fatty acid elongation in epidermal structure and function. Dermatoendocrinol 2011, 3 (2), 65-9.
232. Hanley, K.; Ng, D. C.; He, S. S.; Lau, P.; Min, K.; Elias, P. M.; Bikle, D. D.; Mangelsdorf, D. J.; Williams, M. L.; Feingold, K. R., Oxysterols induce differentiation in human keratinocytes and increase Ap-1-dependent involucrin transcription. J Invest Dermatol 2000, 114 (3), 545-53.
233. Denning, M. F.; Kazanietz, M. G.; Blumberg, P. M.; Yuspa, S. H., Cholesterol sulfate activates multiple protein kinase C isoenzymes and induces granular cell differentiation in cultured murine keratinocytes. Cell Growth Differ 1995, 6 (12), 1619-26.
234. Hanley, K.; Wood, L.; Ng, D. C.; He, S. S.; Lau, P.; Moser, A.; Elias, P. M.; Bikle, D. D.; Williams, M. L.; Feingold, K. R., Cholesterol sulfate stimulates involucrin transcription in keratinocytes by increasing Fra-1, Fra-2, and Jun D. J Lipid Res 2001, 42 (3), 390-8.
235. Elias, P. M.; Williams, M. L.; Holleran, W. M.; Jiang, Y. J.; Schmuth, M., Pathogenesis of permeability barrier abnormalities in the ichthyoses: inherited disorders of lipid metabolism. J Lipid Res 2008, 49 (4), 697-714.
236. Feingold, K. R.; Jiang, Y. J., The mechanisms by which lipids coordinately regulate the formation of the protein and lipid domains of the stratum corneum: Role of fatty acids, oxysterols, cholesterol sulfate and ceramides as signaling molecules. Dermatoendocrinol 2011, 3 (2), 113-8.
237. Elias, P. M.; Crumrine, D.; Rassner, U.; Hachem, J. P.; Menon, G. K.; Man, W.; Choy, M. H.; Leypoldt, L.; Feingold, K. R.; Williams, M. L., Basis for abnormal desquamation and permeability barrier dysfunction in RXLI. J Invest Dermatol 2004, 122 (2), 314-9.
238. Sato, J.; Denda, M.; Nakanishi, J.; Nomura, J.; Koyama, J., Cholesterol sulfate inhibits proteases that are involved in desquamation of stratum corneum. J Invest Dermatol 1998, 111 (2), 189-93.
239. Cox, P.; Squier, C. A., Variations in lipids in different layers of porcine epidermis. J Invest Dermatol 1986, 87 (6), 741-4.
240. Ranasinghe, A. W.; Wertz, P. W.; Downing, D. T.; Mackenzie, I. C., Lipid composition of cohesive and desquamated corneocytes from mouse ear skin. J Invest Dermatol 1986, 86 (2), 187-90.
241. Akiyama, M., Corneocyte lipid envelope (CLE), the key structure for skin barrier function and ichthyosis pathogenesis. J Dermatol Sci 2017, 88 (1), 3-9.
242. Feingold, K. R., Thematic review series: skin lipids. The role of epidermal lipids in cutaneous permeability barrier homeostasis. J Lipid Res 2007, 48 (12), 2531-46.
243. Greene, S. L.; Muller, S. A., Netherton's syndrome. Report of a case and review of the literature. J Am Acad Dermatol 1985, 13 (2 Pt 2), 329-37.
244. Traupe, H., The ichthyoses : a guide to clinical diagnosis, genetic counseling, and therapy. In Springer-Verlag, Berlin; New York, 1989.
245. Stone, D. L.; Carey, W. F.; Christodoulou, J.; Sillence, D.; Nelson, P.; Callahan, M.; Tayebi, N.; Sidransky, E., Type 2 Gaucher disease: the collodion baby phenotype revisited. Arch Dis Child Fetal Neonatal Ed 2000, 82 (2), F163-6.
246. Holleran, W. M.; Takagi, Y.; Menon, G. K.; Legler, G.; Feingold, K. R.; Elias, P. M., Processing of epidermal glucosylceramides is required for optimal mammalian cutaneous permeability barrier function. J Clin Invest 1993, 91 (4), 1656-64.
247. Holleran, W. M.; Ginns, E. I.; Menon, G. K.; Grundmann, J. U.; Fartasch, M.; McKinney, C. E.; Elias, P. M.; Sidransky, E., Consequences of beta-glucocerebrosidase deficiency in epidermis. Ultrastructure and permeability barrier alterations in Gaucher disease. J Clin Invest 1994, 93 (4), 1756-64.
248. Holleran, W. M.; Takagi, Y.; Menon, G. K.; Jackson, S. M.; Lee, J. M.; Feingold, K. R.; Elias, P. M.,

Permeability barrier requirements regulate epidermal beta-glucocerebrosidase. J Lipid Res 1994, 35 (5), 905-12.
249. Doering, T.; Holleran, W. M.; Potratz, A.; Vielhaber, G.; Elias, P. M.; Suzuki, K.; Sandhoff, K., Sphingolipid activator proteins are required for epidermal permeability barrier formation. J Biol Chem 1999, 274 (16), 11038-45.
250. Freinkel, R. K.; Traczyk, T. N., Lipid composition and acid hydrolase content of lamellar granules of fetal rat epidermis. J Invest Dermatol 1985, 85 (4), 295-8.
251. Grayson, S.; Johnson-Winegar, A. G.; Wintroub, B. U.; Isseroff, R. R.; Epstein, E. H., Jr.; Elias, P. M., Lamellar body-enriched fractions from neonatal mice: preparative techniques and partial characterization. J Invest Dermatol 1985, 85 (4), 289-94.
252. Madison, K. C.; Sando, G. N.; Howard, E. J.; True, C. A.; Gilbert, D.; Swartzendruber, D. C.; Wertz, P. W., Lamellar granule biogenesis: a role for ceramide glucosyltransferase, lysosomal enzyme transport, and the Golgi. J Investig Dermatol Symp Proc 1998, 3 (2), 80-6.
253. Takagi, Y.; Kriehuber, E.; Imokawa, G.; Elias, P. M.; Holleran, W. M., Beta-glucocerebrosidase activity in mammalian stratum corneum. J Lipid Res 1999, 40 (5), 861-9.
254. Schmuth, M.; Schoonjans, K.; Yu, Q. C.; Fluhr, J. W.; Crumrine, D.; Hachem, J. P.; Lau, P.; Auwerx, J.; Elias, P. M.; Feingold, K. R., Role of peroxisome proliferator-activated receptor alpha in epidermal development in utero. J Invest Dermatol 2002, 119 (6), 1298-303.
255. Hachem, J. P.; Crumrine, D.; Fluhr, J.; Brown, B. E.; Feingold, K. R.; Elias, P. M., pH directly regulates epidermal permeability barrier homeostasis, and stratum corneum integrity/cohesion. J Invest Dermatol 2003, 121 (2), 345-53.
256. van Smeden, J.; Dijkhoff, I. M.; Helder, R. W. J.; Al-Khakany, H.; Boer, D. E. C.; Schreuder, A.; Kallemeijn, W. W.; Absalah, S.; Overkleeft, H. S.; Aerts, J.; Bouwstra, J. A., In situ visualization of glucocerebrosidase in human skin tissue: zymography versus activity-based probe labeling. J Lipid Res 2017, 58 (12), 2299-2309.
257. Schmuth, M.; Man, M. Q.; Weber, F.; Gao, W.; Feingold, K. R.; Fritsch, P.; Elias, P. M.; Holleran, W. M., Permeability barrier disorder in Niemann-Pick disease: sphingomyelin-ceramide processing required for normal barrier homeostasis. J Invest Dermatol 2000, 115 (3), 459-66.
258. Jensen, J. M.; Schutze, S.; Forl, M.; Kronke, M.; Proksch, E., Roles for tumor necrosis factor receptor p55 and sphingomyelinase in repairing the cutaneous permeability barrier. J Clin Invest 1999, 104 (12), 1761-70.
259. Oyoshi, M. K.; He, R.; Kumar, L.; Yoon, J.; Geha, R. S., Cellular and molecular mechanisms in atopic dermatitis. Adv Immunol 2009, 102, 135-226.
260. Wollenberg, A.; Rawer, H. C.; Schauber, J., Innate immunity in atopic dermatitis. Clin Rev Allergy Immunol 2011, 41 (3), 272-81.
261. David Boothe, W.; Tarbox, J. A.; Tarbox, M. B., Atopic Dermatitis: Pathophysiology. Adv Exp Med Biol 2017, 1027, 21-37.
262. Leung, D. Y.; Bieber, T., Atopic dermatitis. Lancet 2003, 361 (9352), 151-60.
263. Seguchi, T.; Cui, C. Y.; Kusuda, S.; Takahashi, M.; Aisu, K.; Tezuka, T., Decreased expression of filaggrin in atopic skin. Arch Dermatol Res 1996, 288 (8), 442-6.
264. Palmer, C. N.; Irvine, A. D.; Terron-Kwiatkowski, A.; Zhao, Y.; Liao, H.; Lee, S. P.; Goudie, D. R.; Sandilands, A.; Campbell, L. E.; Smith, F. J.; O'Regan, G. M.; Watson, R. M.; Cecil, J. E.; Bale, S. J.; Compton, J. G.; DiGiovanna, J. J.; Fleckman, P.; Lewis-Jones, S.; Arseculeratne, G.; Sergeant, A.; Munro, C. S.; El Houate, B.; McElreavey, K.; Halkjaer, L. B.; Bisgaard, H.; Mukhopadhyay, S.; McLean, W. H., Common loss-of-function variants of the epidermal barrier protein filaggrin are a major predisposing factor for atopic dermatitis. Nat Genet 2006, 38 (4), 441-6.
265. Cole, C.; Kroboth, K.; Schurch, N. J.; Sandilands, A.; Sherstnev, A.; O'Regan, G. M.; Watson, R. M.; McLean, W. H.; Barton, G. J.; Irvine, A. D.; Brown, S. J., Filaggrin-stratified transcriptomic analysis of pediatric skin identifies mechanistic pathways in patients with atopic dermatitis. J Allergy Clin Immunol 2014, 134 (1), 82-91.
266. Jungersted, J. M.; Scheer, H.; Mempel, M.; Baurecht, H.; Cifuentes, L.; Hogh, J. K.; Hellgren, L. I.; Jemec, G. B.; Agner, T.; Weidinger, S., Stratum corneum lipids, skin barrier function and filaggrin mutations in patients with atopic eczema. Allergy 2010, 65 (7), 911-8.
267. Farwanah, H.; Raith, K.; Neubert, R. H.; Wohlrab, J., Ceramide profiles of the uninvolved skin in atopic dermatitis and psoriasis are comparable to those of healthy skin. Arch Dermatol Res 2005, 296 (11), 514-21.
268. Ishikawa, J.; Narita, H.; Kondo, N.; Hotta, M.; Takagi, Y.; Masukawa, Y.; Kitahara, T.; Takema, Y.; Koyano, S.; Yamazaki, S.; Hatamochi, A., Changes in the ceramide profile of atopic dermatitis patients. J Invest Dermatol 2010, 130 (10), 2511-4.

269. Yamamoto, A.; Serizawa, S.; Ito, M.; Sato, Y., Stratum corneum lipid abnormalities in atopic dermatitis. Arch Dermatol Res 1991, 283 (4), 219-23.
270. Bleck, O.; Abeck, D.; Ring, J.; Hoppe, U.; Vietzke, J. P.; Wolber, R.; Brandt, O.; Schreiner, V., Two ceramide subfractions detectable in Cer(AS) position by HPTLC in skin surface lipids of non-lesional skin of atopic eczema. J Invest Dermatol 1999, 113 (6), 894-900.
271. Di Nardo, A.; Wertz, P.; Giannetti, A.; Seidenari, S., Ceramide and cholesterol composition of the skin of patients with atopic dermatitis. Acta Derm Venereol 1998, 78 (1), 27-30.
272. Janssens, M.; van Smeden, J.; Gooris, G. S.; Bras, W.; Portale, G.; Caspers, P. J.; Vreeken, R. J.; Hankemeier, T.; Kezic, S.; Wolterbeek, R.; Lavrijsen, A. P.; Bouwstra, J. A., Increase in short-chain ceramides correlates with an altered lipid organization and decreased barrier function in atopic eczema patients. J Lipid Res 2012, 53 (12), 2755-66.
273. van Smeden, J.; Janssens, M.; Kaye, E. C.; Caspers, P. J.; Lavrijsen, A. P.; Vreeken, R. J.; Bouwstra, J. A., The importance of free fatty acid chain length for the skin barrier function in atopic eczema patients. Exp Dermatol 2014, 23 (1), 45-52.
274. Macheleidt, O.; Kaiser, H. W.; Sandhoff, K., Deficiency of epidermal protein-bound omega-hydroxyceramides in atopic dermatitis. J Invest Dermatol 2002, 119 (1), 166-73.
275. Ohno, Y.; Suto, S.; Yamanaka, M.; Mizutani, Y.; Mitsutake, S.; Igarashi, Y.; Sassa, T.; Kihara, A., ELOVL1 production of C24 acyl-CoAs is linked to C24 sphingolipid synthesis. Proc Natl Acad Sci U S A 2010, 107 (43), 18439-44.
276. Danso, M.; Boiten, W.; van Drongelen, V.; Gmelig Meijling, K.; Gooris, G.; El Ghalbzouri, A.; Absalah, S.; Vreeken, R.; Kezic, S.; van Smeden, J.; Lavrijsen, S.; Bouwstra, J., Altered expression of epidermal lipid bio-synthesis enzymes in atopic dermatitis skin is accompanied by changes in stratum corneum lipid composition. J Dermatol Sci 2017, 88 (1), 57-66.
277. Imokawa, G., A possible mechanism underlying the ceramide deficiency in atopic dermatitis: expression of a deacylase enzyme that cleaves the N-acyl linkage of sphingomyelin and glucosylceramide. J Dermatol Sci 2009, 55 (1), 1-9.
278. Ishibashi, M.; Arikawa, J.; Okamoto, R.; Kawashima, M.; Takagi, Y.; Ohguchi, K.; Imokawa, G., Abnormal expression of the novel epidermal enzyme, glucosylceramide deacylase, and the accumulation of its enzymatic reaction product, glucosylsphingosine, in the skin of patients with atopic dermatitis. Lab Invest 2003, 83 (3), 397-408.
279. Higuchi, K.; Hara, J.; Okamoto, R.; Kawashima, M.; Imokawa, G., The skin of atopic dermatitis patients contains a novel enzyme, glucosylceramide sphingomyelin deacylase, which cleaves the N-acyl linkage of sphingomyelin and glucosylceramide. Biochem J 2000, 350 Pt 3, 747-56.
280. Kim, H. J.; Kim, K. M.; Noh, M.; Yoo, H. J.; Lee, C. H., Glucosylsphingosine Induces Itch-Scratch Responses in Mice. Biomol Ther 2010, 18 (3), 316-320.
281. Afzal, R.; Shim, W. S., Glucosylsphingosine Activates Serotonin Receptor 2a and 2b: Implication of a Novel Itch Signaling Pathway. Biomol Ther (Seoul) 2017, 25 (5), 497-503.
282. Jin, K.; Higaki, Y.; Takagi, Y.; Higuchi, K.; Yada, Y.; Kawashima, M.; Imokawa, G., Analysis of beta-glucocerebrosidase and ceramidase activities in atopic and aged dry skin. Acta Derm Venereol 1994, 74 (5), 337-40.

Chapter 3

In situ visualization of glucocerebrosidase in human skin tissue: zymography versus activity-based probe labeling

In situ visualization of glucocerebrosidase in human skin tissue: zymography versus activity-based probe labeling

J. van Smeden, I.M. Dijkhoff , R.W.J. Helder, H. Al-Khakany, **D.E.C. Boer**, A. Schreuder, W.W. Kallemeijn, S. Absalah, H.S. Overkleeft, J.M.F.G. Aerts, J.A. Bouwstra.

Abstract

Epidermal β-glucocerebrosidase (GCase), an acid β-glucosidase normally located in lysosomes, converts (glucosyl)ceramides into ceramides, which is crucial to generate an optimal barrier function of the outermost skin layer, the stratum corneum (SC). Here we report on two developed *in situ* methods to localize active GCase in human epidermis: i) an optimized zymography method that is less labor intensive and visualizes enzymatic activity with higher resolution than currently reported methods using either substrate 4-methylumbelliferyl-β-D-glucopyranoside or resorufin-β-D-glucopyranoside; and ii) a novel technique to visualize active GCase molecules by their specific labeling with a fluorescent activity-based probe (ABP), MDW941. The latter method pro¬ved to be more robust and sensitive, provided higher resolution microscopic images, and was less prone to sample preparation effects. Moreover, in contrast to the zymography substrates that react with various β-glucosidases, MDW941 specifically labeled GCase. We demonstrate that active GCase in the epidermis is primarily located in the extracellular lipid matrix at the interface of the viable epidermis and the lower layers of the SC. With ABP-labeling, we observed reduced GCase activity in 3D-cultured skin models when supplemented with the reversible inhibitor, isofagomine, irrespective of GCase expression. This inhibition affected the SC ceramide composition: MS analysis revealed an inhibitor-dependent increase in the glucosylceramide:ceramide ratio.

Introduction

Epidermal β-glucocerebrosidase (GCase), an acid β-glucosidase normally located in lysosomes, converts (glucosyl)ceramides into ceramides, which is crucial to generate an optimal barrier function of the outermost skin layer,

the stratum corneum (SC). Here we report on two developed *in situ* methods to localize active GCase in human epidermis: *i*) an optimized zymography method that is less labor intensive and visualizes enzymatic activity with higher resolution than currently reported methods using either substrate 4-methylumbelliferyl-β-D-glucopyranoside or resorufin-β-D-glucopyranoside; and *ii*) a novel technique to visualize active GCase molecules by their specific labeling with a fluorescent activity-based probe (ABP), MDW941. The latter method pro¬ved to be more robust and sensitive, provided higher resolution microscopic images, and was less prone to sample preparation effects. Moreover, in contrast to the zymography substrates that react with various β-glucosidases, MDW941 specifically labeled GCase. We demonstrate that active GCase in the epidermis is primarily located in the extracellular lipid matrix at the interface of the viable epidermis and the lower layers of the SC. With ABP-labeling, we observed reduced GCase activity in 3D-cultured skin models when supplemented with the reversible inhibitor, isofagomine, irrespective of GCase expression. This inhibition affected the SC ceramide composition: MS analysis revealed an inhibitor-dependent increase in the glucosylceramide:ceramide ratio.

β-Glucocerebrosidase (GCase; also referred to as acid β-glucosidase or GBA; EC 3.2.1.45) is a lysosomal enzyme that hydrolyzes glucosylceramides (GlcCers) into ceramides [1, 2]. Inherited GCase deficiency (as occurs in Gaucher disease) results in lysosomal accumulation of GlcCers, primarily in macrophages located in the liver, spleen, and bone marrow [3]. Complete absence of GCase causes an extreme Gaucher disease phenotype (so-called collodion baby) with fatal skin abnormalities [4]. Newly synthesized GCase is normally transported to

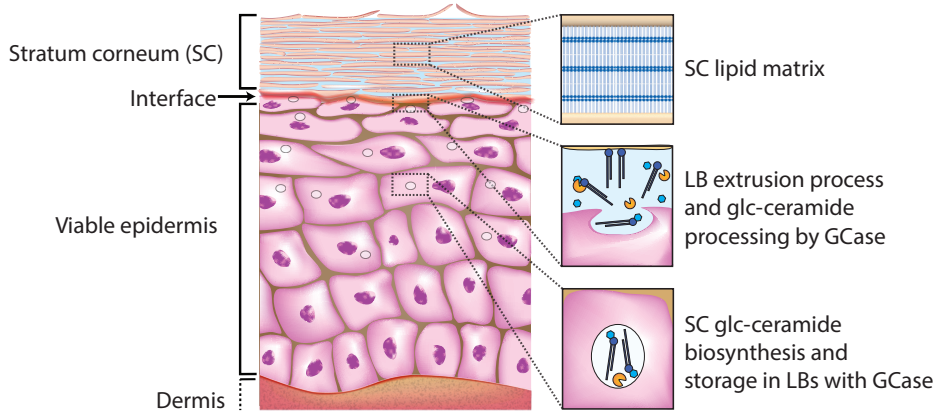

Figure 1: Epidermis with the outermost layer (SC) functioning as the primary skin barrier. The biosynthesis of the SC ceramides is located in the lower and middle epidermal layers, while storage takes place at the lamellar bodies together with processing enzymes like GCase. Once extruded at the interface of the viable epidermis and the SC, GCase converts the GlcCers into their final barrier components, the ceramides, which become part of the ordered SC lipid matrix.

the lysosomal compartment by binding to the lysosomal integral membrane protein type-2 [5]. In lysosomes, GCase is active at its optimal pH of around 5.2–5.6, assisted by the activator protein, saposin C [6, 7]. Besides lysosomal GCase, two other β-glucosidases can be present in cells (GBA2 and GBA3). GBA2 can also convert GlcCers into ceramides, implicating that such conversion may also occur outside the lysosomes [8]. Here, GCase is used when specifically referring to lysosomal β-glucosidase, whereas any β-glucosidase is indicated as GBA.

To date, over 270 *GBA* mutations have been identified (https://research.cchmc.org/LOVD2/) that may either lead to reduced protein expression or result in nonfunctional GCase or a reduced enzyme activity [9]. GCase expression levels do not often relate to enzyme activity because of various aspects, like posttranslational modifications of the protein or cofactors [10]. This suggests that GCase activity (rather than gene or protein expression) is indicative for the clinical outcome. However, current studies on lipid metabolic enzymes mainly focus on methods to quantify gene expression or protein levels, rather than enzyme activity. To date, enzyme activity is often performed via zymography studies in which a selective substrate is converted to a fluorescent product by the enzyme of interest. Many *in vitro* and *in situ* methods have been established, particularly for studies on proteases [11-13]. Reports on zymography of other enzymes are less common, but GCase is an excellent example in which established methods have proven their value: 4-methylumbelliferyl-β-D-glucopyranoside (4-MU-β-glc) has been used as a substrate and is converted by GCase into the blue fluorophore, 4-methylumbelliferone ($\lambda em,max \approx$ 450 nm; supplemental Figure S1) [7]. A common alternative is resorufin-β-D-glucopyranoside (res-β-glc), which results in red fluorescent resorufin ($\lambda em,max \approx 580$ nm). The substrates are limited in their sensitivity and substrate specificity is a matter of concern. Alternatives to zymography are therefore needed to examine the presence of active GCase, like the use of activity-based probes (ABPs) [14, 15]. This technique relies on mechanism-based labeling of GCase with a fluorescent suicide inhibitor [16, 17]. MDW941 is a cyclophellitol β-epoxide tagged with a BODIPY red dye (supplemental Figure S1) [16]. It binds covalently to the catalytic nucleophile, E340, of GCase with high affinity and specificity. Fluorescent ABPs like MDW941 have been successfully used to visualize *in situ* active GCase molecules in cultured cells and tissues of rodents [16, 18], but human skin tissue has so far never been examined with these ABPs.

The aim of this study was to develop, optimize, and compare zymography and ABP-labeling to visualize *in situ* active GCase in human skin tissue. Human skin contains a dermal and an epidermal component, the latter consisting of several layers, including the stratum corneum (SC), the nonviable outermost skin layer (Figure 1). This layer acts as a pivotal barrier and contains terminally differentiated enucleated cells embedded in a ceramide-rich lipid matrix [19]. In this matrix, ceramides are a major component and have uniquely long

hydrocarbon chains [20]. Changes in the composition of SC ceramides or the expression of GCase may lead to an impaired barrier function that has been encountered in several inflammatory skin diseases (e.g., eczema) [21, 22]. These ceramides are synthesized in the endoplasmic reticulum of viable epidermal cells [23-25] and are subsequently stored as GlcCers in vesicles (so-called lamellar bodies) together with GCase and other enzymes that convert the lipid precursors into barrier lipids [26]. This conversion occurs during the lamellar body extrusion process: the lamellar bodies fuse with the cell membrane and extrude their lipid and enzyme content into the extracellular space between the viable epidermis and the SC [20]. To date, it has been reported that the conversion of GlcCers into ceramides by GCase takes place in this lipid-rich environment [27, 28]. Subsequently, the ceramides are arranged into lipid layers (together with other barrier lipids, like fatty acids and cholesterol) forming

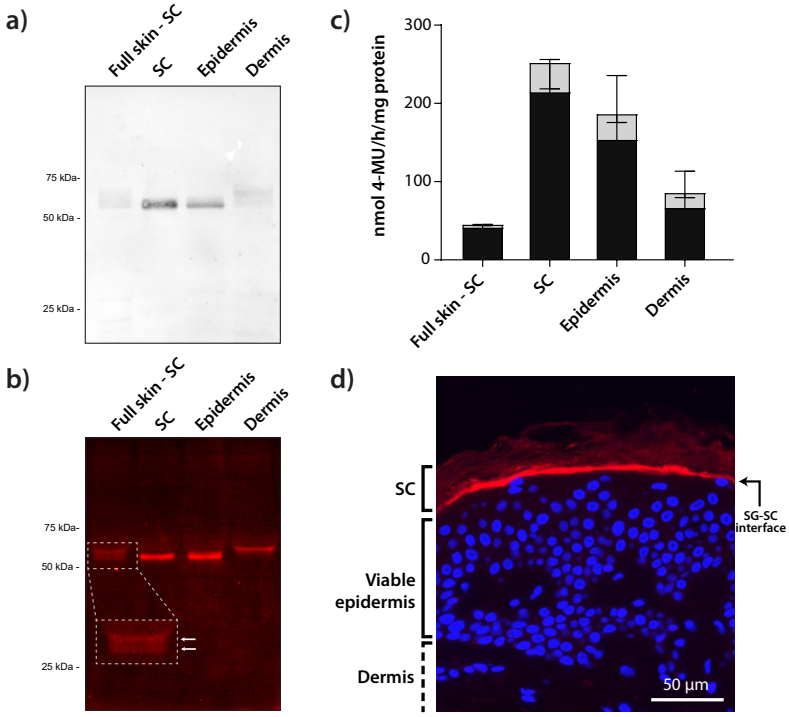

Figure 2: Labeling of GCase in human skin tissue. A: Western blot of GCase in different human skin tissue layers using monoclonal anti-GCase (50 mg of protein per lane were loaded on the SDS-PAGE gel). Full skinSC, full thickness skin without SC. B: Fluorescent labeling of active GCase (5 mg of protein per lane were loaded on the SDS-PAGE gel) in skin tissues exposed to MDW941. C: Bar plots of the enzymatic activity of GCase in skin tissue, as determined by a 4-MU-b-glc substrate assay (gray + black bars). The fraction of 4-methylumbelliferone converted by GCase is indicated by black bars (n = 3, mean ± SD). D: Immunohistochemical fluorescent staining of expressed GCase (red), and counterstaining with DAPI (blue) for cell nuclei. Objective lens magnification 20×.

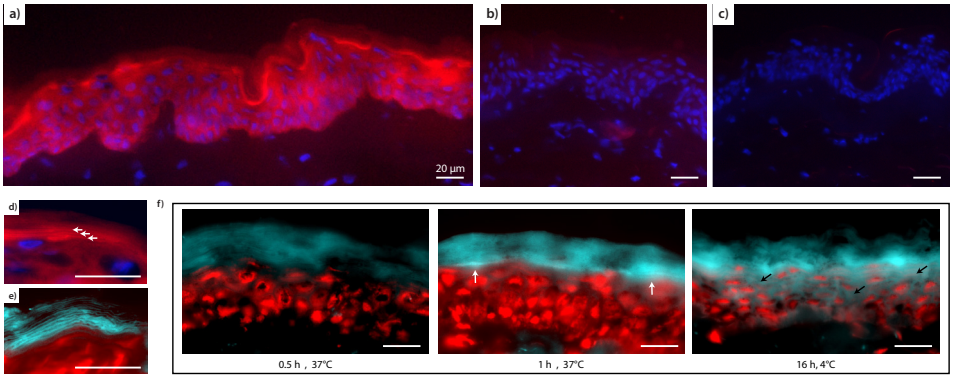

Figure 3: GCase *in situ* zymography assay on human skin sections. A: Microscopy photographs of 20× magnification using res-β-glc substrate (red) and DAPI counterstaining to detect cell nuclei (blue). B: Additional preincubation with competitive GCase inhibitor, resorufin, successfully obstructs substrate conversion. C: No red fluorescence is observed when no substrate is applied (negative control). D: Photograph (63× magnification) in which the red fluorescent product layers are indicated by the white arrows. E: Images (63× magnification) using 4-MU--β-glc substrate focusing on the blue fluorescent product layers. Red counterstaining was performed using propidium iodide to stain cell nuclei. F: Microscopy images (63× magnification) of the results from different substrate incubation periods (0, 1, and 16 h). White arrows indicate highest signal contrast, whereas black arrows illustrate the diffusion effect of the fluorescent product at longer time periods. Scale bars represent 20 mm.

lamellar stacks. These lamellar stacks function as the principal barrier and are crucial to protect the body from the environment [29, 30]. The conversion of GlcCers into ceramides by GCase in the extracellular space is contradictory to the notion that GCase is solely active in the lysosomal compartment [2, 31]. Using two newly developed techniques (zymography and ABP-labeling), we were able to visualize active β-glucosidase and, more specifically, active GCase.

First, the presence of GCase from isolated skin layers was demonstrated and the specificity of the ABP for GCase (MDW941) in skin lysate was determined. Second, an optimized *in situ* zymography method was developed, as current methods for visualizing GCase activity in skin sections have substantial (conflicting) differences in their procedures [7, 32, 33]. Third, a new method to detect GCase in human epidermis by means of *in situ* ABP-labeling was optimized in regard to ABP concentration, buffer conditions, and washing procedures. This method was applied on a cultured 3D-human skin equivalent (HSE) model that mimics human skin [34], while the culture medium was supplemented with the GCase inhibitor, isofagomine (supplemental Figure S1). Isofagomine selectively inhibits GCase at low nanomolar concentration, but not the other β-glucosidases, GBA2 and GBA3 [35, 36]. This enabled us to study whether inhibition of GCase activity directly affects the SC glucosyl (ceramide) composition.

Results

GCase is primarily located near the interface of the viable epidermis and the SC.

IsIsolated lysates of human dermis, epidermis, SC, and the viable skin layers minus the SC (full skin-SC) were analyzed by Western blotting for the presence of GCase protein. GCase (~60 kDa) was expressed more in the epidermis than the dermis (Figure 2A). More specifically, GCase was predominantly located in the SC, as the viable skin layers (skin without SC) showed protein bands with much lower intensity. In addition to the Western blot procedure, we used the ABP, MDW941, to fluorescently label active GCase in skin tissue (Figure 2B; fluorescent bands at ~60 kDa; Coomassie brilliant blue staining for total protein content is provided in supplemental Figure S2). Interestingly, GCase located in the dermis appears to have a slightly higher molecular mass compared with GCase in the epidermis, which matches the presence of two bands in the lysate with epidermis and dermis (full-thickness skin minus SC). Subsequently, a 4-MU-β-glc activity assay was performed to quantify the activity of GCase in the different skin layers (Figure 2C). In all skin layers, GCase was shown to be primarily GCase and had the highest activity in epidermal tissue and SC tissue. This is in line with the Western blot and gel electrophoresis results presented in Figure 2A, B, where the most pronounced bands were observed in the epidermis and SC as well. We then performed *in situ* immunohistochemical staining to determine the exact location of GCase expression (Figure 2D). In line with the aforementioned results, GCase proved to be expressed in the viable epidermis and SC layers, predominantly along the whole interface of the viable epidermis and the SC. Having confirmed that GCase was predominantly expressed and active in epidermal skin layers and amenable to selective labeling by MDW941, we next established detailed protocols for localizing active GCase in human skin tissue. We focused on two *in situ* techniques: i) zymography of GCase, and ii) ABP-labeling of GCase.

In situ *zymography of epidermal GCase: method development of 4-MU-β-glc and res-β-glc substrates.*

We optimized the zymography protocol for two commonly used substrates, 4-MU-β-glc and res-β-glc, which, upon conversion by GCase, lead to their fluorescent products, 4-methylumbelliferone (indigo) and resorufin (orange/red). The procedure to obtain the high resolution *in situ* zymography images was an important aspect of the optimization procedure. We optimized the protocol for the following four important aspects concerning substrate reconstitution, washing procedure, substrate incubation buffer, and incubation period and temperature. First, res-β-glc is relatively insoluble in buffer solution, leading to fluorescent clusters that interfere with imaging. Dissolving the substrate in dimethylsulfoxide (i.e., 1 mM) prior to dilution in

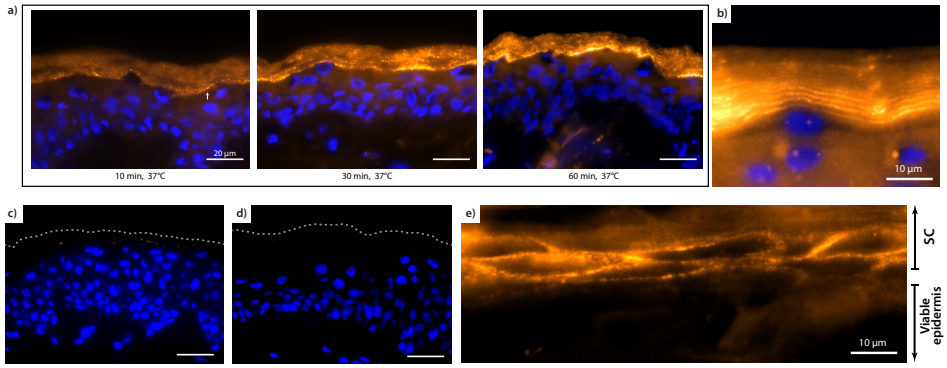

Figure 4: *In situ* GCase labeling by MDW941 ABP. Microscope images (63× magnification) of human skin sections incubated with the ABP, MDW941 (yellow/orange), and counterstained with DAPI (blue). Scale bar represents 20 mm unless stated otherwise. A: Incubation period assay of 10, 30, and 60 min incubation periods. At 10 min, some weak ABP-labeling is already present (white arrow). B: When zooming in on the viable epidermis-SC interface, prominent labeling of active GCase is observed. C: Competition assay of ABPs in which human skin sections were preincubated with nonfluorescent ABP (cylophellitol-epoxide tagged with a nonfluorescent moiety) prior to incubation with MDW941. The dotted line indicates the outermost SC layer. D: Human skin sections incubated without any ABP (negative control). E: High magnification of the viable epidermis-SC interface at skin sections in which the SC was not flattened, illustrating MDW941 labeling around the corneocytes (DAPI-counterstaining of nuclei in the viable epidermis is not visualized for better visualization of GCase in the extracellular lipid matrix).

buffer completely removed this. The 4-MU-β-glc could be dissolved directly in buffer, without any additional steps. Second, after incubation with substrate, washing is necessary to successfully remove background staining. Three short rinses with MilliQ water (the first one in addition with Tween-20) resulted in the best contrast between fluorescent signal and aspecific staining. Longer or more wash steps resulted in significant loss of fluorescent signal, whereas less washing led to reduced contrast. Third, we incubated the samples with two commonly used substrate buffers for zymography, 10 mM MES solution and 150 mM McIlvaine solution. Fourth, the effect of incubation period and temperature was investigated, using an incubation period between 0 and 16 h at 4°C or 37°C.

The results on the optimized protocol are depicted in Figure 3 (and supplemental Figure S3). Both substrates visualized GCase in skin sections and provided similar results: fluorescent product was observed at the viable epidermis-SC interface of human skin sections (Figure 3A). To exclude nonspecific staining, we performed a competition assay in which we preincubated skin sections with a commonly used competitive GCase-specific inhibitor, isofagomine. Consecutive incubation with substrate res-β-glc (in addition to equimolar concentrations of isofagomine to maintain

competition) resulted in no significant staining (Figure 3B), indicating that isofagomine successfully inhibited GCase activity and that the substrates were indeed converted by GCase. Without any substrate (negative control), no staining was observed either (Figure 3C). When studying the catalytic conversion of substrate by GCase at higher magnification levels (e.g., 63×), "layers" of fluorescent product were formed, as can be seen from Figure 3D and the zoomed section. The presence of GCase activity in the intercellular SC regions was also clearly visualized when using 4-MU-β-glc as substrate (Figure 3E). Incubation for at least 1 h at 37°C did result in sufficient fluorescent signal at the viable epidermis-SC interface. It was determined that longer incubation periods (e.g., 16 h) should be avoided to prevent excessive diffusion of fluorescent product throughout the section, even at the reduced temperature of 4°C (Figure 3F).

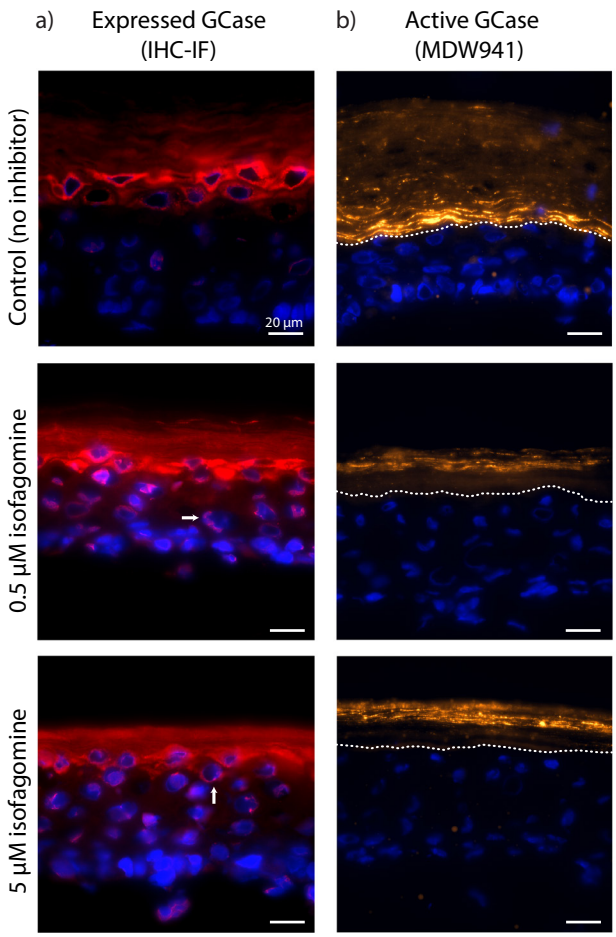

Figure 5:
A: Immunohistochemical fluorescent staining of expressed GCase (red) in HSEs cultured with isofagomine or without (control). DAPI was used for counterstaining, indicating blue-labeled cell nuclei. White arrows point to GCase labeling near the nuclei of viable keratinocytes. B: In situ visualization of active GCase labeled with MDW941 in HSEs cultured with isofagomine. Yellow/orange staining (MDW941) indicates active GCase. Blue indicates cell nuclei (DAPI). All images were taken at a 63× magnification. Scale bar represents 20 µm. The dotted line indicates the viable epidermis-SC interface.

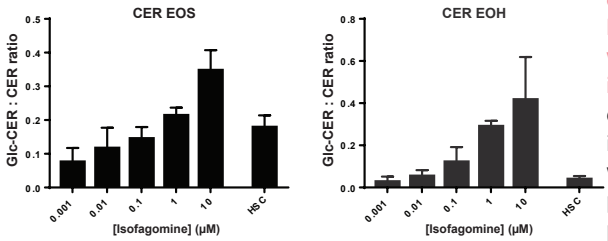

Figure 6: GlcCer:ceramide ratios of ceramide (CER) subclasses EOS and EOH in HSEs cultured with different concentrations isofagomine. Bar plots depict mean ± SD from three independent donor experiments with at least two or more cultures per experiment. As a control, a pool of >10 human SC samples was analyzed (HSC condition).

Developing an in situ *ABP-labeling procedure for localizing active GCase in the epidermis.*

We established a new method for visualizing active GCase in human epidermal skin tissue by means of ABP-labeling. We optimized the method for ABP concentration, incubation period, buffer type, and washing procedure. Concerning ABP concentration, labeling was already successful at 10 nM MDW941; however, more robust and high contrast staining was obtained at 100 nM concentrations. Higher concentrations (e.g., 1 μM) did not result in more intense staining, but increased the risk of nonspecific labeling (precipitation of the probe) (see supplemental Figure S4). When optimizing incubation period, we demonstrated that labeling was already observable after 30 min of incubation, but an ~1 h incubation period proved optimal (Figure 4A). At 63× objective lens magnification, it became apparent that GCase was present not only at the viable epidermis-SC interface but also in the lower SC layers, as fluorescent layers of ABP-labeling appeared (Figure 4B), similar to the fluorescent layers observed with the zymography method. To exclude that MDW941 labels at nonspecific sites of the skin sections, we preincubated sections in excess of a nonfluorescent selective GCase probe [37, 38]. This nonfluorescent probe binds covalently to E340 of GCase only. Its irreversible binding prohibits binding of MDW941 in the subsequent incubation period. Indeed, Figure 4C demonstrated no visible fluorescent signal (thus no MDW941 binding), illustrating specific labeling of active GCase by MDW941 in human skin sections. No background staining was observed, as incubation without ABP (negative control samples) resulted in no detectable staining (Figure 4D). MDW941 labeling on skin that was not fully differentiated (and thus shows no full flattening of the corneocytes in the SC) revealed that the ABP was located in the lipid matrix surrounding the corneocytes (Figure 4E). Note that when optimizing buffer, we obtained identical results when using MES and McIlvaine buffer; therefore, both buffers are considered suitable for ABP-labeling. Regarding washing procedure, we observed that washing at least three times proved superior over washing once, as the latter procedure did not always remove all unlabeled MDW941. The newly developed GCase

ABP-labeling proved quick and very reproducible, resulting in high resolution imaging, even at low concentrations of MDW941. This method was therefore used to study GCase expression in HSEs in which GCase activity was modulated.

Altered GCase activity in HSEs cultured with isofagomine.

We applied our optimized *in situ* ABP method to a HSE that resembles, to a large extent, the morphology and lipid composition in human skin. During generation of these HSEs, the medium was supplemented with 0–100 μM isofagomine, a potent reversible GCase inhibitor. We analyzed to what extent GCase expression and activity were affected by isofagomine in culture medium. Figure 5A shows that GCase in HSEs (as visualized with a specific antibody) was mainly located at the viable epidermis-SC interface, similar to the observations made for human skin (Figure 2D). This expression at the viable epidermis-SC interface was not decreased when cultured with 0.5 or 5 μM isofagomine in the medium. In fact, GCase expression was observed throughout all SC layers. Besides, adding isofagomine to the culture medium resulted in more GCase staining near the nuclei of viable epidermal cells (see arrows in Figure 5A), which implied an increase in *de novo* GCase expression and thus GCase synthesis. When analyzing the presence of active GCase using the ABP, MDW941, in the absence of isofagomine, labeling was observed at the viable epidermis-SC interface and the lower SC layers (Figure 5B), in line with the expression pattern observed in Figure 5A. Interestingly, labeling of active GCase at the viable epidermis-SC interface was lost when inhibitor (0.5 and 5 μM) isofagomine was added to the medium. Only a weak staining at the outermost SC layers remained.

SC ceramides in HSEs are altered when cultured with isofagomine.

Because we observed changes in GCase in HSEs cultured with the inhibitor, isofagomine, we analyzed the SC ceramides of these HSEs by means of LC/MS. Figure 6 depicts the GlcCer:ceramide ratios of two acylceramide subclasses, EOS and EOH, respectively. At 1 nM isofagomine concentration (far below the Ki,isofagomine of ~20 nM) [39], a ratio around 0.8 was observed, indicating that ~7% of ceramide EOS remained glycosylated at this culturing condition. When the isofagomine concentration was increased, the GlcCer:ceramide ratio was also increased for both ceramide EOS and EOH. At concentrations of 10 μM isofagomine, the ratio increased significantly to 0.35 ± 0.06 and 0.42 ± 0.20 for EOS and EOH, respectively. This indicated that the conversion of GlcCers into ceramides was successfully hampered by the competitive inhibitor, isofagomine. The HSE model can therefore be supplemented with specific concentrations to modulate the exact amount of GlcCers:ceramides.

Discussion

This study first reported on the presence of active GCase in human skin, which was primarily located outside the lysosomes in the extracellular space of the inner layers of the lipophilic SC lipid matrix. GCase activity in such an environment is unique and has hitherto not been observed in any other tissues. We described two independent methods to visualize the presence of active GCase in the extracellular space: zymography and ABP-labeling. Although the presence of GCase at the viable epidermis-SC interface has been reported before using zymography [7, 32, 33, 40-42], the specificity of the substrates (res-β-glc and 4-MU-β-glc) has been debated, as both are converted by several β-glucosidases [43-45]. Therefore, we developed a new method that uses the ABP, MDW941. This aziridine-based probe has unmatched sensitivity and specificity toward lysosomal GCase and delivers superior spatial resolution images. Below, we discuss and compare both methods (summarized in Table 1).

Zymography.

The developed procedure is compatible with the two most commonly used substrates in relation to GCase activity. The method is robust, less time-consuming, and provides higher resolution images than most reported protocols. The following optimization steps proved crucial for the improved results, and are related to sample preparation, incubation period, choice of substrate, incubation buffer, and washing procedures.

First, reported *in situ* methods sometimes use fixation solvents to localize GCase activity [7, 32], but this mitigates GCase activity and should be avoided [46-48]. Cryo-fixed sections without fixation solvent on SuperFrost glass slides are therefore preferred.

Second, the optimal incubation period with 4-MU-β-glc or res-β-glc was around 1–2 h. Shorter incubation periods led to significantly less fluorescent product, whereas longer incubation periods caused diffusion of the fluorescent product. Takagi et al. [7] proposed an incubation period of 16 h at the reduced temperature of 4°C to minimize diffusion of product, but our proposed method demonstrated clearer contrast of converted product when applying an incubation period of less than 2 h at 37°C. Besides, incubation at 37°C more closely resembles the *in vivo* situation and, thus, the physiological activity of GCase.

Third, no significant difference was observed between the two substrates, res-β-glc (orange/red) and 4-MU-β-glc (indigo), for *in situ* visualization of active GCase. Neither substrate showed significant overlap in its emission wavelength with its respective counterstain (DAPI and propidium iodide). Green fluorophores were avoided because of the autofluorescence of skin tissue caused by components like collagen, elastin, melanin, and keratin [49,

50]. We did not observe any emitted fluorescence signal for res-β-glc at the excitation and emission wavelengths proposed by Hachem et al. [33] (588 and 644 nm, respectively).

Fourth, GCase activity is optimal around pH 5.2–5.6 [6, 7]. The use of appropriate buffers is therefore crucial and preferred over the use of deionized water as the substrate solvent, as has been used in other protocols [33]. MES buffer (10 mM) was preferred over 150 mM McIlvaine buffer, as the images were more consistent and more often resulted in clear "layered" patterns of converted fluorescent product in the SC. This could be related to the high salt concentration of McIlvaine buffer, which may affect the surface charge and tertiary structure of GCase, leading to changes in enzyme activity [51].

Fifth, we noticed significantly better results after optimizing the washing steps. Directly after cryo-sectioning, protocols should include a washing procedure to remove specimen matrix (e.g., Tissue-Tek). In agreement with Man et al. [52], we observed that the matrix was easily removed when washing with 1% Tween-20 in water. A second washing step was introduced directly after the substrate incubation step. A dip-wash with deionized water that was repeated three times appeared to be optimal; the first wash was with the addition of 1% Tween-20.

ABP-labeling.

ABP-lABP-labeling has several advantages compared with the zymography procedure: *i*) MDW941 labeling proved much more sensitive, as incubation with 100 nM ABP was sufficient for proper localization, whereas 1 mM substrate was preferred for zymography. *ii*) MDW941 is GCase specific, in contrast to 4-MU-β-glc and res-β-glc, which are ligands for all β-glucosidase subtypes (GCase, GBA2–3). Hence, only the ABP-labeling method demonstrated that visualized protein is indeed lysosomal GCase. *iii*) Covalent binding of ABP was less dependent on incubation period and washing procedures, and labeling with the ABP, MDW941, does not require enzyme-based protonation (thus incubation near optimal pH) [37]. *iv*) Generally, reproducibility of *in situ* zymography is a main concern and repeated measurements are necessary to compensate for irregular results [53]. In contrast, ABP-labeling delivers more robust images of active GCase along the entire skin section. As a consequence, ABP-labeling requires a significantly lower number of skin sections for reliable conclusions in comparison to zymography.

Recapitulating, this is the first time that the highly sensitive and selective MDW941 label demonstrates that active GCase is located in the lipophilic extracellular matrix outside the lysosomes of human skin, which is unique with respect to both environmental condition and localization as observed in cells of other tissues [16, 18]. ABP sensitivity also becomes apparent when comparing ABP-labeling to the *in vitro* Western blotting procedure:

for successful visualization of GCase, only 5 µg of protein was loaded for the ABP-labeling procedure, whereas 50 µg was required for the Western blot procedure. ABP-labeling of skin lysates demonstrated that active GCase in the dermis is of different molecular size than active GCase in the epidermis. This suggests that different isoforms are present in both skin layers, consistent with our finding that N-glycanase treatment converted both dermal and epidermal GCase to an identical molecular weight [54-56]. In the dermis, GCase is likely located in the lysosomes of cells (fibroblasts, macrophages, and adipocytes), where it degrades GlcCer as the penultimate step in cellular glycosphingolipid turnover.

The unmatched sensitivity of ABP-labeling proved useful when studying HSEs. GCase expression and activity in HSEs is localized at the same epidermal layers compared with human skin. Supplementation of isofagomine, a commonly used potent reversible inhibitor of GCase [45, 57, 58], to the medium demonstrated that the activity of GCase can be altered without significantly reducing GCase expression or inducing any morphological effects. Localization of active GCase in the epidermis is therefore essential for understanding the consequences of the SC ceramide composition. Inhibition of GCase by isofagomine resulted in a concentration-dependent increase of the precursors, acyl-GlcCer EOS and acyl-GlcCer EOH, compared with their acyl-ceramide products. We specifically studied these two ceramide subclasses, as it is known that ceramides EOS and EOH are not substrates for a second enzyme (acid sphingomyelinase) that converts sphingomyelins into ceramides [59]. A high concentration of isofagomine in the medium led to complete inhibition of GCase at the viable epidermis-SC interface and only a weak ABP-labeling in the outer SC layers was observed. This indicates that isofagomine reaches the SC layers and proves that GCase activity is crucial for the SC ceramide composition. We explain GCase activity in the outer SC layers by the fact that isofagomine may not sufficiently diffuse into the upper SC layers and inhibit GCase. Besides, competition between substrates, endogenous GCase, and isofagomine still occurs, as isofagomine is a reversible inhibitor and the medium is refreshed twice a week. Any remaining GCase activity is therefore expected to be at the lowest isofagomine concentration, i.e., the outermost SC layers. Nevertheless, the concentration-dependent effect indicates that the conversion by GCase can be modulated by hampering enzyme activity, irrespective of GCase expression. This supplement may therefore be useful to target GCase to model skin barrier dysfunction related to specific diseases. Gaucher disease is an obvious candidate, but a dysfunction in GCase expression is also observed in skin disorders like Netherton syndrome and atopic dermatitis [21, 60]. The significance of GCase activity in these skin diseases remains inconclusive [61, 63] and the presented methods here will be used in future studies to unravel this aspect, along with the relationship to environmental factors, like skin

Table 1: Overview of the optimized *in situ* protocols to visualize epidermal GCase by zymography and ABP-labeling.

Parameter	*In situ* Zymography	*In situ* ABP-Labeling
Section fixation	Cryo-samples (no fixation)	Cryo-samples (no fixation)
[Fluorogenic compound]	~1 mM 4-MU-b-glc or res-b-glc	~100 nM MDW941
Incubation period/temperature	1–2 h, 37°C	1 h, 37°C
Preferred buffer	MES	MES or McIlvaine
Washing protocol	1× 1% Tween, 3× short rinses in MilliQ	1× 1% Tween, 3× short rinses in MilliQ

hydration and the SC pH gradient. We observed active GCase primarily in the innermost SC layers, which may be related to the slightly acidic pH gradient across the SC. The pH of the inner SC layers (~5–6) is at the optimal pH of GCase [64]. This acidic pH may aid GCase activity in the extracellular SC environment, even at the outermost SC layers that are extremely lipophilic. In relation to Netherton syndrome and atopic dermatitis, changes in environmental factors, like SC humidity and pH gradient, have been reported as possible causes for changes in GCase activity [33, 40, 64- 66]. GCase has been reported as a key mediator for skin barrier homeostasis, as changes in epidermal GCase activity have been observed in cases of skin barrier disruption [67].

In conclusion, we provided two independent methods to visualize epidermal GCase and demonstrated that, in both human skin and our HSEs, active GCase was predominantly present in the extracellular space of the SC lipid matrix. ABP-labeling demonstrated changes in GCase activity for HSEs cultured with inhibitor, explaining the altered SC (glucosyl)ceramide composition in these HSEs. In combination with immunohistochemical staining for the expression of GCase and the use of MS to quantify endogenous GlcCers and ceramides, these methods that visualize active GCase bridge the gap between analysis on protein expression level and the final phenotype, the SC ceramide profile. ABP-labeling is superior to zymography in terms of sensitivity, specificity, and robustness, and the ABP, MDW941, is compatible with skin of human and murine origin [16, 37]. ABP-labeling may therefore be used in future studies to address GCase activity in relation to skin barrier diseases.

Experimental procedures

Processing human skin. Human skin was processed in accordance with the Declaration of Helsinki principles. Skin from mammoplasty or abdominoplasty was obtained from local hospitals directly after surgery. Skin was dermatomed to a thickness of 400 µm after removal of the adipose tissue. Skin samples were either processed to culture HSEs, used for *in vitro* GCase analysis, or cryo-frozen

for sectioning and labeling: small skin samples were put in gelatin capsules filled with matrix specimen Tissue-Tek OCT (Sakura Finetek Europe, Alphen a/d Rijn, The Netherlands) and snap-frozen in liquid nitrogen. Snap-frozen skin tissue from human skin or HSEs was cut to 5 µm-thick sections (Leica CM3050s; Leica Microsystems, Germany). Sections were placed on SuperFrost Plus micro slides (VWR International, The Netherlands) and used for immunohistochemical stainings or enzyme activity studies (*in situ* zymography and ABP-labeling).

Culturing and harvesting HSEs. HSEs were cultured as described previously [34, 68, 69]. Briefly, the epidermis was separated from the dermis by Dispase digestion (Roche, Almere, The Netherlands). Primary fibroblasts were isolated after incubation of the dermis in collagenase (Gibco-Invitrogen, Carlsbad, CA) and Dispase II (Roche). Keratinocytes were isolated from the epidermis after trypsin digestion (Sigma-Aldrich, Steinheim, Germany). The dermal compartment was cultured using isolated rat collagen populated with fibroblasts. Dermal equivalents were cultured submerged for 1 week. Then human keratinocytes were seeded on the dermal equivalent and the HSEs were cultured for 2 days under submerged conditions. The HSEs were lifted to the air-liquid interface and cultured for an additional 2 weeks while supplementing different concentrations of the GCase inhibitor, isofagomine (0, 0.001, 0.01, 0.1, 0.5, 1, 5, or 10 µM; $n \geq 3$ for each condition) to the culture medium. Medium was refreshed twice a week. After the culture period, HSEs were harvested: HSEs cultured with 0, 0.5, or 5.0 µM (isofagomine) were snap-frozen (unfixed) and cut in 5 µm-thick sections, as described above for human skin. These samples were analyzed for *in situ* immunohistochemistry-immunofluorescence staining and ABP-labeling of GCase. The remaining HSEs were used to analyze the SC (glucosyl)ceramides by LC/MS.

In vitro *analysis of GCase in human skin lysates.* From dermatomed skin, the individual skin layers were isolated according to the procedures described elsewhere [70, 71]: dermis, epidermis, SC, and viable skin layers (full thickness skin minus SC). Dermis was isolated from the epidermis using a 2.4 U/ml dispase II solution (Roche). SC was isolated by 0.1% trypsin digestion (Sigma-Aldrich). Human skin was left overnight in 0.1% trypsin in PBS at 4°C. After an incubation period of 1 h at 37°C, the SC was isolated and washed once with 0.1% (w/v) trypsin inhibitor in PBS solution and twice in MilliQ. The GCase content was determined in various isolated skin layers for: i) the presence of GCase by Western blotting; ii) the presence of active GCase by ABP-labeling; and iii) quantitation of GCase activity by a 4-MU-β-glc assay. All procedures are described briefly below.

Western blot analysis of GCase. Western blot analysis was performed to examine the presence of GCase in human skin. Skin lysates were prepared in KPI buffer (25 mM potassium phosphate, pH 6.5) and 0.1% (v/v) Triton with cOmplete protease inhibitor (Roche) in tubes with 1.0 mm glass beads (BioSpec Products, Bartlesville, OK). These tubes were processed on a FastPrep-24 5G for 10 cycles of 20 s at a speed of 6 m/s. Samples were filtered on a 1 ml disposable spin column (G-Biosciences, St. Louis, MO) and spun down for 10 min at 15,000 rpm. The protein concentration was quantified by BCA kit (Thermo Scientific, Rockford, IL). Subsequently, lysates were denatured with Laemmli loading buffer [312.5 mM Tris-HCl (pH 6.8), 0.1% (w/v) bromophenol blue, 50% (v/v) glycerol, 10% (w/v) SDS, and 8% (w/v) DTT] and heated for 5 min at 98°C. Samples were subjected to 10% SDS-PAGE and transferred to 0.2 µm nitrocellulose membranes by using a Trans-Blot Turbo system (Bio-Rad). The blots were blocked in 5% (w/v) Protifar in PBS 0.1% (v/v) Tween-20 and incubated overnight at 4°C with anti-GCase monoclonal antibody (8E4 [72]) at 1:1,000 dilution in 2% (w/v) Protifar PBS 0.1% (v/v) Tween-20. After washing three times in PBST, membranes were incubated for 1 h at room temperature with secondary antibody, Alexa Fluor 647 donkey anti-mouse (Life Technologies, Bleiswijk, The Netherlands), at 1:10,000 dilution in 2% (w/v) Protifar PBS 0.1% (v/v) Tween-20. Blots were washed twice in PBST and once in PBS, followed by scanning on a Typhoon FLA 9500 scanner (λex = 653 nm, λem = 669 nm). Precision Plus Protein unstained standard #1610373 (Bio-Rad) was used as reference ladder.

ABP-labeling of GCase. To examine whether active GCase was present in lysates of isolated human skin layers, labeling was performed as described previously [16]. Samples were first incubated in 100 nM ABP MDW941 in McIlvaine buffer (150 mM citric acid-Na2HPO4, pH 5.2), 0.2% (w/v) sodium taurocholate, 0.1% (v/v) Triton X-100, and 0.1% (w/v) BSA at 37°C for 1 h. Afterwards, samples were denatured with Laemmli loading buffer and heated for 5 min at 98°C. Gel electrophoresis was performed on 10% SDS-polyacrylamide gels, washed afterwards in demineralized water and visualized using a Typhoon FLA 9500 scanner, deep red (λex = 649 nm, λem = 670 nm) and green (λex = 532 nm, λem = 554 nm). Bio-Rad #1610373 was used as reference ladder and no significant autofluorescence of the skin layers was observed that could possibly interfere with the results.

GCase activity assay. 4-MU-β-Glc (Santa Cruz, Dallas, TX) was used to measure the GCase activity in the separate skin layers (16). Skin lysates were incubated on ice with and without 100 nM MDW933 (nonfluorescent GCase inhibitor) for 30 min, followed by incubation with the 4-MU-β-Glc mixture at 37°C for 30 min. This incubation mixture contained McIlvaine buffer (150 mM

citric acid-Na2HPO4, pH 5.2), 0.2% (w/v) sodium taurocholate, 0.1% (v/v) Triton X-100, 0.1% (w/v) BSA, and 3.7 mM 4-MU-β-Glc substrate. Afterwards, the substrate reaction was stopped with glycine-NaOH (pH 10.3) and the amount of fluorescent product (4-methylumbelliferone) was measured with a fluorescence spectrometer (LS-55; Perkin Elmer) at λex = 366 nm and λem = 445 nm. No significant autofluorescence of the lysates was observed. By subtracting the activity obtained when incubated with GCase inhibitor from the activity obtained without incubation with inhibitor (nonspecific GCase activity), the actual GCase hydrolysis activity was determined.

Immunofluorescence staining for GCase expression. Skin sections (5 μm-thick) were fixed with acetone and washed with PBS (pH 7.4). Sections were blocked using 2.5% (v/v) goat serum in 1% (v/v) BSA/PBS. Incubation with primary monoclonal GCase antibody (ab125065; Abcam, Cambridge, UK) was performed overnight at 4°C. Sections were labeled with secondary antibody (Rhodamine Red AffiniPure goat anti-rabbit IgG; Jackson ImmunoResearch Laboratories, West Grove, PA). Afterwards, sections were washed twice in PBS and once in demineralized water and subsequently mounted using Vectashield with DAPI solution (Vector Laboratories, Burlingame, CA).

In situ *zymography of epidermal GCase.* Skin sections were washed with 1% (v/v) Tween-20 in MilliQ. Afterwards, 1 mM fluorogenic substrate in either 10 mM MES buffer (pH 5.4) or McIlvaine buffer (150 mM citric acid-Na2HPO4, pH 5.2) were added to the sections and incubated at 37°C for 0 min, 10 min, 30 min, 1 h, 2 h, or 16 h. Substrate was either 4-MU-β-glc or res-β-glc (Marker Gene Technologies, Oregon). For the zymography competition assay, an additional preincubation step of 1 h at 37°C with 1 mM isofagomine (Toronto Research Chemicals, Toronto, Canada) was performed. Thereafter, the sections were washed briefly with 1% (v/v) Tween-20 solution and subsequently either one or three additional washes with MilliQ water. Sections were mounted with Vectashield containing either DAPI or propidium iodide for appropriate counterstaining of cell nuclei. The main parameters of the optimized protocol are listed in Table 1.

In situ *ABP-labeling of active GCase in the epidermis.* Skin sections were washed with 1% (v/v) Tween-20 (Bio-Rad Laboratories) in MilliQ. Afterwards, different concentrations of the ABP, MDW941 (10, 100, or 1,000 nM), in either McIlvaine buffer or MES buffer were added to the sections and incubated for different periods (0, 10, 30, or 60 min) at 37°C. Negative control samples were preincubated with a 10 μM cyclophellitol-epoxide ABP tagged with a nonfluorescent moiety in 150 mM McIlvaine buffer [150 mM citric acid-Na2HPO4 (pH 5.2), 0.2% (w/v) sodium taurocholate, 0.1% (v/v) Triton X-100].

Thereafter, the samples were washed either once or three times in MilliQ water (first wash in addition of 1% Tween-20) and mounted using Vectashield with DAPI solution. An overview of the final method is provided in Table 1.

Fluorescence microscopy. Images were taken using a Zeiss Imager.D2 microscope connected to a Zeiss AxioCam MRm camera (Zeiss, Germany). Images were taken at objective lens magnifications of 20× and 63× (with immersion oil) and with an ocular lens magnification of 10×. Images were processed using Zen 2 2012, blue edition (Zeiss). Exposure times were kept constant for each individual experiment. Gamma was set to 1.0 for all measurements.

SC lipid isolation and (glucosyl)ceramide analysis. SC was isolated from small skin samples by trypsin digestion (as described above). Then, lipids were extracted from the SC using an extended Bligh and Dyer procedure described by Boiten et al. [73] The obtained lipid fraction was reconstituted in heptane:chloroform:methanol (95:21/2:21/2) prior to analysis by LC/MS, as explained previously [73]. In short, chromatography of (glucosyl) ceramides was achieved by an Acquity UPLC H-class (Waters, Milford, MA) using gradient elution of heptane toward 50% heptane:isopropanol:ethanol (50:25:25) by means of a normal phase PVA-silica column (100 × 2.1 mm inner diameter, 5 µm particle size; YMC, Kyoto, Japan). A Xevo TQ-S MS, equipped with an atmospheric pressure chemical ionization source was used for mass analysis in positive-ion full-scan MS mode for scanning from m/z 350 to 1,200 amu (ceramides) and from m/z 500 to 1,350 amu (GlcCers). Deuterated non-hydroxy fatty acid/sphingosine base ceramide (ceramide NS, Evonik Industries, Germany) was used as internal standard. The ratio of the areas under the curve of acyl-GlcCers and acyl-ceramides (specifically ceramide subclasses EOS and EOH, see supplemental Figure S1e, f for the molecular architecture) were subsequently calculated and will be referred to as GlcCer:ceramide ratio, as reported previously [60]. We focused specifically on acyl-ceramide subclasses because: i) the precursors of these ceramides are solely GlcCers and, therefore, only conversion by GCase plays a role in the final step of the acyl-ceramide synthesis and results could not be obscured by other enzymes (i.e., ceramides that can also be generated by acid sphingomyelinase); and ii) these ceramides are crucial for a proper SC lipid matrix structure and are therefore relevant when studying HSEs in relation to the SC barrier.

Acknowledgements

The authors thank Evonik Industries (Essen, Germany) for providing deuterated ceramide NS to quantify LC/MS data.

Supplemental data

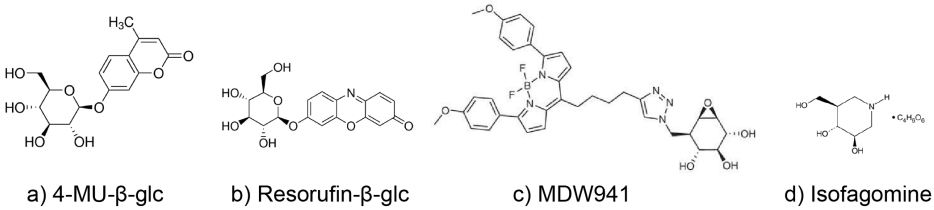

a) 4-MU-β-glc b) Resorufin-β-glc c) MDW941 d) Isofagomine

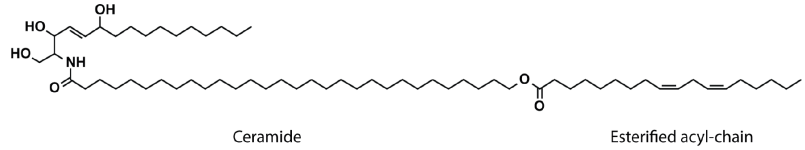

e) Ceramide EOS

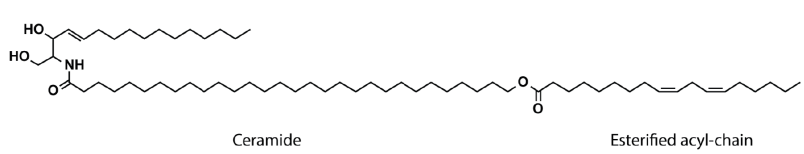

f) Ceramide EOH

Supplemental Figure S1: Molecular structures of a-b) substrates 4-methylumbelliferyl-β-D-glucopyranoside (4-MU-β-glc) and resorufin-β-D-glucopyranoside (Res-β-glc) used for *in situ* zymography that result in respectively blue and red fluorescent products; c) activity-based GCase probe: d) Potent reversible GCase inhibitor. e) Ultra long Esterified Omega-hydroxyacyl-Sphingosine ceramide (Ceramide EOS). f) Ultra long Esterified Omega-hydroxyacyl-6-Hydroxy sphingosine ceramide (Ceramide EOH).

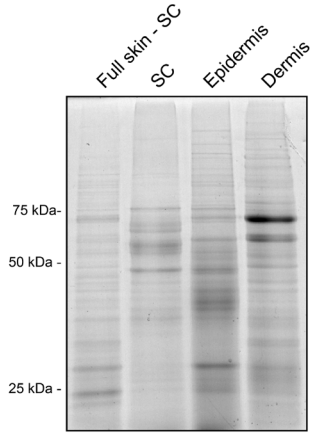

Supplemental Figure S2: Coomassie G250 stain of protein in skin lysate and homogenate. Per lane, 50 µg protein was loaded on the 1.5 mm SDS Page gel.

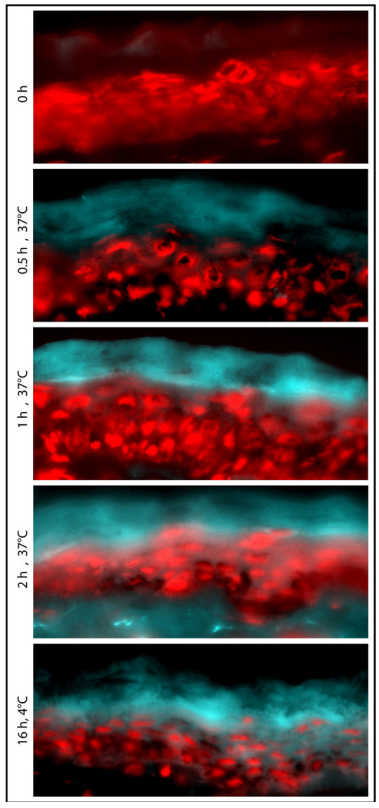

Supplemental Figure S3: Effect of incubation time of zymography assay visualizing GCase activity in human skin sections. 63x magnification images using 4-MU-β-glc substrate focusing on the blue fluorescent product 'layers'. Red counterstaining was performed using propidium iodide to stain cell nuclei. At incubation periods <1 hour, fluorescent signal is relatively low. At incubation periods of 2 hour or longer, diffusion of fluorescent product is observed, particularly after 16 h, when label is 'diffused' at the lower epidermal layers.

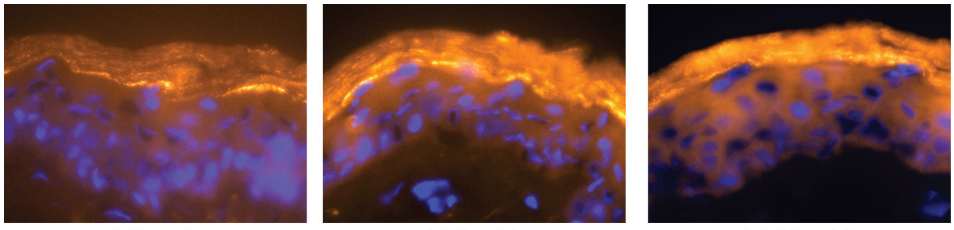

Supplemental Figure S4: *In situ* GCase labeling by MDW941 ABP. 63x Microscope images of human skin sections incubated with different concentrations (10, 100, 1000 nM) of ABP MDW941 (Yellow/Orange), and counterstained with DAPI (blue). GCase labeling was observed for all three MDW941 concentrations, but was optimal around 100 nM.

References

1. W.M. Holleran, Y. Takagi, Y. Uchida, Epidermal sphingolipids: metabolism, function, and roles in skin disorders, FEBS Lett, 580 (2006) 5456–5466.
2. T. Wennekes, R.J. van den Berg, R.G. Boot, G. A. van der Marel, H.S. Overkleeft, J.M. Aerts, Glycosphingolipids–nature, function, and pharmacological modulation, Angew Chem Int Ed Engl, 48 (2009) 8848–8869.
3. B.E. Rosenbloom, N.J. Weinreb, Gaucher disease: a comprehensive review, Crit Rev Oncog, 18 (2013) 163–175.
4. D.L. Stone, W. F. Carey, J. Christodoulou, D. Sillence, P. Nelson, M. Callahan, N. Tayebi, E. Sidransky, Type 2 Gaucher disease: the collodion baby phenotype revisited, Arch Dis Child Fetal Neonatal Ed, 82 (2000) F163–F166.
5. D. Reczek, M. Schwake, J. Schröder, H. Hughes, J. Blanz, X. Jin, W. Brondyk, S. Van Patten, T. Edmunds, P. Saftig, LIMP-2 is a receptor for lysosomal mannose-6-phosphate-independent targeting of beta-glucocerebrosidase, Cell. 131 (2007) 770–783.
6. A.M. Vaccaro, M. Muscillo, K. Suzuki, Characterization of human glucosylsphingosine glucosyl hydrolase and comparison with glucosylceramidase, Eur J Biochem, 146 (1985) 315–321.
7. Y. Takagi, E. Kriehuber, G. Imokawa, P.M. Elias, W.M. Holleran, Beta-glucocerebrosidase activity in mammalian stratum corneum, J Lipid Res, 40 (1999) 861–869.
8. S. van Weely, M. Brandsma, A Strijland, J.M. Tager, J.M. Aerts, Demonstration of the existence of a second, non-lysosomal glucocerebrosidase that is not deficient in Gaucher disease, Biochim Biophys Acta, 1181 (1993) 55–62.
9. M. Horowitz, A. Zimran, Mutations causing Gaucher disease, Hum Mutat, 3 (1994) 1–11.
10. H. Ryšlavá, V. Doubnerová, D. Kavan, O. Vaněk, Effect of posttranslational modifications on enzyme function and assembly, J Proteomics, 92 (2013) 80–109.
11. J. Wilkesman, L. Kurz, Protease analysis by zymography: a review on techniques and patents, Recent Pat Biotechnol, 3 (2009) 175–184.
12. J. Vandooren, N. Geurts, E. Martens, P.E. Van den Steen, G. Opdenakker, Zymography methods for visualizing hydrolytic enzymes. Nat. Methods. 10 (2013) 211–220.
13. S.J. George, J.L. Johnson J. L, In situ zymography, Methods Mol Biol, 622 (2010) 271–277.
14. B.F. Cravatt, A.T. Wright, J.W. Kozarich, Activity-based protein profiling: from enzyme chemistry to proteomic chemistry, Annu Rev Biochem, 77 (2008) 383–414.
15. L.I. Willems, H.S. Overkleeft, S.I. van Kasteren, Current developments in activity-based protein profiling, Bioconjug Chem, 25 (2014) 1181–1191.
16. M.D. Witte, W.W. Kallemeijn, J. Aten J, K.Y. Li, A. Strijland, W.E. Donker-Koopman, A.M. van den Nieuwendijk, B. Bleijlevens, G. Kramer, B.I. Florea, et al, Ultrasensitive in situ visualization of active glucocerebrosidase molecules, Nat Chem Biol, 6 (2010) 907–913.
17. M.D. Witte, G.A. van der Marel, J.M.F.G. Aerts, H.S. Overkleeft, Irreversible inhibitors and activity-based probes as research tools in chemical glycobiology, Org Biomol Chem, 9 (2011) 5908–5926.
18. D. Herrera Moro Chao, W.W. Kallemeijn, A.R. Marques, M. Orre, R. Ottenhoff, C. van Roomen, E. Foppen, M.C. Renner, M. Moeton, M. van Eijk, et al, Visualization of active glucocerebrosidase in rodent brain with high spatial resolution following in situ labeling with fluorescent activity based probes, PLoS One, 10 (2015) e0138107.
19. P.M. Elias, Epidermal lipids, barrier function, and desquamation, J Invest Dermatol 80 (Suppl.) (1983) 44s–49s.
20. K.R. Feingold, P.M. Elias, Role of lipids in the formation and maintenance of the cutaneous permeability barrier, Biochim Biophys Acta, 1841 (2014) 280–294.
21. J. van Smeden, M. Janssens, G.S. Gooris, J.A. Bouwstra. The important role of stratum corneum lipids for the cutaneous barrier function, Biochim Biophys Acta, 1841 (2014) 295–313.
22. J. Ishikawa, H. Narita, N. Kondo, M. Hotta, Y. Takagi, Y. Masukawa, T. Kitahara, Y. Takema, S. Koyano, S. Yamazaki, et al, Changes in the ceramide profile of atopic dermatitis patients, J Invest Dermatol 130 (2010) 2511–2514.
23. Y. Pewzner-Jung, S. Ben-Dor, A.H. Futerman, When do lasses (longevity assurance genes) become CerS (ceramide synthases)? Insights into the regulation of ceramide synthesis, J Biol Chem 281 (2016) 25001–25005.
24. M. Rabionet, K. Gorgas, R. Sandhoff, Ceramide synthesis in the epidermis, Biochim Biophys Acta 1841 (2014) 422–434.
25. M.A. Lampe, M.L. Williams, P.M Elias, Human epidermal lipids: characterization and modulations during

differentiation, J Lipid Res 24 (1983) 131–140.
26. M. Fartasch, The epidermal lamellar body as a multifunctional secretory organelle. In Skin Barrier. P.M. Elias and K.R. Feingold, editors. CRC Press, Boca Raton, FL (2005) 261–272.
27. S. Hamanaka, M. Hara, H. Nishio, F. Otsuka, A. Suzuki, Y. Uchida, Human epidermal glucosylceramides are major precursors of stratum corneum ceramides, J Invest Dermatol, 119 (2002) 416–423.
28. Y.A. Hannun, L.M. Obeid, Principles of bioactive lipid signalling: lessons from sphingolipids, Nat Rev Mol Cell Biol, 9 (2008) 139–150.
29. D. Groen, D.S. Poole, G.S. Gooris, J.A. Bouwstra, Is an orthorhombic lateral packing and a proper lamellar organization important for the skin barrier function? Biochim Biophys Acta 1808 (2011) 1529–1537.
30. J. Bouwstra, G. Gooris, M. Ponec M, The lipid organisation of the skin barrier: liquid and crystalline domains coexist in lamellar phases, J Biol Phys, 28 (2002) 211–223.
31. G.M. Cooper, R.E. Hausman, The Cell: A Molecular Approach. 7th edition Sinauer Associates, Inc, Sunderland, MA (2016)
32. M. Schmuth, K. Schoonjans, Q.C. Yu, J.W. Fluhr, D. Crumrine, J.P. Hachem, P. Lau, J. Auwerx, P.M. Elias, K.R. Feingold, Role of peroxisome proliferator-activated receptor alpha in epidermal development in utero, J Invest Dermatol, 119 (2002) 1298–1303.
33. J.P. Hachem, D. Crumrine, J. Fluhr, B.E. Brown, K.R. Feingold, P.M. Elias, pH directly regulates epidermal permeability barrier homeostasis, and stratum corneum integrity/cohesion, J Invest Dermatol, 121 (2003) 345–353
34. V.S. Thakoersing, G.S. Gooris, A. Mulder, M. Rietveld, A. El Ghalbzouri, J.A. Bouwstra, Unraveling barrier properties of three different in-house human skin equivalents, Tissue Eng Part C Methods, 18 (2012) 1–11.
35. Z. Berger, S. Perkins, C. Ambroise, C. Oborski, M. Calabrese, S. Noell, D. Riddell, W.D. Hirst, Tool compounds robustly increase turnover of an artificial substrate by glucocerebrosidase in human brain lysates, PLoS One, 10 (2015) e0119141.
36. C. Dulsat, N. Mealy, Isofagomine tartrate, Drugs Future, 34 (2009) 23.
37. W.W. Kallemeijn, K.Y. Li, M.D. Witte, A.R. Marques, J. Aten, S. Scheij, J. Jiang, L.I. Willems, T.M. Voorn-Brouwer, C.P. van Roomen, Novel activity-based probes for broad-spectrum profiling of retaining beta-exoglucosidases in situ and in vivo, Angew Chem Int Ed Engl, 51 (2012) 12529–12533.
38. B. Chandrasekar, T. Colby, A. Emran Khan Emon, J. Jiang, T.N. Hong, J.G. Villamor, A. Harzen, H.S. Overkleeft, R.A. van der Hoorn, Broad-range glycosidase activity profiling, Mol Cell Proteomics, 13 (2014) 2787–2800.
39. C. Kuriyama, O. Kamiyama, K. Ikeda, F. Sanae, A. Kato, I. Adachi, T. Imahori, H. Takahata, T. Okamoto, N. Asano, In vitro inhibition of glycogen-degrading enzymes and glycosidases by six-membered sugar mimics and their evaluation in cell cultures, Bioorg Med Chem, 16 (2008) 7330–7336.
40. Y. Hatano, M.Q. Man, Y. Uchida, D. Crumrine, T.C. Scharschmidt, E.G. Kim, T.M. Mauro, K.R. Feingold, P.M. Elias, W.M. Holleran, Maintenance of an acidic stratum corneum prevents emergence of murine atopic dermatitis, J Invest Dermatol, 129 (2009) 1824–1835.
41. D. Ilic, M. Mao-Qiang, D. Crumrine, G. Dolganov, N. Larocque, P. Xu, M. Demerjian, B.E. Brown, S.T. Lim, V. Ossovskaya, et al, Focal adhesion kinase controls pH-dependent epidermal barrier homeostasis by regulating actin-directed Na+/H+ exchanger 1 plasma membrane localization, Am J Pathol, 170 (2007) 2055–2067.
42. J.P. Hachem, T. Roelandt, N. Schurer, X. Pu, J. Fluhr, C. Giddelo, M.Q. Man, D. Crumrine, D. Roseeuw, K.R. Feingold, et al, Acute acidification of stratum corneum membrane domains using polyhydroxyl acids improves lipid processing and inhibits degradation of corneodesmosomes, J Invest Dermatol, 130 (2010) 500–510.
43. Y. Ben-Yoseph, H.L. Nadler, Pitfalls in the use of artificial substrates for the diagnosis of Gaucher's disease, J Clin Pathol, 31 (1978) 1091–1093.
44. F.Y. Choy, R.G. Davidson, Gaucher disease. III. Substrate specificity of glucocerebrosidase and the use of nonlabeled natural substrates for the investigation of patients, Am J Hum Genet, 32 (1980) 670–680.
45. O. Motabar, E. Goldin, W. Leister, K. Liu, N. Southall, W. Huang, J.J. Marugan, E. Sidransky, W. Zheng, A high throughput glucocerebrosidase assay using the natural substrate glucosylceramide, Anal Bioanal Chem, 402 (2012) 731–739.
46. Z.S. Galis, G.K. Sukhova, P. Libby, Microscopic localization of active proteases by in situ zymography: detection of matrix metalloproteinase activity in vascular tissue, FASEB J, 9 (1995) 974–980.
47. S.J. Yan, E.A. Blomme, In situ zymography: a molecular pathology technique to localize endogenous protease activity in tissue sections, Vet Pathol, 40 (2003) 227–236.
48. W.M. Frederiks, O.R. Mook, Metabolic mapping of proteinase activity with emphasis on in situ

zymography of gelatinases: review and protocols, J Histochem Cytochem, 52 (2004) 711–722.
49. R. Patalay, C. Talbot, Y. Alexandrov, I. Munro, M.A.A. Neil, K. Konig, P.M.W French, A. Chu, G.W. Stamp, C. Dunsby, Quantification of cellular autofluorescence of human skin using multiphoton tomography and fluorescence lifetime imaging in two spectral detection channels, Biomed Opt Express, 2 (2011) 3295–3308.
50. K. König, Clinical multiphoton tomography, J Biophotonics, 1 (2008) 13–23.
51. K.D. Collins, Charge density-dependent strength of hydration and biological structure, Biophys J, 72 (1997) 65–76.
52. M.Q. Man, T.K. Lin, J.L. Santiago, A. Celli, L. Zhong, Z.M. Huang, T. Roelandt, M. Hupe, J.P. Sundberg, K.A. Silva, et al, Basis for enhanced barrier function of pigmented skin, J Invest Dermatol, 134 (2014) 2399–2407.
53. R. Nemori, T. Tachikawa, A review for in situ zymography: method for localization of protease activities in a tissue, The Tissue Culture Engineering, 25 (1999) 29–32.
54. S. Fabrega, P. Durand, P. Codogno, C. Bauvy, C. Delomenie, B. Henrissat, B.M. Martin, C. McKinney, E.I. Ginns, J.P. Mornon, et al, Human glucocerebrosidase: heterologous expression of active site mutants in murine null cells, Glycobiology, 10 (2000) 1217–1224.
55. J.M. Aerts, S. Brul, W.E. Donker-Koopman, S. van Weely, G.J. Murray, J.A. Barranger, J.M. Tager, A.W. Schram, Efficient routing of glucocerebrosidase to lysosomes requires complex oligosaccharide chain formation, Biochem Biophys Res Commun, 141 (1986) 452–458.
56. S. Van Weely, J.M. Aerts, M.B. Van Leeuwen, J.C. Heikoop, W.E. Donker-Koopman, J.A. Barranger, J.M. Tager, A.W. Schram, Function of oligosaccharide modification in glucocerebrosidase, a membrane-associated lysosomal hydrolase, Eur J Biochem, 191 (1990) 669–677.
57. F. Ben Bdira, W.W. Kallemeijn, S.V. Oussoren, S. Scheij, B. Bleijlevens, B.I. Florea, C van Roomen, R. Ottenhoff, M. van Kooten, M.T.C. Walvoort, et al, 2017. Stabilization of glucocerebrosidase by active site occupancy, ACS Chem Biol, 12 (2017) 1830–1841.
58. D.J. Urban, W. Zheng, O. Goker-Alpan, A. Jadhav, M.E. Lamarca, J. Inglese, E. Sidransky, C.P. Austin, Optimization and validation of two miniaturized glucocerebrosidase enzyme assays for high throughput screening, Comb Chem High Throughput Screen, 11 (2008) 817–824.
59. Y. Uchida, M. Hara, H. Nishio, E. Sidransky, S. Inoue, F. Otsuka, A. Suzuki, P.M. Elias, W.M. Holleran, S. Hamanaka, Epidermal sphingomyelins are precursors for selected stratum corneum ceramides, J Lipid Res, 41 (2000) 2071–2082.
60. J. van Smeden, M. Janssens, W.A. Boiten, V. van Drongelen, L. Furio, R.J. Vreeken, A. Hovnanian, J.A. Bouwstra, Intercellular skin barrier lipid composition and organization in Netherton syndrome patients, J Invest Dermatol, 134 (2014) 1238–1245.
61. M. Danso, W. Boiten, V. van Drongelen, K. Gmelig Meijling, G. Gooris, A. El Ghalbzouri, S. Absalah, R. Vreeken, S. Kezic, J. van Smeden, et al, Altered expression of epidermal lipid bio-synthesis enzymes in atopic dermatitis skin is accompanied by changes in stratum corneum lipid composition, J Dermatol Sci, 88 (2017) 57–66.
62. A. Sugiura, T. Nomura, A. Mizuno, G. Imokawa, Reevaluation of the non-lesional dry skin in atopic dermatitis by acute barrier disruption: an abnormal permeability barrier homeostasis with defective processing to generate ceramide, Arch Dermatol Res, 306 (2014) 427–440.
63. K. Jin, Y. Higaki, Y. Takagi, K. Higuchi, Y. Yada, M. Kawashima, G. Imokawa, Analysis of beta-glucocerebrosidase and ceramidase activities in atopic and aged dry skin, Acta Derm Venereol, 74 (1994) 337–340.
64. J.W. Fluhr, P.M. Elias, Stratum corneum pH: formation and function of the 'acid mantle', Exogenous Dermatology, 1 (2002) 163–175.
65. M. Abdul-Hammed, B. Breiden, G. Schwarzmann, K. Sandhoff, Lipids regulate the hydrolysis of membrane bound glucosylceramide by lysosomal beta-glucocerebrosidase, J Lipid Res, 58 (2017) 563–577.
66. M.H. Schmid-Wendtner, H. C. Korting, The pH of the skin surface and its impact on the barrier function, Skin Pharmacol Physiol, 19 (2006) 296–302.
67. W.M. Holleran, Y. Takagi, G.K. Menon, S.M. Jackson, J.M. Lee, K.R. Feingold, P.M. Elias, Permeability barrier requirements regulate epidermal beta-glucocerebrosidase, J Lipid Res, 35 (1994) 905–912.
68. A. El Ghalbzouri, S. Commandeur, M.H. Rietveld, A.A. Mulder, R. Willemze, Replacement of animal-derived collagen matrix by human fibroblast-derived dermal matrix for human skin equivalent products, Biomaterials, 30 (2009) 71–78.
69. M. Ponec, A. Weerheim, J. Kempenaar, A. Mulder, G.S. Gooris, J. Bouwstra, A.M. Mommaas, The formation of competent barrier lipids in reconstructed human epidermis requires the presence of vitamin C, J Invest Dermatol, 109 (1997) 348–355.

70. A.K. Nugroho, L. Li, D. Dijkstra, H. Wikstrom, M. Danhof, J.A. Bouwstra, Transdermal iontophoresis of the dopamine agonist 5-OH-DPAT in human skin in vitro, J Control Release, 103 (2005) 393–403.
71. E.M. Haisma, M.H. Rietveld, A. de Breij, J.T. van Dissel, A. El Ghalbzouri, P.H. Nibbering, Inflammatory and antimicrobial responses to methicillin-resistant Staphylococcus aureus in an in vitro wound infection model, PLoS One, 8 (2013) e82800.
72. J.M. Aerts, W.E. Donker-Koopman, G.J. Murray, J.A. Barranger, J.M. Tager, A.W. Schram, A procedure for the rapid purification in high yield of human glucocerebrosidase using immunoaffinity chromatography with monoclonal antibodies, Anal Biochem, 154 (1986) 655–663.
73. W. Boiten, S. Absalah, R. Vreeken, J. Bouwstra, J. van Smeden J, Quantitative analysis of ceramides using a novel lipidomics approach with three dimensional response modelling, Biochim Biophys Acta, 1861 (2016) 1652–1661.

Chapter 4

Skin of Atopic Dermatitis patients shows disturbed β-glucocerebrosidase and acid sphingomyelinase activity that relates to changes in stratum corneum lipid composition

Skin of Atopic Dermatitis patients shows disturbed β-glucocerebrosidase and acid sphingomyelinase activity that relates to changes in stratum corneum lipid composition

D.E.C. Boer, J. van Smeden, H. Al-Khakany, E. Melnik, R. van Dijk, S. Absalah, R. J. Vreeken, C.C.P. Haenen, A.P.M. Lavrijsen, H.S. Overkleeft, J.M.F.G Aerts, J.A. Bouwstra.

Abstract

Patients with Atopic Dermatitis (AD) suffer from inflamed skin and skin barrier defects. Proper formation of the outermost part of the skin, the stratum corneum (SC), is crucial for the skin barrier function. In this study we analyzed the localization and activity of lipid enzymes β-glucocerebrosidase (GCase) and acid sphingomyelinase (ASM) in the skin of AD patients and controls. Localization of both the expression and activity of GCase and ASM in the epidermis of AD patients was altered, particularly at lesional skin sites. These changes aligned with the altered SC lipid composition. More specifically, abnormal localization of GCase and ASM related to an increase in specific ceramide subclasses [AS] and [NS]. Moreover we related the localization of the enzymes to the amounts of SC ceramide subclasses and free fatty acids (FFAs).

We report a correlation between altered localization of active GCase and ASM and a disturbed SC lipid composition. Localization of antimicrobial peptide beta-defensin-3 (HBD-3) and AD biomarker Thymus and Activation Regulated Chemokine (TARC) also appeared to be diverging in AD skin compared to control. This research highlights the relation between correct localization of expressed and active lipid enzymes and a normal SC lipid composition for a proper skin barrier.

Introduction

Atopic Dermatitis (AD) is a multifactorial disease in which both immunological aspects and skin barrier defects contribute to clinical manifestations as erythema, xerosis and pruritis. The interplay between inflammation and skin barrier in this disease is complex, and it is hypothesized that a skin barrier dysfunction may facilitate exogenous compounds (e.g. pathogens, allergens) to penetrate the skin and provoke an immune response [1]. Subsequently,

this immune response may also affect the barrier properties of the skin. This is also known as the "outside–inside–outside" model of AD pathogenesis [2, 3]. Nonetheless, AD is known to be a heterogeneous disease that can be driven by activation of the adaptive immune response, along with being the initiator that activates key TH1, TH17 and TH22 cytokine pathways [4].

The strongest predisposing factor for developing AD is loss-of-function mutations in the *filaggrin* gene (*flg*) [5, 6]. The protein filaggrin is an essential component for a proper formation of the Stratum Corneum (SC), the outermost skin layer that functions as the primary physical skin barrier. The SC is the non-vital final keratinocyte differentiation product forming the outermost layer of the skin. It consists of multiple layers of corneocytes (dead cells) embedded in an extracellular lipid matrix and plays an eminent role in the barrier function of the skin. The breakdown products of filaggrin – forming a substantial part of the natural moisturizing factor (NMF) – are essential for water retention in theSC. Additionally, the NMF is important for maintaining a physiologic acidic environment in the SC, supporting an optimal skin-pH and water level for proper enzyme activity in the skin [7, 8]. Several of these skin enzymes play a crucial role in generating key barrier components of the SC, the SC lipids, which form a highly ordered intercellular matrix [9, 10]. The composition of the SC lipid matrix is crucial for a proper skin barrier, and changes in these lipids are related to several skin barrier diseases [11, 12]. The main SC lipids are ceramides, free fatty acids (FFAs) and cholesterol. Ceramide synthases are essential for the formation of ceramides *de novo*. To store the ceramides in the viable cells, the ceramides are converted to glucosylceramides and sphingomyelin by the enzymes glucosylceramide synthase and sphingomyelin synthase, respectively (as reviewed in [13]). Besides ceramides also free fatty acids (FFAs)

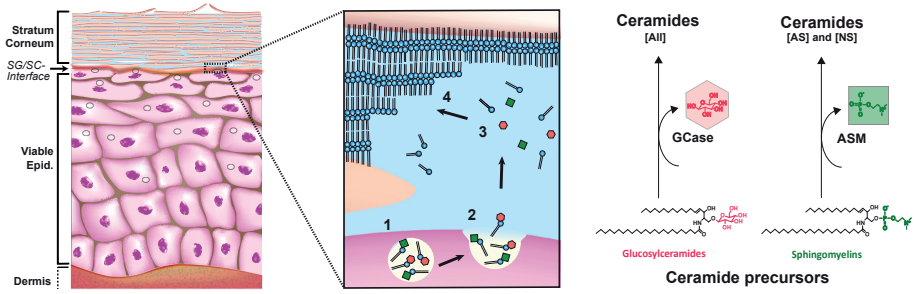

Figure 1: Schematic overview of formation SC lipid layers at the SG/SC-interface. 1. Lamellar Bodies (LBs) in the keratinocytes are filled with ceramide precursors glucosylceramides and sphingomyelins together with the enzymes GCase and ASM. 2. Extrusion process of the lipids and lipid enzymes. 3. Conversion of glucosylceramides and sphingomyelins by respectively GCase and ASM to ceramides. 4. Formation of the extracellular stacked lipid layers: the lipid barrier in the SC.

reside in the lipid matrix of the SC. Proper expression of stearoyl CoA desaturase (SCD) and ELOVL1-7 (elongation of very long chain fatty acids 1–7) have been shown to be key for a proper FFA and ceramide composition [13]. An impaired skin barrier is typically monitored by an increased transepidermal water loss (TEWL. AD patients suffer from an increased TEWL (reduced skin barrier). This increased TEWL is correlated to changes in the SC lipids, particularly in two key classes: the ceramides, and their precursors the FFAs [14]. Whereas FFAs contain a single acyl chain, ceramides contain two long chains attached to one polar head group. In SC both the head group and carbon chain length show a wide variation in molecular architecture [15]. To distinguish all SC ceramides, they are categorized in subclasses based on their architecture, illustrated in Supplemental Figure 1. The SC ceramide composition in AD patients is changed. Compared to control skin, lesional AD skin demonstrates a significant decrease in the average carbon chain length of both ceramides and FFAs [16-18]. In addition, a (relative) increase in [AS] and [NS] ceramides in lesional skin has been observed [19-21]. The reason why particularly ceramides [AS] and [NS] are increased in barrier disrupted skin is not fully understood, but likely originates from changes in the epidermal biosynthesis of the SC ceramides [12, 22].

A pivotal step in this ceramide conversion is the final process in which ceramide precursors – glucosylceramides and sphingomyelins – are extruded from the Stratum Granulosum (SG) keratinocytes into the extracellular environment at the SG/SC interface [14]. During this extrusion process of lipids and their corresponding enzymes, the ceramide precursors transform into their final barrier constituents. Here, glucosylceramides and sphingomyelins are converted by respectively β-glucocerebrosidase (GCase) and acid sphingomyelinase (ASM) (Figure 1). Both GCase and ASM will convert their substrates into ceramides, but conversion by ASM will lead to only ceramide subclasses [AS] and [NS], whereas ceramide formation via GCase may lead to ceramides of any subclass [23, 24]. It is known that the expression of these enzymes is mildly changed in the epidermis of some AD subjects, particular at lesional skin sites [25-27]. However, not all reported changes in the SC ceramides in AD patients could be explained by the expression of GCase and ASM [28]. Literature suggests that micro-environmental factors like SC water content and local skin-pH are essential for proper activity (besides expression) of these enzymes [29, 30]. The skin microbiome and inflammation are changed in AD [31-33] and could therefore consequently have an effect on the SC lipid composition. This has not been studied previously, thus we additionally examined the localization of Human beta defensing (HBD)-3 as a readout for the microbiome, plus it has been reported to be decreased in AD. Furthermore we included Thymus and Activation Regulated Chemokine (TARC), which is

involved in Th2 cell migration and has been confirmed as a biomarker for AD severity [32, 33]. This also provides the opportunity to research whether the localization of these AD markers change concordantly with GCase and ASM localization.

We visualized *in situ* enzyme expression and activity of GCase and ASM in human skin tissue of AD subjects and controls and analyzed the SC ceramides and FFas by LC/MS. In addition, we examined several AD markers (both locally and systemically) to study the relationship between the SC lipids and the inflammatory aspects, as it is known that cytokines may induce lipid abnormalities in atopic skin [34, 35]. Our findings elucidate the relation between localization of – particularly active – GCase and ASM, versus the SC lipid composition. In addition, this study elaborates on the clinical relevance by relating these enzymes and SC lipid composition to biologically/clinically important parameters like TEWL and disease severity scores [36].

Results

This study cohort consisted of ten patients diagnosed with AD and five controls. Three AD patients had lesional regions on their arms during the study period. A summary of the results with respect to (local) SCORAD, EASI, TEWL and skin-pH per time point is provided in figure 2. In agreement with previous studies, our AD cohort demonstrated an elevated baseline TEWL for non-lesional as well as lesional skin regions in comparison to control skin [37]. In addition, skin-pH values were in similar ranges as reviewed elsewhere [38]. These general parameters support the representativeness of this AD cohort in relation to established literature [37-40].

Location of expressed enzyme does not predict the location of active enzyme.

We first studied the localization of GCase expression in the skin cryosections of the control subjects. The top panel in figure 3 shows the expression of GCase mainly concentrated at the interface between the viable epidermis and SC (SG/SC-interface). Active GCase was visualized using the activity based probe MDW941. Concerning the intensity of the signal, a substantial intra- and inter-individual variation was observed. Therefore, we focused on the location of the activity in this study (supplemental figure S2). In all controls, the active enzyme was primarily observed in the SC, no active GCase was observed in the viable epidermis. Active GCase was present in the SC lipid matrix surrounding the corneocytes: either throughout all SC layers, or in the lower regions of the SC. Note that the signal intensity is very heterogeneous between subjects and even within a single skin section, but localization remains in the SC lipid matrix for all controls.

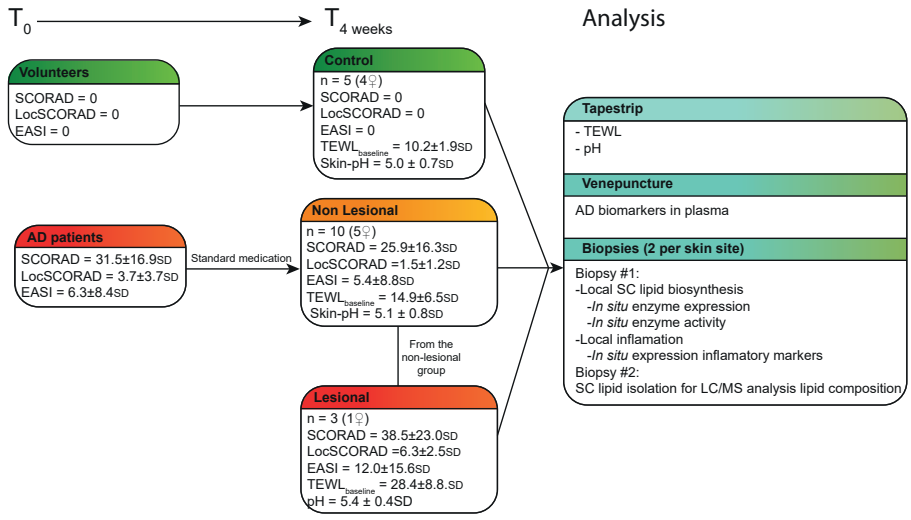

Figure 2: Schematic overview experimental set up and scoring of the cohort. T_0: SCORAD and EASI parameters of volunteers and AD patients. T_4 weeks: SCORAD, EASI, TEWL and pH parameters of controls and AD patients. Skin samples from arm regions and two biopsies were taken from all subjects. From 3 AD patients non-lesional and lesional skin samples were taken. Furthermore venipuncture and tape stripping was performed.

When focusing on ASM expression in the control skin sections, the expression was present throughout the viable epidermis. The activity of ASM was determined by zymography. The intensity of this signal was also very heterogeneous, even within a single skin cryosection of a subject. In one subject (nr. 5) no ASM activity was detected. The location of ASM activity was detected mainly in the lower layers of the SC near the SG/SC-interface or scattered throughout the whole SC, but no activity signal was encountered in the viable epidermis.

Location of expressed enzyme does not predict the location of active enzyme.

We first studied the localization of GCase expression in the skin cryosections of the control subjects. The top panel in figure 3 shows the expression of GCase mainly concentrated at the interface between the viable epidermis and SC (SG/SC-interface). Active GCase was visualized using the activity based probe MDW941. Concerning the intensity of the signal, a substantial intra- and inter-individual variation was observed. Therefore, we focused on the location of the activity in this study (supplemental figure S2). In all controls, the active enzyme was primarily observed in the SC, no active GCase was observed in the viable epidermis. Active GCase was present in the SC lipid matrix surrounding the corneocytes: either throughout all SC layers, or in the lower regions of the SC. Note that the signal intensity is very heterogeneous between subjects and

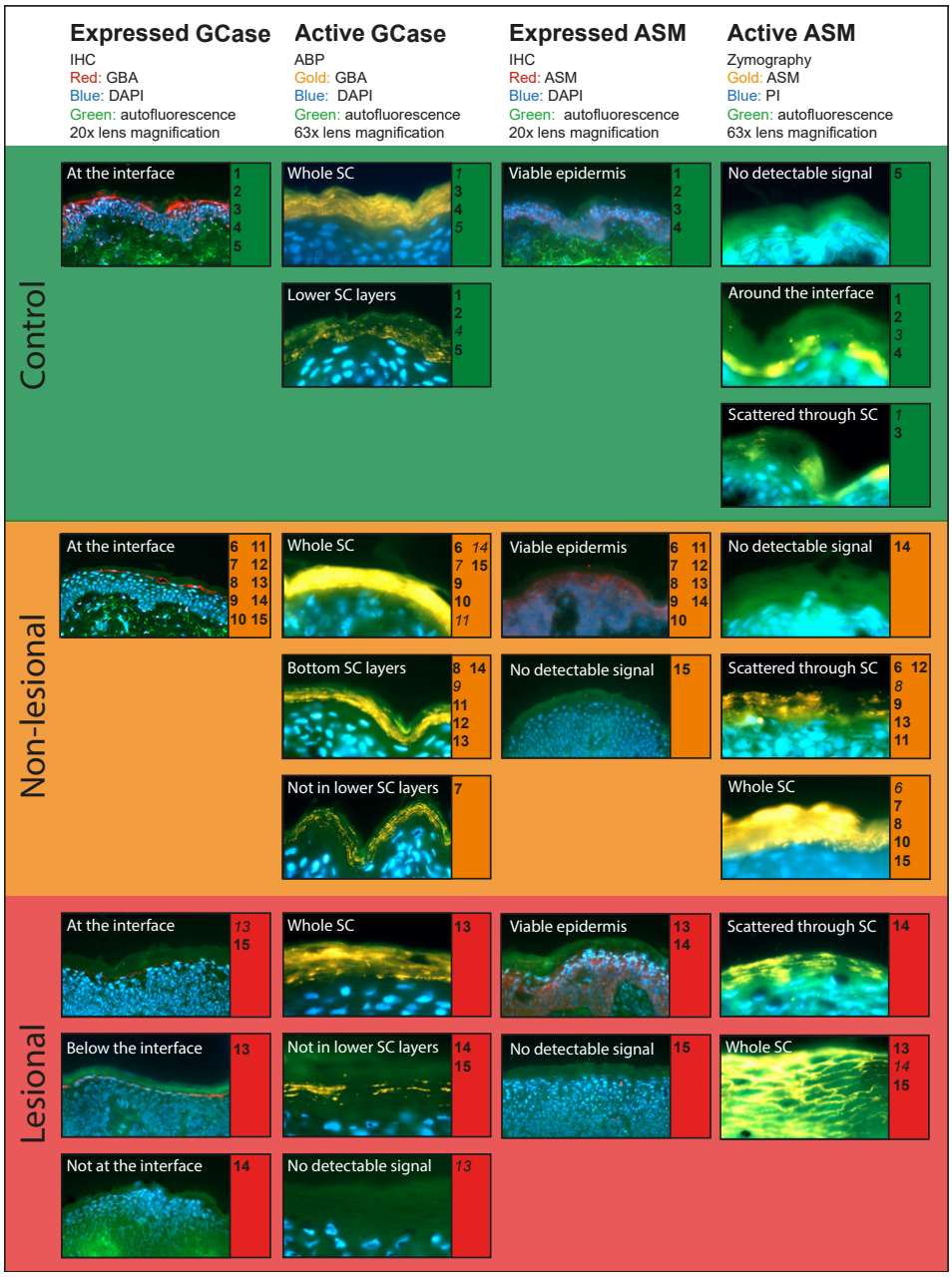

Figure 3: *In situ* expression and activity localization of GCase and ASM within skin sections of control, non-lesional AD and lesional AD skin. Microscopy images showing in which skin layers expressed and active enzymes are localized. Depicted are which localization patterns can be found in each subject. Bold numbers show its main occurrence per subject. Italic numbers demonstrate the less abundant patterns.

even within a single skin section, but localization remains in the SC lipid matrix for all controls.

When focusing on ASM expression in the control skin sections, the expression was present throughout the viable epidermis. The activity of ASM was determined by zymography. The intensity of this signal was also very heterogeneous, even within a single skin cryosection of a subject. In one subject (nr. 5) no ASM activity was detected. The location of ASM activity was detected mainly in the lower layers of the SC near the SG/SC-interface or scattered throughout the whole SC, but no activity signal was encountered in the viable epidermis.

Lesional AD skin shows less localized active GCase and ASM compared to control skin.

Lesional skin sections from three subjects were available for analysis. We first noted more keratinocyte layers in the viable epidermis compared to the control skin sections (supplemental figure S2). Moreover, in the lesional skin of patient #15 the SC appeared thicker and at some sections, corneocytes appeared swollen (supplemental figure S2). The expression of GCase at lesional skin sites was examined (figure 3, bottom panel). In patient #15 the expression of GCase was very similar to that in the control skin. In patient #13, GCase expression was sometimes observed at the SG/SC-interface, but mostly in the outermost keratinocyte layer in the viable epidermis close to the SG/SC-interface. Concerning patient #14, no GCase expression was detected at the lesional site, instead a diffuse signal was present in the whole viable epidermis. Additionally, in this patient nuclear expression was observed. When focusing on active GCase, in general this was localized in the SC matrix. In some parts of the sections of subject #13, no active GCase could be detected. However, in the majority of the cases of areas where activity was observed, a distribution throughout all the SC layers was observed. In skin sections of the other two patients active GCase was observed in the SC matrix, but mainly in the middle and outer layers of the SC and not in the lower layers of the SC.

ASM expression was not detected in patient #15, whereas the lesional sites of the other two subjects demonstrated expression at locations similar to that observed in the control skin sections. As far as active ASM is concerned, all lesional sections throughout all the SC lipid layers demonstrated activity. In the case of patient #14 the distribution throughout the SC was more scattered compared to the more evenly spread localization observed in the other two AD patients. Because the signal of ASM activity was throughout the whole SC of subject #15, the swollen corneoctes at the lesional sites of the SC were even more apparent.

Non-lesional AD skin demonstrates a high variety in localization of active enzymes.

A large variation was observed between the different subjects for GCase and ASM of non-lesional AD skin: localization patterns of active GCase and ASM varied between very comparable to control skin and similar to a lesional appearance. All the sections showed a GCase and ASM expression pattern similar to the control subjects, with two exceptions: i) Patient #9 showed additionally intra nuclear GCase expression; ii) non-lesional skin sections of patient #15 showed no ASM expression signal. The localization of active GCase was observed throughout the whole SC or in the lower layers of the SC, as described above for the control subjects. However, the localization in patient #7 was sometimes absent in the lower layers of the SC, corresponding with a more lesional distribution pattern. Active ASM localization was confined throughout the whole SC, either in a smooth or in a scattered pattern. Only patient #14 demonstrated no active ASM signal.

When combining all these findings we observe that the localization of active enzyme appeared more variable than the location of expressed enzyme. In general, active GCase and ASM are less localized near the SG/SC-interface in lesional and some non-lesional AD skin regions. As these changes in localization of enzyme activity may affect the SC ceramide composition, we thoroughly analyzed the SC lipids for each subject.

Increase in [AS] and [NS] ceramides relate with enzyme phenotype and disease severity.

We quantified the SC ceramides for each specific subclass and chain length Additional data on specific ceramides or glucosylceramides is listed in supplemental Figure S3 and supplemental Tables 2, 3 and Figure 4A demonstrates that AD patients have less absolute amount of total ceramides, particularly at lesional skin sites. Ceramide [NP] and [NH] were mostly reduced, as well as the EO ceramides. In contrast, ceramides [NS] and [AS] increased in absolute (and relative) amount in AD. Close examination revealed that the increase in these subclasses was dominated by ceramides with a very short chain length being 34 carbon atoms in total chain length, the so called C34 ceramides (Figure 4B and supplemental figure S4). We then related the amount of ceramides [AS]+[NS] to the different categories of activity patterns observed for ASM as described above (Figure 4C). The absence of clear ASM activity or clear localization near the viable epidermis and SG/SC-interface coincided with a relatively low [AS] and [NS] amount. In addition, subjects that had a more dispersed ASM activity localization compared to control subjects, demonstrated the most deviating amount of ceramides [AS] and [NS]. Thus, less localized active ASM around the SG/SC-interface correlates with an increased (and more varying) amount of [AS] and [NS]. We also observed the amount of ceramides [AS] and [NS] coinciding with an increase in local disease

severity (Figure 4D). Furthermore, a correlation was observed for active GCase and the ceramides that are synthesized by this enzyme only (all ceramides minus [AS] and [NS]), as is depicted in figure 4E. Absence of GCase activity near the SG/SC-interface results in a reduced amount of ceramides synthesized by GCase. Therefore, active GCase near the SG/SC-interface is crucial for a normal amount of ceramides synthesized by that enzyme.

The increase in short chain length ceramides and decrease in very long EO ceramides reduces the mean ceramide chain length in patients with AD, especially in lesional skin [18]. As the changes in ceramide chain length may be related to an impaired fatty acid elongation process [41], we quantified the FFA composition as well (Figure 4F). The calculated molar ratio *ceramides* : *FFAs* was 0.61±0.18 in the control group, 0.59±0.13 in non-lesional AD and 1.06±0.66 in lesional AD skin. Note that we excluded the short chain FFAs due to notorious contamination of C16:0 and C18:0, even nowadays in ultra-pure organic

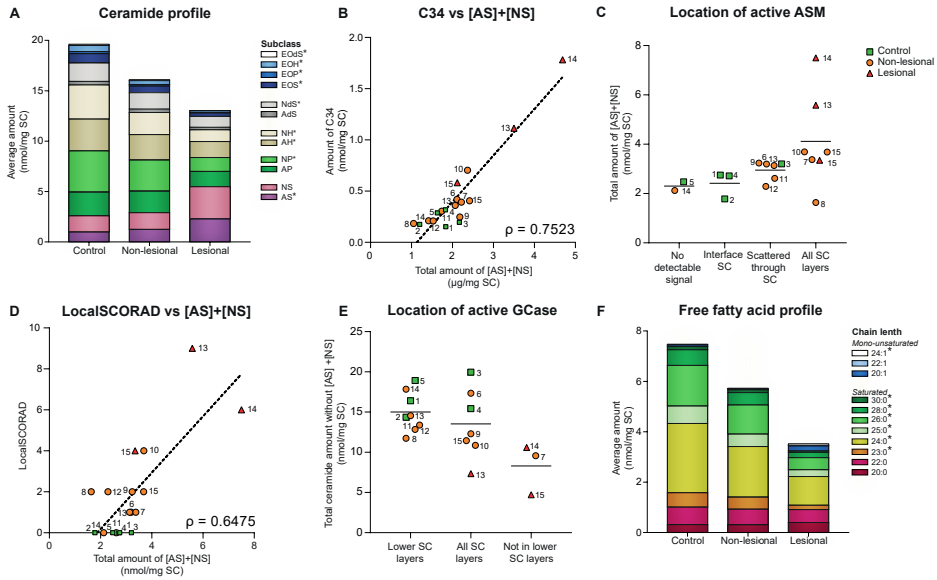

Figure 4: SC lipid data in control, non-lesional and lesional AD skin. A. Bar plots of average amount of ceramide subclasses in the SC. B. Dot plot amount of C34 ceramides plotted versus the total amount of [AS]+[NS] ceramides. C. Dot plot total amount of [AS]+[NS] ceramides plotted against the location of active ASM in the skin. D. Dot plot LocalSCORAD plotted against the total amount of [AS]+[NS] ceramides, E. Dot plot total amount of SC ceramides without¬ [AS]+[NS] compared to the location of active GCase location in the skin. F. Bar plots of average amount of SC FFAs categorized by length and degree of unsaturation. Significant ordinal trends (Jonckheere-Terpstra tests) for the ceramide and FFA quantities in A and F, respectively are shown for each lipid with a * ($p<0.05$). Horizontal lines in C and E represent means, and ρ-values in B and D depict Spearman correlations.

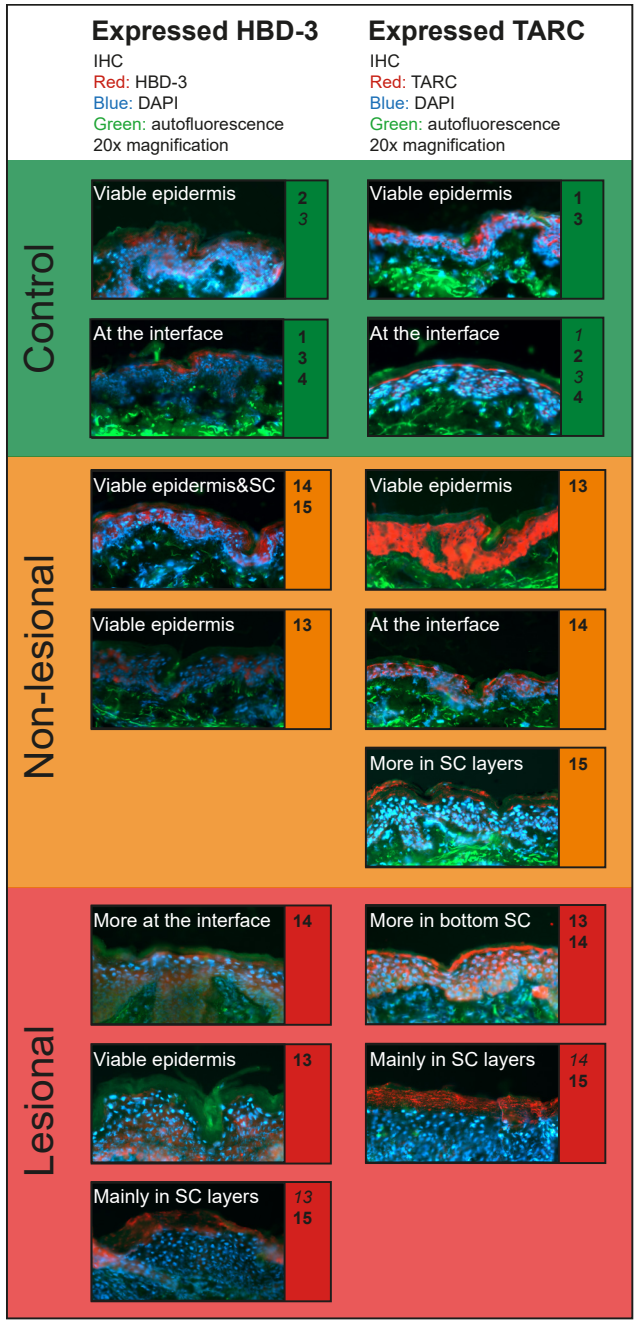

Figure 5: *In situ* localization of HBD-3 and TARC within skin sections of control, non-lesional AD and lesional AD skin. Microscopy images of skin sections showing in which skin layers HBD-3 and TARC are localized. Depicted are which localization patterns can be found in each subject. Bold numbers show its main occurrence per subject. Italic numbers demonstrate which patterns also appear in subjects, but are not the main pattern found in that individual.

solvents. This explains the difference in ratio-outcomes when comparing them to literature values [42, 43]. We observed also a decrease in absolute amount of FFAs in AD skin, particularly for ceramides with chain length of 23 carbon atoms or higher. This could be an indication for a relation between the decrease in FFA chain length to the increase in short chain ceramides belonging to the [AS] and [NS] subclass.

TARC and HBD-3 are less localized around the SG/SC-interface in lesional AD skin sections.

Besides the lipid enzymes, we also studied whether key inflammation markers (for AD) were changed systemically and locally. Systemically, we studied levels of TARC, Interleukin-22 and soluble IL-2 receptorin plasma, but no difference in these parameters between control and AD subjects was observed in this study cohort (data not shown).

In the skin the localization of TARC and HBD-3 were studied as a readout for inflammation and skin microbiome respectively. This is shown in Figure 5, for the control subjects and AD patients #13, #14 and #15 non-lesional and lesioanl regions. HBD-3 is mainly localized in the viable epidermis and occasionally slightly more confined around the SG/SC-interface in most control and non-lesional skin sections. There are non-lesional and lesional skin sections where HBD-3 is also present in the SC (non-lesional of subjects #14 and #15, lesional skin of subject #13). And in one patient, at the lesional site HBD-3 was more profound in the SC layers (#15).

Concerning the localization of AD marker TARC, its presence was generally in the viable epidermis and localized around the SG/SC-interface in control and non-lesional skin sections. In the lesional and some non-lesional skin sites, the expression of TARC was more abundant in the SC, either mainly in the bottom layers (non lesional section of #15 and lesional sites of #11 and #12) or throughout the whole SC (lesional skin section #15). Thus, delocalization of TARC was mainly detected in (inflamed) lesional AD skin as was observed with the active enzymes GCase and ASM.

Discussion

This study is the first that determines in one cohort of AD patients altogether the location of expressed and active SC lipid enzymes, and additionally relates this to a fully quantified SC ceramide and FFA composition. Here we demonstrate AD patients have an altered localization of GCase and ASM, particularly at lesional skin sites. The changes observed in (active) enzyme localization relate to altered ceramide levels and the ceramide subclass profile. These changes in SC lipids correlated with a disturbed skin barrier and

increased local disease severity.

Although our study cohort is small, it has identical clinical characteristics as comparable studies reported previously (i.e. TEWL, SCORAD, SC, skin barrier lipid properties) [17-19, 28, 44, 45]: i) On a general level, AD patients demonstrate a decrease in amount of SC lipids (both ceramides and FFAs), which is more substantial at lesional skin sites. ii) When observing the SC lipids in more detail, a shift towards shorter ceramides and FFAs is seen in AD patients. iii) An increase in subclasses that are particularly related to ASM ([AS] and [NS]) was observed at the expense of ceramide [NP] and [NH], a feature of AD that is observed in almost every AD cohort.

When correlating the SC lipid composition to the enzyme expression/activity, one should realize that there is a time-aspect difference between both parameters: The ceramide composition is the result of an accumulation of the lipid synthesis products for at least 20 days prior to the study day, whereas the biopsies and *in situ* expression/activity images are visualizations at a specific time point – the study day itself. Nevertheless, despite this time-issue and the small sample-size of our cohort, we were able to establish clear changes in the lipid enzymes and correlate these to the SC ceramide phenotype.

A previous study has shown reduced ASM activity in non-lesional and lesional AD epidermis compared to controls, while proposing reduced sphingomyelin levels were not caused by the downregulated ASM levels [26]. In addition normal GCase activity in AD SC has been reported [25]. The present study is the first to study in which both, active GCase and ASM were localized throughout the whole epidermis and related to changes observed in SC ceramide subclass profile in AD. More specifically, we demonstrate that the location of active enzyme rather than the location of expressed enzyme correlates with AD disease manifestation. This elucidates why previously no correlations between enzymes and SC lipids were observed [28], as detailed localization of active GCase and ASM has never been described in AD. Due to the recent development of visualization techniques by ABP-labeling and *in situ* zymography for GCase and ASM [46, 47], their localization can now be studied in detail. Besides to the aforementioned changes in localization of active GCase and ASM in AD, we also observed, on a micro-level scale, a high variation in location of active GCase and ASM. Lipid content over depth has previously been shown to be homogeneous [48]. However, because local changes are observed for the (active) enzymes GCase and ASM, local differences in lipid composition cannot be excluded. No techniques with sufficient resolution are available yet to measure these changes in lipid compositions locally. The underlying reason for high variation in the location of active enzyme is unknown, but literature mentions changes in the micro-environment as one of the most plausible reasons [29]. Changes in micro-environment may affect the local distribution of microflora (which relates to our local changes in antimicrobial peptide

HBD-3 expression), and also the local acidic environment (so-called skin-pH). Literature reports slightly elevated levels in skin-pH in AD [38], even in non-lesional skin [49]. This change in skin-pH could affect the activity of GCase and ASM *in vivo*, as the optimal pH value for GCase and ASM are respectively 4.5 and 5.6 [50]. In addition, we analyzed the skin-pH, but did not observe substantial differences between healthy subjects and AD-patients. However, if these environmental changes in acidity vary to a high extent on a micro-scale, this would align with the micro-scale localization differences in active GCase and ASM. Another important factor for optimal enzyme activity is the presence of cofactors. Saposin C is necessary for proper GCase activity, and dysfunction in this cofactor could lead to insufficient ceramide conversion, as is the case in specific Gaucher cohorts [51]. The role of saposin C in relation to AD is unknown, but it has been reported that protein amount of precursor prosaposin is decreased in AD [52] which could hamper proper functioning of GCase.

GCase converts glucosylceramides into the final SC barrier ceramides. Previously no difference in GCase activity between lesional and control skin was found [25]. However, we observed that active GCase is less localized around the SG/SC-interface and lower SC layers in lesional AD skin compared to control. This is in line with previous observations by Holleran et al., who demonstrated changes in localization of GCase activity (relative increase in upper parts of the epidermis) in mice with a skin barrier disruption [53]. In our study, the altered location of active GCase correlates with a decreased amount of overall SC ceramide levels, particularly the subclasses that cannot be synthesized by ASM. This corresponds with the localization of active ASM being present in additional (more outer) SC layers besides being mainly localized at the SG/SC-interface, as observed in the control group. The increase of ceramides [AS] and [NS] correlated to clinically relevant parameters for skin barrier function (TEWL) and disease severity (SCORAD). Other reported studies in different cohorts and skin diseases that found comparable changes in ceramides [AS] and [NS] (reviewed by [19]), implies that the by ASM derived [AS] and [NS] ceramides are involved in circumstances relate to stressed/diseased skin. This could indicate ASM has a different function than GCase in the skin, as they also have different roles in other organs and tissues: GCase is a key lysosomal enzyme, responsible for main physiological functions of almost every cell, and a key enzyme in glucosylceramide metabolism under healthy/physiological conditions and is considered a housekeeping enzyme [54]. On the contrary, ASM is usually referred as a mediator in pathological processes like cell stress and apoptosis [55]. A switch from physiological conditions towards pathophysiological conditions, like observed here between healthy and AD, may imply that these enzymes have comparable (patho)physiological roles in the skin as they have elsewhere in the human body. Besides, the localization

of expressed TARC, a chemokine triggered in inflammatory diseases like AD, is also changed in AD subjects and could be observed throughout the SC rather than only in the viable epidermis or at the SG/SC-interface [56, 57]. Note that these AD subjects did also demonstrate active ASM throughout the SC.

Literature reports TARC as one of the most significant biomarkers to date for diagnosing AD [58]. We did not observe a correlation between the localization of TARC in the skin and systemic TARC analyzed from plasma. However, visualizing this expressed biomarker in the epidermis does already demonstrate local changes, that might not be visible systemic yet. This all indicates that for interpreting local changes in AD severity, visualization of the local epidermal environment may facilitate in elucidating differences between clinical appearance of AD patients.

The reduction we found in [NP] ceramides (and increase in [AS] and [NS]), can also – at least partially – be explained by changes in dihydroceramide desaturase enzymes (DEGS1 and DEGS2), involved in the conversion of [dS]-ceramides into respectively [S]-ceramides and [P]-ceramides. An increase in expression/activity of DEGS1 relative to DEGS2 would increase the amount of [S] ceramides at the expense of [P] ceramides. The analysis of DEGS-enzymes is beyond the scope of this manuscript, and currently no methods are available for visualizing *in situ* DEGS activity.

We have shown the importance of correct localization of SC enzymes and how this correlates with previously published characteristics of AD, as well as SC lipid composition. We demonstrated changes in SC lipid composition directly affect the skin barrier function (and indirectly disease severity). As these changes originate (at least partially) from changes in the activity of the enzymes, a possible new target for therapy would be to restore the activity of GCase and ASM in AD skin to that of control skin, thereby aiming for repairing the ceramide composition in AD.

Acknowledgements

We thank Walter Boiten for his valuable input regarding the analysis of the ceramide data.

Materials and Methods

Subject inclusion and skin sample processing. The study was conducted according to the Declaration of Helsinki principles. Caucasian AD patients and control volunteers of age 18-40 were included in the study and assessed using SCORAD (SCORing Atopic Dermatitis) [40] and EASI (Eczema Area and Severity Index) [39]. A full overview of all exclusion criteria is provided in supplemental materials and methods. Individuals had a 4-week washout period during which it was not allowed to use soaps or cosmetics on the ventral forearms. Subjects with lesional AD skin were put on standard medication that did not contain any interfering lipids (see 'Use of standardized formulations' in the supplement). After 4 weeks the participants were scored again for SCORAD and EASI. This was followed by monitoring skin-pH and TEWL in depth after SC removal by tape stripping from a marked area on their ventral forearm. TEWL was measured with a closed chamber evaporimeter (Aqua Flux AF200: Biox Systems Ltd, London, UK) and skin-pH was measured with a skin-pH Portable Meter - HI99181 – (Hanna Instruments, Nieuwegein, NL). Subsequently two 4 mm punch biopsies were collected from the non-lesional AD skin and skin from controls, adjacent to the tape stripped sites. Two additional biopsies were obtained from three AD patients that had lesional skin sites on their ventral forearms. Biopsies were used either for SC lipid analysis or were snap frozen with matrix specimen Tissue-Tek (Sakura Finetek, Alphen a/d Rijn, Netherlands) in liquid nitrogen. Frozen samples were cut to 5 µm thick sections (Leica CM3050s, Leica Microsystems, Germany), placed on SuperFrost plus microscope slides (VWR International, Netherlands) and stored at -80°C prior to being used for enzyme studies.

SC lipid isolation and analysis. The SC of one of the biopsies was isolated by a common trypsin digestion procedure [59], followed by SC lipid isolation with use of an extended Bligh and Dyer extraction [60, 61]. The SC lipids were reconstituted in heptane:chloroform:methanol (95:2.5:2.5) and the exact ceramide and FFA composition was finally determined by liquid chromatography/mass spectrometry (LC/MS), as previously reported [61]. Briefly, a normal phase pva-column (100 x 2.1mm i.d., 5µm particle size; YMC Kyota, Japan) attached to and Acquity UPLC H-class device (Waters, Milford, MA, USA), programmed with an elution gradient of heptane toward heptane:isopropanol:ethanol (50:25:25), was used to separate the ceramides subclasses by chromatography. A Waters Xevo TQ-S MS, equipped with an atmospheric pressure chemical ionization (APCI) source was used for all mass analysis in positive ion full scan mode of the lipids. Data presented in absolute amounts (nmol/µg SC) was obtained by applying our reported quantitative model by using deuterated internal standards (Ceramides EOS and NS).

For FFA analysis, a new method was developed based on our previously

reported analysis [62]. A Purospher Star LiChroCART column (55x2 mm i.d., 3 µm particle size; Merck, Darmstadt, Germany) was used to separate FFAs while a solvent gradient of acetonitrile:H2O (90:10) to methanol:heptane (90:10) was maintained at 0.5 mL/min. For ionization optimization, addition of 2% chloroform and 0.005% acetic acid led to stable [M+Cl]- and [M-H]- traces, both analyzed in SIR negative ion mode using a Waters XEVO TQ-S MS with an IonSabre APCI MkII probe. Details of this method are provided in the supplement.

Statistics. Statistical tests were performed using Graphpad Prism v6 (GraphPad Software, La Jolla California USA) and IBM SPSS Statistics v24 (IBM, New York, NY). Most data appeared non-normally distributed, hence we used non-parametric statistics: significant ordinal trends in the SC lipid quantities (ceramides and FFAs) were determined using the Jonckheere-Terpstra trend tests. Spearman's ρ were calculated to indicate correlation coefficients. Significance was set at the $p<0.05$ level.

Immunohistochemical staining of ASM, GCase, HBD-3 and TARC. Skin cryosections were washed three times with PBS and blocked in PBS containing 1% (v/v) BSA and 2.5% (v/v) horse serum. Next, sections were incubated overnight at 4°C with any of the primary antibodies diluted in 1% BSA in PBS. Thereafter, sections were washed with PBS and labeled for one hour at room temperature with secondary antibody diluted in 1% BSA in PBS. Then sections were washed twice in PBS, once in demi-H2O and finally mounted with Vectashield with diamidino-phenylindole solution (DAPI, Vector Laboratories, Burlingame, CA). Antibody details and dilution factors are depicted in table 1.

In-situ *ABP labeling GCase.* Active GCase was visualized by labeling with the ABP MDW941 as we reported previously [63]. Briefly, skin cryosections were washed in MilliQ with 1% (v/v) Tween-20 (Bio-Rad Laboratories), followed by

Table 1: Overview primary and secondary antibodies.

	Antibody	Dilution ratio	Binding	Antibody brand
1st	Anti-GCase	1:150	Human anti rabbit	Abcam (ab125065)
	Anti-ASM	1:150	Human anti mouse	Novus (NBP2-45889)
	Anti-HBD-3	1:1500	Human anti rabbit	Abcam (ab19270)
	Anti-TARC	1:100	Human/rat/mouse anti rabbit	Abcam (ab182793)
2nd	Rhodamine red	1:300	Goat anti rabbit	Jackson ImmunoResearch (711-295-152)
	Cy3	1:1000	Goat anti mouse	Abcam (ab97035)

incubation with 100nM of MDW941 in McIlvain buffer (150 mM citric acid-Na2HPO4 (pH 5.2)) with 0.2% (w/v) sodium taurocholate and 0.1% (v/v) Triton X-100 for 1 hour at 37°C. Then samples were washed once with MilliQ with 1% (v/v) Tween-20 and afterwards three times with MilliQ water. Mounting was performed using Vectashield with DAPI solution.

In-situ *zymography ASM.* Active ASM was visualized by our recently developed *in situ* zymography method using 6-HMU-PC (Moscerdam, Oegstgeest, the Netherlands) as ASM specific substrate [47]. Skin samples were washed in MilliQ with 1% (v/v) Tween-20. The sections were incubated in 0.1M sodium acetate buffer pH5.2 containing 0.5mM 6-HMU-PC in, 0.02% (w/v) sodium azide and 0.2% (w/v) sodium taurocholate at 37°C for one hour. Subsequently, samples were dip-washed twice with MilliQ with 1% (v/v) Tween-20. Mounting was performed using Vectashield with Propidium iodide (PI, Vector Laboratories, Burlingame, CA).

Fluorescence microscopy. Microscopy images were taken with a Zeiss Imager. D2 microscope connected to a ZeissCam MRm camera (Zeiss, Göttingen, Germany) with objective magnification 10x and lens magnification between 10-63x (with immersion oil). Zen 2 2012, blue edition (Zeiss) was used for image processing. Exposure times were kept constant for each individual experiment. Gamma was set to 1.0 for all measurements. Enzyme activity was determined at its optimal magnification 63x. Activity of ASM was visualized by 6-HMU at λex=380 nm and λem=460 nm, whereas active GCase was visualized with ABP MDW941 at λex=549nm, λem=610nm. Microscopy images were independently scored by two researchers on the location of GCase, ASM, HBD-3 and TARC.

Supplemental Materials and Methods

Exclusion criteria for participation in the study. A potential subject who met any of the following criteria was excluded from participation in this study:

Exclusion criteria for healthy subjects and AE patients

- Aged under 18 or over 40.
- Non-Caucasian.
- Abundant hair presence on the ventral forearms.
- Unnatural abnormalities on one of their ventral forearms (e.g. skin lesions, tattoos).
- Using any systemic drug therapy (e.g. cholesterol-lowering drugs, insulin related drugs, steroids and immunosuppressants).
- Who received phototherapy in the past 2 years.
- Pregnancy.

Additional exclusion criteria for healthy subjects:
- No chronically inflammatory disease.
- Use of dermatological products (e.g. creams) on their ventral forearms on a daily basis.
- Dermatological disorders or a history of dermatological disorders.

Additional exclusion criteria for AE patients:
- The absence of both lesional and non-lesional skin sites on their ventral forearms at day 0 of the study. Thus, when patients only have non-lesional skin sites at their ventral forearms of Day 0, but not inflamed, red lesions, they will be excluded as one of the key objectives is to investigate within the same subject non-lesional skin with lesional skin.
- The use of corticosteroids class IV or higher. Patients with corticosteroids class I-III need to give informed consent about changing their medication to a standardized regimen (see "3) study design").

Besides, all subjects were requested:
- Not to change their usual skin care regimen (except for topical corticosteroids, as described above).
- The forearms should not be exposed to excessive sun- or artificial UV-light.
- Not to smoke or start smoking 3 weeks prior or during the experiment;
- Not to drink warm and/or caffeine containing beverages on the day of the experiment.
- Not to apply any topical formulation on their ventral forearms on day 28 (study day).
- To leave the application site(s) untouched during the day of the experiment.
- To keep an agenda for 3 weeks in advance in which they describe and take photographs of their ventral forearms once every day. In this way, we have more information about the history of the lesional skin prior to the primary investigation day.

Use of standardized formulations. Patients with atopic eczema often do apply topical formulations of any kind on their body. This includes sometimes class 1-4 corticosteroids. These formulations highly influence with the primary analysis and objectives:
1) Many topical formulations and emollients contain lipids that are also present in human skin. This highly interferes with our lipid composition data.
2) Corticosteroids have a systemic effect on the inflammation, thereby significantly altering the inflammation markers locally and systemically.

Stardardized treatment during the study period was therefore as follows:
- Patients that did not apply any topical continue this until day 28.
- Patients that applied non-corticosteroid formulation switched to a cetomacrochol cream.
- Patients that applied class 1 corticosteroids switched to a 0.1% hydrocortisone

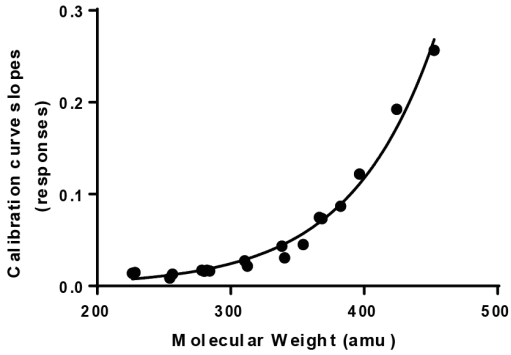

acetate in cetomacrochol cream with emollient cetomacrochol.
- Patients that applied class 2 or 3 corticosteroids switched to 0.1% triamcinolon acetonide in cetomacrochol with emollient cetomacrochol.
- Patients that applied class 4 corticosteroids were excluded from the study.

Analysis of Stratum Corneum fatty acid composition by LC/MS. Isolated Stratum Corneum fatty acids from biopsies of all AD patients and controls were quantitatively analyzed by ultra performance liquid chromatography/mass spectrometry (UPLC/MS), adapted from our previously reported analysis (van Smeden et al., BBA, 2014). Tables I, II, and III below provide all detailed

Table I: UPLC setup

UPLC system	Waters Acquity UPLC H-Class
UPLC reverse phase C18	Purospher Star LiChroCART (55x2 mm, 3µm)
UPLC reverse phase C18	
- Heating tray temperature	- +40°C
- Wash solvent	- MeOH:Heptane:IPA (25:50:25%)
- Injection volume	- 10µl
Mobile Phase	
- Flow rate	- 0.5 mL/min
- Solvents	
- Acetonitrile	- ULC/MS grade, Biosolve (012041)
- Methanol	- ULC/MS grade, Biosolve (136841)
- Heptane	- ULC/MS grade, Boom (76025346.2500)
- Ionization enhancers/stabilizers	
- Chloroform (2%)	- HPLC grade, Labscan (C07C11X)
- Acetic acid (0.005%)	- HPLC grade, Biosolve (01070601)

information on parameters for respectively LC, MS, and validation parameters of the quantified analytes.
Absolute quantification was achieved taking into account the different response factors for each ion trace (see Figure on the right). The individual response factors were obtained via analysis of calibrators (see table III) in addition to an internal standard (ISTD) correction using deuterated ISTDs C18:0 D35 and C24:0 D47. Mass Lynx and Target Lynx Software (Waters) was used to process the data.

Table II: MS setup.

MS System	MS System
LC/MS interface	LC/MS interface
- Probe	- Probe
- Corona discharge current	- Corona discharge current
- Cone voltage	- Cone voltage
- APCI probe temperature	- APCI probe temperature
- Desolvation gas volume	- Desolvation gas volume
- Cone gas volume	- Cone gas volume
Scan Method	Scan Method
- Ionization mode	- Ionization mode
Scan settings/trace	Scan settings/trace
- Scan time	- Scan time
- Inter scan Delay	- Inter scan Delay
- Collision gas flow (Q2)	- Collision gas flow (Q2)
- Collision Voltage (Q2)	- Collision Voltage (Q2)
MS Resolution	MS Resolution
- Q1	- Q1
- Q3	- Q3

Table III: Validation parameters.

	Fatty acid (length : saturation)	Ion trace(s)* (amu)	Rt (min. ± SD)	Calibration curves (R-value)**
Saturated Fatty Acids	20:0	311.46 + 347.37	2.23 ± 0.012	0.993
	22:0	339.37 + 375.35	2.68 ± 0.008	0.995
	23:0	353.36 + 389.33	2.87 ± 0.005	0.998
	24:0	367.41 + 403.38	3.03 ± 0.022	0.995
	25:0	381.46 + 417.37	3.16 ± 0.005	0.997
	26:0	395.51 + 431.42	3.29 ± 0.003	0.996
	28:0	423.48 + 459.46	3.55 ± 0.004	0.994
	30:0	451.52 + 487.43	3.83 ± 0.005	0.995
Unsaturated Fatty Acids	20:1	309.38 + 345.36	1.63 ± 0.024	0.991
	22:1	337.36 + 373.33	2.19 ± 0.004	0.996
	24:1	365.39 + 401.31	2.68 ± 0.049	0.995

*: Masses correspond to ions [M-H]- + [M+Cl]-. ** Correlation values of 3 independent calibration curves (range 1-100 pmol) with a mixture of 11 fatty acids and two deuterated internal standards.

Supplemental data

Supplemental table S1 - Disease manifestation and main location of the (active) enzymes per individual subject: The main localization pattern is mentioned first, italic depicts the less abundant pattern that sometimes is also found in the subject. Green = control; orange = non-lesional AD ; red = lesioanl AD.

Nr	Sex	TEWL	SCORAD day28	local SCORAD day 28	EASI day 28	Expressed GCase	Active GCase	Expressed ASM	Active ASM
1	F	12.44	0	0	0	At the interface	Lower layers SC *Whole SC*	Viable epidermis	Around interface *Scattered through SC*
2	M	8.81	0	0	0	At the interface	Lower layers SC	Viable epidermis	Around interface
3	F	11.65	0	0	0	At the interface	Whole SC	Viable epidermis	Scattered through SC *Around interface*
4	F	10.32	0	0	0	At the interface	Whole SC *Lower layers SC*	Viable epidermis	Around interface
5	F	7.92	0	0	0	At the interface	Lower layers SC *Whole SC*	Viable epidermis	No detectable signal
6	M	12.83	15.4	1	3.2	At the interface	Whole SC	Viable epidermis	Scattered through SC *Whole SC*
7	F	19.19	18.2	1	1.8	At the interface	Not in lower SC layers *Whole SC*	Viable epidermis	Whole SC
8	F	8.37	23	2	1	At the interface	Bottom SC layers	Viable epidermis	Whole SC *Scattered through SC*
9	F	11.34	13.9	2	5	At the interface	Whole SC *Bottom SC layers*	Viable epidermis	Scattered through SC

Continuation supplemental table S1 - Disease manifestation and main location of the (active) enzymes per individual subject: The main localization pattern is mentioned first, italic depicts the less abundant pattern that sometimes is also found in the subject. Green = control; orange = non-lesional AD ; red = lesioanl AD.

Nr	Sex	TEWL	SCORAD day28	local SCORAD day 28	EASI day 28	Expressed GCase	Active GCase	Expressed ASM	Active ASM
10	M	25.3	41.16	4	5.7	At the interface	Whole SC	Viable epidermis	Whole SC
11	F	14.99	8.8	0	0.3	At the interface	Bottom SC layers *Whole SC*	Viable epidermis	Scattered through SC
12	M	17.94	22.6	2	1.4	At the interface	Bottom SC layers	Viable epidermis	Scattered through SC
13	M	8.39	64.3	1	29.8	Below interface *At the interface*	Bottom SC layers *Whole SC*	Viable epidermis	Scattered through SC
13	M	24.46	64.3	9	29.8	At the interface	Whole SC *No detectable signal*	Viable epidermis	Whole SC
14	F	5.03	20.1	0	1.2	Not at the interface	Bottom SC layers *Whole SC*	Viable epidermis	No detectable signal
14	F	38.51	20.1	6	1.2	At the interface	Not in lower SC layers	Viable epidermis	Scattered through SC *Whole SC*
15	M	23.74	31.1	2	4.9	At the interface	Whole SC	No detectable signal	Whole SC
15	M	22.36	31.1	4	4.9	At the interface	Not in lower SC layers	No detectable signal	Whole SC

Supplemental table S2 – Ceramide class data per individual subject.: Green = control; orange = non-lesional AD ; red = lesioanl AD.

Code	NdS	NS	NP	NH	AdS	AS	AP	AH	EOdS	EOS	EOP	EOH
1	1587.3	1736.1	3831.7	3543.1	290.2	977.7	1918.5	3130.1	94.0	1103.0	184.9	724.2
2	1774.2	1076.3	3516.9	2595.4	374.8	709.4	2357.5	2639.4	88.6	536.4	128.3	350.3
3	1897.8	2020.1	4550.2	4308.3	372.2	1182.8	2427.2	3890.1	110.8	1300.2	231.5	870.9
4	1663.9	1452.4	3317.1	2424.2	396.8	1296.6	3114.9	3445.0	74.0	541.0	116.3	342.9
5	2257.2	1632.5	5242.4	3943.6	378.3	846.0	2023.9	2681.0	145.3	1113.9	311.9	827.0
6	2608.2	1823.0	4186.4	2669.9	573.7	1373.1	3008.3	3064.2	100.8	653.8	143.8	343.9
7	1014.5	1898.7	1587.9	1848.3	224.7	1475.6	1176.5	2392.2	82.1	778.3	80.0	389.9
8	1408.3	1085.0	2938.7	2486.0	224.3	548.6	1408.5	1952.8	97.4	644.5	138.4	443.5
9	1994.0	1733.8	2591.5	1622.8	439.2	1503.3	2458.6	2566.1	67.5	299.0	95.5	163.1
10	1371.9	1955.9	2273.7	1656.8	403.7	1736.8	2035.6	2212.4	55.4	501.9	105.8	255.5
11	1556.8	1562.6	2861.8	2538.1	324.4	1056.7	1757.0	2392.8	124.3	1082.6	175.3	568.3
12	1425.6	1371.0	3189.9	2214.0	259.1	921.9	2261.6	2502.1	66.6	501.3	130.0	301.3
13	1633.9	1664.2	3283.4	1930.9	390.7	1469.2	2931.1	3269.0	86.2	566.1	140.2	310.1
13	892.7	3082.5	1356.3	973.5	249.3	2500.5	1814.1	1593.1	23.3	278.4	54.7	118.5
14	1931.9	1410.4	5705.6	3383.0	306.1	713.7	1975.8	2321.0	109.0	1050.2	299.4	758.4
14	1774.6	4666.9	2034.8	1658.5	400.3	2834.0	1797.1	1986.3	44.3	582.3	95.7	229.5
15	1269.3	1968.3	2290.4	1540.6	287.5	1714.6	2512.3	2449.0	70.4	624.4	114.4	293.0
15	541.9	1798.5	772.1	814.0	146.1	1548.8	941.3	1176.1	11.5	187.5	32.3	92.3

Supplemental tables S3 – Semi-quantitative GlcCer data: Top: Average GlcCer/Cer ratio EOH subclass as mean +/- SEM. Bottom: Average GlcCer/Cer ratio EOS subclass as mean +/- SEM.

	EOH66	EOH67	EOH68	EOH69	EOH70
Control	0.09 ± 0.03	0.09 ± 0.03	0.09 ± 0.03	0.07 ± 0.03	0.06 ± 0.03
Non-lesional	0.18 ± 0.04	0.17 ± 0.04	0.16 ± 0.03	0.14 ± 0.04	0.13 ± 0.03
Lesional	0.28 ± 0.17	0.23 ± 0.13	0.22 ± 0.15	0.21 ± 0.14	0.18 ± 0.12

	EOS64	EOS66	EOS67	EOS68	EOS69	EOS70	EOS71	EOS72	EOS74
Control	0.13 ± 0.10	0.32 ± 0.11	0.28 ± 0.08	0.23 ± 0.07	0.19 ± 0.06	0.18 ± 0.04	0.18 ± 0.04	0.20 ± 0.05	0.14 ± 0.02
Non-lesional	0.37 ± 0.13	0.64 ± 0.14	0.51 ± 0.09	0.42 ± 0.08	0.32 ± 0.06	0.28 ± 0.05	0.26 ± 0.04	0.24 ± 0.04	0.18 ± 0.02
Lesional	0.32 ± 0.25	0.60 ± 0.31	0.50 ± 0.26	0.47 ± 0.22	0.54 ± 0.31	0.46 ± 0.22	0.80 ± 0.43	0.47 ± 0.20	0.23 ± 0.06

Supplemental figures

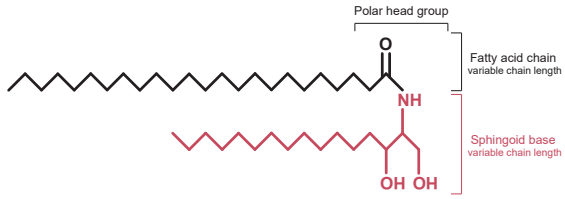

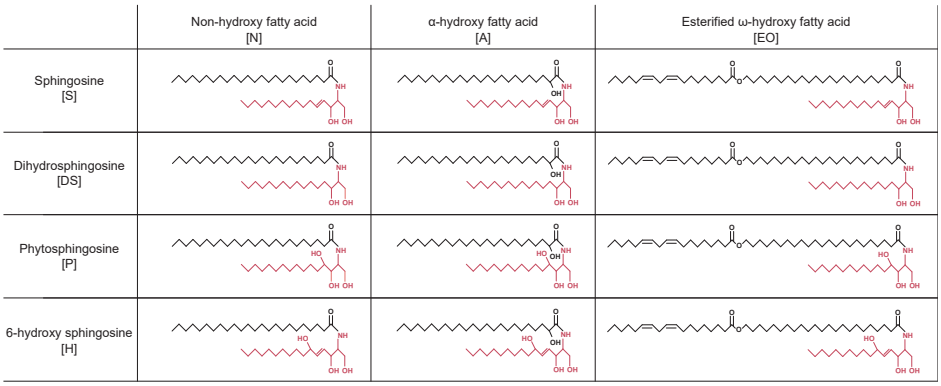

Supplemental figure S1: Table of the 12 common SC ceramide subclasses. Ceramide nomenclature including the molecular architecture. A ceramide is composed of a fatty acid chain (labeled in gray) linked via an amide bond to a sphingoid base (depicted in blue). In human skin, both chains vary in length (red arrows), leading to a total chain length (the two combined chains together) that varies from very short (~34 carbon atoms) to very long (>80 carbon atoms) chains. In addition, both chains can have additional functional groups at the carbon positions marked in red. This results in 4 different sphingoid bases (dihydrosphingosine [dS], sphingosine [S], phytosphingosine [P], 6-hydroxysphingosine [H]) and 3 different acyl chains (non-hydroxy fatty acid [N], α-hydroxy fatty acid [A] and the ultra-long esterified ω-hydroxy fattyacid [EO]). Together, this results in the presence of the 12 most common presented subclasses. As an example, a cer with a non-hydroxy fatty acid of 16 carbon atoms long and a sphingosine base of 18 carbon atoms will be denoted as ceramide [NS] C34.

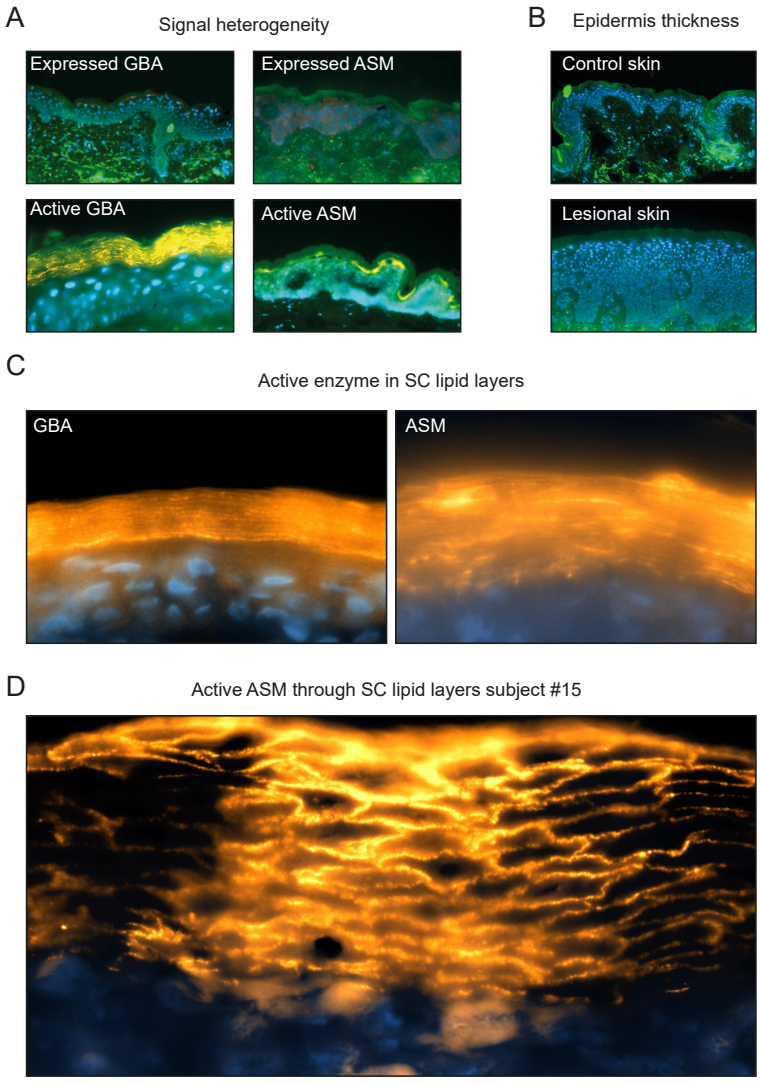

Supplemental figure S2: *In situ* heterogeneity localization GCase and ASM, lesional AD skin morphology and localization of active GCase and ASM in the SC lipid layers. A. Examples of heterogeneity of the fluorescence signal of expressed and active GCase and ASM. Left top: Expressed GCase (red) in subject #11. DAPI staining in blue and autofluorescence in green, 20x magnification. Left bottom: Active GCase (gold) in subject #7. DAPI staining in blue and autofluorescence in green, 63x magnification. Right top: expressed ASM (red) in subject #3. DAPI staining in blue and autofluorescence in green, 20x magnification. Right bottom: active ASM (gold) in subject #2. PI staining in blue and autofluorescence in green, 20x magnification. B. Epidermis in control skin (top) and in lesional skin (bottom). DAPI staining in blue and autofluorescence in green, 20x magnification. C. Active SC enzymes in the SC lipid layers. GCase (left, gold. DAPI in blue) in subject #1 and ASM(right, gold. PI in blue) in subject #10, 63x magnification. D. Example of swollen corneocytes in the SC of lesional skin of subject #15, active ASM in gold, PI in blue, 63x magnification.

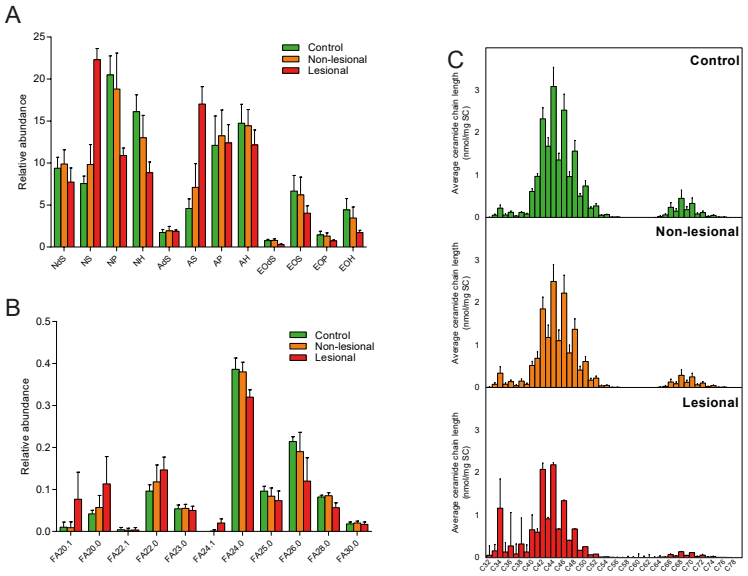

Supplemental figure S3: Lipid data SC. A. Bar plot of the relative amount of ceramides in the SC classified by category (mean ±SD). B. Bar plot of the relative amount of SC fatty acids categorized by length and saturation (mean ±SD). C. Bar plots of the abundances of the ceramide chain length subclasses per control, non-lesional and lesional group (mean±SD).

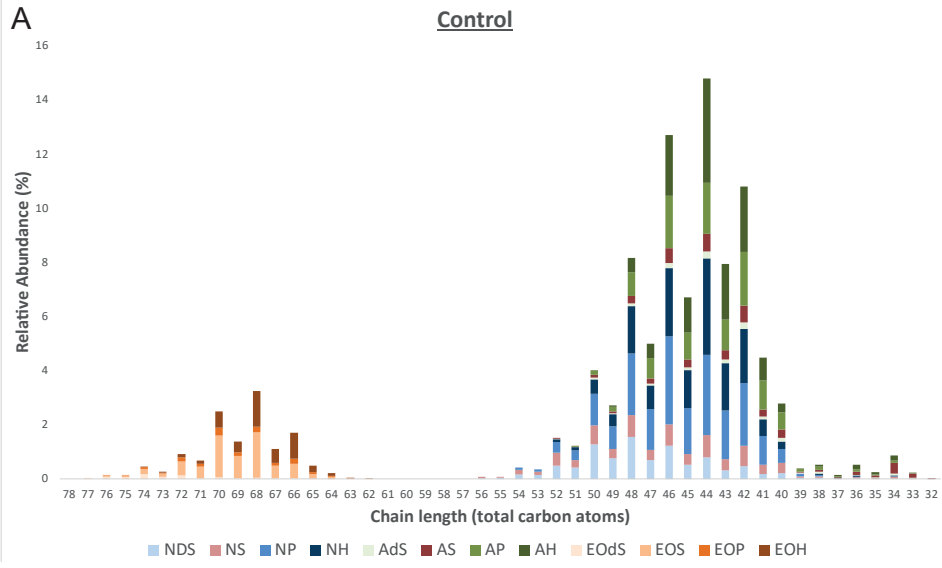

Supplemental Figure S4A: Bar plots of the relative abundances (%) of the ceramide chain lengths, labelled for each individual subclass, displayed for control

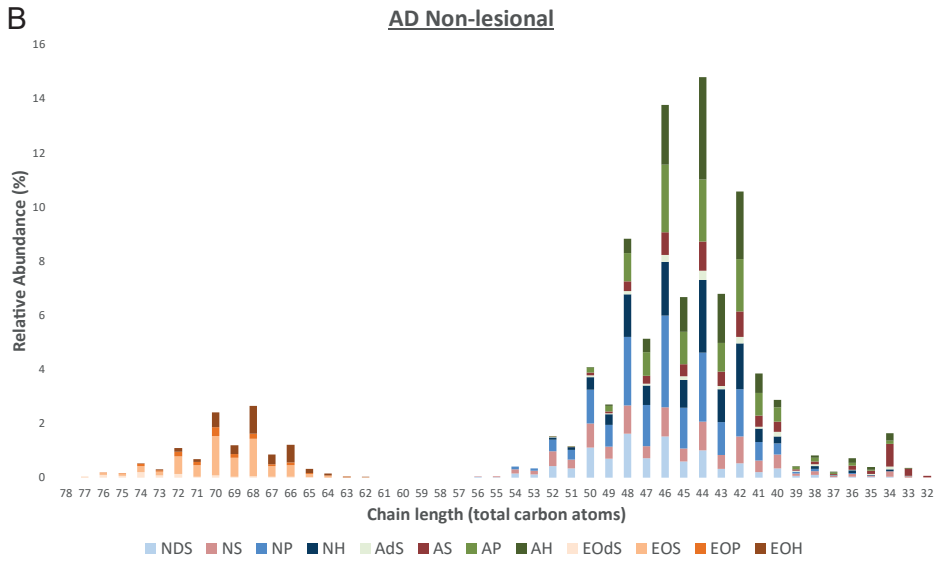

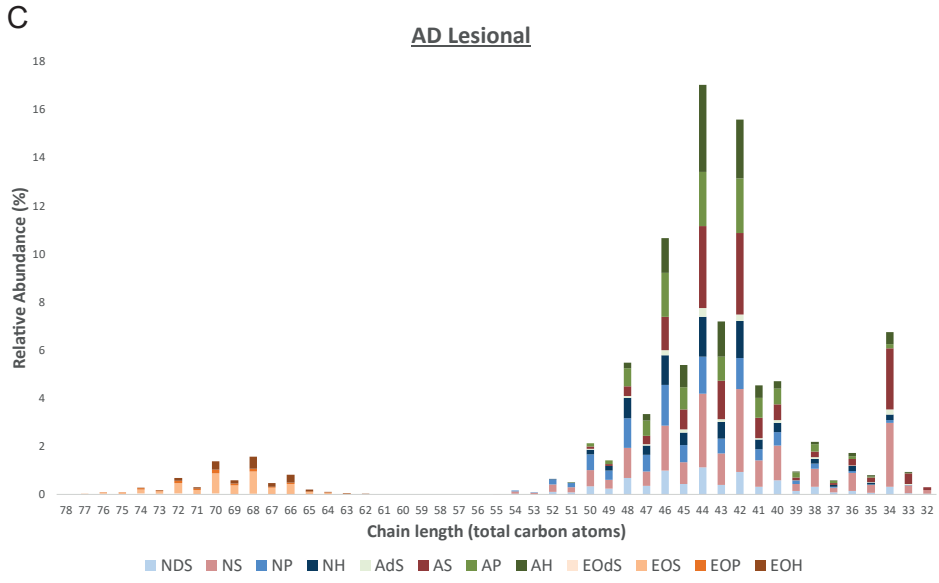

Supplemental Figure S4B and S4C: B. Bar plots of the relative abundances (%) of the ceramide chain lengths, labelled for each individual subclass, displayed for non-lesioanl AD. C. Bar plots of the relative abundances (%) of the ceramide chain lengths, labelled for each individual subclass, displayed for lesional AD.

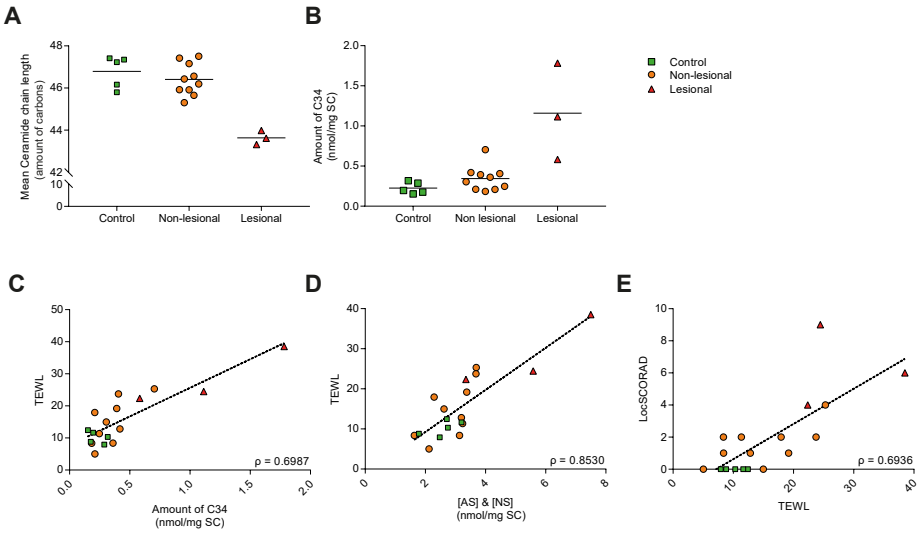

Supplemental figure S5: SC barrier lipid data. A. Dot plot of the mean ceramide chain length in the SC categorized by control, non-lesional or lesional AD skin. B. Dot plot of the absolute amount of C34 ceramides categorized by control, non-lesional or lesional AD skin. C. Dot plot TEWL and amount of C34 per subject. D. Dot plot TEWL and amount of ceramide [AS]&[NS] per subject E. Dot plot locSCORAD and TEWL per subject. All ρ's are calculated according to Spearman correlation test.

References

1. K.C. Madison, Barrier function of the skin: "la raison d'etre" of the epidermis, J Invest Dermatol, 121 (2003) 231-241.
2. P.M. Elias, M. Steinhoff, "Outside-to-inside" (and now back to "outside") pathogenic mechanisms in atopic dermatitis, J Invest Dermatol, 128 (2008) 1067-1070.
3. N.B. Silverberg, J.I. Silverberg, Inside out or outside in: does atopic dermatitis disrupt barrier function or does disruption of barrier function trigger atopic dermatitis?, Cutis, 96 (2015) 359-361.
4. P.M. Brunner, E. Guttman-Yassky, D.Y. Leung, The immunology of atopic dermatitis and its reversibility with broad-spectrum and targeted therapies, J Allergy Clin Immunol, 139 (2017) S65-S76.
5. C.N. Palmer, A.D. Irvine, A. Terron-Kwiatkowski, Y. Zhao, H. Liao, S.P. Lee, D.R. Goudie, A. Sandilands, L.E. Campbell, F.J. Smith, G.M. O'Regan, R.M. Watson, J.E. Cecil, S.J. Bale, J.G. Compton, J.J. DiGiovanna, P. Fleckman, S. Lewis-Jones, G. Arseculeratne, A. Sergeant, C.S. Munro, B. El Houate, K. McElreavey, L.B. Halkjaer, H. Bisgaard, S. Mukhopadhyay, W.H. McLean, Common loss-of-function variants of the epidermal barrier protein filaggrin are a major predisposing factor for atopic dermatitis, Nat Genet, 38 (2006) 441-446.
6. A.D. Irvine, W.H. McLean, Breaking the (un)sound barrier: filaggrin is a major gene for atopic dermatitis, J Invest Dermatol, 126 (2006) 1200-1202.
7. S. Kezic, A. Kammeyer, F. Calkoen, J.W. Fluhr, J.D. Bos, Natural moisturizing factor components in the stratum corneum as biomarkers of filaggrin genotype: evaluation of minimally invasive methods, Br J Dermatol, 161 (2009) 1098-1104.
8. G.M. O'Regan, A. Sandilands, W.H.I. McLean, A.D. Irvine, Filaggrin in atopic dermatitis, J Allergy Clin Immunol, 122 (2008) 689-693.
9. P.M. Elias, Structure and function of the stratum corneum extracellular matrix, J Invest Dermatol, 132 (2012) 2131-2133.
10. J.A. Bouwstra, F.E. Dubbelaar, G.S. Gooris, M. Ponec, The lipid organisation in the skin barrier, Acta Derm Venereol Suppl (Stockh), 208 (2000) 23-30.
11. J. van Smeden, J.A. Bouwstra, Stratum Corneum Lipids: Their Role for the Skin Barrier Function in Healthy Subjects and Atopic Dermatitis Patients, Curr Probl Dermatol, 49 (2016) 8-26.
12. K.R. Feingold, Thematic review series: skin lipids. The role of epidermal lipids in cutaneous permeability barrier homeostasis, J Lipid Res, 48 (2007) 2531-2546.
13. M. Rabionet, K. Gorgas, R. Sandhoff, Ceramide synthesis in the epidermis, Biochim Biophys Acta, 1841 (2014) 422-434.
14. K.R. Feingold, P.M. Elias, Role of lipids in the formation and maintenance of the cutaneous permeability barrier, Biochim Biophys Acta, 1841 (2014) 280-294.
15. S. Motta, M. Monti, S. Sesana, R. Caputo, S. Carelli, R. Ghidoni, Ceramide composition of the psoriatic scale, Biochim Biophys Acta, 1182 (1993) 147-151.
16. M. Janssens, J. van Smeden, G.S. Gooris, W. Bras, G. Portale, P.J. Caspers, R.J. Vreeken, T. Hankemeier, S. Kezic, R. Wolterbeek, A.P. Lavrijsen, J.A. Bouwstra, Increase in short-chain ceramides correlates with an altered lipid organization and decreased barrier function in atopic eczema patients, J Lipid Res, 53 (2012) 2755-2766.
17. J. Ishikawa, H. Narita, N. Kondo, M. Hotta, Y. Takagi, Y. Masukawa, T. Kitahara, Y. Takema, S. Koyano, S. Yamazaki, A. Hatamochi, Changes in the ceramide profile of atopic dermatitis patients, J Invest Dermatol, 130 (2010) 2511-2514.
18. J. van Smeden, M. Janssens, E.C. Kaye, P.J. Caspers, A.P. Lavrijsen, R.J. Vreeken, J.A. Bouwstra, The importance of free fatty acid chain length for the skin barrier function in atopic eczema patients, Exp Dermatol, 23 (2014) 45-52.
19. J. van Smeden, M. Janssens, G.S. Gooris, J.A. Bouwstra, The important role of stratum corneum lipids for the cutaneous barrier function, Biochim Biophys Acta, 1841 (2014) 295-313.
20. S. Ito, J. Ishikawa, A. Naoe, H. Yoshida, A. Hachiya, T. Fujimura, T. Kitahara, Y. Takema, Ceramide synthase 4 is highly expressed in involved skin of patients with atopic dermatitis, J Eur Acad Dermatol Venereol, 31 (2017) 135-141.
21. C.P. Shen, M.T. Zhao, Z.X. Jia, J.L. Zhang, L. Jiao, L. Ma, Skin Ceramide Profile in Children With Atopic Dermatitis, Dermatitis, 29 (2018) 219-222.
22. Y. Uchida, Ceramide signaling in mammalian epidermis, Biochim Biophys Acta, 1841 (2014) 453-462.
23. S. Hamanaka, M. Hara, H. Nishio, F. Otsuka, A. Suzuki, Y. Uchida, Human epidermal glucosylceramides are major precursors of stratum corneum ceramides, J Invest Dermatol, 119 (2002) 416-423.
24. Y. Uchida, M. Hara, H. Nishio, E. Sidransky, S. Inoue, F. Otsuka, A. Suzuki, P.M. Elias, W.M. Holleran, S. Hamanaka, Epidermal sphingomyelins are precursors for selected stratum corneum ceramides, J Lipid Res,

41 (2000) 2071-2082.
25. K. Jin, Y. Higaki, Y. Takagi, K. Higuchi, Y. Yada, M. Kawashima, G. Imokawa, Analysis of beta-glucocerebrosidase and ceramidase activities in atopic and aged dry skin, Acta Derm Venereol, 74 (1994) 337-340.
26. J.M. Jensen, R. Folster-Holst, A. Baranowsky, M. Schunck, S. Winoto-Morbach, C. Neumann, S. Schutze, E. Proksch, Impaired sphingomyelinase activity and epidermal differentiation in atopic dermatitis, J Invest Dermatol, 122 (2004) 1423-1431.
27. S. Kusuda, C.Y. Cui, M. Takahashi, T. Tezuka, Localization of sphingomyelinase in lesional skin of atopic dermatitis patients, J Invest Dermatol, 111 (1998) 733-738.
28. M. Danso, W. Boiten, V. van Drongelen, K. Gmelig Meijling, G. Gooris, A. El Ghalbzouri, S. Absalah, R. Vreeken, S. Kezic, J. van Smeden, S. Lavrijsen, J. Bouwstra, Altered expression of epidermal lipid bio-synthesis enzymes in atopic dermatitis skin is accompanied by changes in stratum corneum lipid composition, J Dermatol Sci, 88 (2017) 57-66.
29. J.P. Hachem, D. Crumrine, J. Fluhr, B.E. Brown, K.R. Feingold, P.M. Elias, pH directly regulates epidermal permeability barrier homeostasis, and stratum corneum integrity/cohesion, J Invest Dermatol, 121 (2003) 345-353.
30. Y. Hatano, M.Q. Man, Y. Uchida, D. Crumrine, T.C. Scharschmidt, E.G. Kim, T.M. Mauro, K.R. Feingold, P.M. Elias, W.M. Holleran, Maintenance of an acidic stratum corneum prevents emergence of murine atopic dermatitis, J Invest Dermatol, 129 (2009) 1824-1835.
31. I. Nomura, E. Goleva, M.D. Howell, Q.A. Hamid, P.Y. Ong, C.F. Hall, M.A. Darst, B. Gao, M. Boguniewicz, J.B. Travers, D.Y. Leung, Cytokine milieu of atopic dermatitis, as compared to psoriasis, skin prevents induction of innate immune response genes, J Immunol, 171 (2003) 3262-3269.
32. T. Kakinuma, K. Nakamura, M. Wakugawa, H. Mitsui, Y. Tada, H. Saeki, H. Torii, A. Asahina, N. Onai, K. Matsushima, K. Tamaki, Thymus and activation-regulated chemokine in atopic dermatitis: Serum thymus and activation-regulated chemokine level is closely related with disease activity, J Allergy Clin Immunol, 107 (2001) 535-541.
33. N. Furusyo, H. Takeoka, K. Toyoda, M. Murata, S. Maeda, H. Ohnishi, N. Fukiwake, H. Uchi, M. Furue, J. Hayashi, Thymus and activation regulated chemokines in children with atopic dermatitis: Kyushu University Ishigaki Atopic Dermatitis Study (KIDS), Eur J Dermatol, 17 (2007) 397-404.
34. E. Berdyshev, E. Goleva, I. Bronova, N. Dyjack, C. Rios, J. Jung, P. Taylor, M. Jeong, C.F. Hall, B.N. Richers, K.A. Norquest, T. Zheng, M.A. Seibold, D.Y. Leung, Lipid abnormalities in atopic skin are driven by type 2 cytokines, JCI Insight, 3 (2018).
35. Y. Hatano, H. Terashi, S. Arakawa, K. Katagiri, Interleukin-4 suppresses the enhancement of ceramide synthesis and cutaneous permeability barrier functions induced by tumor necrosis factor-alpha and interferon-gamma in human epidermis, J Invest Dermatol, 124 (2005) 786-792.
36. L.A. Gerbens, C.A. Prinsen, J.R. Chalmers, A.M. Drucker, L.B. von Kobyletzki, J. Limpens, H. Nankervis, A. Svensson, C.B. Terwee, J. Zhang, C.J. Apfelbacher, P.I. Spuls, i. Harmonising Outcome Measures for Eczema, Evaluation of the measurement properties of symptom measurement instruments for atopic eczema: a systematic review, Allergy, 72 (2017) 146-163.
37. H. Alexander, S. Brown, S. Danby, C. Flohr, Research Techniques Made Simple: Transepidermal Water Loss Measurement as a Research Tool, J Invest Dermatol, 138 (2018) 2295-2300 e2291.
38. S.G. Danby, M.J. Cork, pH in Atopic Dermatitis, Curr Probl Dermatol, 54 (2018) 95-107.
39. J.M. Hanifin, M. Thurston, M. Omoto, R. Cherill, S.J. Tofte, M. Graeber, The eczema area and severity index (EASI): assessment of reliability in atopic dermatitis. EASI Evaluator Group, Exp Dermatol, 10 (2001) 11-18.
40. Severity scoring of atopic dermatitis: the SCORAD index. Consensus Report of the European Task Force on Atopic Dermatitis, Dermatology, 186 (1993) 23-31.
41. Y. Uchida, The role of fatty acid elongation in epidermal structure and function, Dermatoendocrinol, 3 (2011) 65-69.
42. M.M. Man, K.R. Feingold, C.R. Thornfeldt, P.M. Elias, Optimization of physiological lipid mixtures for barrier repair, J Invest Dermatol, 106 (1996) 1096-1101.
43. A. Weerheim, M. Ponec, Determination of stratum corneum lipid profile by tape stripping in combination with high-performance thin-layer chromatography, Arch Dermatol Res, 293 (2001) 191-199.
44. C. Tawada, H. Kanoh, M. Nakamura, Y. Mizutani, T. Fujisawa, Y. Banno, M. Seishima, Interferon-gamma decreases ceramides with long-chain fatty acids: possible involvement in atopic dermatitis and psoriasis, J Invest Dermatol, 134 (2014) 712-718.
45. S. Borodzicz, L. Rudnicka, D. Mirowska-Guzel, A. Cudnoch-Jedrzejewska, The role of epidermal sphingolipids in dermatologic diseases, Lipids Health Dis, 15 (2016) 13.

46. J. van Smeden, I.M. Dijkhoff, R.W.J. Helder, H. Al-Khakany, D.E.C. Boer, A. Schreuder, W.W. Kallemeijn, S. Absalah, H.S. Overkleeft, J. Aerts, J.A. Bouwstra, In situ visualization of glucocerebrosidase in human skin tissue: zymography versus activity-based probe labeling, J Lipid Res, 58 (2017) 2299-2309.
47. J. van Smeden, H. Al-Khakany, Y. Wang, D. Visscher, N. Stephens, S. Absalah, H.S. Overkleeft, J.M.F.G. Aerts, A. Hovnanian, J.A. Bouwstra, Epidermal barrier lipid enzyme activity in Netherton patients relates with serine protease activity and stratum corneum ceramide abnormalities. Submitted.
48. W.A. Boiten, T. Berkers, S. Absalah, J. van Smeden, A.P.M. Lavrijsen, J.A. Bouwstra, Applying a vernix caseosa based formulation accelerates skin barrier repair by modulating lipid biosynthesis, J Lipid Res, 59 (2018) 250-260.
49. S. Seidenari, G. Giusti, Objective assessment of the skin of children affected by atopic dermatitis: a study of pH, capacitance and TEWL in eczematous and clinically uninvolved skin, Acta Derm Venereol, 75 (1995) 429-433.
50. F. Rippke, V. Schreiner, H.J. Schwanitz, The acidic milieu of the horny layer: new findings on the physiology and pathophysiology of skin pH, Am J Clin Dermatol, 3 (2002) 261-272.
51. R.J. Tamargo, A. Velayati, E. Goldin, E. Sidransky, The role of saposin C in Gaucher disease, Mol Genet Metab, 106 (2012) 257-263.
52. C.Y. Cui, S. Kusuda, T. Seguchi, M. Takahashi, K. Aisu, T. Tezuka, Decreased level of prosaposin in atopic skin, J Invest Dermatol, 109 (1997) 319-323.
53. W.M. Holleran, Y. Takagi, G.K. Menon, S.M. Jackson, J.M. Lee, K.R. Feingold, P.M. Elias, Permeability barrier requirements regulate epidermal beta-glucocerebrosidase, J Lipid Res, 35 (1994) 905-912.
54. E.B. Kelly, Encyclopedia of human genetics and disease, Greenwood, Santa Barbara, Calif., 2013.
55. R.W. Jenkins, D. Canals, Y.A. Hannun, Roles and regulation of secretory and lysosomal acid sphingomyelinase, Cell Signal, 21 (2009) 836-846.
56. J. Thijs, T. Krastev, S. Weidinger, C.F. Buckens, M. de Bruin-Weller, C. Bruijnzeel-Koomen, C. Flohr, D. Hijnen, Biomarkers for atopic dermatitis: a systematic review and meta-analysis, Curr Opin Allergy Clin Immunol, 15 (2015) 453-460.
57. D. Hijnen, M. De Bruin-Weller, B. Oosting, C. Lebre, E. De Jong, C. Bruijnzeel-Koomen, E. Knol, Serum thymus and activation-regulated chemokine (TARC) and cutaneous T cell- attracting chemokine (CTACK) levels in allergic diseases: TARC and CTACK are disease-specific markers for atopic dermatitis, J Allergy Clin Immunol, 113 (2004) 334-340.
58. Y. Kataoka, Thymus and activation-regulated chemokine as a clinical biomarker in atopic dermatitis, J Dermatol, 41 (2014) 221-229.
59. H. Tanojo, A. Bos-van Geest, J.A. Bouwstra, H.E. Junginger, H.E. Boodé, In vitro human skin barrier perturbation by oleic acid: Thermal analysis and freeze fracture electron microscopy studies, Thermochimica Acta, 293 (1997) 77-85.
60. E.G. Bligh, W.J. Dyer, A rapid method of total lipid extraction and purification, Can J Biochem Physiol, 37 (1959) 911-917.
61. W. Boiten, S. Absalah, R. Vreeken, J. Bouwstra, J. van Smeden, Quantitative analysis of ceramides using a novel lipidomics approach with three dimensional response modelling, Biochim Biophys Acta, 1861 (2016) 1652-1661.
62. J. van Smeden, W.A. Boiten, T. Hankemeier, R. Rissmann, J.A. Bouwstra, R.J. Vreeken, Combined LC/MS-platform for analysis of all major stratum corneum lipids, and the profiling of skin substitutes, Biochim Biophys Acta, 1841 (2014) 70-79.
63. M.D. Witte, W.W. Kallemeijn, J. Aten, K.Y. Li, A. Strijland, W.E. Donker-Koopman, A.M. van den Nieuwendijk, B. Bleijlevens, G. Kramer, B.I. Florea, B. Hooibrink, C.E. Hollak, R. Ottenhoff, R.G. Boot, G.A. van der Marel, H.S. Overkleeft, J.M. Aerts, Ultrasensitive in situ visualization of active glucocerebrosidase molecules, Nat Chem Biol, 6 (2010) 907-913.

Chapter 5

Glucosylated cholesterol in skin: Synthetic role of extracellular glucocerebrosidase

Glucosylated cholesterol in skin: Synthetic role of extracellular glucocerebrosidase

D.E.C. Boer, M.J. Ferraz, A. Nadaban, M. Mirzaian, A. Hovnanian , J. van Smeden, J.A. Bouwstra, J.M.F.G Aerts.

Abstract

The existence of glucosylated cholesterol (GlcChol) in tissue has recently been recognized. GlcChol is generated from glucosylceramide (GlcCer) and cholesterol through transglucosylation by two retaining β-glucosidases, GBA and GBA2. Given the abundance of GBA, GlcCer and cholesterol in the skin's stratum corneum (SC), we studied the occurrence of GlcChol.

A significant amount of GlcChol was detected in SC (6 pmol/mg weight). The ratio GlcChol/GlcCer is higher in SC than epidermis, 0.083 and 0.011, respectively. Examination of GlcChol in patients with Netherton syndrome revealed comparable levels (11 pmol/mg).

Concluding, GlcChol was identified as a novel component in SC and is likely locally metabolized by GBA. The physiological function of GlcChol in the SC warrants future investigation.

Introduction

The existence of glucosylated cholesterol (GlcChol) has relatively recent been documented [1-3]. GlcChol is present in various tissues in significant amounts. It has become apparent that two cellular retaining β-glucosidases, the lysosomal glucocerebrosidase (GCase; GBA) and cytosol-facing membrane associated glucosylceramidase (GBA2) are able to generate GlcChol from glucosylceramide (GlcCer) and cholesterol (Chol) via a transglucosylation reaction (see Figure 1). Normally, the enzyme GBA2 synthesizes GlcChol and the glycolipid is degraded by the lysosomal GCase [1]. However, when GCase is surrounded by a high concentration of Chol as is the case in Niemann-Pick disease type C, the enzyme also generates GlcChol [1]. In view of occurrence of GlcChol, the skin is of interest, in particular its outer extracellular layer the stratum corneum (SC). Lamellar bodies rich in GlcCer are extruded into the SC

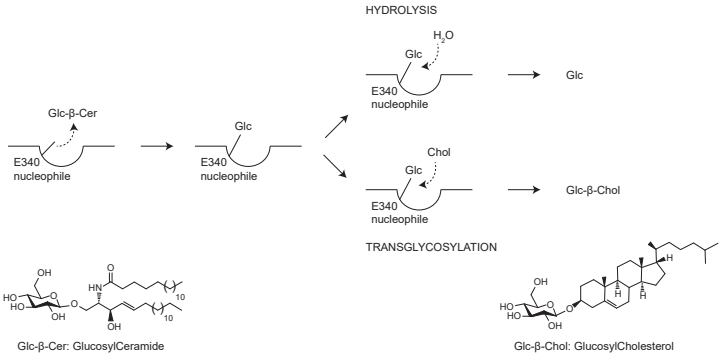

Figure 1. Metabolism of GlcCer by lysosomal GCase. The attack of the glucosidic bond results in cleavage of GlcCer in Cer and the covalent linkage of the glucose (Glc) to the catalytic nucleophile, glutamate 340 [6]. Subsequently, hydrolysis releases Glc. Alternatively, transglucosylation with cholesterol as acceptor results in formation of GlcChol [1].

and the lipid is locally converted by GCase to ceramide (Cer) [4]. This process is essential for the generation of desired barrier properties. The abundant presence of active GCase molecules in the SC has earlier been demonstrated by zymography and labeling with activity-based probes [5, 6]. The importance of GCase in the skin is demonstrated by the dramatic outcome of complete GCase deficiency. GCase-deficient humans and mice do not survive after birth due to major disruption of skin permeability [7]. The collodion baby is the most severe phenotype of Gaucher disease, the inherited lysosomal storage disorder caused by deficiency of GCase [8].

Since the SC contains besides GCase and GlcCer also relative high amounts of Chol, all ingredients for formation of GlcChol appear present. We therefore examined skin regarding the presence of GlcChol. In addition, we studied SC of patients suffering from Netherton syndrome (NTS). Patients with NTS have scaling and superficial peeling of the skin and skin inflammation as a result of uncontrolled serine protease activity [9, 10]. A sensitive LC-MS/MS method for quantitative detection of GlcChol employing an isotope encoded identical standard was used in the investigation [1]. Skin Cer can vary in composition of sphingoid base and fatty acyl moieties. The fatty acyl moiety of the skin Cers is very diverse, ranging from esterified w-hydroxy fatty acids [EO], non-hydroxy fatty acids [N] and a-hydroxy fatty acids [A] [11]. In addition to this, distinct sphingoid base-isoforms of Cers occur like regular sphingosine [S], dihydrosphingosine [DS], phytosphingosine [P] and 6-hydroxysphingosine [H]. The composition of NTS skin regarding [EOS], [NS] and [AS] forms of GlcCer and Cers was earlier studied [12]. In the present investigation we quantified the major GlcCer[S] isoform [13].

Our investigation firstly documents the presence of GlcChol in the SC and the findings are discussed.

Results and discussion

GlcChol levels were measured in full thickness skin, dermatomed skin and SC samples from abdominal skin by LC-MS/MS with $^{13}C_6$-encoded GlcChol as internal standard (see Figure 2). In parallel, samples were deacylated and GlcCer with regular sphingosine (GlcCer[S]) was determined with C17-sphinganine as internal standard.

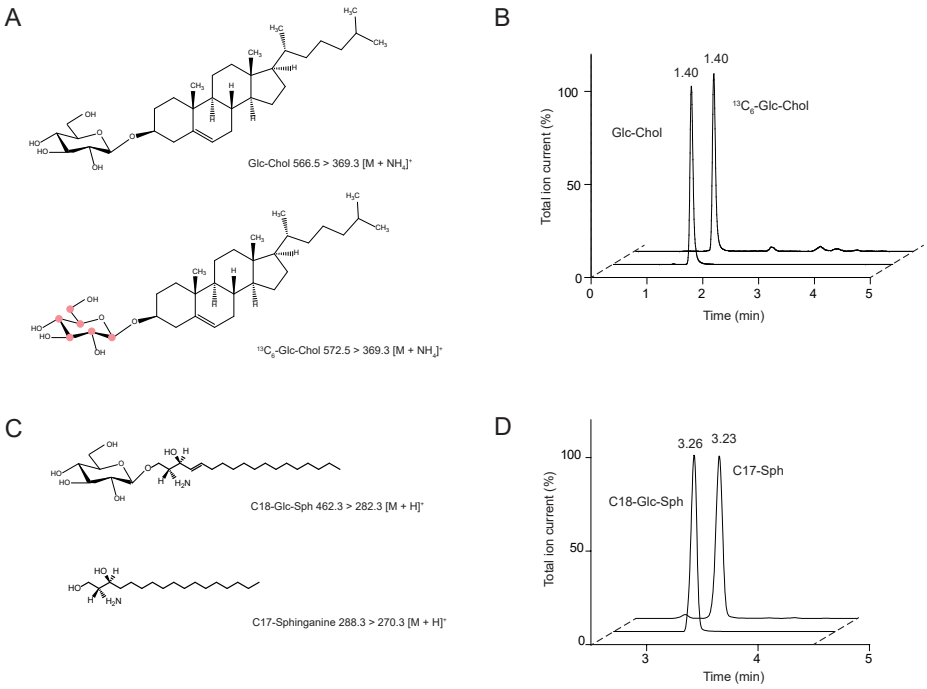

Figure 2. Quantification of GlcChol and C18-GlcSph in skin samples by LC-MS/MS. A. The structure of GlcChol and its isotope, 13C6-labeled GlcChol. B. LC-MS/MS chromatogram of pure GlcChol and its ^{13}C-labeled isotope added to SC lipid extract. The ammonium-adduct is the most abundant m/z for both compounds. The product ion, m/z 369.3, is the common fragment for both compounds. C. The structure of deacylated forms of C18-GlcCer[S] and internal standard Cer[DS] d17.0/16.0. D. LC-MS/MS chromatogram after deacylation: C18-GlcSph in SC lipid extract and Cer[DS] d17.0/16.0 after addition of pure Cer[DS] d17.0/16.0. The H^+-adduct is the most abundant m/z for both compounds.

Table 1 shows the levels of GlcChol and GlcCer[S] and the ratio GlcChol/GlcCer[S] in full thickness and dermatomed human abdominal skin and SC. GlcChol was detected in all samples. The highest levels of GlcChol as well as the highest GlcChol/GlcCer ratio were detected in the SC.

Next, we determined GlcChol and GlcCer[S] in NTS SC samples, being 11.1 +/- 3.7 pmol/mg and 44 +/- 14.6 pmol/mg. Lower levels of GlcCer[S] were detected

Table 1: GlcChol and GlcCer[S] in different fractions of human abdominal skin.

	pmol/mg wet weight		ratio
Sample	**GlcChol**	**GlcCer [S]**	**GlcChol/GlcCer[S]**
Full thickness skin	0.63	63.54	0.010
Epidermis	3.12	272.49	0.011
SC	5.98	72.21	0.083

compared to the levels in the abdominal SC, resulting in a higher ratio GlcChol/GlcCer. Higher levels of GlcCer can be found when the outermost cell layer of the viable epidermis is still present after SC isolation by trypsinization. This method was used to isolate SC from abdominal skin, but was not required for the NTS SC sheets. In Figure 3 lipid data for individual skin samples are shown.

Table 2: Absolute amounts of GlcChol and GlcCer[S] as mean +/- SEM (pmol/mg SC).

	pmol/mg wet weight		ratio
	GlcChol	**GlcCer [S]**	**GlcChol/GlcCer[S]**
NTS	11.1 ± 3.7	44.0 ± 14.6	0.37 ± 0.08

Our investigation reveals the presence of GlcChol in the SC of human skin. Our finding is not entirely surprising given the local abundance of the enzyme GCase, GlcCer and Chol in the SC. The occurrence of GlcChol has earlier been noted for snake skin as well as chicken skin [14, 15], but these investigations received no follow-up. Glucosylated sterols are actually not rare in nature. In plants and algae, glucosylated sterols (sterolins) are abundant metabolites [16].

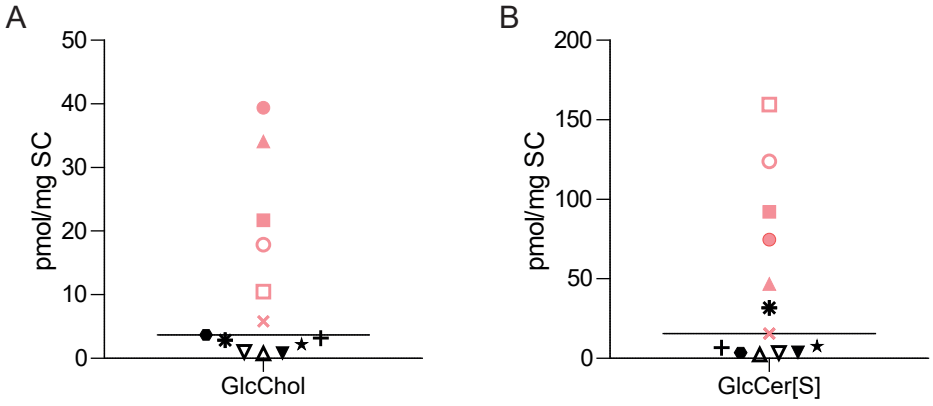

Figure 3. Individual distribution of lipid data. A. Dot plot GlcChol level per individual NTS subject. B. Dot plot GlcCer[S] level per individual NTS subject. Individuals with GlcChol levels above median are depicted in pink.

The likely biosynthetic pathway for GlcChol in the SC involves transglucosylation of cholesterol with GlcCer as glucose donor (see Figure 4). The physiological function of GlcChol in the skin is presently unknown. It might be speculated that it assists, similar to cholesterol sulfate, desquamation [30]. Our investigation of SC samples obtained from NTS and AD patients indicates that GlcChol is still formed in these pathological conditions. Clearly, further research is warranted to establish the function of GlcChol in the SC.

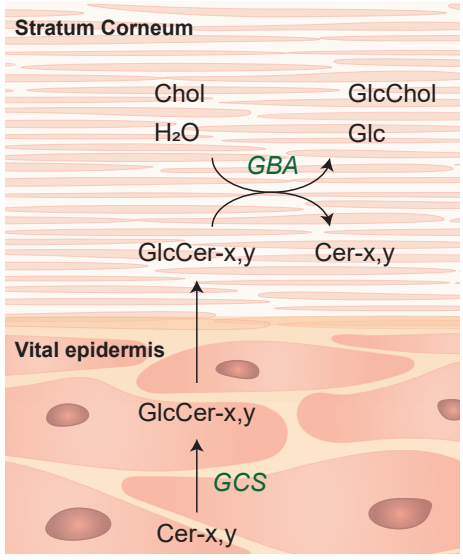

Figure 4. GlcChol formation in the skin.

Materials and Methods

Skin acquisition and preparation. All human skin samples used were obtained with consent and in accordance with the Declaration of Helsinki. Abdominal skin was obtained from a local hospital following cosmetic surgery and used within 24 h after surgery. Subcutaneous fat was removed from full thickness skin using a surgical scalpel. The SC side of the skin was wiped with 70% ethanol in deionized water. After fixing the full skin on a stryofoam support and using a Padgett Electro Dermatome Model B (Kansas City, USA), the skin was dermatomed to a thickness off 300-400 µm as described previously. Subsequently the SC was isolated using a trypsin digestion procedure. SC sheets were harvested from 13 patients suffering from NTS after informed consent.

Lipid extraction. After wet weight determination lipids were extracted with a methanol chloroform extraction (1:1 v/v). ^{13}C-labelled GlcChol and Cer[DS] d17.0/16.0 in methanol (both used as an internal standard) were added followed by a Bligh and Dyer extraction as described previously [1, 13]. Half of the lipid extract was deacylated prior to GlcCer[S] measurement [17].

LC-MS/MS analysis. For all experiments a Waters Xevo-TQS micro instrument was used. The instrument consisted of a UPLC system combined with a tandem quadruple mass spectrometer as mass analyzer. Acquired data were analyzed with Masslynx 4.1 Software (Waters, Milford MA, USA). Tuning conditions and MS settings for GlcChol and GlcCer[S] in ES+ (electrospray positive) mode are as published previously [1, 13].

References

1. A.R. Marques, M. Mirzaian, H. Akiyama, P. Wisse, M.J. Ferraz, P. Gaspar, K. Ghauharali-van der Vlugt, R. Meijer, P. Giraldo, P. Alfonso, P. Irun, M. Dahl, S. Karlsson, E.V. Pavlova, T.M. Cox, S. Scheij, M. Verhoek, R. Ottenhoff, C.P. van Roomen, N.S. Pannu, M. van Eijk, N. Dekker, R.G. Boot, H.S. Overkleeft, E. Blommaart, Y. Hirabayashi, J.M. Aerts, Glucosylated cholesterol in mammalian cells and tissues: formation and degradation by multiple cellular beta-glucosidases, J Lipid Res, 57 (2016) 451-463.
2. H. Akiyama, S. Kobayashi, Y. Hirabayashi, K. Murakami-Murofushi, Cholesterol glucosylation is catalyzed by transglucosylation reaction of beta-glucosidase 1, Biochem Biophys Res Commun, 441 (2013) 838-843.
3. H. Akiyama, Y. Hirabayashi, A novel function for glucocerebrosidase as a regulator of sterylglucoside metabolism, Biochim Biophys Acta Gen Subj, 1861 (2017) 2507-2514.
4. M. Rabionet, K. Gorgas, R. Sandhoff, Ceramide synthesis in the epidermis, Biochim Biophys Acta, 1841 (2014) 422-434.
5. J. van Smeden, I.M. Dijkhoff, R.W.J. Helder, H. Al-Khakany, D.E.C. Boer, A. Schreuder, W.W. Kallemeijn, S. Absalah, H.S. Overkleeft, J. Aerts, J.A. Bouwstra, In situ visualization of glucocerebrosidase in human skin tissue: zymography versus activity-based probe labeling, J Lipid Res, 58 (2017) 2299-2309.
6. M.D. Witte, W.W. Kallemeijn, J. Aten, K.Y. Li, A. Strijland, W.E. Donker-Koopman, A.M. van den Nieuwendijk, B. Bleijlevens, G. Kramer, B.I. Florea, B. Hooibrink, C.E. Hollak, R. Ottenhoff, R.G. Boot, G.A. van der Marel, H.S. Overkleeft, J.M. Aerts, Ultrasensitive in situ visualization of active glucocerebrosidase molecules, Nat Chem Biol, 6 (2010) 907-913.
7. V.L. Tybulewicz, M.L. Tremblay, M.E. LaMarca, R. Willemsen, B.K. Stubblefield, S. Winfield, B. Zablocka, E. Sidransky, B.M. Martin, S.P. Huang, et al., Animal model of Gaucher's disease from targeted disruption of the mouse glucocerebrosidase gene, Nature, 357 (1992) 407-410.
8. D.L. Stone, W.F. Carey, J. Christodoulou, D. Sillence, P. Nelson, M. Callahan, N. Tayebi, E. Sidransky, Type 2 Gaucher disease: the collodion baby phenotype revisited, Arch Dis Child Fetal Neonatal Ed, 82 (2000) F163-166.
9. H. Traupe, The ichthyoses : a guide to clinical diagnosis, genetic counseling, and therapy Springer-Verlag, Berlin ; New York, (1989).
10. S.L. Greene, S.A. Muller, Netherton's syndrome. Report of a case and review of the literature, J Am Acad Dermatol, 13 (1985) 329-337.
11. S. Motta, M. Monti, S. Sesana, R. Caputo, S. Carelli, R. Ghidoni, Ceramide composition of the psoriatic scale, Biochim Biophys Acta, 1182 (1993) 147-151.
12. J. van Smeden, M. Janssens, W.A. Boiten, V. van Drongelen, L. Furio, R.J. Vreeken, A. Hovnanian, J.A. Bouwstra, Intercellular skin barrier lipid composition and organization in Netherton syndrome patients, J Invest Dermatol, 134 (2014) 1238-1245.
13. M. Mirzaian, P. Wisse, M.J. Ferraz, H. Gold, W.E. Donker-Koopman, M. Verhoek, H.S. Overkleeft, R.G. Boot, G. Kramer, N. Dekker, J.M. Aerts, Mass spectrometric quantification of glucosylsphingosine in plasma and urine of type 1 Gaucher patients using an isotope standard, Blood Cells Mol Dis, 54 (2015) 307-314.
14. P.W. Wertz, P.M. Stover, W. Abraham, D.T. Downing, Lipids of chicken epidermis, J Lipid Res, 27 (1986) 427-435.
15. W. Abraham, P.W. Wertz, R.R. Burken, D.T. Downing, Glucosylsterol and acylglucosylsterol of snake epidermis: structure determination, J Lipid Res, 28 (1987) 446-449.
16. V.A. Stonik, I.V. Stonik, Sterol and Sphingoid Glycoconjugates from Microalgae, Mar Drugs, 16 (2018).
17. J.E. Groener, B.J. Poorthuis, S. Kuiper, M.T. Helmond, C.E. Hollak, J.M. Aerts, HPLC for simultaneous quantification of total ceramide, glucosylceramide, and ceramide trihexoside concentrations in plasma, Clin Chem, 53 (2007) 742-747.

Chapter 6

β-Xylosidase and transxylosidase activities of human glucocerebrosidase

β-Xylosidase and transxylosidase activities of human glucocerebrosidase

D.E.C. Boer, M. Mirzaian, M.J. Ferraz, K.C. Zwiers, M. Hazeu, M.V. Baks, R. Ottenhoff, A.R.A. Marques, R. Meijer, J.C.P. Roos, T. Cox, R.G. Boot, N.j. Pannu, H.S. Overkleeft, M.E. Artola, J.M.F.G. Aerts.

Abstract

Glucocerebrosidase (GCase) is a lysosomal retaining β-glucosidase that hydrolyzes β-glucosidic substrates and transglucosylates cholesterol to cholesterol-β-glucoside (GlcChol). Here we demonstrate that recombinant human GCase also cleaves 4-methylumbelliferyl-β-D-xylose (4-MU-β-Xyl) and is able to transxylosylate cholesterol. Formed xylosyl-cholesterol (XylChol) acts as subsequent acceptor to render di-xylosyl-cholesterol. Examination of mutant forms of GCase from Gaucher disease patients revealed no marked abnormalities in relative β-glucosidase, β-xylosidase, transglucosidase and transxylosidase activities. The presence of low levels of XylChol in mouse and human tissue was detected and its origin studied. Intact cultured cells were found to form XylChol, in GCase dependent manner, when exposed to 4-MU-β-Xyl or a plant-derived cyanidine-β-xyloside. Unlike GCase, the cytosol-facing β-glucosidase GBA2 shows no β-xylosidase or transxylosidase activity. Likewise glucosylceramide synthase (GCS) is unable to synthesize XylChol. Next, we detected xylosylated ceramide (XylCer) in tissues. XylCer was found to also act as donor in XylChol formation by GCase. Unexpectedly, GCS was observed to be able to generate XylCer. Thus, food derived β-D-xyloside and XylCer are potential donors for GCase driven formation of XylChol in cells and tissues formed via transxylosylation by GCase. In conclusion, our findings point to further catalytic versatility of GCase and warrant examination of occurrence and function of xylosylated lipids.

Introduction

The aldopentose xylose resembles the six-membered cyclic pyranose glucose except for lacking the pendant CH2OH group. As main building block of xylan, xylose is a major plant sugar [1]. In animals xylose is added

by uridine diphosphate D-xylose (UDP-Xyl) dependent xylosyltransferases as the first saccharide to sidechain hydroxyls of serine or threonine residues during O-glycosylation of proteoglycans. This step is essential in synthesis of glycosaminoglycans like heparan sulfate, keratan sulfate and chondroitin sulfate [2]. The human body is unable to synthesize xylose de novo. UDP-Xyl is however formed from UDP-glucuronate by UDP-glucuronic acid decarboxylase 1 encoded by the UXS1 gene [3]. Since the first investigations by Fisher & Kent and Patel & Tappel in the late sixties, degradation of β-xylosides in animals is thought to rely on β-glucosidases [4, 5]. This does not come as a surprise in view of the structural similarity of xylose with glucose. We earlier demonstrated that indeed the lysosomal acid β-glucosidase GCase, also known as glucocerebrosidase, hydrolyzes 4-methylumbelliferyl-β-xyloside (4-MU-β-Xyl), in contrast to the non-lysosomal β-glucosidase GBA2 [6]. Inherited defects in GCase cause Gaucher disease (GD), a progressive disorder characterized by the accumulation of macrophages loaded with glucosylceramide (GlcCer) in tissues [7, 8]. No accumulation of β-D-xylose-containing glycopeptides in GD patients has been reported, but this possibility has not been actively studied. More recently another catalytic capacity of GCase has been recognized: the transfer of glucose from β-glucoside substrates to cholesterol, thus generating glucosyl-β-D-cholesterol (GlcChol) [9-11]. Generation of GlcChol by GCase is not merely a test tube phenomenon, but also takes place *in vivo* [10]. In Niemann Pick type C disease (NPC), intralysosomal cholesterol is markedly increased due to genetic defects in any of the two proteins NPC1 or NPC2 mediating the egress of the sterol from lysosomes [12]. During this pathological condition, GCase actively generates GlcChol [10]. Formation of GlcChol can also be experimentally induced by incubating cells with U18666A, an inhibitor of efflux of cholesterol from lysosomes. The transglucosylation reaction in cells is prohibited by concomitant inhibition of GCase [10]. The β-glucosidase GBA2, tightly associated to the cytoplasmic leaflet of membranes, also exerts transglucosidase activity *in vitro* and *in vivo* [10, 13-15].

The earlier findings on glycon substrate specificity of GCase and the recently noted transglucosidase activity of the enzyme prompted us to examine whether GCase is also able to generate xylosyl-β-D-cholesterol (XylChol). We here report on the *in vitro* xylosylation of cholesterol by GCase, rendering not only XylChol, but also di-xylosyl-cholesterol and even small amounts of tri-xylosyl-cholesterol (Xyl_2Chol and Xyl_3Chol, respectively). Cells and tissues were found to contain low levels of XylChol. Subsequent investigations indicated that GBA2 plays no role in the metabolism (formation of degradation) of xylosylated lipids. Cells when exposed to 4-MU-β-Xyl produce XylChol in an entirely GCase-dependent manner. This reaction is favored during intralysosomal cholesterol accumulation as induced with the agent U88666A. Formation of XylChol

also occurs in cells incubated with the plant cyanidin 3-D-xyloside occurring in berries. Our subsequent studies revealed the presence of xylosylated ceramide (XylCer) in cells and tissues. This lipid is apparently synthesized by glucosylceramide synthase (GCS) using UDP-xylose as sugar donor. The same enzyme doesn't synthesize XylChol. Our findings on the unexpected existence of xylosylated lipids and their metabolism by glucocerebrosidase are discussed in relation to Gaucher disease.

Results

Cleavage of 4-methylumbelliferyl-β-D-xylose by GCase.

We first compared the ability of pure recombinant hGCase to cleave 4-MU-β-Xyl and 4-MU-β-Glc. The enzyme releases fluorescent 4-MU from both substrates, but the noted activity towards 4-MU-β-Xyl is around 70-fold lower as the result of a higher Km and lower Vmax (Table 1). The activity of GCase towards both substrates shows a similar pH optimum (Figure 1A) and stimulation by taurocholate (Figure 1B). The stimulatory effect of recombinantly produced saposin C on GCase-mediated cleavage of 4-MU-β-Glc and 4-MU-β-Xyl is comparable (Figure 1C). The kcat//Km of recombinant GCase is about 40-fold higher for 4-MU-β-Glc than 4-MU-β-Xyl (Table 1). The retaining β-glucosidase GCase employs the double displacement mechanism for catalysis with E340 as nucleophile and E325 as acid/base [16]. Blocking glutamate E340 by covalent linkage of the suicide inhibitor cyclophellitol abolishes activity of GCase [17]. The activity of GCase towards 4-MU-β-Glc and 4-MU-β-Xyl substrates was found to be both inhibited by pre-incubation for 90 minutes followed by an activity assay with the substrates for 60 minutes. The slightly higher apparent

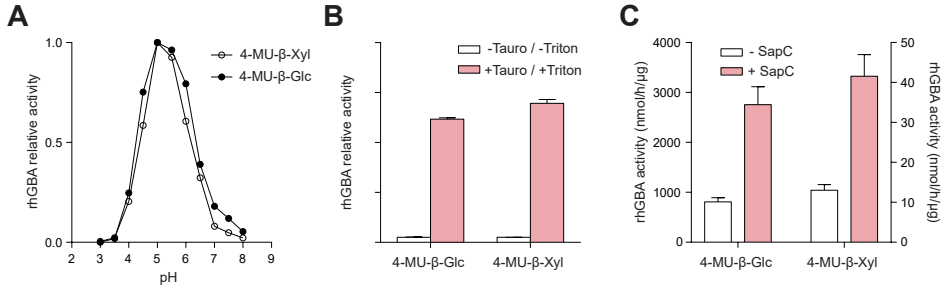

Figure 1: Cleavage of 4-MU-β-Glc and 4-MU-β-Xyl by recombinant hGCase. A. pH optimum of 4-MU release by GCase from 4-MU-β-Glc (closed circles) and 4-MU-β-Xyl (open circles). B. Stimulation by 0.2 % (w/v) taurocholate of 4-MU release from the substrates 4-MU-β-Glc (left) and 4-MU-β-Xyl (right). Expressed as 100 % is the activity measured in the absence of taurocholate at pH 5.2 with 0.1% (v/v) Triton X-100. C. Stimulation of 4-MU release from the substrates 4-MU-β-Glc (left axis) and 4-MU-β-Xyl (right axis) by recombinant saposin C at pH 4.5 in the presence of phosphatidylserine.

Table 1: Kinetic parameters hGCase

hGCase	4-MU-β-Glc	4-MU-β-Xyl
Km (mM)	0.76 ± 0.06	5.24 ± 1.04
Vmax (nmol/h.mg)	1.23 ± 0.03 x 106	1.88 ± 0.3 x 105
Kcat/Km (mM/s-1)	25.03	0.55
IC50 cyclophellitol (μM)	0.085 ± 0.002	0.061 ± 0.002
IC50 D-xylo-cyclophellitol (μM)	10.16 ± 1.03	6.41 ± 0.47

IC50 observed with 4-MU-β-Glc (85 nM) than with 4-MU-β-Xyl (61 nM) is likely explained by the greater protection against irreversible inhibition of GCase by the β-D-Glucose substrate. Recently a xylose analogue of cyclophellitol was synthesized [18]. It was observed that GCase is also irreversibly inactivated by D-Xylo-cyclophellitol, although with lower affinity than cyclophellitol (Table 1). Again, the apparent IC50 determined with 4-MU-β-Glc (10.16 μM) is slightly higher than with 4-MU-β-Xyl substrate (6.41 μM), presumably due to better protection of GCase against irreversible inhibition by the presence of 4-MU-β-Glc.

Transxylosidase activity of GCase.

We investigated recombinant GCase with respect to transxylosidase activity. For this, the enzyme was incubated for 16 hours with 4-MU-β-Glc or 4-MU-β-Xyl as donor and fluorescent 25-NBD-cholesterol as acceptor and next the products were analyzed by HPTLC and fluorescence scanning. Formation of fluorescent sterol metabolites occurred with both donors (Figure 2A). With 4-MU-β-Glc, glucosylated 25-NBD-cholesterol is formed as earlier described [10]. With 4-MU-β-Xyl, two novel fluorescent metabolites were detected, presumed to be mono- and di-xylosylated 25-NBD-cholesterol (Figure 2A).

Next, we used natural cholesterol as acceptor in the same assay with 4-MU-β-Xyl as donor and the formed products were analyzed by LC-MS/MS. In this way, formation of XylChol, Xyl_2Chol, and traces of Xyl_3Chol was detected (Figure 2B). In sharp contrast, incubation of GCase and cholesterol with 4-MU-β-Glc only renders GlcChol as product (Figure 2C).

Time dependence of glycosidase and transglycosidase activities of GCase.

GCase and cholesterol were incubated with 4-MU-β-Glc or 4-MU-β-Xyl at 37 ˚C for different time periods. The release of 4-MU and formation of glycosylated products was determined. The formed GlcChol was already maximal after an incubation of 30 min and subsequently declined with time (Figure 2C). This suggests that the formed GlcChol is subject to subsequent hydrolysis by GCase. In sharp contrast, XylChol showed no prominent reduction over time, and Xyl_2Chol was formed after a lag period (Figure 2D). This suggests

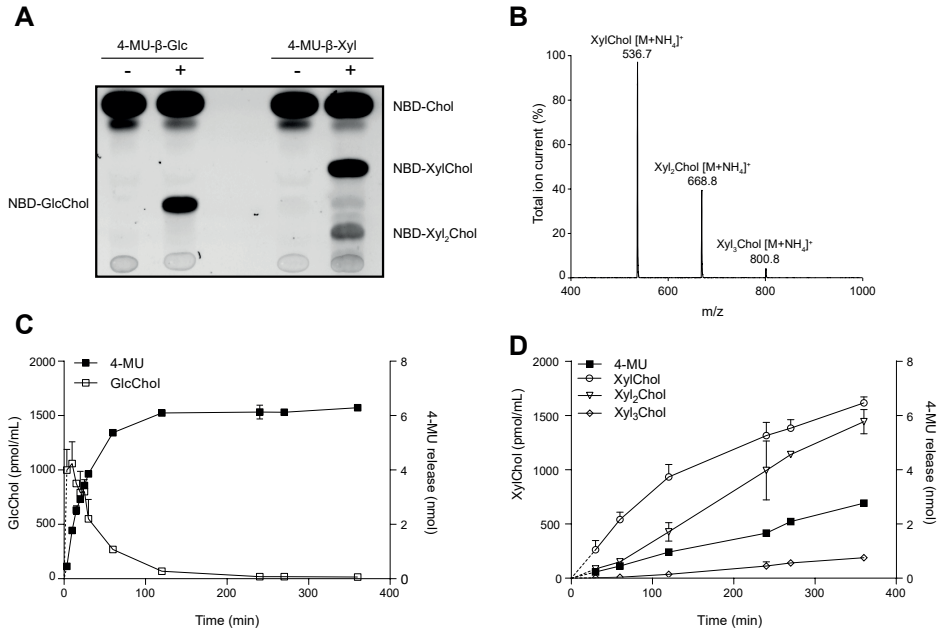

Figure 2: Transxylosylation and transglucosylation of cholesterol by GCase. A. HPTLC analysis of fluorescent products formed from 25-NBD-cholesterol following incubation with rGCase in the presence of 4-MU-β-Glc or 4-MU-β-Xyl for 16h. B. LC-MS/MS analysis of products formed during 1h incubation of rGCase, cholesterol and 4-MU-β-Xyl. C. Release of 4-MU from 4-MU-β-Glc and concomitant formation of glucosylated cholesterol in time. D. Release of 4-MU from 4-MU-β-Xyl and concomitant formation of xylosylated cholesterol in time. rGCase was incubated at pH 5.2 in the presence of taurocholate and Triton X-100 with 3.7 mM 4-MU-substrates for indicated times.

that XylChol is hardly hydrolyzed and acts as acceptor for further xylosylation. This process continues with Xyl_2Chol acting as acceptor rendering Xyl_3Chol (Figure 2D). A comparison of the release of 4-MU with concomitant formation of glycosylated sterol indicates that GCase shows considerably higher net transxylosylation than transglucosylation (Figure 2). We next studied the outcome of the incubation of GCase and cholesterol with 4-MU-β-Xyl (3 h) followed by 4-MU-β-Glc (1 h). Formation of GlcXylChol (with m/z 698.5 > 369.3) was demonstrable at these conditions, again pointing to XylChol acting as excellent acceptor in glycosylation reaction (Supplemental Table 2).

Time dependence of glycosidase and transglycosidase activities of GCase.

GCase and cholesterol were incubated with 4-MU-β-Glc or 4-MU-β-Xyl at 37 ˚C for different time periods. The release of 4-MU and formation of glycosylated products was determined. The formed GlcChol was already maximal after an incubation of 30 min and subsequently declined with time (Figure 2C). This suggests that the formed GlcChol is subject to subsequent

hydrolysis by GCase. In sharp contrast, XylChol showed no prominent reduction over time, and Xyl_2Chol was formed after a lag period (Figure 2D). This suggests that XylChol is hardly hydrolyzed and acts as acceptor for further xylosylation. This process continues with Xyl_2Chol acting as acceptor rendering Xyl_3Chol (Figure 2D). A comparison of the release of 4-MU with concomitant formation of glycosylated sterol indicates that GCase shows considerably higher net transxylosylation than transglucosylation (Figure 2). We next studied the outcome of the incubation of GCase and cholesterol with 4-MU-β-Xyl (3 h) followed by 4-MU-β-Glc (1 h). Formation of GlcXylChol (with m/z 698.5 > 369.3) was demonstrable at these conditions, again pointing to XylChol acting as excellent acceptor in glycosylation reaction (Data not shown).

In vivo *formation of xylosylated cholesterol.*

To substantiate our *in vitro* findings, potential transxylosylation by cultured RAW264.7 cells exposed to 3.7 mM 4-MU-β-Xyl was investigated. Cells were

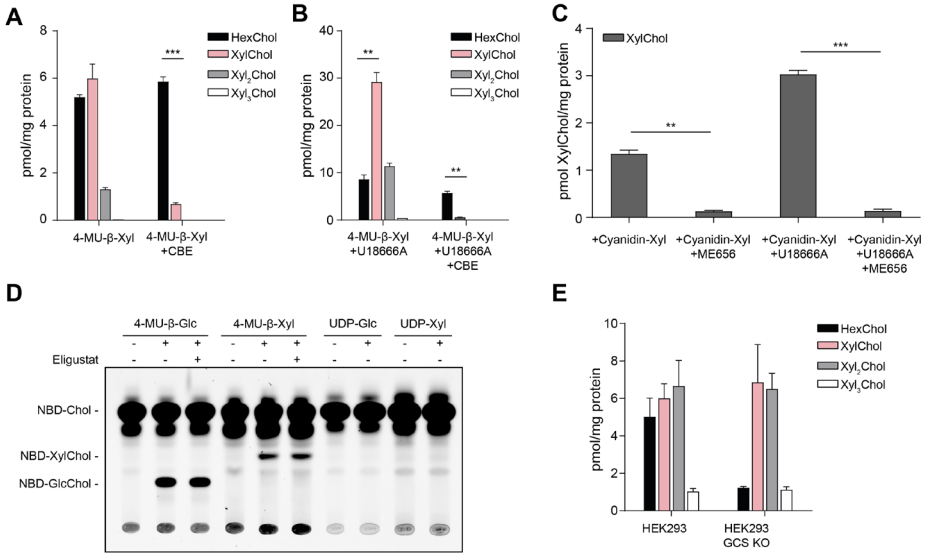

Figure 3: Formation of xylosylated cholesterols. A. LC-MS/MS detection of formed XylChol and HexChol (GlcChol or GalChol) in RAW264.7 cells incubated with 3.7 mM 4-MU-β-Xyl for 24 hours in the presence/absence of CBE, n=3 technical replicates and $p<0.05$. B. Idem in the presence of 10 μM U18666A. C. LC-MS/MS detection of formed xylosylated cholesterol in RAW264.7 cells incubated with 3.7 mM cyanidin 3-D-xyloside for 24 hours in the presence/absence of U18666A with/without GCase inhibitor ME656, n=2 technical replicates and $p<0.05$. D. HPTLC of in vitro formation of xylosylated cholesterols by HeLa cell lysate using NBD-Chol as acceptor and 4-MU-Glc, 4-MU-Xyl, UDP-Glc and UDP-Xyl as (potential) sugar donors in the prescence/absence of GCS inhibitor Eligustat. E. LC-MS/MS detection of formed xylosylated and glucosylated cholesterols in HEK293 and HEK293 GCS KO cells exposed to 3.7 mM 4-MU-β-Xyl and U18666A for 24 hours, n=3 technical replicates and $p<0.05$.

incubated with or without the irreversible GCase inhibitor conduritol B-epoxide (CBE) either in the absence (Figure 3A) or presence of 10 μM U18666A (Figure 3B) to induce lysosomal accumulation of cholesterol [10]. Formation of XylChol, Xyl_2Chol and Xyl_3Chol was detected by LC-MS/MS. The levels of xylosylated cholesterols were markedly increased by the exposure of cells to U18666A and prohibited by prior inhibition of GCase with CBE (Figure 3A and 3B). Several β-xylosidic compounds are known to be produced by plants and their uptake via food is likely [19, 20]. We therefore investigated whether cyanidin 3-D-xyloside from berries (Supplemental figure 3) can act as sugar donor in cellular formation of XylChol. For this purpose, RAW264.7 cells were incubated with cyanidin 3-D-xyloside for 24 hours and the formation of XylChol was monitored. Indeed, xylosylated cholesterol was formed by the exposed cells in GCase-dependent manner, as indicated by lack of its formation upon GCase inactivation by GCase specific inhibitor ME656 (Figure 3C). Addition of U18666A to the cells during incubation resulted in a little increase of the formed XylChol (Figure 3C). We next tested the possible involvement of UDP-glucose dependent GCS [21, 22]. Lack of involvement of GCS in the synthesis of XylChol was confirmed with an *in vitro* GCS assay by HPTLC (Figure 3D). Additionally, HEK cells made deficient in GCS by CRISPR-Cas9 produced XylChol on a par to corresponding cells when exposed to 4-MU-β-Xyl and U18666A (Figure 3E).

Specificity of transxylosylation.

We studied potential transxylosylation by the two other human retaining β-glucosidases, GBA2 and GBA3. We earlier noticed that GBA2, but not GBA3, can mediate transfer of the glucosyl moiety from 4-MU-β-D-Glc to cholesterol or ceramide [10]. While this finding was recapitulated (Supplemental figure 4), concomitantly no xylosylation by GBA2 was detectable consistent with GBA2's inability to hydrolyze 4-MU-β-D-Xyl [6]. However, GBA3, albeit less prominent than GCase, is able to hydrolyze 4-MU-β-Xyl as well as to transxylosylate cholesterol (Supplemental figure 4).

Table 2: Catalytic features of mutant GCase enzymes. Relative enzymatic activities in lysates of fibroblasts from GD patients incubated with 4-MU-Glc or 4-MU-Xyl to determine glucosidase and xylosidase activity. Cholesterol was added for trans activity determination. n=2 and values are expressed ± SD.

	Ratio	pmol/nmol	
Mutation	**Xylosidase /Glucosidase**	**Transglucosylation /Glucosidase**	**Transxylosylation /Glucosidase**
Control	0.035 ± 0.007	0.654 ± 0.076	0.044 ± 0.006
N370S	0.018 ± 0.001	0.391 ± 0.081	0.029 ± 0.012
L444P	0.028 ± 0.000	0.571 ± 0.066	0.044 ± 0.004
D409H	0.028 ± 0.004	0.182 ± 0.071	0.030 ± 0.001

β-Xylosidase and transxylosidase activities of mutant glucocerebrosidase of Gaucher disease patients.

Mutant forms of *GBA* commonly encountered in GD patients were compared to rGCase enzyme activity by using control and GD patient fibroblasts homozygous for N370S, L444P and D409H mutations in GCase. Cell lysates were incubated with either 4-MU-Glc or 4-MU-Xyl to determine their glucosidase and xylosidase activity by measuring the 4-MU release. Lysates were also incubated with 4-MU-Glc and 4-MU-Xyl concurrently with cholesterol as acceptor, followed by GlcChol and XylChol measurement (Table 2). These analyses showed a small reduction in xylosidase/glucosidase ratio in N370S compared to the control. Additionally we found a minor reduction in transglucosylation/glucosidase activity in GD fibroblasts with a D409H mutation compared to control.

Natural occurrence of xylosylated cholesterol.

We investigated next the presence of XylChol in cells and tissues. For this purpose, XylChol was synthesized to be used as internal standard in LC-MS/MS based quantitation of this lipid in materials. Figure 4A shows XylChol detection in fibroblast, HeLa, HEK293T and RAW264.7 cells as well as in human spleen and mouse liver. The XylChol levels are relatively low as compared to those of HexChol (GlcChol or GalChol), although the ratio HexChol:XylChol differs per cell type and tissue (data not shown). In cells, XylChol levels are on average 130 fold less than those of HexChol. In liver relatively much lower amounts of XylChol were noted. However, relatively more XylChol was detected in liver of $Npc1^{-/-}$ mice, earlier found to also contain high levels of GlcChol [10]. Of note, in spleens of type 1 GD patients reduced XylChol concentrations were observed.

Xylosylated ceramide as a potential xylose donor for GCase.

In search for an endogenous xylose donor in the generation of XylChol, the occurrence of xylosylated ceramide (XylCer) was examined. For this purpose, a LC-MS/MS based quantitation was developed, based on microwave-assisted deacylation to xylosylated sphingosine of which a standard was synthesized. We measured XylCer levels in the same materials previously used for XylChol measurement (Figure 4B). Of note, XylCer is increased in GD spleen, whereas XylChol is reduced in the patient's organ (Figure 4A). Apparently, GCase does not degrade XylChol but synthetizes it. On the other hand, GCase can degrade XylCer and thus might use XylCer as sugar donor in the formation of XylChol. To test whether XylCer is a suitable sugar donor in formation of XylChol we generated XylCer and next incubated it with cholesterol and recombinant GCase. Formation of XylChol was detected by LC-MS/MS (Figure 5A), confirming XylCer might act as a sugar donor.

Glucosylceramide synthase synthesizing cylosylated ceramide.

Our discovery of XylCer stimulated the search for a XylCer generating enzyme. As candidate the enzyme GCS was tested. First, an *in vitro* assay with UDP-Xyl as donor and NBD C6-ceramide as acceptor incubated for 16 h with lysate of HEK293T cells led to formation NBD-XylCer and possibly NBD-Xyl$_2$Cer was detected (Figure 5B). The same assay was performed with ceramide d18.1/18.1 as acceptor and resulted likewise in formation of XylCer, as detected by LC-MS/MS (Figure 5C). Lysates of cells lacking GCS were found to be unable to generate XylCer. Upon overexpression of GCS in the GCS KO

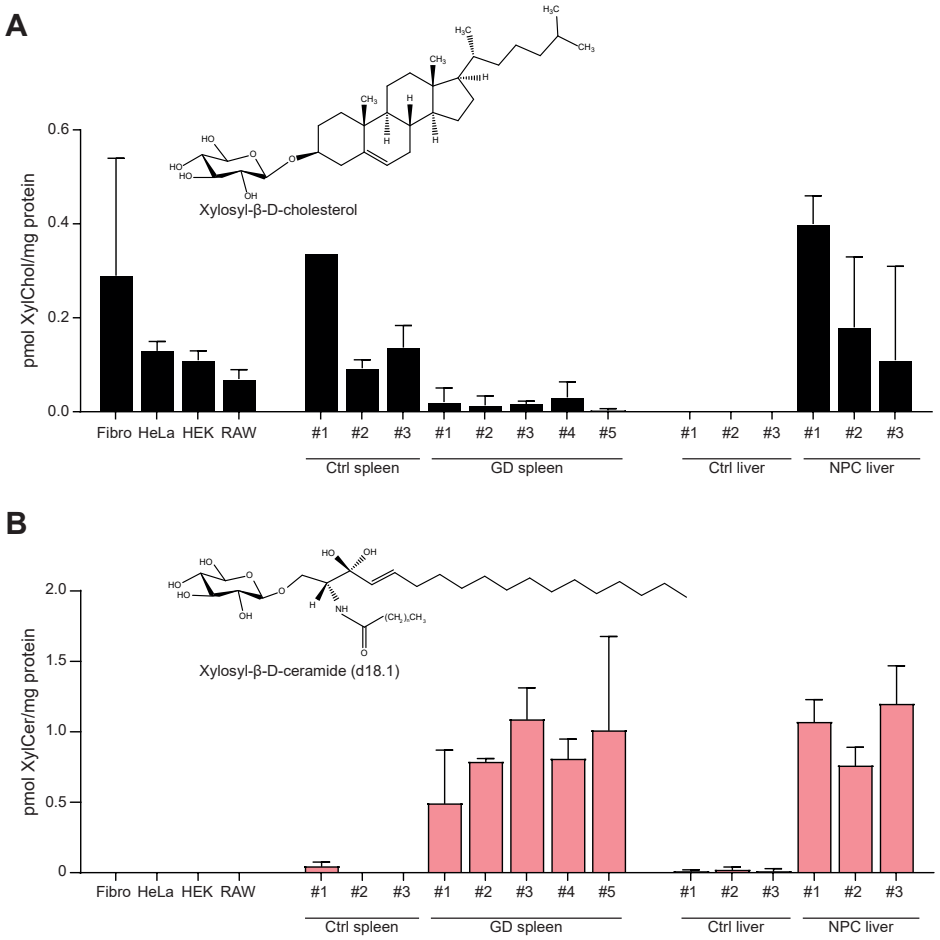

Figure 4: Levels of xylosylated cholesterol and ceramide found in cells and organs. A. LC-MS/MS analysis of XylChol occurrence in Fibroblasts, HeLa, HEK293, RAW264.7 cells, human control spleens, human GD spleens, mouse control livers and mouse NPC livers. B. LC-MS/MS analysis of XylCer occurrence in Fibroblasts, HeLa, HEK293, RAW264.7 cells, human control spleens, human GD spleens, mouse control livers and mouse NPC livers. Error bars are standard deviation of technical duplicates.

cells corresponding the cell lysates were regained the ability to produce XylCer (Figure 5C). This novel function of GCS was further confirmed using lysates of the GCS-deficient GM95 cells and the parental GCS-competent MEB4 B16 cells incubated with UDP-Xyl and ceramide d18.1/18.1, where only the MEB4 cells showed formation of XylCer (Figure 5D).

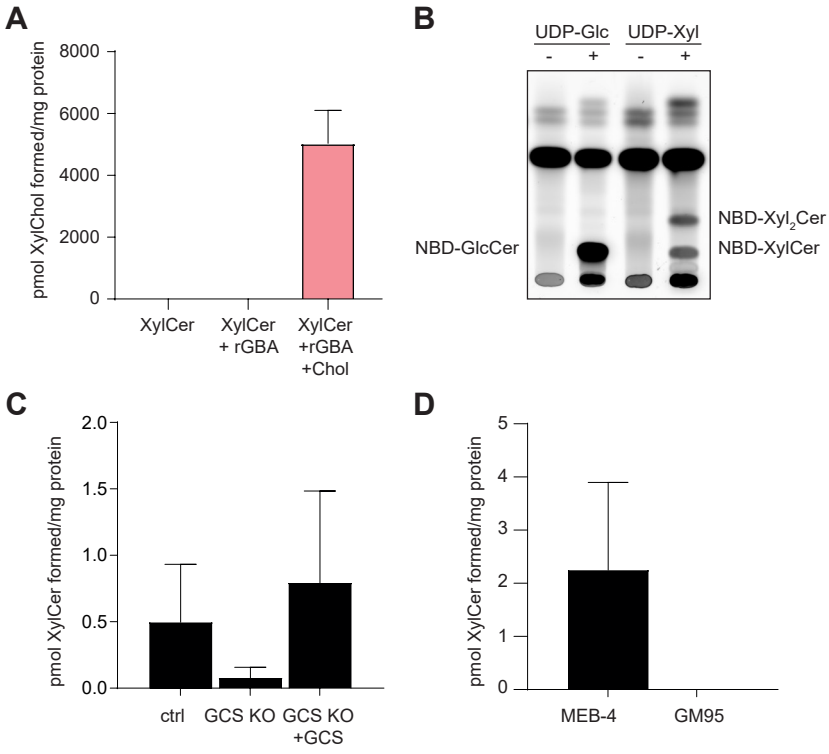

Figure 5: XylCer is a donor for GCase to transxylosylate cholesterol and can be synthesized by GCS. A.XylCer (formed by incubation 4-MU-Xyl, Ceramide d18.1/18.1 and rGCase at pH 5.2) was incubated with rGCase and cholesterol at pH 5.2 for 18 hours at 37°C. The figure depicts LC-MS/MS measurement of formed XylChol. Errorbars represent standard deviation of technical duplicate. B. HPTLC analysis of formation of glycosylated NBD C6-ceramide by GCS with UDP-Glc or UDP-Xyl as donor. C. LC-MS/MS analysis of formed glycosylated ceramide after incubation of cell lysates of HeLa, HeLa GCS KO or HeLa GCS KO with a reintegrated overexpression of GCS with UDP-Glc or UDP-Xyl and ceramide d18.1/18.1. Incubations were 16 hours, errorbars represent standard deviation n=2. D. LC-MS/MS analysis of formed glycosylated ceramide after incubation of mouse fibroblast lysates with UDP-Glc or UDP-Xyl and ceramide d18.1/18.1. Incubations were 16 hours, errorbars represent standard deviation n=2.

Discussion

Our present investigation reveals an intriguing novel catalytic feature of human GCase, the lysosomal glucocerebrosidase. First, we noted that GCase cleaves *in vitro* besides 4-MU-β-Glc also 4-MU-β-Xyl. Moreover, the enzyme uses both substrates as sugar donors in transglycosylation of cholesterol molecules. Next, we observed the generation of xylosylated cholesterol in living cells exposed to 4-MU-β-Xyl. Induction of lysosomal cholesterol accumulation in cells with U18666A increases formation of xylosylated cholesterols, a reaction prohibited by inactivation of GCase with the irreversible inhibitor CBE. Remarkably, both *in vitro* and *in vivo*, GCase may even produce di-xylosyl-cholesterol using 4-MU-β-Xyl as sugar donor, a repetitive transglucosylation not seen with 4-MU-β-Glc as sugar donor [10]. The affinity of GCase for 4-MU-β-Glc as substrate for cleavage is higher than that for 4-MU-β-Xyl. Likewise, XylChol is a much poorer substrate for hydrolysis by GCase than GlcChol. Following exposure of GCase to cholesterol and 4-MU-β-Xyl, the concentration of XylChol steadily builds up and it starts to act as acceptor in a second round of transxylosylation, rendering Xyl_2Chol. Incubation of GCase and cholesterol with a mixture of 4-MU-β-Xyl and 4-MU-β-Glc leads to formation of GlcXylChol, further highlighting the suitability of XylChol as acceptor in transglycosylation by GCase. Of note, Aerts and co-workers earlier noted also relative higher net transxylosylase than transglucosylase efficiency of a β-D-glucosidase from Stachybotrys atra [19], quite comparable to our findings with GCase. We modelled XylChol in the crystal structure of human GCase (data not shown). Indeed, XylChol can be positioned in the pocket as acceptor for another round of transglycosylation. Obviously real life crystallography experiments with soaked lipids in the crystal will be required to obtain conclusive data and further insight.

The possible physiological relevance of transxylosylation by GCase warrants discussion. Mass spectrometry shows the presence of significant amounts of XylChol in liver of Npc1-/- mice. XylChol was also detected in low quantities in cells, liver and spleen. Interestingly, in type 1 GD spleens XylChol levels were clearly reduced as compared to control spleens. This finding substantiates the notion that GCase is largely responsible for formation of XylChol and the same enzyme is only poorly able to degrade it, in contrast to its ability to hydrolyze 4-MU-β-xyloside. Of interest, the β-glucosidase GBA2 shown earlier to be a potent transglucosidase generating GlcChol has no significant activity towards β-xyloside substrates. Apparently the pendant CH2OH group in glucoside substrates contributes crucially to the interaction of substrate with GBA2. The importance of the presence of the additional CH2OH group in glucose is also suggested by the much lower affinity of GBA2 for the inhibitor conduritol-B-epoxide as compared to cyclophellitol (with the pendant CH2OH group) [23]. In

contrast to GBA2, the enzyme GBA3, a cytosolic broad-specificity glycosidase implicated in metabolism of xenophobic glycosides [24], shows xylosidase and transxylosidase activity in *in vitro* experiments. The contribution of this enzyme in metabolism of xylosides is presently still unclear.

Our discovery of catalytic activities of GCase (β-glucosidase, β-xylosidase, transglucosylase and transxylosylase) prompted us to look into the possibility that specific mutant forms of GCase as occurring in GD patients may have selective abnormalities in one of the activities. Analyzing patient fibroblast with common GD mutations N370S, L444P and D409H GCase did not point to specific abnormalities in one of the catalytic activities as tested with 4-MU-Glc and 4-MU-Xyl as substrates and cholesterol as acceptor. We were particularly interested in any abnormalities in catalytic features of D409H GCase since this mutation is associated with an unique symptomatology involving valve calcification [25-27]. Although we detected no specific abnormalities for this particular mutant enzyme it nevertheless remains of interest to study in biopsy materials of GD patients with D409H patients the presence of abnormal β-xylosides.

In the course of our investigation a key question concerned the nature of physiological xyloside donors. Several β-xylosidic compounds are known to be produced by plants and their uptake via food is a priori not excluded [19, 20]. We did show the ability of *in vivo* formation of XylChol in cells when incubated with cyanidin 3-D-xyloside, which is found in plums and berries. Making it likely there might be other plant originated β-xylosides that are suitable donors for GCase-mediated formation of xylosylated sterols. An alternative endogenous donor of β-D-xylosyl moieties might be degradation products of proteoglycans. During their lysosomal degradation β-D-xylosyl-peptides are formed. Our investigation also revealed another, somewhat unexpected, candidate: xylosylated ceramide. Actually, the occurrence of XylCer has been previously reported in the salt gland of the herring gull [28]. Our investigation demonstrated the presence of XylCer in human and mouse materials, although at very low levels as compared to GlcCer. Additionally, XylCer can serve as a donor for transxylosylation of cholesterol by GCase. Extension of these findings resulted in the finding of a novel function of GCS, that is able to use UDP-Xyl to form XylCer, although with much lower affinity than UDP-Glc. XylCer was found to be elevated in GD spleen, consistent with this lipid being a substrate for GCase and possible sugar donor in transylosylation mediated by the lysosomal enzyme. The physiological relevance of the relatively tiny amounts of XylCer is presently enigmatic. It requires further studies to establish whether exogenous β-xylosides of plant origin or endogenous β-xylosides (β-D-xylosyl-peptides or XylCer) acts donors in formation of XylChol.

In conclusion, human GCase is more versatile in catalysis as hitherto considered. Investigation of the (patho)physiological relevance of various reactions catalyzed by GCase and xylosylated lipids is needed to further complete understanding of the full symptomatology of Gaucher disease [7, 8] and other conditions for which abnormal GCase imposes a risk such as multiple myeloma and α-synucleinopathies like Parkinsonism and Lewy-body dementia [29].

Materials and Methods

Materials. 25-[N-[(7-nitro-2-1,3-benzoxadiazol-4-yl)methyl]amino]-27-norcholesterol (25-NBD-cholesterol) were purchased from Avanti Polar Lipids (Alabaster, AL, USA). (6-((N-(7-Nitrobenz-2-Oxa-1,3-Diazol-4-yl)amino) hexanoyl)Sphingosine) (NBD C6-Ceramide) was purchased from Invitrogen (Waltham, MA, USA). 4-methylumbelliferyl β-D-glucose (4-MU-Glc) and 4-methylumbelliferyl β-D-xylose (4-MU-Xyl) were purchased from Glycosynth™ (Winwick Quay Warrington, Cheshire, England). Cyanidin 3-Xyloside was obtained from Toronto Research Chemicals (Martin Ross Ave, North York, Canada). Uridine diphosphate glucose (UDP-Glc), Cholesterol, cholesterol trafficking inhibitor U18666A, 1-O-cholesteryl-β-D-glucose (β-cholesteryl glucose, β-GlcChol) and ammonium formate (LC-MS quality) were from Sigma-Aldrich (St Louis, MO, USA). Uridine diphospho- alpha-D-xylopyranoside (UDP-Xyl) was purchased from CarboSource Services (Riverbend Rd, Athens, USA - Supported in part by Grant #DE-FG02-93ER20097). GCase inhibitor Conduritol-β-epoxide (D, L-1,2-anhydro-myo-inositol; CBE) was from Enzo Life Sciences Inc. (Farmingdale, NY, USA), GCase inhibitor cyclophellitol, GBA2 inhibitor N-(5-adamantane-1-yl-methoxy-pentyl)-deoxynojirimycin (AMP-DNM), GBA3 inhibitor α-1-C-nonyl-DIc (anDIX) and 1-O-cholesteryl-β-D-xylose (XylChol) were synthesized at Leiden Institute of Chemistry (Leiden, The Netherlands) [24, 30]. Cerezyme®, a recombinant human GCase was obtained from Genzyme (Genzyme Nederland, Naarden, The Netherlands). LC-MS–grade methanol, 2-propanol, water, and HPLC-grade chloroform was purchased from Biosolve. D-xylo-cyclophellitol was synthesized as reported earlier [18].

Collection of Niemann-Pick type C mouse livers and GD patient spleens. Livers from Npc1-/- mice (Npc1nih), along with wild-type littermates (Npc1+/+), were collected in a previous study [10]. All human spleens were obtained either as surgical specimens during therapeutic splenectomy or at autopsy. The phenotype of the subjects was established by clinical examination. All organs were stored at -80 °C. Later, homogenates were made from the frozen material in water.

Cloning and expression of cDNAs encoding GBA2, GBA3 and GCS. The design of cloning primers was based on NCBI reference sequences NM_020944.2 for human GBA2, and NM_020973.3 for human GBA3 as described previously [10]. Glucosylceramide synthase (GCS) in HEK293 cells was knocked-down by the CRISPR/Cas9 system [31]. The coding sequence of GCS was amplified by PCR (using the following oligonucleotides: sense. 5'-GGGGACAAGTTTG TACAAAAAAGCAGGCTACCACCATGGCGCTGCTGGACCTG-3'and antisense '-GGGGACCACTTTGTACAAGAAAGCTGGGTCTTATACATCTAGGATTTCCTCTG-3') and cloned into pDNOR-221 and sub cloned in pcDNA3.1-Zeo via Gateway cloning system (Invitrogen). Correctness of the construct was verified by sequencing. HEK293 cells were obtained from the "American Type Culture Collection" and cultured in Iscove's modified Dulbecco's medium with 5% FBS and penicillin/streptomycin under 5% CO2 at 37°C. For transfection cells were seeded at 75% confluence in 6-well plates and transfected using PEI Transfection reagent (Polysciences Inc, Valley Rd, Warrington, USA) according to the manufacturer's instructions, at a PEI:DNA ratio of 3:1.

Culturing and collection of GD fibroblasts. Control and GD patient fibroblasts homozygous for N370S, L444P and D409H mutations in *GBA* were cultured in HAMF12-DMEM medium supplied with 10% FBS and penicillin/streptomycin at 37°C under 7% CO2. Fibroblasts were collected by trypsinization followed by 3x washing with ice cold PBS. Cells were homogenized in 25mM potassium phosphate buffer pH 6.5 supplemented with 0.1 % (v/v) Triton X-100 by sonication on ice.

In vitro *assays with fluorogenic 4-methylumbelliferyl-β-D-glycosides.* Enzymatic activity of GCase was measured with 3.7 mM 4-MU-β-Glc or 4-MU-β-Xyl, dissolved in 150 mM McIlvaine buffer (pH 5.2 supplemented with 0.2 % (w/v) sodium taurocholate, 0.1 % (v/v) Triton X-100) and 0.1 % (w/v) BSA) [32]. The reaction was stopped with NaOH-glycine (pH 10.3), and fluorescence was measured with a fluorimeter LS-55 (Perkin-Elmer, Beaconsfield, UK) at λex 366 nm and λex 445 nm. Enzymatic activity of GBA2 was measured in lysates of cells overexpressing the enzyme using the same conditions as above but without the presence of detergents and at pH 5.8. Enzymatic activity of GBA3 was measured in the absence of detergents in 100mM HEPES buffer at pH 7.0 [24]. Stimulation of GCase activity by the activator protein saposin C, produced recombinantly in *E. coli* [33], was monitored with 3.7 mM 4-MU-β-Glc as substrate in 150 mM McIlvaine buffer pH 4.5 containing 0.1 % (w/v) BSA and 0.4 mg/mL phosphatidylserine [34].

In vitro *assay of transglycosidase activity with fluorescent 25-NBD-cholesterol as acceptor.* Recombinant GCase and lysates of HEK293 cells overexpressing GBA2 and GBA3 were used to determine transglycosidase activity of each enzyme. The assays were performed as described earlier [10]. First, lysates overexpressing GBA2, or GBA3 were pre-incubated with 5 µM CBE for 20 min (samples containing diluted recombinant GCase were pre-incubated in the absence of CBE). To each of the samples the appropriate buffer containing 4-MU-Xyl or 4-MU-Glc was added for a final donor concentration of 3 mM and a final concentration of 40 µM 25-NBD-cholesterol as acceptor. Transglycosidase activity of GBA2 overexpressing cells was measured in a 150 mM McIlvaine buffer pH 5.8 and the assay for recombinant GCase was done in a 150 mM McIlvaine buffer pH 5.2 containing 0.1% BSA, 0.1% Triton X-100 and 0.2% sodium taurocholate. For GBA3 the assay contained 100 mM HEPES buffer, pH 7.0. The reaction was terminated by addition of chloroform/methanol (1:1, v/v) and lipids were extracted according to Bligh and Dyer [35]. Thereafter lipids were separated by thin layer chromatography on HPTLC silica gel 60 plates (Merck, Darmstadt, Germany) using chloroform/methanol (85:15, v/v) as eluent followed by detection of NBD-labelled lipids using a Typhoon Variable Mode Imager (GE Healthcare Bio-Science Corp., Piscataway, NJ, USA) [6].

In vitro *assay of GCS activity with fluorescent NBD C6-ceramide as acceptor.* HeLa, HeLa GCS KO and HeLa GCS KO with overexpression of GCS cell were homogenized in 100mM potassium phosphate buffer pH 7.5 supplemented with 4mM MgCl2 by sonication on ice. These homogenates were incubated with 35µM NBD C6-ceramide and 10 mM of UDP-Glc or UDP-Xyl for 16 hours. Lipids were extracted, separated and visualized as described above.

In vitro *assay of transglycosidase activity with cholesterol as acceptor.* Assays with natural cholesterol or ceramide d18:1/18:1 as acceptor were performed exactly as described in the sections above and the subsequent analysis of products was performed by LC-MS/MS as described in the section below. In brief for cholesterol: pure recombinant GCase was incubated at 37 ˚C with 32 µM cholesterol and 3.0 mM 4-MU-β-Xyl or 4-MU-β-Glc in 150 mM McIlvaine buffer pH 5.2 containing 0.1% BSA, 0.1% Triton X-100 and 0.2% sodium taurocholate for the indicated time periods. In short for ceramide: 10mM of UDP-Glc or UDP-Xyl was incubated with 0.16 µM ceramide d18.1/18:1 for 16 hours. All the incubations were stopped by addition of chloroform/methanol (1:1, v/v) and lipids were extracted according to Bligh and Dyer.

Assays with cultured RAW264.7 and HEK293 cells. Experiments with cultured RAW264.7 and HEK293 cells exposed to 3.7 mM 4-MU-β-Xyl or cyanidin 3-D-xyloside in the medium, either in the absence or presence of U18666A

(10 µM), inducing lysosomal cholesterol accumulation, were performed as described earlier [10]. Lysosomal GCase was irreversibly inhibited by prior incubation of cells with 300 µM CBE or 20nM ME656. Cells were harvested and lipids extracted as earlier described [10].

Synthesis Xylosylated Cholesterol. A complete overview of the synthesis of β-cholesteryl xyloside can be found in the supplemental materials and methods.

LC-MS/MS analysis. A Waters Xevo-TQS micro instrument was used in all experiments. The instrument consisted of an UPLC system combined with a tandem quadruple mass spectrometer as mass analyzer. Data were analyzed with Masslynx 4.1 Software (Waters,Milford MA, USA). Tuning conditions for GlcChol, XylChol's, GlcXylChol's, GlcSph and XylSph in ES+ (electrospray positive) mode are presented in Supplemental Table 1. All lipids during this study were separated using an Acquity BEH C18 reversed-phase column (2.1x 50 mm, particle size 1.7 µm; Waters). The column temperature and the temperature of the auto sampler were kept at 23°C and 10°C respectively during the run. The flow rate was 0.250 mL/min and volume of injection 10µL.

Analysis of GlcChol, and XylChol by LC-MS/MS. For the identification of XylChol, the extracted sample was dried and dissolved in methanol. MS parents scan and daughters scan were performed (Figure 2). As for GlcChol [10], the most abundant species of XylChol are ammonium adducts, [M+NH4]+ and the product ion 369.3 represents the cholesterol part of the molecule after loss of the xylose moiety. Ammonium adducts of XylChol, Xyl_2Chol and Xyl_3Chol showed the transitions 536.5>369.3, 668.5>369.3 and 800.5>369.3 respectively. For Multiple Reaction Monitoring (MRM) the UPLC program was applied during 5.5 minutes consisting of 10% eluent A (2-propanol:H2O 90:10 (v/v) containing 10 mM ammonium formate) and 90% eluent B (methanol containing 10 mM ammonium formate) The divert valve of the mass spectrometer was programmed to discard the UPLC effluent before (0 to 0.8 min) and after (4.5 to 5.5 min) the elution of the analytes to prevent system contamination. The retention time of both GlcChol and the internal standard $^{13}C_6$-GlcChol was 1.36 min. XylChol's were either synthesized or generated *in vitro* by incubation of GCase with 4-MU-β-Xyl and cholesterol. The retention time of XylChol, Xyl_2Chol and Xyl_3Chol was 1.71 min, 1.49 min and 1.40 min respectively (Supplemental Figure 1). Lastly, plasma was spiked with pure XylChol (0-1000 pmol XylChol/mL of plasma), internal standard $^{13}C_6$-GlcChol was added and samples were extracted. The area from transition XylChol over the area from the transition of internal standard (the ratio) was plotted against the concentration of XylChol in the plasma samples. The limit of detection was 0.1 pmol/mL plasma with

a sinal-to-noise ratio of three and the limit of quantification was 10 pmol/mL pasma with a signal-to-noise ratio of ten. Calculation of the signal-to-noise ratio was done using the peak-to-peak method.

LC-MS/MS quantitation of GlcChol and XylChols produced in vitro. Following incubation of rGCase and cholesterol with either 4-MU-β-Glc or 4-MU-β-Xyl, lipids were extracted according to the method of Bligh and Dyer by addition of methanol, chloroform and water (1:1:0.9, v/v/v). The lower phase was taken to dryness in an Eppendorf concentrator. Isolated lipids were purified by water/butanol extraction (1:1, v/v). The upper phase (butanol phase) was dried and dissolved in methanol, sonicated in a bath sonicator and samples were analyzed by LC-MS.

LC-MS/MS quantitation of GlcChol and XylChol's in cultured cells and organs. Cells were homogenized in 25mM potassium phosphase buffer pH 6.5 containing 0.1% (v/v) triton, by sonication on ice. Livers and spleens were homogenized in water. Prior to extraction, ^{13}C-labelled GlcChol and ceramide d17.0/16.0 in methanol (both used as an internal standard) were added to the homogenate. Samples were then treated with methanol:chloroform (1:1, v/v) to precipitate the proteins, following the supernatant was further extracted as described above.

Analysis of GlcCer, and XylCer by LC-MS/MS. To measure GlcCer and XylCer, lipids were deacylated [36] after Bligh and Digher extraction with methanol, chloroform and 100mM formate buffer pH 3.0 (1:1:0.9, v/v/v). Next, sample was evaporated and purified by water/butanol extraction (1:1, v/v). The butanol phase was dried, the final sample dissolved in methanol and GlcSph and XylSph levels measured. GlcSph was analyzed as published previously [37]. For Xylsph identification the sample was introduced in the mass spectrometer using LC-MS/MS (from 0 to 6.5 min to the detector), using eluent A (H2O:formic acid 99.5/0.5 (v/v) containing 1 mM ammonium formate) and eluent B (methanol:formic acid 99.5/0.5 (v/v) containing 1 mM ammonium formate). A mobile phase gradient was used during the run: 0.00 min 0% B, 2.50 min 100% B, 6.00 min 100% B, 6.05 min 0% B and 6.50 min 0% B.
MS parents scan and daughters scan were performed (Supplemental figure 2). Single reaction monitoring of precursor -> fragment ions (m/z GlcSph 462.30 > 282.30 and XylSph 432.67 > 282.30) was used for quantification.

Protein determination. Protein was measured with the Pierce BCA Protein Assay kit (Thermo Scientific). Absorbance was measured in EL808 Ultra Microplate Reader (BIO-TEK Instruments Inc.) at 562 nm.

Statistical Analysis. Values in figures are presented as a mean ± S.D. Data were analyzed by unpaired Student's t-test or Mann-Whitney u-test. P values < 0.05 were considered significant. * P < 0.05, ** P < 0.01 and *** P < 0.001.

Supplemental Materials and Methods

Synthesis of β-cholesteryl xyloside (β-Xyl-Chol).

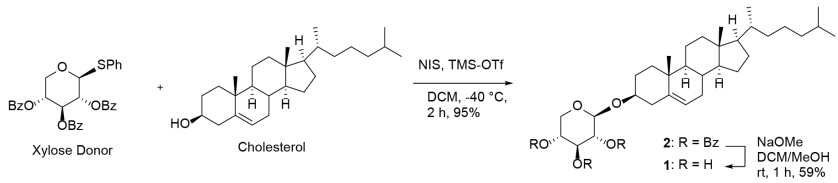

Unless stated otherwise, starting materials, reagents and solvents were purchased as high-grade commercial products from Sigma-Aldrich and were used without further purification. Dichloromethane (DCM) stored over 4 Å molecular sieves, which were dried in vacuo before use. Reactions were monitored by analytical thin-layer chromatography (TLC) using Merck aluminum sheets pre-coated with silica gel 60 with detection by UV absorption (254 nm) and by spraying with a solution of (NH4)6Mo7O24·H2O (25 g/L) and (NH4)4Ce(SO4)4·H2O (10 g/L) in 10% sulfuric acid followed by charring at ~150 ˚C or by spraying with an aqueous solution of KMnO4 (7%) and K2CO3 (2%) followed by charring at ~150 °C. Column chromatography was performed manually using either Baker or Screening Device silica gel 60 (0.04 - 0.063 mm), or with a Biotage Isolera™ flash purification system using silica gel cartridges (Screening devices SiliaSep HP, particle size 15-40 µm, 60A) in the indicated solvents. 1H NMR and ^{13}C NMR spectra were recorded on Bruker AV-500 (500/125 MHz) spectrometer in the given solvent. Chemical shifts are given in ppm relative to the chloroform, methanol, or dimethylsulfoxide residual solvent peak or tetramethylsilane (TMS) as internal standard. The following abbreviations are used to describe peak patterns when appropriate: s (singlet), d (doublet), t (triplet), q (quartet), qt (quintet), m (multiplet), br (broad), ar (aromatic), app (apparent). LC/MS analysis was performed on A Waters Acquity TM TQD instrument. The instrument consisted of a UPLC system combined with a tandem quadrupole mass spectrometer as mass analyzer using a BEH C18 reversed-phase column (2.1 × 50 mm, particle size 1.7 µm; Waters Corporation), by applying an isocratic elution of mobile phases, 2-propanol:water 90:10 (v/v) containing 10 mM ammonium formate (eluent A) and methanol containing 10 mM ammonium formate (eluent B).

β-cholesteryl xylosyl benzoate 2. (2S,3R,4S,5R)-2-(phenylthio)tetrahydro-2H-pyran-3,4,5-triyl tribenzoate donor1 (111 mg. 0.20 mmol) and cholesterol (62 mg, 167 mmol) were co evaporated in toluene (2x) and re-dissolved in 2 mL of DCM. 4Å molecular sieves were added and the mixture was stirred for 30 min at room temperature. Then the mixture was cooled to -40 °C and NIS (45 mg, 0.20 mmol) and TMS-OTf (42 µL, 0.23 mmol) were added. After stirring for 2 h at -40 °C the reaction was quenched with Et3N and warm up to room temperature. The mixture was diluted with DCM (30 mL) and aqueous 10% Na2S2O3 (20 mL). The extracted organic phase was then washed with brine, dried and purified by silica gel column chromatography (from pentane to pentane:EtOAc 9:1) to afford the protected β-cholesteryl xyloside 2 in 95% yield. 1H NMR (500 MHz, CDCl3): δ 7.99 (ddd, J = 7.1, 4.1, 1.2 Hz, 5H), 7.55 – 7.47 (m, 3H), 7.36 (q, J = 8.0 Hz, 6H), 5.76 (t, J = 7.4 Hz, 1H), 5.34 (dd, J = 7.5, 5.6 Hz, 1H), 5.29 – 5.27 (m, 1H), 4.95 (d, J = 5.6 Hz, 1H), 4.44 (dd, J = 12.1, 4.4 Hz, 1H), 3.68 (dd, J = 12.1, 7.3 Hz, 1H), 3.57 (tt, J = 11.3, 4.6 Hz, 1H), 2.46 – 2.33 (m, 1H), 2.27 (ddd, J = 13.3, 4.9, 2.2 Hz, 1H), 2.20 – 2.11 (m, 1H), 2.06 – 1.90 (m, 2H), 1.90 – 1.76 (m, 3H), 1.73 – 1.47 (m, 8H), 1.47 – 1.19 (m, 6H), 1.19 – 1.02 (m, 6H), 1.02 – 0.97 (m, 2H), 0.95 (s, 3H), 0.91 (d, J = 6.6 Hz, 3H), 0.87 (d, J = 2.2 Hz, 3H), 0.85 (d, J = 2.2 Hz, 3H), 0.66 (s, 3H). 13C NMR (126 MHz, CDCl3) δ 165.7, 165.6, 165.4, 140.5, 133.5, 133.3, 130.0, 129.6, 129.4, 129.4, 128.5, 122.2, 98.8, 79.0, 77.4, 77.2, 76.9, 70.9, 70.7, 69.5, 61.5, 56.9, 56.3, 50.3, 42.5, 39.9, 39.7, 38.8, 37.4, 36.9, 36.3, 35.9, 32.1, 32.0, 29.9, 29.7, 28.4, 28.3, 28.2, 24.4, 24.0, 23.0, 22.7, 21.2, 19.5, 18.9, 12.0.

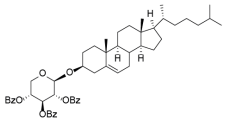

β-cholesteryl xyloside1. Intermediate 2 (63 mg, 0.076 mmol) was dissolved in a mixture of DCM/MeOH (1:2, v/v, 3 mL) and NaOMe (5.4 M in MeOH, 7.6 µL). After stirring for 1 h the reaction mixture was neutralized by addition of Et3N·HCl and purified by silica gel column chromatography (from DCM to DCM:MeOH 9:1), yielding the title compound cholesteryl-D-β-Xylopyranoside (β-Xyl-Chol) 1 as a white solid in 59% yield. 1H NMR (500 MHz, CDCl3): δ 5.37 (d, J = 5.1 Hz, 1H), 4.50 (d, J = 6.1 Hz, 1H), 4.05 (dd, J = 11.9, 4.4 Hz, 1H), 3.75 (dq, J = 8.0, 4.0 Hz, 1H), 3.65 – 3.53 (m, 2H), 3.47 – 3.40 (m, 1H), 3.36 (dd, J = 11.9, 8.1 Hz, 1H), 2.94 (s, 1H), 2.64 (d, J = 4.1 Hz, 1H), 2.42 – 2.34 (m, 2H), 2.23 (t, J = 12.5 Hz, 1H), 2.04 – 1.95 (m, 2H), 1.91 – 1.81 (m, 2H), 1.64 – 1.43 (m, 10H), 1.36 – 1.23 (m, 6H), 1.16 – 1.04 (m, 6H), 1.00 (s, 3H), 0.91 (d, J = 6.5 Hz, 3H), 0.87 (d, J = 2.3 Hz, 3H), 0.86 (d, J = 2.4 Hz, 3H), 0.67 (s, 3H). 13C NMR (126 MHz, CDCl3) δ 140.2, 122.5, 100.8, 78.7, 74.6, 72.5, 69.9, 64.3, 56.9, 56.3, 50.3, 42.5, 39.9, 39.7, 38.8, 37.4, 36.9, 36.3, 35.9, 32.1, 32.0, 29.8, 28.4, 28.2, 24.4, 24.0, 23.0, 22.7, 21.2, 19.5, 18.9, 12.0. LC-MS/MS: calcd. for [C32H54O5+NH3]+ 518.8; found 536.7.

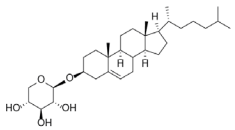

Supplemental data

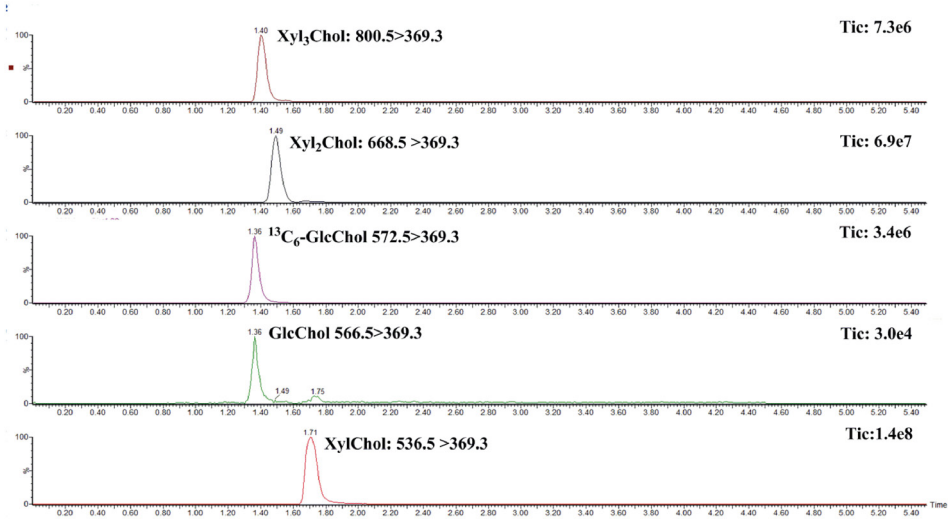

Supplemental Figure 1: Chromatogram of XylChol, Xyl_2Chol, Xyl_3Chol, GlcChol and $^{13}C_6$-GlcChol.

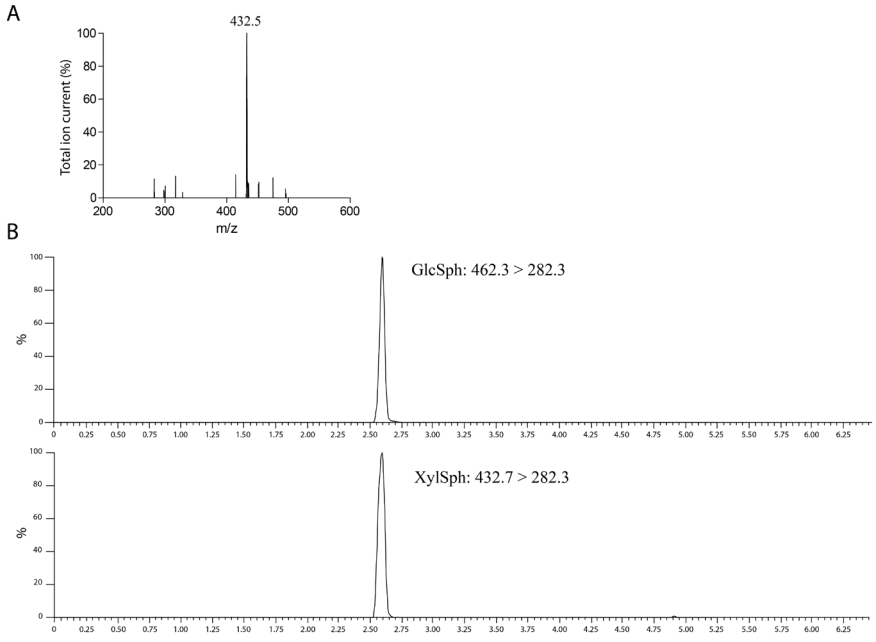

Supplemental Figure 2: A. MS/MS Fragmentation spectrum of parent scan XylSph B. Chromatogram GlcSph and XylSph.

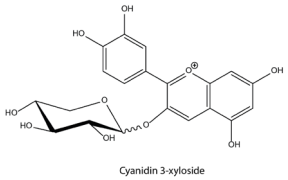

Supplemental Figure 3: Chemical structure Cyanidin 3-xyloside.

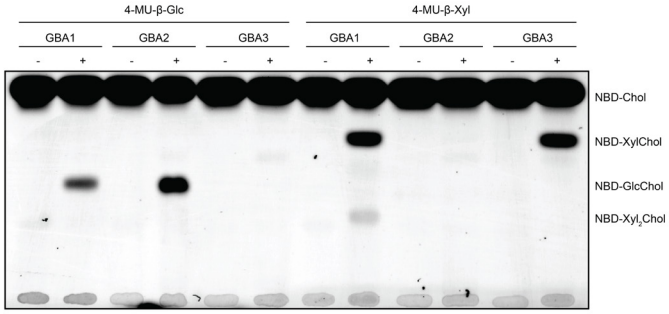

Supplemental Figure 4: Lack of transxylosylation by GBA2. HPTLC analysis of formation of glycosylated 25-NBD-cholesterol by β-glucosidases with 4-MU-β-Xyl and 4-MU-β-Glc as donor. Enzymes: recombinant hGCase; lysate of HEK293 cells overexpressing GBA2; lysate of HEK293 cells overexpressing GBA3. Incubation for 16 hours with (+) or without (-) enzyme preparation.

Supplemental Tables 1. MS/MS instrument parameters.

Mass spectrometer	Xevo-TQS-Micro (Waters)
Ionization mode	ESI+
Capillary voltage	3.50 kV
Source temperature	150 °C
Desolvation temperature	450 °C
Cone gas flow	50 L/h
Desolvation gas flow	950 L/h

Compound	Parent (m/z)	Daughter (m/z)	Cone voltage (V)	Collision energy (V)	RT (min)
GlcChol	566.5	369.3	20	15	1.34
^{13}C-GlcChol	572.0	369.3	20	15	1.34
XylChol	536.5	369.3	20	15	1.69
Xyl_2Chol	668.5	369.3	20	15	1.47
Xyl_3Chol	800.5	369.3	20	15	1.38
GlcSph	462.3	282.3	30	20	3.23
XylSph	432.67	282.3	25	15	3.25
C17-Sphinganine	288.3	270.3	20	15	3.26

References

1. E.A. Rennie, H.V. Scheller, Xylan biosynthesis, Curr Opin Biotechnol, 26 (2014) 100-107.
2. J.D. Esko, K. Kimata, U. Lindahl, Proteoglycans and Sulfated Glycosaminoglycans, in: nd, A. Varki, R.D. Cummings, J.D. Esko, H.H. Freeze, P. Stanley, C.R. Bertozzi, G.W. Hart, M.E. Etzler (Eds.) Essentials of Glycobiology, Cold Spring Harbor (NY), 2009.
3. J.L. Moriarity, K.J. Hurt, A.C. Resnick, P.B. Storm, W. Laroy, R.L. Schnaar, S.H. Snyder, UDP-glucuronate decarboxylase, a key enzyme in proteoglycan synthesis: cloning, characterization, and localization, J Biol Chem, 277 (2002) 16968-16975.
4. D. Fisher, P.W. Kent, Rat liver beta-xylosidase, a lysosomal membrane enzyme, Biochem J, 115 (1969) 50P-51P.
5. V. Patel, A.L. Tappel, Identity of beta-glucosidase and beta-xylosidase activities in rat liver lysosomes, Biochim Biophys Acta, 191 (1969) 86-94.
6. S. van Weely, M. Brandsma, A. Strijland, J.M. Tager, J.M. Aerts, Demonstration of the existence of a second, non-lysosomal glucocerebrosidase that is not deficient in Gaucher disease, Biochim Biophys Acta, 1181 (1993) 55-62.
7. E. Beutler, G.A. Grabowski, Gaucher disease, in: The Metabolic and Molecular Bases of Inherited Disease, McGraw-Hill Publishing Company, New York, United States, 1995, pp. 2641-2670.
8. M.J. Ferraz, W.W. Kallemeijn, M. Mirzaian, D. Herrera Moro, A. Marques, P. Wisse, R.G. Boot, L.I. Willems, H.S. Overkleeft, J.M. Aerts, Gaucher disease and Fabry disease: new markers and insights in pathophysiology for two distinct glycosphingolipidoses, Biochim Biophys Acta, 1841 (2014) 811-825.
9. H. Akiyama, S. Kobayashi, Y. Hirabayashi, K. Murakami-Murofushi, Cholesterol glucosylation is catalyzed by transglucosylation reaction of beta-glucosidase 1, Biochem Biophys Res Commun, 441 (2013) 838-843.
10. A.R. Marques, M. Mirzaian, H. Akiyama, P. Wisse, M.J. Ferraz, P. Gaspar, K. Ghauharali-van der Vlugt, R. Meijer, P. Giraldo, P. Alfonso, P. Irun, M. Dahl, S. Karlsson, E.V. Pavlova, T.M. Cox, S. Scheij, M. Verhoek, R. Ottenhoff, C.P. van Roomen, N.S. Pannu, M. van Eijk, N. Dekker, R.G. Boot, H.S. Overkleeft, E. Blommaart, Y. Hirabayashi, J.M. Aerts, Glucosylated cholesterol in mammalian cells and tissues: formation and degradation by multiple cellular beta-glucosidases, J Lipid Res, 57 (2016) 451-463.
11. H. Akiyama, Y. Hirabayashi, A novel function for glucocerebrosidase as a regulator of sterylglucoside metabolism, Biochim Biophys Acta Gen Subj, 1861 (2017) 2507-2514.
12. M.T. Vanier, Complex lipid trafficking in Niemann-Pick disease type C, J Inherit Metab Dis, 38 (2015) 187-199.
13. Y. Yildiz, H. Matern, B. Thompson, J.C. Allegood, R.L. Warren, D.M. Ramirez, R.E. Hammer, F.K. Hamra, S. Matern, D.W. Russell, Mutation of beta-glucosidase 2 causes glycolipid storage disease and impaired male fertility, J Clin Invest, 116 (2006) 2985-2994.
14. R.G. Boot, M. Verhoek, W. Donker-Koopman, A. Strijland, J. van Marle, H.S. Overkleeft, T. Wennekes, J.M. Aerts, Identification of the non-lysosomal glucosylceramidase as beta-glucosidase 2, J Biol Chem, 282 (2007) 1305-1312.
15. H.G. Korschen, Y. Yildiz, D.N. Raju, S. Schonauer, W. Bonigk, V. Jansen, E. Kremmer, U.B. Kaupp, D. Wachten, The non-lysosomal beta-glucosidase GBA2 is a non-integral membrane-associated protein at the endoplasmic reticulum (ER) and Golgi, J Biol Chem, 288 (2013) 3381-3393.
16. W.W. Kallemeijn, M.D. Witte, T.M. Voorn-Brouwer, M.T. Walvoort, K.Y. Li, J.D. Codee, G.A. van der Marel, R.G. Boot, H.S. Overkleeft, J.M. Aerts, A sensitive gel-based method combining distinct cyclophellitol-based probes for the identification of acid/base residues in human retaining beta-glucosidases, J Biol Chem, 289 (2014) 35351-35362.
17. M.D. Witte, W.W. Kallemeijn, J. Aten, K.Y. Li, A. Strijland, W.E. Donker-Koopman, A.M. van den Nieuwendijk, B. Bleijlevens, G. Kramer, B.I. Florea, B. Hooibrink, C.E. Hollak, R. Ottenhoff, R.G. Boot, G.A. van der Marel, H.S. Overkleeft, J.M. Aerts, Ultrasensitive in situ visualization of active glucocerebrosidase molecules, Nat Chem Biol, 6 (2010) 907-913.
18. S.P. Schroder, R. Petracca, H. Minnee, M. Artola, J.M.F.G. Aerts, J.D.C. Codee, G.A. van der Marel, H.S. Overkleeft, A Divergent Synthesis of L-arabino- and D-xylo-Configured Cyclophellitol Epoxides and Aziridines, Eur J Org Chem, (2016) 4787-4794.
19. W. Wiczkowski, E. Romaszko, M.K. Piskula, Bioavailability of cyanidin glycosides from natural chokeberry (Aronia melanocarpa) juice with dietary-relevant dose of anthocyanins in humans, J Agric Food Chem, 58 (2010) 12130-12136.
20. Y. Liu, D. Zhang, Y. Wu, D. Wang, Y. Wei, J. Wu, B. Ji, Stability and absorption of anthocyanins from blueberries subjected to a simulated digestion process, Int J Food Sci Nutr, 65 (2014) 440-448.
21. G.M. Aerts, O. Vanopstal, C.K. Debruyne, Beta-D-Glucosidase-Catalyzed Transfer of the Glycosyl Group

from Aryl Beta-D-Gluco-Pyranosides and Beta-D-Xylo-Pyranosides to Phenols, Carbohyd Res, 100 (1982) 221-233.
22. C.D. Kay, G. Mazza, B.J. Holub, J. Wang, Anthocyanin metabolites in human urine and serum, Br J Nutr, 91 (2004) 933-942.
23. C.L. Kuo, W.W. Kallemeijn, L.T. Lelieveld, M. Mirzaian, I. Zoutendijk, A. Vardi, A.H. Futerman, A.H. Meijer, H.P. Spaink, H.S. Overkleeft, J. Aerts, M. Artola, In vivo inactivation of glycosidases by conduritol B epoxide and cyclophellitol as revealed by activity-based protein profiling, FEBS J, 286 (2019) 584-600.
24. N. Dekker, T. Voorn-Brouwer, M. Verhoek, T. Wennekes, R.S. Narayan, D. Speijer, C.E. Hollak, H.S. Overkleeft, R.G. Boot, J.M. Aerts, The cytosolic beta-glucosidase GBA3 does not influence type 1 Gaucher disease manifestation, Blood Cells Mol Dis, 46 (2011) 19-26.
25. E. Uyama, K. Takahashi, M. Owada, R. Okamura, M. Naito, S. Tsuji, S. Kawasaki, S. Araki, Hydrocephalus, corneal opacities, deafness, valvular heart disease, deformed toes and leptomeningeal fibrous thickening in adult siblings: a new syndrome associated with beta-glucocerebrosidase deficiency and a mosaic population of storage cells, Acta Neurol Scand, 86 (1992) 407-420.
26. A. Chabas, B. Cormand, D. Grinberg, J.M. Burguera, S. Balcells, J.L. Merino, I. Mate, J.A. Sobrino, R. Gonzalez-Duarte, L. Vilageliu, Unusual expression of Gaucher's disease: cardiovascular calcifications in three sibs homozygous for the D409H mutation, J Med Genet, 32 (1995) 740-742.
27. A. Abrahamov, D. Elstein, V. Gross-Tsur, B. Farber, Y. Glaser, I. Hadas-Halpern, S. Ronen, M. Tafakjdi, M. Horowitz, A. Zimran, Gaucher's disease variant characterised by progressive calcification of heart valves and unique genotype, Lancet, 346 (1995) 1000-1003.
28. K.A. Karlsson, B.E. Samuelsson, G.O. Steen, Identification of a xylose-containing cerebroside in the salt gland of the herring gull, J Lipid Res, 13 (1972) 169-176.
29. W. Westbroek, M. Nguyen, M. Siebert, T. Lindstrom, R.A. Burnett, E. Aflaki, O. Jung, R. Tamargo, J.L. Rodriguez-Gil, W. Acosta, A. Hendrix, B. Behre, N. Tayebi, H. Fujiwara, R. Sidhu, B. Renvoise, E.I. Ginns, A. Dutra, E. Pak, C. Cramer, D.S. Ory, W.J. Pavan, E. Sidransky, A new glucocerebrosidase-deficient neuronal cell model provides a tool to probe pathophysiology and therapeutics for Gaucher disease, Dis Model Mech, 9 (2016) 769-778.
30. H.S. Overkleeft, G.H. Renkema, J. Neele, P. Vianello, I.O. Hung, A. Strijland, A.M. van der Burg, G.J. Koomen, U.K. Pandit, J.M. Aerts, Generation of specific deoxynojirimycin-type inhibitors of the non-lysosomal glucosylceramidase, J Biol Chem, 273 (1998) 26522-26527.
31. S. Ichikawa, H. Sakiyama, G. Suzuki, K.I. Hidari, Y. Hirabayashi, Expression cloning of a cDNA for human ceramide glucosyltransferase that catalyzes the first glycosylation step of glycosphingolipid synthesis, Proc Natl Acad Sci U S A, 93 (1996) 4638-4643.
32. J.M. Aerts, W.E. Donker-Koopman, M.K. van der Vliet, L.M. Jonsson, E.I. Ginns, G.J. Murray, J.A. Barranger, J.M. Tager, A.W. Schram, The occurrence of two immunologically distinguishable beta-glucocerebrosidases in human spleen, Eur J Biochem, 150 (1985) 565-574.
33. V.E. Ahn, P. Leyko, J.R. Alattia, L. Chen, G.G. Prive, Crystal structures of saposins A and C, Protein Sci, 15 (2006) 1849-1857.
34. J.M. Aerts, M.C. Sa Miranda, E.M. Brouwer-Kelder, S. Van Weely, J.A. Barranger, J.M. Tager, Conditions affecting the activity of glucocerebrosidase purified from spleens of control subjects and patients with type 1 Gaucher disease, Biochim Biophys Acta, 1041 (1990) 55-63.
35. E.G. Bligh, W.J. Dyer, A rapid method of total lipid extraction and purification, Can J Biochem Physiol, 37 (1959) 911-917.
36. J.E. Groener, B.J. Poorthuis, S. Kuiper, M.T. Helmond, C.E. Hollak, J.M. Aerts, HPLC for simultaneous quantification of total ceramide, glucosylceramide, and ceramide trihexoside concentrations in plasma, Clin Chem, 53 (2007) 742-747.
37. M. Mirzaian, P. Wisse, M.J. Ferraz, H. Gold, W.E. Donker-Koopman, M. Verhoek, H.S. Overkleeft, R.G. Boot, G. Kramer, N. Dekker, J.M. Aerts, Mass spectrometric quantification of glucosylsphingosine in plasma and urine of type 1 Gaucher patients using an isotope standard, Blood Cells Mol Dis, 54 (2015) 307-314.

Chapter 7

Discussion and Future Prospects

Discussion and Future Prospects

The studies described in this thesis were aimed to increase insight in the catalytic versatility and potential functions of glucocerebrosidase, inside and beyond the lysosome. The specific goals of investigations are formulated in the introductory chapter. General background on glycosphingolipids and their metabolizing enzymes is provided in **chapter 2**. Special attention is focused to the acid β-glucosidase aka glucocerebrosidase (GCase; GBA), the main object of the conducted investigations. Historically, the function of GCase inside lysosomes has received considerable interest. For half a century it is known that deficiency of the enzyme causes Gaucher disease, a relatively common lysosomal storage disorder characterized by accumulation of glucosylceramide (GlcCer) laden macrophages in tissues [1]. The relatively recent recognition that carriers of a mutant *GBA* allele have a markedly increased risk for developing α-synucleinopathies (Parkinson's disease and Lewy-body dementia) has further boosted interest in the function of the enzyme [2]. Complete GCase deficiency proves to be incompatible with terrestrial life due to disturbed skin barrier function [3, 4]. This finding has raised interest in the role of GCase beyond the lysosome.

Beyond the lysosome: the stratum corneum of the skin

The first section of this thesis concerns the role of GCase in the human skin. **Chapter 3** describes the use of fluorescent activity-based probes (ABP) to visualize active GCase molecules *in situ* in the skin. This method is more robust and sensitive than zymography using either substrate 4-methylumbelliferyl-β-D-glucopyranoside or resorufin-β-D-glucopyranoside as substrate rendering diffusing products, the blue fluorophore, 4-methylumbelliferone and the red fluorescent resorufin, respectively. Active GCase was found to be primarily located in the extracellular lipid matrix of the most outer part of the skin, the

stratum corneum (SC). This location of active GCase molecules is consistent with literature reports on the enzyme's role in generating ceramides in the SC [5-7]. The lipid rich environment and low pH (ranging from 4.5–5.3 on the outside, to 6.8 on the inside) of the SC likely contributes to the local stability of GCase [8, 9].

In recent times 3D cultured skin models mimic the properties of native human skin, called full thickness models (FTMs), have been successfully developed (as reviewed in [10]). ABPs targeting GCase can be used to visualize active enzyme molecules in these models. Moreover, the ABPs and their cyclophellitol-epoxide scaffold are potent suicide inhibitors of GCase and could therefore be used to generate on demand an enzyme deficiency in a FTM. The importance of GCase in features of skin could thus be studied in unprecedented manner. Also a superior, entirely GCase-specific suicide inhibitor, a cyclophellitol tagged at C8 with a hydrophobic bulky adamantyl, has recently been developed [11, 12].

Meanwhile, multiple ABPs reacting with various retaining glycosidases have been designed [13-18]. Active enzyme molecules visualized with these ABPs are lysosomal exo-glycosidases (galactocerebrosidase, α-galactosidases A and B, acid α-mannosidases, acid α-glucosidase, α-fucosidase, α-iduronidase, acid β-galactosidase, β-mannosidase and β-glucuronidase). Available are also ABPs labeling other non-lysosomal human β-glucosidases (GBA2 and GBA3) and the intestinal lactase-phlorizin hydrolase that also shows β-glucosidase activity [19-21]. With all these ABPs in place, the presence of active glycosidase molecules can now be rigorously studied in samples of normal and diseased human skin as well as in FTMs. The presence of lysosomal enzymes in the SC is still poorly documented and little is known about the possible presence of enzymes like GBA2 and GBA3 in the epidermis.

Two other hydrolases are also of specific interest in relation to the SC: acid sphingomyelinase (ASM) and acid ceramidase (AC). ASM crucially converts sphingomyelin (SM) molecules to their ceramide backbones in the SC. AC is able to fragment ceramides to sphingosine and free fatty acid (FFA) moieties. Both ceramide and FFA are crucial components of intercellular lipid lamellae in the SC constituting the skin barrier [22]. At the moment the only way to visualize the activity of ASM is zymography using 6-hexadecanoyl-4-methylumbelliferyl-phosphorylcholine (6-HMU-PC) as substrate [23, 24]. It is appealing to consider the use of ABPs to render more detailed information on ASM and AC in the skin. Arenz and co-workers have designed fluorescent phosphosphingolipids capable of Förster resonance energy transfer [25]. The compound is a structure mimic of SM in terms of its polarity, conformation, and steric bulk and can be used to determine ASM activity by fluorescence

spectroscopy. Recently, Fabrias and coworkers have designed very specific ABPs for AC, based on analogues of the AC inhibitor SABRAC [26]. It will be valuable to establish with the ABPs the precise location of ASM and AC in the human skin and to determine the ratios between active GCase, active ASM and AC molecules in normal and diseased tissue.

The lipid composition of the SC is crucial for a proper barrier feature of the skin that is determined by a delicate balance between ceramide, fatty acid and cholesterol in lipid lamellae [22]. **Chapter 4** illustrates the great value of ABPs in determining the location of active enzyme molecules. Described is the altered localization of active GCase and ASM in the epidermis of atopic dermatitis (AD) patients that is related to abnormal barrier function and SC lipid changes, particularly at lesional skin sites.

Altered localization of ASM relates to increased ceramide subclasses [AS] and [NS] in AD SC, lipids known to be crucial for proper SC lipid lamellae and barrier function [27-30]. In the study described in **chapter 4**, the altered location of active GCase molecules in the epidermis was found to correlate with reduction of total SC ceramides, particularly the subclasses [NP], [NH] and EO ceramides that are not derived from the catabolism of SM by ASM. At the moment it can't be distinguished whether the observed changes in SC lipid organization (partially) originate from altered active enzyme distribution or that the disturbed barrier causes the changed location of enzymes. It is conceivable that abnormal enzyme location and changed SC lipid composition enforce each other. It will be informative to test how fast acute inactivation of GCase with suicide inhibitors causes a disturbed barrier over time. Moreover, it could be analyzed whether the location of ASM is influenced by such imposed change in SC lipid lamellae. Likewise, it could be studied with FTMs whether available inhibitors of glucosylceramide synthase (GCS; Miglustat and Eliglustat) [31, 32] can balance a deficiency in active GCase with respect to desired barrier features. If so, topical administration of GCS inhibitors could be developed as therapeutic avenue.

The occurrence of glucosylated cholesterol (GlcChol) in human cells and tissues has recently been documented [33-35]. It has become apparent that GlcCer is the biosynthetic precursor of GlcChol. The cytosol-faced GBA2 normally generates GlcChol using GlcCer as sugar donor and cholesterol as acceptor via transglucosylation [33]. During extreme lysosomal accumulation of cholesterol (as occurs in Niemann Pick type C disease), GlcChol can be also formed by GCase via transglucosylation, however under normal conditions GCase catalyzes the cleavage of GlcChol to free glucose and sterol [33].

Chapter 5 demonstrates the existence of GlcChol in the SC. Local formation of GlcChol in the SC by GCase via a transglucosylation reaction seems the plausible biosynthetic pathway: active GCase molecules are present in the SC (**chapter 3**) and GlcCer and cholesterol are abundant local lipids.

At present the physiological function of GlcChol in the SC is unclear. It can be speculated that GlcChol has a role in natural desquamation (shedding of the outermost layer of the skin), similar to that postulated for cholesterol sulfate [36]. An additional and/or alternative function of SC GlcChol might involve barrier features. To investigate this, the TEWL (Trans Epidermal Water Loss) in a SC substitute model (porous substrate covered with synthetic SC lipids) with and without GlcChol could be measured [37]. It could be also experimentally investigated whether GlcChol content of skin samples (or cultured 3D skin) can be increased by exposure to exogenous glucosylated sterol and if so whether this impacts the barrier function.

Formation of GlcChol in the SC seems dependent on GCase. Therefore, the SC content on GlcChol could in theory offer a readout for presence of active GCase in the SC of individuals with lesions. Such hypothetical diagnostic application for SC GlcChol warrants further investigation. It can be confirmed with FTM that pharmacological inactivation of GCase prohibits formation of GlcChol and reduces the levels of the glucosylated sterol. Of note, GlcChol and GlcCer were measured in SC sheets obtained from patients suffering from Netherton syndrome (NTS) with severely impaired skin barrier (**chapter 5**). The ratio GlcChol/GlcCer in the patient samples was found to be quite normal. In samples of some patients supra-high levels of both GlcChol and GlcCer were observed, but inter-subject differences were very high, as earlier reported for lipid abnormalities in skin of NTS patients [38].

Lamellar bodies

To conclude the thesis section dealing with skin, a more in-depth discussion of lamellar bodies (LBs) is of interest. LBs play a key role in the delivery of lipids into the SC [39-41]. They are specialized intracellular organelles packed with lipids, including GlcCer and SM [22]. In upwards migrating keratinocytes of the stratum spinosum the formation of LBs is initiated. The organelles have a surrounding membrane and contain internal lipid membrane structures. The membrane protein ATP-binding cassette sub-family A member 12 (ABCA12) is responsible for the transport of GlcCer's into the LBs [42-44]. Moreover, the LBs contain enzymes such as GCase and ASM. Following extrusion of LBs at the interface between the stratum granulosum and the SC, the enzymes GCase

and ASM metabolize their lipid substrates to ceramides, essential steps for proper SC lipid lamellae [40, 41]. LBs are lysosome related organelles (LROs), sometimes referred to as secretory lysosomes [45]. They share features of late endosomes and lysosomes. The latter are cytoplasmic organelles that serve as a major degradative compartment in eukaryotic cells, carried out by more than 50 acid-dependent hydrolases [46].

As discussed in **chapter 2**, newly formed and correctly folded GCase molecules bind in the ER to LIMP2 (lysosomal integrated membrane protein 2), which is essential for proper transport of GCase to lysosomes [47, 48]. At first glance it therefore seems likely that LIMP2 also mediates the transport of GCase to LBs, and thus could co-determine skin features. However, acute myoclonic renal failures syndrome (AMRF) patients with a defective LIMP2 develop no overt skin problems, despite reduced GCase in most cell types [48]. Since GCase in LIMP2 deficient cells is secreted by default, it might be that the SC of AMRF patients contains sufficient, directly secreted, enzyme to allow local degradation of GlcCer. It is unlikely that some other β-glucosidase compensates for GCase in the SC since such compensation does not occur in

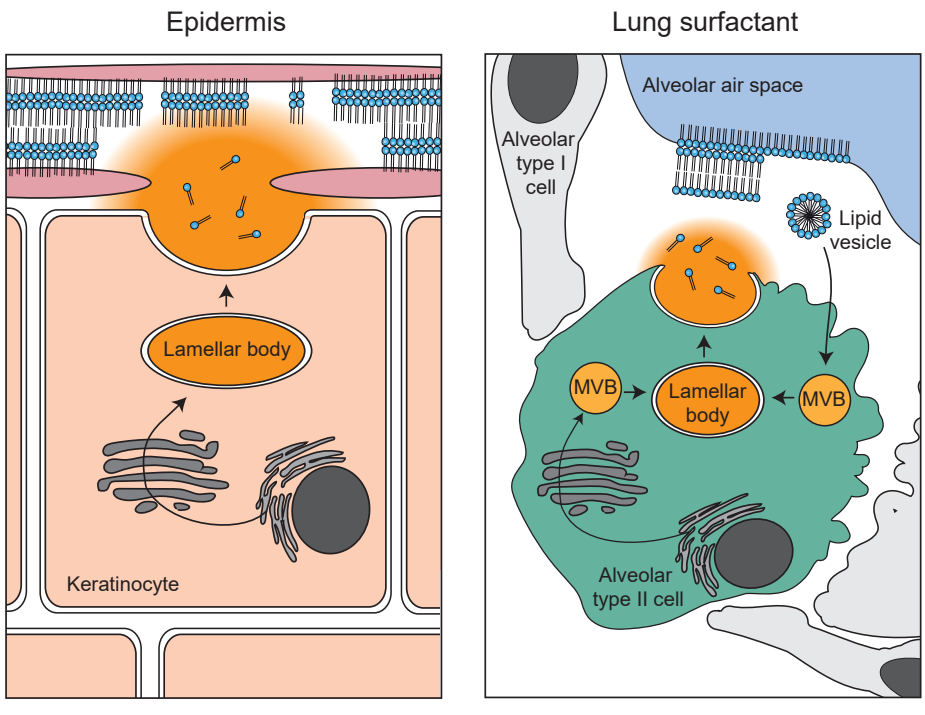

Figure 1: The similarities in the epidermal and lung lamellar body extrusion. MVB: Multivescular body.

collodion Gaucher disease patients [49-52]. Alternatively, delivery of GCase to LBs keratinocytes might take place by another, yet unidentified, receptor protein.

Apart from the skin there are other tissues where structures similar to lipid-rich LBs are formed [45]. One example of this is the lung epithelium. The alveolar system of the lung is a body barrier and is composed of two types of epithelial cells, pneumocytes I and II [53]. LBs in pneumocyte type II cells store lung surfactant that is composed of phospholipids and proteins [54, 55]. The surfactant lipid components (dipalmitoylphosphatidylcholine as major one) are extruded from LBs and form a protective layer at the alveolar air-liquid interface essential for appropriate surface tension [56]. During LB formation in pneumocytes lipids are imported by ABCA3, phylogenetically close to ABCA12 [57, 58]. An ABCA3 mutation underlies a fatal lung disease in newborns in which the surface surfactant function is impaired [59]. Thus, there is a striking parallel with the severe ichthyotic skin in patients with ABCA12 mutations [43, 44, 58]. Additionally, immediate lung alveolar collapse after birth has been demonstrated in ABCA12 deficient mice, showing it has a crucial role in both skin and lung barrier function [60]. The similarities in the lung and skin (Figure 1) spark curiosity whether glycosphingolipids also play a role in surfactant LBs and the lung barrier. Interestingly proteomic analysis of rat LB's showed significant overlap with other LRO's, but surprisingly little with LB's from the skin [61]. Moreover, little is known on lysosomal enzyme content of LBs in pneumocytes and surfactant [62]. It is therefore appealing to study in lung LBs and surfactant the presence of glycosidases using ABPs. An old study by de Vries et al. reports high amounts of lysosomal α-glucosidase (GAA), however GCase activity in LBs from the lung was low [63]. In another study with rats, six lysosomal hydrolases were identified as components of lung LBs: acid phosphatase, β-hexosaminidase, β-galactosidase, α-mannosidase, α-fucosidase and β-glucosidase. Interestingly, acute ozone stress in rats was found to result in reduced hydrolase activities voor all hydrolases, except α -mannosidase, in the LB's of alveolar type II cells [64]. More recently decreased levels of phosphatidylcholine in the lung surfactant of patients suffering from Gaucher disorder and other lysosomal storage diseases were detected, suggesting a potential link between lysosomal enzymes and barrier function [65].

LBs have also been detected in rat stomach [66] minipig kidney [67], guinea pig organ of Corte [68], canine tong papillae [69], rabbit eustachian tube [70], human oral epithelium [71] and mucosa of the nose [72]. These tissues all share an epithelial character and their LBs seem to mediate lipid transport to the extracellular space. It can be therefore attractive to research these "barrier

tissues" for glycosphingolipids and metabolizing enzymes. Another tissue in this connection of potential interest might be the placenta. The placenta is a highly specialized organ that mediates exchange of various endogenous and exogenous substances between the mother and fetus and can therefore be seen as a "barrier tissue" [73, 74]. Markedly increased GCase expression and activity has been observed in preeclamptic placenta [75]. There is still a lot unknown about this barrier in relation to lipids and lamellar bodies, but there are reports suggesting that lipid rafts in the fetal tissue are able to prevent maternal-fetal virus cell transmission [76, 77]. Blundell et al. have engineered a model that mimics structural and functional complexity of the human placenta barrier [78]. The cultured trophoblasts on their "placenta-on-a-chip" develop dense microvilli that make it possible to reconstitute the expression and localization of certain membrane transport proteins. Such models might be of interest to study in more detail regarding expression and localization of lysosomal enzymes like GCase. Besides the maternal-fetal barrier and the fetal skin, another barrier is formed during the last trimester of pregnancy: the fetus is covered in vernix caseosa, which is a protective biofilm. The vernix caseosa substitutes the immature epidermal barrier in fetal skin and forms a barrier against bacterial infection [79]. All main SC lipids have been shown to be present in the vernix caseosa [80] and research has shown 30% of the lipids in the vernix caseosa to be similar to the SC lipid content [81].

Catalytic versatility of GCase

The second section of the thesis deals with the catalytic versatility of GCase that exceeds hydrolysis of GlcCer. Expanding earlier observations [82, 83], **chapter 6** provides evidence that GCase is remarkably versatile in catalysis. It is not only able to use β-glucosides as substrate, but also β-xylosides. In addition, GCase is shown to also transxylosylate cholesterol rendering xylosylated sterol (XylChol). It was noted that recombinant GCase can even generate Xyl_2Chol and trace amounts of Xyl_3Chol. An attractive explanation for this repetitive xylosylation is the noted poor hydrolysis of XylChol by GCase, contrary to that of GlcChol. Transxylosylation is not solely a test tube phenomenon but also takes place in intact cells with lysosomal cholesterol accumulation and exposed to the sugar donor 4-metylumbelliferyl-β-xyloside (4-MU-Xyl).

β-Glucosidases are a heterogeneous group of enzymes and are known to sporadically hydrolyze other substrates that are structurally similar to β-glucosides [84-87]. Previously xylosidase activity has been reported for beta-D-glucosidases from *Stachybotrys Atra* [88], *Agrobacterium Tumefaciens* [89], *Aspergillus Niger* [90], and *Erwinia Chrysanthemi* [91]. It is also not uncommon for xylosidases to display transglycosidase activity: this has been described

for β-xylosidases from *Aspergillus Sp* [92], *Agrobacterium Tumefaciens* [89], and *Talaromyces Amestolkiae* [93]. Therefore, the observed transxylosidase activity of human GCase is not completely unexpected, nevertheless it's the first time it has been documented and characterized.

A subsequent investigation of tissues and cells revealed the presence of small but significant amounts of XylChol. Apparently, the formation of XylChol occurs also *in vivo*. A key question after the discovery of endogenous XylChol concerned the nature of β-xylosides donors that allow its formation by transxylosylation. Considered donors were exogenous β-xylosides. Indeed, XylChol was found to be formed by cultured cells after exposure to the plant derived cyanidin-β-xyloside, a colored component of berries that has been shown to accumulate in plasma after intake of berry supplements [94]. Next, endogenous β-xylosides were considered as donors. One possible candidate in this respect would be serine-linked β-xylosides arising from lysosomal degradation of proteoglycans [95]. Another considered candidate was xylosylated ceramide (XylCer). So far, there is just one report on the presence of XylCer in the salt gland of herring gull, however no follow up research on this has apparently been performed [96]. As described in **chapter 6**, tissues were found to contain small amounts of XylCer. Somewhat surprisingly, it was detected that GCS is able to use UDP-xylose (UDP-Xyl) to form XylCer, although the affinity for UDP-Xyl is much lower compared to that for UDP-Glc. It was next demonstrated that XylCer is an excellent sugar donor for GCase to generate XylChol. Therefore, at present the most likely biosynthetic pathway for formation of endogenous XylChol is the generation of XylCer by GCS followed by its use as sugar donor for GCase-mediated formation of XylChol. Consistent with this pathway is the reduced XylChol level in spleen from a type 1 Gaucher patient with a reduced GCase activity.

The identification of GlcChol in the SC of skin (**chapter 5**), prompted us to look for the possible presence of XylChol in the SC. In vital epidermis and full skin of a normal individual the presence of significant amounts of XylChol could be observed: levels of approximately 3 and 15 pmol/mg wet weight, respectively. These preliminary findings should be reproduced by analysis of samples from different subjects. Pilot studies with SC sheets from NTS patients revealed the presence of XylChol in 10 out of 13 of samples, ranging from 12 to 77 fmol/mg dry weight. This finding suggests that XylChol manages to reach the SC in diseased skin with breached barrier function.

Future investigations

Other β-glucosidases.

The discovery of significant activity of the enzyme GCase towards β-xylosidase led to investigation of similar activity of the two other cellular retaining β-glucosidases: the cytosol-facing membrane-associated GBA2 and the soluble cytosolic GBA3 (Klotho-Related Protein, KLrP) [83, 97]. GBA2 was found to exert no β-xylosidase or transxylosidase activity. In contrast, GBA3 (formerly known as 'broad-specific beta-glucosidase') is active towards β-xylosides, showing hydrolytic and transxylosylation activities similar to GCase. The physiological role of GBA3 is still not entirely clear. Common in humans is an inherited deficiency in the enzyme [98, 99]. The enzyme is thought to play a role in detoxification of toxic plant glucoside [100, 101]. A preliminary investigation has revealed that GBA3 can use 4-MU-β-galactoside and 4-MU-β-xyloside to transglycosylate 25-NBD-cholesterol. GBA3 when incubated with 4-MU-β-glucoside was only able to transglucosylate natural cholesterol but not 25-NBD-cholesterol. As observed with GCase, the ability of GBA3 to generate xylosylated products was relative prominent as compared to its ability to degrade β-xylosides. In an earlier study, Glew and co-workers did observe transgalactosylation activity of pig liver GBA3 with alcohol or another substrate molecule as acceptor, generating digalactosyl-PNP [102]. Apparently, the catalytic pocket of GBA3 can harbor (near) simultaneously two substrate molecules in the pocket. An extended careful analysis of pure GBA3 regarding transxylosylation capacity is of interest.

Another player: Acylglucosides?

The pendant CH_2OH group in a β-glucoside seems not essential be a substrate for GCase (**chapter 6**). This finding is not surprising given the observation that GCase tolerates a hydrophobic extension at C8 of cyclophellitol-epoxide (equivalent to C6 of glucose during the covalent binding to the catalytic nucleophile E340 [103]. Actually, the affinity of the suicide inhibitor is markedly improved by this modification [103]. Likewise, Vocadlo and co-workers designed a highly specific GCase substrate containing a bulky modification at the C6 of the glucoside [104].

These observations prompted the investigation whether a β-glucoside with an O-acyl extension at C6 is a suitable substrate for GCase. Four different 6-O-acyl-glucoside-methylumbelliferones (4-MU-AGlc's) were synthesized by Marta Artola (figure 2A). GCase was found to be able to hydrolyze all 4-MU-AGlc substrates showing even lower Km values than 4-MU-Glc. The Vmax of GCase was significantly higher for 4-MU-Glc than 4-MU-AGlc's. Next, the transfer of the 6-O-acylglucoside moiety from 4-MU-AG to cholesterol was confirmed by LC-MS/MS analysis. Of note, GBA2 does not accept 4-MU-AG as a substrate. Again,

this is consistent with lack of reactivity of GBA2 with a cyclophellitol with C8 modification. Meanwhile, a norbornadiene-6 glucoside-methylumbelliferone (4-MU-AG-NBD) has been generated by Artola (Figure 2B). This compound was found to be still hydrolyzed by GCase with high affinity. Such type of substrate is envisioned to be of great use to identify acceptors in transglycosylation catalyzed by GCase since the glycosylated products should be fluorescent due to the NBD attached to the sugar moiety. However, the NBD linked via an ester bond to the glucose moiety is intrinsically susceptible to hydrolysis. At the moment it is attempted to synthesize the same compound with a more stable thio-ester.

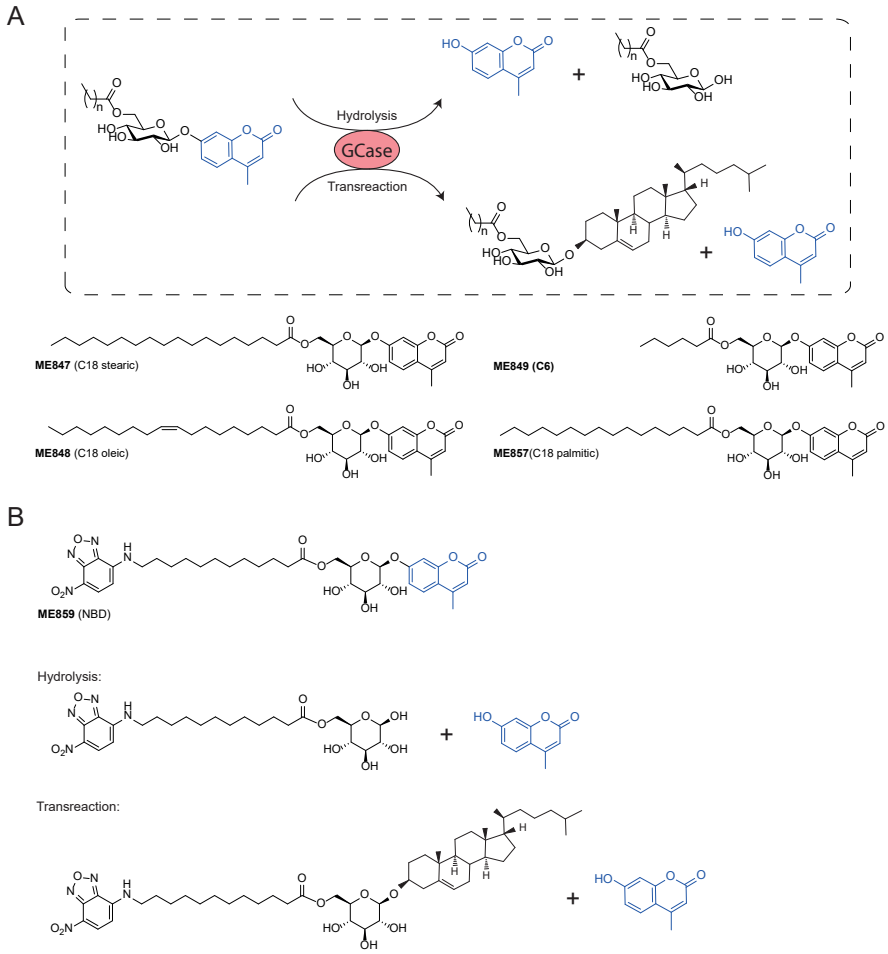

Figure 2: Acylglucosides as a substrate for GCase. A: Hydrolysis and transreaction by GCase of 4-MU glucose acylated substrates, with their acyl group differing in length and saturation. B. Chemical structure NBD-Acyl-Glucose-D-β 4-methylumbelliferyl compound (ME859) as a substrate for GCase and formed products.

The question can be raised whether 6-O-acylglucosides occur in human tissues and if so, whether they they are physiological substrates for GCase. This is amenable to investigation since in principle 6-O-acylglucosyl-cholesterol can be sensitively measured with LC-MS/MS. More than thirty years ago, Wertz and colleagues actually reported the presence of 6-O-acylated glucosylated sterol in the epidermis of chicken, being a stunning 2% of the total lipid [105]. Another research paper from around that time reports on the existence of GlcChol in snake skin [106]. The 6-O-acylated glucosylated sterols are also well known and abundant compounds in plants and usually named acyl steryl glucosides (ASGs). Several plant-derived food products are rich in ASGs, like soybean and potato [107]. Very high levels are reported for tomatoes and olive oil [108, 109]. It is conceivable that consumed ASGs (chicken skin used in snacks, various plant products) may enter intact and/or deacylated the body from the intestine [110]. Of note, oral exposure of rodents to a mixture of ASGs and SGs induces α-synucleinopathies, suggesting even their entry into the brain [110]. Likely, ASGs and de-acylated SGs are substrates of GCase and thus could interfere with endogenous GlcCer metabolism.

It will be of interest to study the presence and role of 6-O-acylglucoside sterols in the SC of human skin. Based on their chemical structure, 6-O-acylglucoside sterols might connect in a flexible way lipid lamellae, in analogy to the assumed action of very long SC ceramides [106]. It will be also exciting to look for the presence of ASG's in various cell types in the body in health and disease and to identify their precise subcellular localization.

Conclusion

This thesis describes the versatile enzyme GCase that fulfills functions inside lysosomes of cells and extracellularly in the skin. In the human skin, GCase acts as biosynthetic enzyme that produces essential SC ceramides from the precursor GlcCer. Contrarily, GCase in the lysosomes catalyzes the penultimate step in the breakdown of glycosphingolipids. The development of the accurate and sensitive *in situ* method for ABP-based detection of active GCase in skin should allow exciting novel investigation on skin in health and disease. As demonstrated in this thesis, the novel method already visualized an altered localization of GCase in AD skin in combination with an altered SC lipid composition. Using LC-MS/MS, the occurrence of GlcChol in human skin could be for the first time demonstrated. Establishing the physiological function of GlcChol in the skin will be of great interest.

The catalytic versatility of GCase is exemplified by its ability to metabolize β-xylosides. The observed natural presence of XylChol and XylCer should prompt a search for additional endogenous β-xylosides. Furtermore, the impact

of intake of food-derived exogenous β-xylosides should be investigated. In this connection, it will be particularly interesting to monitor xylosylated lipids in Gaucher disease and other conditions for which abnormal GCase imposes a risk, such as multiple myeloma and α-synucleinopathies like Parkinsonism and Lewy-body dementia [111]. Additionally, the effect of topical administration of β-glucosides, β-xylosides and sterol-like structures to the skin barrier deserves attention since it might provide clues for novel therapies.

References

1. E. Beutler, G.A. Grabowski, Glucosylceramide Lipidosis-Gaucher Disease. , The metabolic and molecular bases of inherited disease eighth edition: Edited by C R Sriver, A L Beaudet, W S Sly and D Valle. McGraw-Hill, New York (2001).
2. Y.V. Taguchi, J. Liu, J. Ruan, J. Pacheco, X. Zhang, J. Abbasi, J. Keutzer, P.K. Mistry, S.S. Chandra, Glucosylsphingosine Promotes alpha-Synuclein Pathology in Mutant GBA-Associated Parkinson's Disease, J Neurosci, 37 (2017) 9617-9631.
3. E. Sidransky, D.M. Sherer, E.I. Ginns, Gaucher disease in the neonate: a distinct Gaucher phenotype is analogous to a mouse model created by targeted disruption of the glucocerebrosidase gene, Pediatr Res, 32 (1992) 494-498.
4. V.L. Tybulewicz, M.L. Tremblay, M.E. LaMarca, R. Willemsen, B.K. Stubblefield, S. Winfield, B. Zablocka, E. Sidransky, B.M. Martin, S.P. Huang, et al., Animal model of Gaucher's disease from targeted disruption of the mouse glucocerebrosidase gene, Nature, 357 (1992) 407-410.
5. Y. Takagi, E. Kriehuber, G. Imokawa, P.M. Elias, W.M. Holleran, Beta-glucocerebrosidase activity in mammalian stratum corneum, J Lipid Res, 40 (1999) 861-869.
6. F. Chang, P.W. Wertz, C.A. Squier, Comparison of glycosidase activities in epidermis, palatal epithelium and buccal epithelium, Comp Biochem Physiol B, 100 (1991) 137-139.
7. A.M. Vaccaro, M. Muscillo, K. Suzuki, Characterization of human glucosylsphingosine glucosyl hydrolase and comparison with glucosylceramidase, Eur J Biochem, 146 (1985) 315-321.
8. E. Proksch, pH in nature, humans and skin, J Dermatol, 45 (2018) 1044-1052.
9. J.W. Fluhr, P.M. Elias, Stratum corneum pH: formation and function of the "acid mantle", Exog Dermatol (2002) 163-175.
10. H. Niehues, J.A. Bouwstra, A. El Ghalbzouri, J.M. Brandner, P. Zeeuwen, E.H. van den Bogaard, 3D skin models for 3R research: The potential of 3D reconstructed skin models to study skin barrier function, Exp Dermatol, 27 (2018) 501-511.
11. G. Legler, Glycoside hydrolases: mechanistic information from studies with reversible and irreversible inhibitors, Adv Carbohydr Chem Biochem, 48 (1990) 319-384.
12. C.L. Kuo, E. van Meel, K. Kytidou, W.W. Kallemeijn, M. Witte, H.S. Overkleeft, M.E. Artola, J.M. Aerts, Activity-Based Probes for Glycosidases: Profiling and Other Applications, Methods Enzymol, 598 (2018) 217-235.
13. L.I. Willems, T.J. Beenakker, B. Murray, S. Scheij, W.W. Kallemeijn, R.G. Boot, M. Verhoek, W.E. Donker-Koopman, M.J. Ferraz, E.R. van Rijssel, B.I. Florea, J.D. Codee, G.A. van der Marel, J.M. Aerts, H.S. Overkleeft, Potent and selective activity-based probes for GH27 human retaining alpha-galactosidases, J Am Chem Soc, 136 (2014) 11622-11625.
14. J. Jiang, C.L. Kuo, L. Wu, C. Franke, W.W. Kallemeijn, B.I. Florea, E. van Meel, G.A. van der Marel, J.D. Codee, R.G. Boot, G.J. Davies, H.S. Overkleeft, J.M. Aerts, Detection of Active Mammalian GH31 alpha-Glucosidases in Health and Disease Using In-Class, Broad-Spectrum Activity-Based Probes, ACS Cent Sci, 2 (2016) 351-358.
15. J. Jiang, W.W. Kallemeijn, D.W. Wright, A. van den Nieuwendijk, V.C. Rohde, E.C. Folch, H. van den Elst, B.I. Florea, S. Scheij, W.E. Donker-Koopman, M. Verhoek, N. Li, M. Schurmann, D. Mink, R.G. Boot, J.D.C. Codee, G.A. van der Marel, G.J. Davies, J. Aerts, H.S. Overkleeft, In vitro and in vivo comparative and competitive activity-based protein profiling of GH29 alpha-l-fucosidases, Chem Sci, 6 (2015) 2782-false.
16. M. Artola, C.L. Kuo, S.A. McMahon, V. Oehler, T. Hansen, M. van der Lienden, X. He, H. van den Elst, B.I. Florea, A.R. Kermode, G.A. van der Marel, T.M. Gloster, J.D.C. Codee, H.S. Overkleeft, J. Aerts, New Irreversible alpha-l-Iduronidase Inhibitors and Activity-Based Probes, Chemistry, 24 (2018) 19081-19088.
17. L. Wu, J. Jiang, Y. Jin, W.W. Kallemeijn, C.L. Kuo, M. Artola, W. Dai, C. van Elk, M. van Eijk, G.A. van der Marel, J.D.C. Codee, B.I. Florea, J. Aerts, H.S. Overkleeft, G.J. Davies, Activity-based probes for functional interrogation of retaining beta-glucuronidases, Nat Chem Biol, 13 (2017) 867-873.
18. A.R. Marques, L.I. Willems, D. Herrera Moro, B.I. Florea, S. Scheij, R. Ottenhoff, C.P. van Roomen, M. Verhoek, J.K. Nelson, W.W. Kallemeijn, A. Biela-Banas, O.R. Martin, M.B. Cachon-Gonzalez, N.N. Kim, T.M. Cox, R.G. Boot, H.S. Overkleeft, J.M. Aerts, A Specific Activity-Based Probe to Monitor Family GH59 Galactosylceramidase, the Enzyme Deficient in Krabbe Disease, Chembiochem, 18 (2017) 402-412.
19. W.W. Kallemeijn, M.D. Witte, T.M. Voorn-Brouwer, M.T. Walvoort, K.Y. Li, J.D. Codee, G.A. van der Marel, R.G. Boot, H.S. Overkleeft, J.M. Aerts, A sensitive gel-based method combining distinct cyclophellitol-based probes for the identification of acid/base residues in human retaining beta-glucosidases, J Biol Chem, 289 (2014) 35351-35362.
20. W.W. Kallemeijn, K.Y. Li, M.D. Witte, A.R. Marques, J. Aten, S. Scheij, J. Jiang, L.I. Willems, T.M. Voorn-Brouwer, C.P. van Roomen, R. Ottenhoff, R.G. Boot, H. van den Elst, M.T. Walvoort, B.I. Florea, J.D. Codee, G.A. van der Marel, J.M. Aerts, H.S. Overkleeft, Novel activity-based probes for broad-spectrum profiling of retaining beta-

exoglucosidases in situ and in vivo, Angew Chem Int Ed Engl, 51 (2012) 12529-12533.
21. J. Jiang, T.J. Beenakker, W.W. Kallemeijn, G.A. van der Marel, H. van den Elst, J.D. Codee, J.M. Aerts, H.S. Overkleeft, Comparing Cyclophellitol N-Alkyl and N-Acyl Cyclophellitol Aziridines as Activity-Based Glycosidase Probes, Chemistry, 21 (2015) 10861-10869.
22. M. Rabionet, K. Gorgas, R. Sandhoff, Ceramide synthesis in the epidermis, Biochim Biophys Acta, 1841 (2014) 422-434.
23. H.A.-K. J. van Smeden, Y. Wang, D. Visscher, N. Stephens, S. Absalah, H. S. Overkleeft, J. M.F.G. Aerts, A. Hovnanian, J. A. Bouwstra, Epidermal barrier lipid enzyme activity in Netherton patients relates with serine protease activity and stratum corneum ceramide abnormalities. Submitted.
24. O.P. van Diggelen, Y.V. Voznyi, J.L. Keulemans, K. Schoonderwoerd, J. Ledvinova, E. Mengel, M. Zschiesche, R. Santer, K. Harzer, A new fluorimetric enzyme assay for the diagnosis of Niemann-Pick A/B, with specificity of natural sphingomyelinase substrate, J Inherit Metab Dis, 28 (2005) 733-741.
25. T. Pinkert, D. Furkert, T. Korte, A. Herrmann, C. Arenz, Amplification of a FRET Probe by Lipid-Water Partition for the Detection of Acid Sphingomyelinase in Live Cells, Angew Chem Int Ed Engl, 56 (2017) 2790-2794.
26. Y.F. Ordonez, J.L. Abad, M. Aseeri, J. Casas, V. Garcia, M. Casasampere, E.H. Schuchman, T. Levade, A. Delgado, G. Triola, G. Fabrias, Activity-Based Imaging of Acid Ceramidase in Living Cells, J Am Chem Soc, 141 (2019) 7736-7742.
27. J. Ishikawa, H. Narita, N. Kondo, M. Hotta, Y. Takagi, Y. Masukawa, T. Kitahara, Y. Takema, S. Koyano, S. Yamazaki, A. Hatamochi, Changes in the ceramide profile of atopic dermatitis patients, J Invest Dermatol, 130 (2010) 2511-2514.
28. J. van Smeden, M. Janssens, G.S. Gooris, J.A. Bouwstra, The important role of stratum corneum lipids for the cutaneous barrier function, Biochim Biophys Acta, 1841 (2014) 295-313.
29. C.P. Shen, M.T. Zhao, Z.X. Jia, J.L. Zhang, L. Jiao, L. Ma, Skin Ceramide Profile in Children With Atopic Dermatitis, Dermatitis, 29 (2018) 219-222.
30. M. Danso, W. Boiten, V. van Drongelen, K. Gmelig Meijling, G. Gooris, A. El Ghalbzouri, S. Absalah, R. Vreeken, S. Kezic, J. van Smeden, S. Lavrijsen, J. Bouwstra, Altered expression of epidermal lipid bio-synthesis enzymes in atopic dermatitis skin is accompanied by changes in stratum corneum lipid composition, J Dermatol Sci, 88 (2017) 57-66.
31. Eliglustat, in: LiverTox: Clinical and Research Information on Drug-Induced Liver Injury, Bethesda (MD), 2012.
32. Miglustat, in: LiverTox: Clinical and Research Information on Drug-Induced Liver Injury, Bethesda (MD), 2012.
33. A.R. Marques, M. Mirzaian, H. Akiyama, P. Wisse, M.J. Ferraz, P. Gaspar, K. Ghauharali-van der Vlugt, R. Meijer, P. Giraldo, P. Alfonso, P. Irun, M. Dahl, S. Karlsson, E.V. Pavlova, T.M. Cox, S. Scheij, M. Verhoek, R. Ottenhoff, C.P. van Roomen, N.S. Pannu, M. van Eijk, N. Dekker, R.G. Boot, H.S. Overkleeft, E. Blommaart, Y. Hirabayashi, J.M. Aerts, Glucosylated cholesterol in mammalian cells and tissues: formation and degradation by multiple cellular beta-glucosidases, J Lipid Res, 57 (2016) 451-463.
34. H. Akiyama, S. Kobayashi, Y. Hirabayashi, K. Murakami-Murofushi, Cholesterol glucosylation is catalyzed by transglucosylation reaction of beta-glucosidase 1, Biochem Biophys Res Commun, 441 (2013) 838-843.
35. H. Akiyama, Y. Hirabayashi, A novel function for glucocerebrosidase as a regulator of sterylglucoside metabolism, Biochim Biophys Acta Gen Subj, 1861 (2017) 2507-2514.
36. P.M. Elias, M.L. Williams, E.H. Choi, K.R. Feingold, Role of cholesterol sulfate in epidermal structure and function: lessons from X-linked ichthyosis, Biochim Biophys Acta, 1841 (2014) 353-361.
37. M. de Jager, W. Groenink, J. van der Spek, C. Janmaat, G. Gooris, M. Ponec, J. Bouwstra, Preparation and characterization of a stratum corneum substitute for in vitro percutaneous penetration studies, Biochim Biophys Acta, 1758 (2006) 636-644.
38. J. van Smeden, M. Janssens, W.A. Boiten, V. van Drongelen, L. Furio, R.J. Vreeken, A. Hovnanian, J.A. Bouwstra, Intercellular skin barrier lipid composition and organization in Netherton syndrome patients, J Invest Dermatol, 134 (2014) 1238-1245.
39. P. Wertz, Epidermal Lamellar Granules, Skin Pharmacol Physiol, 31 (2018) 262-268.
40. N.Y. Schurer, P.M. Elias, The biochemistry and function of stratum corneum lipids, Adv Lipid Res, 24 (1991) 27-56.
41. K.R. Feingold, Lamellar bodies: the key to cutaneous barrier function, J Invest Dermatol, 132 (2012) 1951-1953.
42. S. Mitsutake, C. Suzuki, M. Akiyama, K. Tsuji, T. Yanagi, H. Shimizu, Y. Igarashi, ABCA12 dysfunction causes a disorder in glucosylceramide accumulation during keratinocyte differentiation, J Dermatol Sci, 60 (2010) 128-129.

43. M. Akiyama, Y. Sugiyama-Nakagiri, K. Sakai, J.R. McMillan, M. Goto, K. Arita, Y. Tsuji-Abe, N. Tabata, K. Matsuoka, R. Sasaki, D. Sawamura, H. Shimizu, Mutations in lipid transporter ABCA12 in harlequin ichthyosis and functional recovery by corrective gene transfer, J Clin Invest, 115 (2005) 1777-1784.
44. M. Akiyama, The roles of ABCA12 in epidermal lipid barrier formation and keratinocyte differentiation, Biochim Biophys Acta, 1841 (2014) 435-440.
45. G. Schmitz, G. Muller, Structure and function of lamellar bodies, lipid-protein complexes involved in storage and secretion of cellular lipids, J Lipid Res, 32 (1991) 1539-1570.
46. C.d.R. de Duve, A. V. S.; Cameron, M. P., The lysosome concept, Churchill London., Lysosomes (1963) 1-35.
47. D. Reczek, M. Schwake, J. Schroder, H. Hughes, J. Blanz, X. Jin, W. Brondyk, S. Van Patten, T. Edmunds, P. Saftig, LIMP-2 is a receptor for lysosomal mannose-6-phosphate-independent targeting of beta-glucocerebrosidase, Cell, 131 (2007) 770-783.
48. S. Rijnboutt, H.M. Aerts, H.J. Geuze, J.M. Tager, G.J. Strous, Mannose 6-phosphate-independent membrane association of cathepsin D, glucocerebrosidase, and sphingolipid-activating protein in HepG2 cells, J Biol Chem, 266 (1991) 4862-4868.
49. D.L. Stone, W.F. Carey, J. Christodoulou, D. Sillence, P. Nelson, M. Callahan, N. Tayebi, E. Sidransky, Type 2 Gaucher disease: the collodion baby phenotype revisited, Arch Dis Child Fetal Neonatal Ed, 82 (2000) F163-166.
50. W.M. Holleran, Y. Takagi, G.K. Menon, G. Legler, K.R. Feingold, P.M. Elias, Processing of epidermal glucosylceramides is required for optimal mammalian cutaneous permeability barrier function, J Clin Invest, 91 (1993) 1656-1664.
51. W.M. Holleran, Y. Takagi, G.K. Menon, S.M. Jackson, J.M. Lee, K.R. Feingold, P.M. Elias, Permeability barrier requirements regulate epidermal beta-glucocerebrosidase, J Lipid Res, 35 (1994) 905-912.
52. W.M. Holleran, E.I. Ginns, G.K. Menon, J.U. Grundmann, M. Fartasch, C.E. McKinney, P.M. Elias, E. Sidransky, Consequences of beta-glucocerebrosidase deficiency in epidermis. Ultrastructure and permeability barrier alterations in Gaucher disease, J Clin Invest, 93 (1994) 1756-1764.
53. V. Castranova, J. Rabovsky, J.H. Tucker, P.R. Miles, The alveolar type II epithelial cell: a multifunctional pneumocyte, Toxicol Appl Pharmacol, 93 (1988) 472-483.
54. D.F. Tierney, Lung surfactant: some historical perspectives leading to its cellular and molecular biology, Am J Physiol, 257 (1989) L1-12.
55. J. Goerke, Lung surfactant, Biochim Biophys Acta, 344 (1974) 241-261.
56. E.R. Weibel, J. Gil, Electron microscopic demonstration of an extracellular duplex lining layer of alveoli, Respir Physiol, 4 (1968) 42-57.
57. V. Besnard, Y. Matsuzaki, J. Clark, Y. Xu, S.E. Wert, M. Ikegami, M.T. Stahlman, T.E. Weaver, A.N. Hunt, A.D. Postle, J.A. Whitsett, Conditional deletion of Abca3 in alveolar type II cells alters surfactant homeostasis in newborn and adult mice, Am J Physiol Lung Cell Mol Physiol, 298 (2010) L646-659.
58. T. Annilo, S. Shulenin, Z.Q. Chen, I. Arnould, C. Prades, C. Lemoine, C. Maintoux-Larois, C. Devaud, M. Dean, P. Denefle, M. Rosier, Identification and characterization of a novel ABCA subfamily member, ABCA12, located in the lamellar ichthyosis region on 2q34, Cytogenet Genome Res, 98 (2002) 169-176.
59. S. Shulenin, L.M. Nogee, T. Annilo, S.E. Wert, J.A. Whitsett, M. Dean, ABCA3 gene mutations in newborns with fatal surfactant deficiency, N Engl J Med, 350 (2004) 1296-1303.
60. T. Yanagi, M. Akiyama, H. Nishihara, K. Sakai, W. Nishie, S. Tanaka, H. Shimizu, Harlequin ichthyosis model mouse reveals alveolar collapse and severe fetal skin barrier defects, Hum Mol Genet, 17 (2008) 3075-3083.
61. R. Ridsdale, C.L. Na, Y. Xu, K.D. Greis, T. Weaver, Comparative proteomic analysis of lung lamellar bodies and lysosome-related organelles, PLoS One, 6 (2011) e16482.
62. J. Perez-Gil, T.E. Weaver, Pulmonary surfactant pathophysiology: current models and open questions, Physiology (Bethesda), 25 (2010) 132-141.
63. A.C. de Vries, A.W. Schram, M. van den Berg, J.M. Tager, J.J. Batenburg, L.M. van Golde, An improved procedure for the isolation of lamellar bodies from human lung. Lamellar bodies free of lysosomes contain a spectrum of lysosomal-type hydrolases, Biochim Biophys Acta, 922 (1987) 259-269.
64. R.H. Glew, A. Basu, S.A. Shelley, J.F. Paterson, W.F. Diven, M.R. Montgomery, J.U. Balis, Sequential changes of lamellar body hydrolases during ozone-induced alveolar injury and repair, Am J Pathol, 134 (1989) 1143-1150.
65. R. Buccoliero, S. Palmeri, G. Ciarleglio, A. Collodoro, M.M. De Santi, A. Federico, Increased lung surfactant phosphatidylcholine in patients affected by lysosomal storage diseases, J Inherit Metab Dis, 30 (2007) 983.
66. Y.C. Kao, L.M. Lichtenberger, Localization of phospholipid-rich zones in rat gastric mucosa: possible origin of a protective hydrophobic luminal lining, J Histochem Cytochem, 35 (1987) 1285-1298.
67. D.C. Dobyan, R.E. Bulger, Morphology of the minipig kidney, J Electron Microsc Tech, 9 (1988) 213-234.

68. Y. Harada, T. Sakai, N. Tagashira, M. Suzuki, Intracellular structure of the outer hair cell of the organ of Corti, Scan Electron Microsc, (1986) 531-535.
69. V.F. Holland, G.A. Zampighi, S.A. Simon, Morphology of fungiform papillae in canine lingual epithelium: location of intercellular junctions in the epithelium, J Comp Neurol, 279 (1989) 13-27.
70. E. Mira, M. Benazzo, P. Galioto, A. Calligaro, A. Casasco, Presence of phospholipidic lamellar bodies on the mucosa of rabbit eustachian tube. Ultrastructural aspects, ORL J Otorhinolaryngol Relat Spec, 50 (1988) 251-256.
71. L. Frithiof, J. Wersaell, A Highly Ordered Structure in Keratinizing Human Oral Epithelium, J Ultrastruct Res, 12 (1965) 371-379.
72. V. Svane-Knudsen, G. Rasmussen, P.P. Clausen, Surfactant-like lamellar bodies in the mucosa of the human nose, Acta Otolaryngol, 109 (1990) 307-313.
73. S. Lager, T.L. Powell, Regulation of nutrient transport across the placenta, J Pregnancy, 2012 (2012) 179827.
74. M.R. Syme, J.W. Paxton, J.A. Keelan, Drug transfer and metabolism by the human placenta, Clin Pharmacokinet, 43 (2004) 487-514.
75. J.M. Jebbink, R.G. Boot, R. Keijser, P.D. Moerland, J. Aten, G.J. Veenboer, M. van Wely, M. Buimer, E. Ver Loren van Themaat, J.M. Aerts, J.A. van der Post, G.B. Afink, C. Ris-Stalpers, Increased glucocerebrosidase expression and activity in preeclamptic placenta, Placenta, 36 (2015) 160-169.
76. A.S. Younes, M. Csire, B. Kapusinszky, K. Szomor, M. Takacs, G. Berencsi, Heterogeneous pathways of maternal-fetal transmission of human viruses (review), Pathol Oncol Res, 15 (2009) 451-465.
77. A. Paradela, S.B. Bravo, M. Henriquez, G. Riquelme, F. Gavilanes, J.M. Gonzalez-Ros, J.P. Albar, Proteomic analysis of apical microvillous membranes of syncytiotrophoblast cells reveals a high degree of similarity with lipid rafts, J Proteome Res, 4 (2005) 2435-2441.
78. C. Blundell, E.R. Tess, A.S. Schanzer, C. Coutifaris, E.J. Su, S. Parry, D. Huh, A microphysiological model of the human placental barrier, Lab Chip, 16 (2016) 3065-3073.
79. V.M. Joglekar, Barrier properties of vernix caseosa, Arch Dis Child, 55 (1980) 817-819.
80. Y. Sumida, M. Yakumaru, Y. Tokitsu, Y. Iwamato, T. Ikemoto, K. Mimura, Studies on the function of vernix caseosa the secrecy of baby's skin., in: International Federation of the Societies of Cosmetic Chemists 20th International Conference, Cannes, France, 1998, pp. 1-7.
81. P.H. Hoeger, V. Schreiner, I.A. Klaassen, C.C. Enzmann, K. Friedrichs, O. Bleck, Epidermal barrier lipids in human vernix caseosa: corresponding ceramide pattern in vernix and fetal skin, Br J Dermatol, 146 (2002) 194-201.
82. V. Patel, A.L. Tappel, Identity of beta-glucosidase and beta-xylosidase activities in rat liver lysosomes, Biochim Biophys Acta, 191 (1969) 86-94.
83. S. van Weely, M. Brandsma, A. Strijland, J.M. Tager, J.M. Aerts, Demonstration of the existence of a second, non-lysosomal glucocerebrosidase that is not deficient in Gaucher disease, Biochim Biophys Acta, 1181 (1993) 55-62.
84. A.R. Plant, J.E. Oliver, M.L. Patchett, R.M. Daniel, H.W. Morgan, Stability and substrate specificity of a beta-glucosidase from the thermophilic bacterium Tp8 cloned into Escherichia coli, Arch Biochem Biophys, 262 (1988) 181-188.
85. S.W. Kengen, E.J. Luesink, A.J. Stams, A.J. Zehnder, Purification and characterization of an extremely thermostable beta-glucosidase from the hyperthermophilic archaeon Pyrococcus furiosus, Eur J Biochem, 213 (1993) 305-312.
86. C. Srisomsap, J. Svasti, R. Surarit, V. Champattanachai, P. Sawangareetrakul, K. Boonpuan, P. Subhasitanont, D. Chokchaichamnankit, Isolation and characterization of an enzyme with beta-glucosidase and beta-fucosidase activities from Dalbergia cochinchinensis Pierre, J Biochem, 119 (1996) 585-590.
87. J.B. Kempton, S.G. Withers, Mechanism of Agrobacterium beta-glucosidase: kinetic studies, Biochemistry, 31 (1992) 9961-9969.
88. C.K. De Bruyne, G.M. Aerts, R.L. De Gussem, Hydrolysis of aryl beta-D-glucopyranosides and beta-D-xylopyranosides by an induced beta-D-glucosidase from Stachybotrys atra, Eur J Biochem, 102 (1979) 257-267.
89. D.K. Watt, H. Ono, K. Hayashi, Agrobacterium tumefaciens beta-glucosidase is also an effective beta-xylosidase, and has a high transglycosylation activity in the presence of alcohols, Biochim Biophys Acta, 1385 (1998) 78-88.
90. P. Thongpoo, C. Srisomsap, D. Chokchaichamnankit, V. Kitpreechavanich, J. Svasti, P.T. Kongsaeree, Purification and characterization of three beta-glycosidases exhibiting high glucose tolerance from Aspergillus niger ASKU28, Biosci Biotechnol Biochem, 78 (2014) 1167-1176.

91. S. Vroemen, J. Heldens, C. Boyd, B. Henrissat, N.T. Keen, Cloning and characterization of the bgxA gene from Erwinia chrysanthemi D1 which encodes a beta-glucosidase/xylosidase enzyme, Mol Gen Genet, 246 (1995) 465-477.
92. E.V. Eneyskaya, H. Brumer, 3rd, L.V. Backinowsky, D.R. Ivanen, A.A. Kulminskaya, K.A. Shabalin, K.N. Neustroev, Enzymatic synthesis of beta-xylanase substrates: transglycosylation reactions of the beta-xylosidase from Aspergillus sp, Carbohydr Res, 338 (2003) 313-325.
93. M. Nieto-Dominguez, A. Prieto, B. Fernandez de Toro, F.J. Canada, J. Barriuso, Z. Armstrong, S.G. Withers, L.I. de Eugenio, M.J. Martinez, Enzymatic fine-tuning for 2-(6-hydroxynaphthyl) beta-D-xylopyranoside synthesis catalyzed by the recombinant beta-xylosidase BxTW1 from Talaromyces amestolkiae, Microb Cell Fact, 15 (2016) 171.
94. J. Fang, J. Huang, Accumulation of plasma levels of anthocyanins following multiple saskatoon berry supplements, Xenobiotica, (2019) 1-4.
95. U. Lindahl, J. Couchman, K. Kimata, J.D. Esko, Proteoglycans and Sulfated Glycosaminoglycans, in: rd, A. Varki, R.D. Cummings, J.D. Esko, P. Stanley, G.W. Hart, M. Aebi, A.G. Darvill, T. Kinoshita, N.H. Packer, J.H. Prestegard, R.L. Schnaar, P.H. Seeberger (Eds.) Essentials of Glycobiology, Cold Spring Harbor (NY), 2015, pp. 207-221.
96. K.A. Karlsson, B.E. Samuelsson, G.O. Steen, Identification of a xylose-containing cerebroside in the salt gland of the herring gull, J Lipid Res, 13 (1972) 169-176.
97. Y. Hayashi, N. Okino, Y. Kakuta, M. Ito, [Novel catabolic pathway of glycosphingolipids that includes a cytosolic glucocerebrosidase, klotho-related protein (KLrP)], Tanpakushitsu Kakusan Koso, 53 (2008) 1462-1467.
98. N. Dekker, T. Voorn-Brouwer, M. Verhoek, T. Wennekes, R.S. Narayan, D. Speijer, C.E. Hollak, H.S. Overkleeft, R.G. Boot, J.M. Aerts, The cytosolic beta-glucosidase GBA3 does not influence type 1 Gaucher disease manifestation, Blood Cells Mol Dis, 46 (2011) 19-26.
99. E. Beutler, Discrepancies between genotype and phenotype in hematology: an important frontier, Blood, 98 (2001) 2597-2602.
100. K.L. LaMarco, R.H. Glew, Hydrolysis of a naturally occurring beta-glucoside by a broad-specificity beta-glucosidase from liver, Biochem J, 237 (1986) 469-476.
101. V. Gopalan, A. Pastuszyn, W.R. Galey, Jr., R.H. Glew, Exolytic hydrolysis of toxic plant glucosides by guinea pig liver cytosolic beta-glucosidase, J Biol Chem, 267 (1992) 14027-14032.
102. V. Gopalan, D.J. Vander Jagt, D.P. Libell, R.H. Glew, Transglucosylation as a probe of the mechanism of action of mammalian cytosolic beta-glucosidase, J Biol Chem, 267 (1992) 9629-9638.
103. M.D. Witte, W.W. Kallemeijn, J. Aten, K.Y. Li, A. Strijland, W.E. Donker-Koopman, A.M. van den Nieuwendijk, B. Bleijlevens, G. Kramer, B.I. Florea, B. Hooibrink, C.E. Hollak, R. Ottenhoff, R.G. Boot, G.A. van der Marel, H.S. Overkleeft, J.M. Aerts, Ultrasensitive in situ visualization of active glucocerebrosidase molecules, Nat Chem Biol, 6 (2010) 907-913.
104. A.K. Yadav, D.L. Shen, X. Shan, X. He, A.R. Kermode, D.J. Vocadlo, Fluorescence-quenched substrates for live cell imaging of human glucocerebrosidase activity, J Am Chem Soc, 137 (2015) 1181-1189.
105. P.W. Wertz, P.M. Stover, W. Abraham, D.T. Downing, Lipids of chicken epidermis, J Lipid Res, 27 (1986) 427-435.
106. W. Abraham, P.W. Wertz, R.R. Burken, D.T. Downing, Glucosylsterol and acylglucosylsterol of snake epidermis: structure determination, J Lipid Res, 28 (1987) 446-449.
107. M. Lepage, Isolation and Characterization of an Esterified Form of Steryl Glucoside, J Lipid Res, 5 (1964) 587-592.
108. R.B. Gomez-Coca, C. Perez-Camino Mdel, W. Moreda, On the glucoside analysis: simultaneous determination of free and esterified steryl glucosides in olive oil. Detailed analysis of standards as compulsory first step, Food Chem, 141 (2013) 1273-1280.
109. B.D. Whitaker, N.E. Gapper, Ripening-specific stigmasterol increase in tomato fruit is associated with increased sterol C-22 desaturase (CYP710A11) gene expression, J Agric Food Chem, 56 (2008) 3828-3835.
110. J.M. Van Kampen, H.A. Robertson, The BSSG rat model of Parkinson's disease: progressing towards a valid, predictive model of disease, EPMA J, 8 (2017) 261-271.
111. S.A. Schneider, R.N. Alcalay, Neuropathology of genetic synucleinopathies with parkinsonism: Review of the literature, Mov Disord, 32 (2017) 1504-1523.

Appendix

Summary
Samenvatting
Curriculum vitae
Dankwoord

Summary

Chapter 1 provides an introduction on glycosphingolipids and their metabolism. The lysosomal β-glucosidase named glucocerebrosidase (GCase, encoded by the *GBA* gene) is highlighted. The scope of the investigations described in this this thesis is presented.

As reviewed in **Chapter 2**, GCase is a retaining β-glucosidase that hydrolyzes the glycosphingolipid glucosylceramide (GlcCer) to ceramide and glucose at acid pH. Inherited deficiency of GCase causes Gaucher disease (GD), a relatively common lysosomal storage disorder. In GD patients GlcCer is stored in lysosomes of cells, particularly tissue macrophages (Gaucher cells). GCase fulfills another crucial function beyond lysosomes. The enzyme generates ceramides from GlcCer molecules in the outer part of the skin, the stratum corneum (SC). This is essential for skin barrier properties compatible with terrestrial life. GCase is catalytically versatile and able to hydrolyze as well as to catalyze transglycosylation.

Chapter 3 describes a novel sensitive *in situ* method for the detection of active GCase in skin sections. With this method use is made of fluorescent activity-based probes (ABP) that covalently bind to the catalytic nucleophile of GCase. As compared to zymography, the ABP-based detection of active GCase offers several advantages. It is less labor intensive and visualizes active enzyme with higher resolution. The investigation on localization of active GCase in skin revealed that the enzyme is present in very high amounts in the SC. With ABP-labeling, active GCase could be detected in 3D-cultured skin models. Labeling with ABP was prohibited by the reversible inhibitor, isofagomine. The inhibitor treatment led to an increase in the *GlcCer* : *ceramide* ratio, illustrating the importance of active GCase.

Chapter 4 focusses on atopic dermatitis. AD patients suffer from inflamed skin accompanied by skin barrier defects. The conducted investigation revealed that the localization and activity of GCase and acid sphingomyelinase (ASM) was abnormal in skin of AD patients, particularly at lesional skin sites. The enzymes GCase and ASM both generate ceramides. Their abnormalities in AD skin correlate to an altered lipid composition of the SC. Specific ceramide subclasses [AS] and [NS] are increased. A correlation between altered localization of active GCase and ASM and a disturbed SC lipid composition was observed.

Chapter 5 deals with the discovery of GlcChol as novel component of human epidermis. GlcChol was already known to generated from GlcCer and cholesterol via transglucosylation catalyzed largely by the enzyme GBA2. At high cconcentration of cholesterol in lysosomes, GCase also forms GlcChol via tranglucsylation. Given the abundance of GCase and cholesterol in the SC, it is not surprising that considerable GlcChol is demonstrable in the human skin, particularly the SC. GlcChol is likely locally metabolized by GCase, however the physiological function of GlcChol in the SC deserves future investigation.

The catalytic versatility of GCase is studied in **Chapter 6**. It is demonstrated that GCase not only cleaves 4-methylumbelliferyl-β-D-glucose, but also 4-methylumbelliferyl-β-D-xylose. It is reported for the first time that GCase is able to transxylosylate cholesterol to render xylosyl-β-cholesterol (XylChol). The formed XylChol can act as a subsequent acceptor for further transxylosylation, rendering di-xylosyl-cholesterol. Synthesis of XylChol occurs in intact cells exposed to 4-MU-Xyl or a plant-derived cyanidine-β-xyloside. This synthesis is entirely GCase dependent and can be increased by the induction of lysosomal cholesterol accumulation. Mutant GCases from GD patients were not found to show marked abnormalities in relative β-glucosidase, β-xylosidase, transglucosidase and transxylosidase activities. Besides GCase, the cytosolic enzyme GBA3 is also able, *in vitro*, to hydrolyze β-xylosides and catalyze a transreaction. In the search for potential endogenous β-xylose donors, xylosylated ceramide (XylCer) was detected in cells and tissues. Glucosylceramide synthase (GCS) was found to form XylCer. Thus, the investigation not only revealed catalytic versatility of GCase but also led to identification of a novel class of glycosphingolipids.

The **Discussion** summarizes the various studies and discusses their outcome in view of the literature. Moreover, suggestions are made regarding future research on the exciting topic of GCase, in particular its cell biology and its broad range of substrates and products.

Samenvatting

Hoofdstuk 1 geeft een introductie over glycosfingolipidenen hun metabolisme. Het lysosomale β-glucosidase genaamd glucocerebrosidase (GCase, gecodeerd door het GBA-gen) wordt hierbij uitgelicht. Het doel van de onderzoeken beschreven in dit proefschrift wordt vervolgens gepresenteerd.

Zoals besproken in **Hoofdstuk 2**, is GCase een vasthoudende β-glucosidase die het glycosfingolipide glucosylceramide (GlcCer) hydrolyseert tot ceramide en glucose bij een zure pH. Erfelijke tekort aan GCase veroorzaakt de ziekte van Gaucher (GD), een relatief veel voorkomende lysosomale stapelingsstoornis. Bij GD-patiënten wordt GlcCer opgeslagen in de lysosomen van cellen, met name weefselmacrofagen (Gaucher-cellen). GCase vervult een andere cruciale functie naast degene in lysosomen. Het enzym genereert ceramiden uit GlcCer-moleculen in het buitenste deel van de huid, het stratum corneum (SC). Dit is essentieel voor huidbarrière-eigenschappen die compatibel zijn met het landleven. GCase is katalytisch veelzijdig en in staat zowel te hydrolysatie als transglycosylatie te katalyseren.

Hoofdstuk 3 beschrijft een nieuwe en gevoelige in situ methode voor de detectie van actieve GCase in huidsecties. Bij deze methode wordt gebruik gemaakt van fluorescerende activity based probes (ABPs) die covalent binden aan het katalytische nucleofiel van GCase. In vergelijking met zymografie biedt de op ABP gebaseerde detectie van actieve GCase verschillende voordelen. Het is namelijk minder arbeidsintensief en visualiseert het actieve enzym met een hogere resolutie. Uit het onderzoek naar de lokalisatie van actieve GCase in de huid is gebleken dat het enzym in zeer grote hoeveelheden in het SC aanwezig is. Met ABP-labeling kon actieve GCase worden gedetecteerd in 3D-gekweekte huidmodellen. Binding van het enzym met ABPs werd voorkomen door de reversibele remmer isofagomine. De behandeling met

deze remmer leidde tot een verhoging van de glucosylceramide: ceramide-verhouding, wat het belang van actieve GCase illustreert.

Hoofdstuk 4 richt zich op atopische dermatitis. AD-patiënten lijden aan een ontstoken huid gepaard met een defecte huidbarrière. Uit het uitgevoerde onderzoek bleek dat de lokalisatie en activiteit van GCase en zure sfingomyelinase (ASM) abnormaal was in de huid van AD-patiënten, met name op de aangedane huid. De enzymen GCase en ASM genereren beiden ceramiden. Hun afwijkingen in AD-huid correleren een gewijzigde lipidesamenstelling van het SC. Specifieke ceramide-subklassen [AS] en [NS] zijn verhoogd. Daarnaast werd er een correlatie waargenomen tussen veranderde lokalisatie van actieve GCase en ASM en een verstoorde SC-lipidesamenstelling.

De katalytische veelzijdigheid van GCase wordt bestudeerd in **hoofdstuk 5**. Aangetoond wordt dat GCase niet alleen 4-methylumbelliferyl-β-D-glucose splitst, maar ook 4-methylumbelliferyl-β-D-xylose. Voor het eerst wordt gerapporteerd dat GCase in staat is om cholesterol te transxylosyleren en hierbij xylosyl-β-cholesterol (XylChol) maakt. Het gevormde XylChol kan dienen als een volgende acceptor voor verdere transxylosylering, waardoor di-xylosyl-cholesterol wordt gevormd. Synthese van XylChol vindt plaats in intacte cellen die zijn blootgesteld aan 4-MU-Xyl of een van planten afkomstig cyanidine-β-xyloside. Deze synthese is volledig GCase-afhankelijk en kan worden verhoogd door het opwekken van lysosomale cholesterolophoping. Mutante GCases van GD-patiënten bleken geen duidelijke afwijkingen te vertonen in relatieve β-glucosidase-, β-xylosidase-, transglucosidase- en transxylosidase-activiteiten. Naast GCase kan het cytosolische enzym GBA3 in vitro ook β-xylosiden hydrolyseren en een transreactie katalyseren. In de zoektocht naar potentiële endogene β-xylosedonoren werd gexylosyleerd ceramide (XylCer) gedetecteerd in cellen en weefsels. Glucosylceramidesynthase (GCS) bleek XylCer te kunnen vormen. Het onderzoek toonde dus niet alleen de katalytische veelzijdigheid van GCase aan, maar leidde ook tot de identificatie van een nieuwe klasse van glycosfingolipiden.

Hoofdstuk 6 behandelt de ontdekking van GlcChol als nieuw component van de menselijke epidermis. Het was al bekend dat GlcChol gegenereerd kan worden uit GlcCer en cholesterol via transglucosylering, grotendeels gekatalyseerd door het enzym GBA2. Bij hoge concentratie van cholesterol in lysosomen vormt GCase ook GlcChol via tranglucsylering. Gezien de overvloed aan GCase en cholesterol in het SC, is het niet verrassend dat een aanzienlijke hoeveelheid GlcChol aantoonbaar is in de menselijke huid, met name in het SC. GlcChol wordt waarschijnlijk lokaal gemetaboliseerd door GCase, maar de

fysiologische functie van GlcChol in de SC verdient toekomstig onderzoek.

De **Discussie** vat de verschillende onderzoeken samen en bespreekt hun resultaten in relatie tot de literatuur. Verder worden suggesties gedaan voor toekomstig onderzoek naar het interessante onderwerp van GCase, met name in relatie tot de celbiologie en het brede scala aan substraten en producten.

Curriculum vitae

Daphne Boer was born on the 16th of November in 1988 in Voorschoten. After graduating from the Adelbert College in Wassenaar in 2007, she started her study Life Science and Technology at the Technical University of Delft and the University of Leiden. She did her minor focused on Life Sciences at the Technical University of Denmark in Kongens Lyngby. During her studies she did three internships. The first was a bachelor research internship at the Human Genetics department of the Leiden University Medical Center (LUMC) entitled "Quantitative gene expression analysis in Oculopharyngeal Muscular Dystrophy and muscle aging." Next, she did a Science Based Business master internship at the Centre for Human Drug Research where she analyzed different types of financing for early stage drug development to "close the biopharmaceutical gap". For her final internship she went to the department of Toxicogenetics at the LUMC for a master research stay titled "The upstream pathway of IL-6 expression in response to UVC induced DNA damage".

After receiving her Master's Degree of Science in 2015 she started as a PhD candidate in the Medical Biochemistry laboratory of Johannes M. F. G. Aerts at the Leiden Institute of Chemistry, which resulted in this thesis. In March 2020 she started as a PostDoc at Human Genetics at the LUMC aiming to unravel mechanisms involved in transcription-coupled DNA repair using genetic and biochemical approaches.

List of Publications

J.M. Aerts, M.J. Ferraz, M. Mirzaian, P. Gaspar, S.V. Oussoren, P. Wisse, C.L. Kuo, L.T. Lelieveld, K. Kytidou, M.D. Hazeu, **D.E.C. Boer**, R. Meijer, M.J.C. van der Lienden, D. Herrera, T.L. Gabriel, J. Aten, H.S. Overkleeft, M.C. van Eijk, R.G. Boot, A.R.A. Marques, Lysosomal Storage Diseases. For Better or Worse: Adapting to Defective Lysosomal Glycosphingolipid, in: *eLs*, John Wiley & Sons, Ltd., Chichester, UK, 2017, pp. 1-13.

J. van Smeden, I.M. Dijkhoff, R.W.J. Helder, H. Al-Khakany, **D.E.C. Boer**, A. Schreuder, W.W. Kallemeijn, S. Absalah, H.S. Overkleeft, J. Aerts, J.A. Bouwstra. In situ visualization of glucocerebrosidase in human skin tissue: zymography versus activity-based probe labeling. *J Lipid Res*, 58 (2017) 2299-2309.

J. Aerts, C.L. Kuo, L.T. Lelieveld, **D.E.C. Boer**, M.J.C. van der Lienden, H.S. Overkleeft, M. Artola, Glycosphingolipids and lysosomal storage disorders as illustrated by gaucher disease, *Curr Opin Chem Biol*, 53 (2019) 204-215.

D.E.C. Boer, J. van Smeden, H. Al-Khakany, E. Melnik, R. van Dijk, S. Absalah, R. J. Vreeken, C.C.P. Haenen, A.P.M. Lavrijsen, H.S. Overkleeft, J.M.F.G Aerts, J.A. Bouwstra. Skin of atopic dermatitis patients shows disturbed β-glucocerebrosidase and acid sphingomyelinase activity that relates to changes in stratum corneum lipid composition. *Biochim Biophys Acta Mol Cell Biol Lipids*, 1865 (2020).

D.E.C. Boer, J. van Smeden, J.A. Bouwstra, J.M.F.G. Aerts. Glucocerebrosidase: Functions in and Beyond the Lysosome. *J Clin Med*, 9 (2020).

D.E.C. Boer, M.J. Ferraz, A. Nadaban, M. Mirzaian, A. Hovnanian , J. van Smeden, J.A. Bouwstra, J.M.F.G Aerts. Glucosylated cholesterol in skin: synthetic role of extracellular glucocerebrosidase. *Clin Chim Acta* (2020)

Submitted

D.E.C. Boer, M. Mirzaian, M.J. Ferraz, K.C. Zwiers, M. Hazeu, M.V. Baks, R. Ottenhoff, A.R.A. Marques, R. Meijer, J.C.P. Roos, T. Cox, R.G. Boot, N.j. Pannu, H.S. Overkleeft, M.E. Artola, J.M.F.G. Aerts. β-Xylosidase and transxylosidase activities of human glucocerebrosidase.

Dankwoord

Dit proefschrift is na een aantal jaren van hard werken geworden tot wat je nu voor je ziet. Ik ben ontzettend trots op het eindresultaat, maar dit was mij nooit alleen gelukt.

Als eerste wil ik mijn promotor **Hans Aerts** bedanken. Voor de introductie in de wereld van lysosomen en zijn vertrouwen in mij, om mij de kans te geven in zijn groep onderzoek te kunnen doen. Bedankt dat je mij de ruimte hebt gegeven om mijzelf te ontwikkelen tot een onafhankelijke onderzoeker, maar dat je in de tussentijd ook in de gaten hield dat ik aan het einde van deze rit ook echt iets had om in dit proefschrift te schrijven. Daarnaast wil ik ook **Joke Bouwstra**, mijn co-promotor, bedanken voor haar hulp en input. Zonder jouw hulp was het nooit mogelijk geweest deze bijdrage te leveren aan het huid onderzoek.

Dit proefschift was natuurlijk niet mogelijk geweest zonder mijn (oud) collega's bij Medische Biochemie, zowel op wetenschappelijk vlak als daarbuiten: **Kim**, **Rolf**, **Marco**, **Marta**, **Rebecca**, **Kassiani**, **Ethan**, **Mina**, **Wouter**, **Marri**, **Eline**, **Per**, **Judith**, **Saskia**, **Remco**, **Bas**, **Hisako**, **Qin**, **René** en **Astrid**. Speciaal bedankje voor 'The party office' mannen **Marc** en **Martijn**. Voornamelijk voor de gezelligheid, maar ook de waardevolle discussies over onderzoek en alles daar omheen.
Ook de studenten die ik heb mogen begeleiden - **Merel**, **Anne**, **Nina**, **Linda**, **Paula** en **Tessa** – wil ik via deze weg bedanken voor hun gezelligheid, harde werk en inzet.

Natuurlijk wil ik ook collega's uit andere onderzoeksgroepen bedanken, zoals **Tom**, **Annelot**, **Timo**, **Bobby** en **Floor** van 'boven'. Maar ook **Walter**, **Richard**, **Andreea** en **Jannik** van DTT. Daarnaast mag **Jeroen** in dit lijstje niet ontbreken, zonder wie ik nooit in de wereld van de huid was geïntroduceerd.

Bedankt voor al je hulp, enthousiasme en dat ik je ten alle tijden kon bereiken voor de meest uiteenlopende vragen.
Verder ook dank aan mijn nieuwe collega's bij de **Luijsterburg groep**, die mij steun en ruimte hebben gegeven de laatste hand aan dit proefschrift en de artikelen en te leggen.

Buitengewone dank gaat uit naar mijn paranimfen **Lindsey** en **Maria**, jullie hebben ontzettend bijgedragen aan mijn fijne tijd bij Medische Biochemie. Lindsey, we hebben veel gelachen en ook af en toe lekker geklaagd. En Maria, bedankt voor je gezelligheid in ons kantoor en al je hulp bij de MS, *obrigado*.

Daarnaast zijn er nog wat mensen buiten het lab die ik hier zou willen bedanken. Want een proefschrift komt niet alleen tot stand op het lab.
Nienke, **Rutger** en **Nora** (en op de valreep ook **Amber**), bij jullie kon ik ontsnappen aan alle hectiek van het onderzoek, en dat is minstens zo belangrijk. Of dit nu met bier bij de basketbal of op de bank met pizza en chips was.
Ook een shout out naar **Tribes** haar docenten en dansers, en dan voornamelijk de **Palermo crew**. Tijdens mijn PhD ben ik er achter gekomen dat dans voor mij de ideale uitlaat klep is en zonder jullie was dit niet mogelijk geweest.
ZVL6, samen spelen en de drankjes daarbuiten waren een goede manier om even met iets anders bezig te zijn. En bedankt voor het begrip als ik in alle drukte niet naar een training kon komen, of weer eens per ongelijk bij het verkeerde zwembad stond.
Speciale dank aan **Jettie**, voor de verschillende discussies die we hebben gehad tijdens het pannenkoeken eten over mijn onderzoek en alles eromheen. Ook was het onwijs prettig om met jou te sparren over wetenschapscommunicatie, zonder jou waren mijn posters en filmpjes nooit zo mooi en duidelijk geworden.

Dan tot slot, de belangrijkste. **Papa** en **mamma**, voor jullie steun tijdens dit proces. Mijn bijkom dagen op de Laan van Meerdervoort en de goeie wijn waren onmisbaar voor wat rust in mijn hoofd tussen alle PhD chaos in. En aan jullie uitleggen waar ik mee bezig was hielp mij vaak alles op een rijtje te zetten en leidde soms tot nieuwe realisaties. Søs, **Tosca**, bedankt voor de opbeurende Disney quotes en concert bezoeken. Ook voor je hulp om te formuleren wat ik nou eigenlijk wilde qua lay-out, of dat nu om dit proefschrift of een youtube filmpje ging. En ook **Roy**, super tof dat je altijd geïnteresseerd was en bedankt voor je input over de kaft.

Iedereen, heel erg bedankt!
- Daphne